Dissertation zur Erlangung des Doktorgrades

der Fakultät für Chemie und Pharmazie

der Ludwig-Maximilians-Universität München

The Rabies Virus Phosphoprotein: Novel Targets and Functions Involved in Interferon Antagonism

Marco Wachowius

aus München, Deutschland

2016

Erklärung

Diese Dissertation wurde im Sinne von § 7 der Promotionsordnung vom 28. November 2011 von Herrn Prof. Dr. Karl-Klaus Conzelmann betreut und von Herrn Prof. Dr. Klaus Förstemann vor der Fakultät für Chemie und Pharmazie vertreten.

Eidesstattliche Versicherung

Diese Dissertation wurde eigenständig und ohne unerlaubte Hilfe erarbeitet.

München, 30.11.2016 .....

Marco Wachowius .....

(Unterschrift des Autors)

Dissertation eingereicht am:	**27.10.2016**
1. Gutachter:	**Prof. Dr. Klaus Förstemann**
2. Gutachter:	**Prof. Dr. Karl-Klaus Conzelmann**
Mündliche Prüfung am:	**30.11.2016**

“Science may be described as the art of systematic over-simplification.”

Karl Popper

This thesis has been prepared in the laboratory of Prof. Dr. Karl-Klaus Conzelmann at the Max von Pettenkofer-Institute and Gene Center of the Ludwig-Maximilians-University Munich.

Danksagung

Im folgenden möchte ich mich sehr herzlich bei allen Menschen bedanken, die meine hier vorliegende Doktorarbeit möglich und die Arbeit daran zu einer angenehmen und spannenden Zeit gemacht haben.

An erster Stelle gilt mein Dank Prof. Karl-Klaus Conzelmann für die Gelegenheit meine Doktorarbeit in seinem Labor und in einem interessanten und herausfordernden Themengebiet anfertigen zu können. Danke für die Betreuung in den letzten Jahren, die allzeit offene Tür, sowie die Begutachtung dieser Arbeit. Desweiteren möchte ich mich bei Prof. Klaus Förstemann bedanken, der sich bereit erklärt hat diese Arbeit als Fachvertreter zu betreuen. Außerdem möchte ich mich beim DFG Graduiertenkolleg 1202 für viele interessante Veranstaltungen und die Finanzierung eines großen Teils dieser Arbeit bedanken.

Bei allen Mitgliedern der Arbeitsgruppe, Alex, ~~A~~Blex, Chloé und Max, sowie bei den ehemaligen Kollegen Kerstin, Konstantin, Tobias und Nadin möchte ich mich sehr herzlich für die produktive und angenehme Atmosphäre bedanken. Vielen Dank an Kerstin, die mir durch ihre hervorragende Betreuung in der Master Arbeit einen guten Start in die Promotion ermöglicht hat. Ein großes Dankeschön an Max für viele großartige Gespräche, Diskussionen und die geteilten Aufreger. Besten Dank an Daniel für viele spannende morgendliche Diskussionen und die Unterstützung beim Virus-Rescue. Desweiteren danke an Alex aka Blex, der das GraKo Dasein und die Seminare am Montag zwei Jahre lang mit mir geteilt hat („Einmal GraKo, immer GraKo“). Außerdem danke an Mr. „gehört zum Inventar“ Alex (der Erste) für viele praktische Ratschläge über die Jahre hinweg und viele spannende Diskussionen. Merci beaucoup auch an Chloé für viele nette Gespräche und hilfreiche Tipps im Labor, sowie die Gelegenheit bei der Arbeit mal wieder mehr Englisch zu reden. Auch ein besonderer Dank an Doro, die mit Ihrem tollen Einsatz unser Labor immer am laufen hält. Ich glaube dass die Atmoshpäre in unserer kleinen aber feinen Gruppe wirklich nicht selbstverständlich ist. Danke Euch allen für eine lehrreiche und angenehme Zeit, die mich in vielerlei Hinsicht weitergebracht hat und an die ich mit Sicherheit noch oft zurückdenken werde.

Mit der größte Dank geht hier natürlich an meine Familie! Herzlichen dank an meine Eltern und an meine einzige Lieblingsschwester, die mich bei eigentlich allen Vorhabungen immer großartig unterstützt haben. Ich denke die hier vorliegende Arbeit war doch eine gute Alternative zur Bootsbauer-Lehre ;). Außerdem einen ganz besonders lieben Dank an meine Freundin Nici. Danke dass du in den letzten Jahren immer für mich da warst und damit sicherlich auch ein großes Stück zu dieser Arbeit beigetragen hast.

Table of contents

1. Summary

In order to counteract invading pathogens, our cells evolved complex signaling cascades and effector proteins which constitute a part of the human innate immune system. Certain molecular characteristics which are normally absent in a healthy cell are used by highly specialized pattern recognition receptors (PRRs) to distinguish between harmless self-structures and non-self molecules potentially indicating a pathogenic threat. Receptor activation leads to the production of interferons (IFNs) and proinflammatory cytokines. For viruses, obligate intracellular parasites, it is essential to circumvent this response in order to establish a productive infection. The phosphoprotein (P) of rabies virus (RABV), the causing agent of a fatal zoonotic disease, has been identified as the central factor in RABV immune evasion. Besides its various crucial functions in the viral life cycle, RABV P antagonizes the innate immune response on two distinct levels. First, RABV P interferes very efficiently with RIG-I-like receptor (RLR) mediated IFN-induction by blocking activation of the central interferon regulatory factor 3 (IRF3). Secondly, RABV P abrogates IFN-signaling using a separate mechanism by retaining activated signal transducer and activator of transcription (STAT) in the cytosol. This dual mode of action makes RABV P one of the most powerful viral IFN antagonists.

Although RABV P is well known as suppressor of IFN induction, the inhibitory mode of action still remained unresolved. In order to shed light on this mechanism, one major goal of the present thesis was to examine which domains and functions of the P protein are vital for its suppressive abilities.

Therefore, different RABV P regions were examined for their potential involvement in subversion of IFN-induction. While the N-terminal domain and a conserved dynein light chain LC8-type 1 (DLC8) binding motif were shown to be non-essential for inhibition, dimerization deficient RABV P was found to be impaired in suppression of a type I interferon response. Further, RABV P strictly relied on the C-terminal domain (CTD) to abrogate RIG-I mediated IFN-induction.

The CTD of RABV P was previously reported to harbor a conformational nuclear localization signal (NLS), which, in concert with its nuclear export signals (NES), makes RABV P a nucleocytoplasmic shuttling protein. In this thesis, RABV P mutant proteins deficient in this CTD-NLS were shown to be defective in their ability to interfere with IRF3 activation. Fusion of NLS-deficient RABV P mutants with an ectopic SV40-NLS restored the suppressive capacities, providing strong evidence that the trafficking behavior of RABV P mediated by the CTD-NLS is required for inhibition of IFN-induction.

Previously, a short stretch of amino acids within a disordered region of RABV P (residues 176-186), was described as essential for the inhibition of IFN induction. However, the exact role of this sequence or the identity of potential molecular interaction partners remained elusive. Therefore, the P-176-186 region was further investigated by site-directed mutagenesis. This approach revealed that tryptophan 186 of RABV P is a critical residue for inhibitory function, since a P mutant protein containing a single alanine substitution at this position (W186A) completely failed in preventing IRF3 activation, equally to the previously characterized internal deletion mutant PΔ176-186. A recombinant virus containing the P-W186A mutant protein could be successfully rescued by a reverse genetics approach. Real-time PCR experiments showed that SAD-L16-P-W186A strongly induced IFN-β transcription, as compared to the parental strain.

Further research employing pulldown assays and mass spectrometry analysis identified members of the HSP70 family as molecular interactors of RABV P. The interaction motif could be narrowed down to RABV P residues 180-186 and *in vitro* studies indicated a direct and sequence specific interaction between the identified P motif and HSP70. The P–HSP70 association was lost in the inhibition defective mutants P-W186A and PΔ176-186. These findings provide a strong correlation between HSP70 binding and the ability of RABV P to suppress the induction of IFN-β, indicating a possible role for HSP70 family members in innate immune signaling.

In contrast to inhibition of IFN-induction, HSP70-binding deficient RABV P proteins were not affected in their ability to interfere with JAK-STAT signaling. Moreover, these P mutants were not impaired in their central role in the viral life cycle, as indicated by the wild type-like growth of the recombinant mutant virus SAD-L16-P-W186A. These findings strongly suggest that the failure of HSP70 binding-deficient RABV P mutants to impair IFN-induction is not due to aberrant protein folding. Furthermore, pulldown assays employing HSP70 mutants and truncation constructs provided evidence that the observed association with RABV P is not depending on heat shock protein ATPase function.

Overexpression of wild type and mutant HSP70 and heat-shock treatment of cells strongly interfered with RLR mediated interferon induction, providing another hint at an involvement of HSP70s in innate immune regulation. Our resulting working hypothesis suggests that RABV P inhibits IFN induction either by abrogating HSP70 function in this pathway, or by misusing the protein to counteract IRF3 activation.

2. Introduction

2.1. Rabies virus

2.1.1. Overview

Rabies is an insidious disease that inevitably leads to a fatal encephalitis in the final stage of a productive infection. Its causative agents are members of the *Lyssavirus* genus with Rabies virus as the type species. They belong to the *Rhabdoviridae*, a family of enveloped viruses exhibiting a rod- or bullet-like shape ("*rhabdos*" meaning rod in Greek). Together with several families, such as the *Filoviridae*, *Paramyxoviridae*, *Bornaviridae* and others, they form the *Mononegavirales*, an order of viruses containing a single-stranded, non-segmented, negative-sense (NNS) RNA genome (Davis et al., 2015).

The first historic phenotypical descriptions that can be attributed to rabies date back to ancient times. Already the Babylonian Talmud described a rabid dog astonishingly accurate and associates its bites with a fatal outcome for the victim: "Five things were mentioned in connection with a mad dog. Its mouth is open, its saliva dripping, its ears flap, its tail is hanging between its thighs, it walks on the edge of the road. Some say, Also it barks without its voice being heard.", "One whom it bites, dies."(*Mishna Yoma*, 83b and 84a) (Rosner, 1974; Rupprecht et al., 2002). Even though no clear concept of pathogens was available in these times, the correlation between human deaths and bites by apparently mad dogs was already correctly recognized. Due to the traces rabies left during the course of human history, it is easy to imagine that the disease had a significant cultural impact and influenced myths and fiction about creatures like vampires and werewolves considerably (Gomez-Alonso, 1998; Metzger, 2013).

It took a long time until microorganisms, such as viruses, were identified as the causing agents of infectious diseases. Before the breakthrough of microbiology, living things were thought to be spontaneously generated from inanimate material under the right circumstances, as it was suggested by the ancient Greek philosopher Aristotle. With the help of newly developed light microscopes, enabling a sufficient magnification, first microorganisms such as yeast were discovered in the nineteenth century. The famous work of the French chemist and microbiologist Louis Pasteur (Photography from around 1885 in Figure 1) demonstrated that fermentation cannot occur in extracts previously sterilized by heat, when atmospheric air is excluded, thus

falsifying the theory of “spontaneous generation” of life and underlining that fermentation is a process that relies on living organisms (Smith, 2012).

Many years later, Louis Pasteur successfully developed a vaccine against chicken cholera, a devastating livestock disease at his time. Pasteur achieved this by prolonged passaging of the causing bacterium *Pasteurella multocida*, leading to an attenuation of the pathogen. Animals treated with this vaccine survived the subsequent challenge with virulent cultures. This achievement of creating a protective vaccine by attenuation of a pathogen is considered to be the birth of the field of immunology. Later on, Louis Pasteur turned to the creation of a vaccine for rabies, in order to establish an interventional therapy for human use. Together with Emile Roux, Pasteur passaged rabies from infected dogs in rabbits, yielding a virulent, however “fixed” strain. The spinal cords of rabbits infected with this virus were dried by desiccation over 15 days, resulting in a loss of pathogenicity. This vaccine successfully protected dogs against inoculation with the highly pathogenic version of the virus. In July 1885, the vaccine was tested on the 9-year-old boy Joseph Meister, who had been previously bitten by a supposedly rabid dog. Pasteur treated the boy over several days, beginning with desiccated apathogenic spinal cord material and proceeding to increasingly less attenuated preparations. Although Pasteur finally inoculated the boy with fresh infectious spinal cord isolations, he survived, providing evidence for the efficacy of this method. Despite the problematic ethical considerations, this experiment paved the ground for the distribution of a protective vaccine against rabies virus, which saved thousands of people even in the following years of the nineteenth century (reviewed in Berche (2012) and Smith (2012)).

Figure 1: Louis Pasteur, around 1885. Picture adapted from Berche (2012).

Although a scientific explanation for rabies and other microbial diseases was only possible much later, the ancient observations of rabies being transmitted to humans by animal bites already correctly outlined the general concept of a zoonotic disease. Rabies virus is widely distributed all over the world due to its ability to infect a large variety of mammalian species, with members of the orders Carnivora and Chiroptera being its primary hosts (Rupprecht et al., 2002). Especially the high prevalence of rabies and other *Lyssaviruses* in different bat species makes it very hard to completely eradicate this disease, since in contrast to terrestrial mammals there are no

measures available for effective mass vaccination so far. Rabies transmitted by hematophagous vampire bats poses a re-emerging health threat for humans and livestock in Latin America, underlining the importance of *Lyssavirus* infected bats as zoonotic reservoir (Johnson et al., 2014). However, by far most human cases are associated with dog bites, especially in the less developed countries (Knobel et al., 2005). Confirmed human-to-human transmissions have only been reported after transplantation of organs from infected donors (Vora et al., 2013). Except for these extremely rare cases, rabies is a strictly zoonotic disease only transmitted to humans by exposure to infected animals.

Because rabies viral particles are enriched in saliva of the host in a later stage of infection, a bite by an infected animal easily brings contagious material in contact with subcutaneous tissue. After primary infection of muscle cells, the RABV particles gain access to primary motor neurons via neuromuscular junctions. Subsequently, by retrograde axonal transport and trans-synaptic neuron-to-neuron spread, RABV is distributed to the CNS of the host (Davis et al., 2015). The incubation time for human rabies is about 20-90 days, however rare cases have been reported showing symptoms not before one year or more after exposure. After initial, rather unspecific, flu-like symptoms, the disease progresses either to encephalitic or paralytic rabies, which differ in specific symptoms but equally end with coma and death of the patient. The encephalitic form of the disease is characterized by astonishing behavioral changes like generalized arousal, hyperexcitability and very frequently severe hydrophobia, which is a unique symptom of rabies. Enrichment of viral particles in saliva in combination with aggressive behavioral changes then provide ideal conditions for the virus to spread to a new host (Jackson, 2013).

Although a very efficacious post-exposure prophylaxis (PEP) consisting of extensive wound cleansing, passive immunization with rabies immune globulin (RIG) and active immunization using a tissue culture rabies vaccine is available (Manning et al., 2008), no effective treatment after onset of clinical signs could be established yet. At this point the timeframe for an effective PEP has expired and the disease exhibits an extreme case fatality rate of almost 100 %, designating rabies as one of the most lethal infectious diseases. Up to now there is only one report of a 15-year-old female who survived a rabies infection without any prophylactic treatment prior to development of clinical symptoms (Willoughby et al., 2005). Rabies mainly transmitted by dog bites is still responsible for approximately 55’000 human deaths worldwide, largely in the less developed regions of Africa and Asia, were many patients have no access to proper PEP (Knobel et al., 2005). Besides the lack of sufficient medical infrastructure, this is due to the relatively high cost and therefore limited availability of human rabies immune globulin (HRIG). Improved immune globulins of equine origin as well as the use of human monoclonal

antibodies might provide more cost effective alternatives in the future, increasing the accessibility to PEP (Smith et al., 2011).

With the lack of an effective treatment for the disease, the focus lies on prevention by human vaccination and control of rabies in domestic animals and the wildlife population. In addition to a reduction of potential animal vectors, mass vaccinations of terrestrial carnivores have been very successful. This was made possible with the development of several efficacious live virus based oral vaccines which can be distributed in baits even to remote areas by aircrafts. Oral vaccines used in the wildlife population encompass attenuated rabies virus strains such as SAD-B19, as well as recombinant viruses expressing the rabies virus glycoprotein based on vaccinia- or human adenovirus. Control tactics comprising this approach could significantly reduce rabies prevalence in wildlife animals in Europe and North America, also resulting in a decline of human cases. Thanks to these efforts, most regions in central Europe are nowadays considered free of rabies (Rosatte, 2013). In addition to the measures mentioned above, it is also important to raise the awareness for rabies in general and in particular for bat associated rabies among the general population, authorities and medical personnel. Exposure to infected bats still accounts for unnecessary human deaths when the risk of infection is not appropriately assessed and a potentially lifesaving PEP is not conducted in time (Harrist et al., 2016).

Moreover, despite many experimental therapeutic approaches, a rational therapy for rabies is still elusive. Also research focusing on novel antiviral drugs like inhibitory peptides or siRNAs could not yet be translated into any promising clinical applications (Smith et al., 2011). Therefore, rabies is still an important global health concern and additional basic research is essential to obtain new insights into rabies virus biology and pathogenesis which might lead the way to the development of new therapeutic strategies.

2.1.2. Organization of RABV particles

The virions of rabies virus (RABV) exhibit a bullet-like shape with a diameter of about 75 nm and a length of 100-175 nm (for schematic representation and EM picture see Figure 2). RABV has a relatively small, non-segmented, negative-sense RNA genome with a length of about 12 kb. Equal to other rhabdoviruses, the genome contains only 5 monocistronic genes that encode their corresponding viral structural proteins: the nucleoprotein (N), phosphoprotein (P), matrix protein (M), glycoprotein (G) and the RNA-dependent RNA polymerase L (large protein). This order (N-P-M-G-L) is highly conserved among the genomes of *Rhabdoviridae* and to a certain extend even among the *Mononegavirales*. N protein is 450 amino acids (aa) in size and tightly

associated with the viral genome. It could be shown to encapsidate the viral RNA by enwrapping up to 9 nucleotides (Iseni et al., 1998), thus shielding it from cellular proteins such as antiviral innate immune receptors (Albertini et al., 2006). Together with P and few copies of L, the packaged genome forms the ribonuclear protein (RNP).

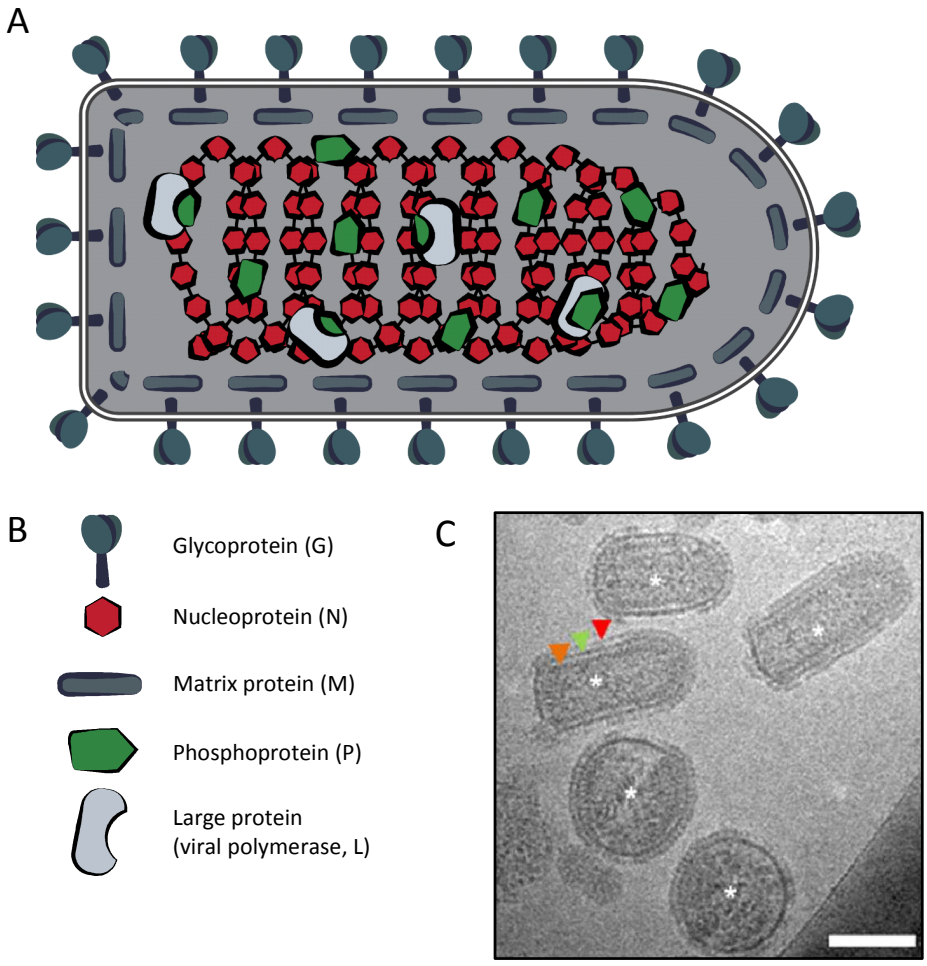

Figure 2: Organization of rabies virus particles.
A) Schematic illustration of a rabies virus virion with RNA genome, envelope and structural proteins. **B)** Legend for the viral proteins depicted in A). **C)** Rabies virus particles visualized by electron microscopy, "M/N-protein (orange arrow head), G-protein (red arrow head) and membrane (green arrow head) are clearly distinguishable." (Guichard et al., 2011).

Exclusively the RNP and not naked RNA can serve as a template for transcription and replication by the polymerase L (2130 aa), whereby P is required as essential cofactor. Inside the viral particle the RNP is condensed into a helical nucleocapsid, which is surrounded by a host cell derived lipid bilayer, exhibiting a bullet-like shape. This envelope contains the trimeric single-pass transmembrane protein G (505 aa), which consists of a glycosylated ectodomain on the outside of the viral particle and a cytoplasmic domain on the inside (Whitt et al., 1991). The G ectodomain is the only viral component that is on the outside of the particle and therefore

mediates tropism. M protein (202 aa) is associated with the membrane on the cytoplasmic side and connects the RNP with the viral envelope. It is a multifunctional protein that is the central factor driving assembly and budding of viral particles (Mebatsion et al., 1999; Okumura and Harty, 2011) and is also involved in the regulation of viral transcription and replication (Finke and Conzelmann, 2003) (organization of viral particle reviewed in Albertini et al. (2011)).

G and M have both been identified to play an important role in viral pathogenicity (Pulmanausahakul et al., 2008). Besides its function as cofactor for L, the phosphoprotein P (297 aa) is a highly versatile and multifunctional protein which is additionally involved in encapsidation of the viral genome and innate immune evasion (Mavrakis et al., 2004; Rieder and Conzelmann, 2009). Since the present thesis mainly focuses on this protein, RABV P will be discussed in more detail separately in 2.1.4.

2.1.3. Rabies virus life cycle

As obligate intracellular parasites, viruses have to infiltrate a host cell in order to replicate. A viral life cycle starts with the attachment of a viral particle to specific receptors on a target cell. The receptors implicated so far in attachment of RABV particles are neuronal cell adhesion molecule (NCAM), p75 neurotrophin receptor (p75NTR) and the nicotinic acetylcholine receptor (nAChR), while the latter is thought to be the primary receptor that mediates entry of the virus in peripheral muscle tissue (Lafon, 2005). After attachment to the extracellular target structure, RABV virions enter the host cell via receptor mediated endocytosis. Increasing acidification of the endosome finally triggers G protein mediated membrane fusion and release of the RNP into the cytosol of the host cell (Gaudin, 2000; Roche and Gaudin, 2004).

With the RNP released into the cytoplasm, including copies of the RNA-dependent RNA-polymerase L and its cofactor P, all requirements are met for the start of an infectious cycle. The viral genome exhibits a negative sense orientation, therefore transcription of viral mRNAs by the L-P polymerase complex is an essential prerequisite for viral gene expression. Viral transcription strictly relies on N encapsidated genomes as template. In addition to the five genes N, P, M, G and L, the viral genome exhibits a 3'-leader and a 5'-trailer sequence, which act as crucial signals in transcription and replication. The 5' end of the viral RNA exhibits a triphosphate modification (genome organization see Figure 3A). The genes of rabies virus are separated by non-coding, intergenic regions (IGRs). Before each IGR, a transcription termination and polyadenylation signal (TTP) mediates transcription stop and polyadenylation of the corresponding mRNA. Downstream of an IGR, a transcription initiation signal (TIS) is located, which allows for

reinitiation of transcription of the following gene. Transcription starts at the 3’ end with generation of the non-coding 5’-triphosphate containing leader-RNA, followed by transcription of the capped and polyadenylated mRNAs of N, P, M, G and L. The viral mRNAs resemble normal cellular mRNAs and are likewise translated by the ribosomes of the host cell.

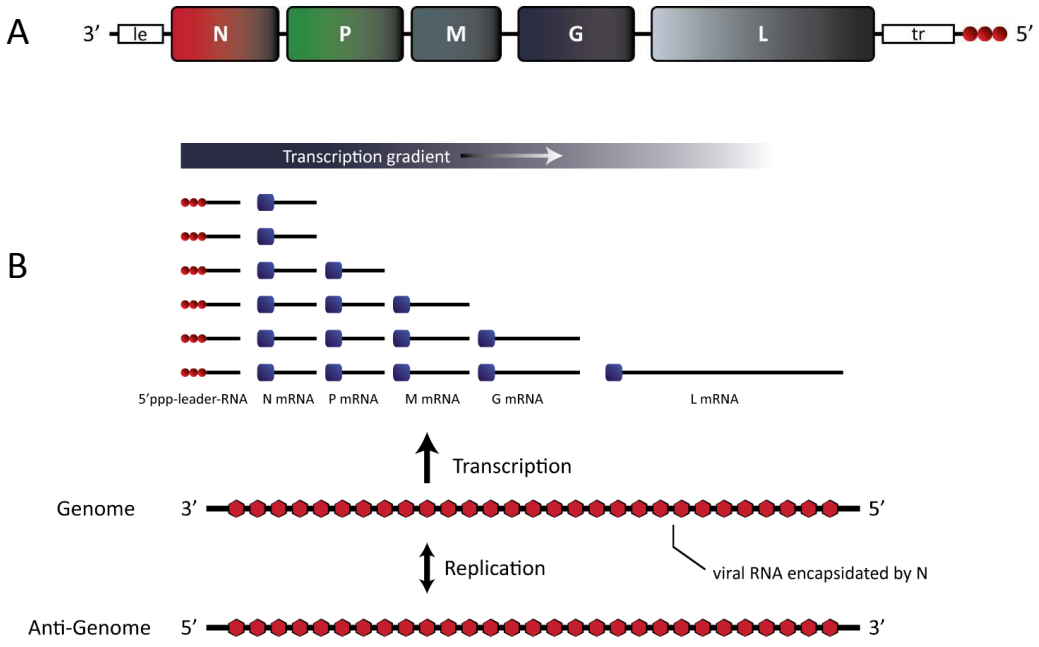

Figure 3: Rabies virus genome organization and transcriptional gradient.
A) Graphical representations of rabies virus genome with the five viral genes N, P, M, G and L. The genome exhibits a 3’ leader and a 5’ trailer sequence, which are essential for initiating transcription and replication. A triphosphate modification is attached to the 5’ end of the genome (5’-ppp). **B)** Transcription starts at the 3’ end of the genome and results in generation of a 5’-ppp containing leader RNA and the capped and polyadenylated N mRNA. After each viral gene, transcription stops and reinitiates with a certain chance, resulting in a transcriptional gradient.

Transcription is terminated after each gene at the TTP and has a certain change to reinitiate at the following TIS. This mechanism leads to a reduced abundance of transcripts with increased distance of the corresponding gene to the 3’ end of the viral genome (Figure 3B). This transcriptional gradient is a typical feature of NNS RNA viruses. However, it is significantly steeper in the case of rabies virus compared to VSV. This is mainly due to the attenuated IGRs in rabies virus, which are much longer than the GA dinucleotides found in VSV, leading most likely to a notable reduction in expression of the L gene (Finke et al., 2000; Rose, 1980). How exactly the polymerase complex gets access to the encapsidated genome and starts transcription is poorly understood. For VSV, it has been suggested that transcription is not limited to begin at the 3’ end but is also able to directly start with N transcription (Whelan and Wertz, 2002) (For review of viral transcription see Albertini et al. (2011)).

How the switch from transcription, which is interrupted at junctions between genes, to full read-through replication is regulated in NNS RNA viruses could not be fully determined yet. In

general, most insights about molecular aspects of the viral life cycle of *Rhabdoviridae* have been obtained by studying VSV. Replication encompasses generation of an anti-genome intermediate, which serves as template for new viral genomes (Figure 3B). The 3' leader sequence acts as promoter to start transcription or replication, while the 3' end of the anti-genome, consisting of the complementary sequence of the 5' trailer of the genome, promotes mainly read-through replication. This process is asymmetric, since much more genomes than anti-genomes are created by the polymerase complex, indicating a higher replicative activity of the 3' promoter of the anti-genome. For rabies virus infected cells, the ratio of genome to anti-genome has been reported to be even as high as 49:1 (Finke and Conzelmann, 1997). The nucleoprotein is essential in viral replication and its abundance is supposed to play a role in the transition from transcription in the early stage of infection to replication later on and in the processivity of replicative RNP synthesis. According to the widely accepted model of replication of NNS RNA viruses, RNA transcription starts at the 3' end of the genome and the leader sequence can be co-transcriptionally encapsidated as soon as a sufficient amount of N is present in the host cell. The discovery of encapsidated leader RNA in VSV infected cells provided some evidence for this hypothesis (Blumberg and Kolakofsky, 1981). If the growing transcript is enwrapped rapidly enough, the polymerase complex switches to replication mode, ignores TTP and TIS sequences, and thus generates full length read-through anti-genome products which can in turn serve as templates for generation of new genome copies (reviewed in Whelan et al. (2004)). In addition to this mechanism depending on N concentration, M protein of SAD-L16 strain rabies virus has been shown to down-regulate mRNA synthesis and promote viral replication (Finke and Conzelmann, 2003; Finke et al., 2003).

The whole process of viral RNA synthesis is not taking place arbitrarily distributed throughout the cytoplasm of the host cell. Recently, the so called "Negri bodies" could be identified as the site of viral transcription and replication (Lahaye et al., 2009). These cytoplasmic inclusion bodies were named after Adelchi Negri, who discovered this diagnostic marker in 1903 as spherical structures in histological sections of infected nervous tissue. Concurrently, the viral proteins N, P and L mainly co-localize in these typical structures, together with viral nucleic acids and host cell factors like HSP70, DLC8 (dynein light chain LC8-type 1) and TLR3 (toll-like receptor 3) (Finke et al., 2004; Lahaye et al., 2009; Menager et al., 2009).

In the late stage of infection, ongoing viral replication results in the assembly of new viral nucleocapsids and budding of viral particles. This process relies on the insertion of the transmembrane protein G into the membrane of the host cell and the matrix protein M, which is the main driver of budding (Mebatsion et al., 1996; Mebatsion et al., 1999). Even though G is

supposed to have rather a supportive function in budding, both proteins cooperatively contribute to the budding process by interactions between M and the cytoplasmatic tail of G (Mebatsion et al., 1999; Okumura and Harty, 2011).

2.1.4. Rabies virus phosphoprotein

The limited coding capacity of small RNA viruses lead to the evolution of highly multifunctional proteins, which are able to fulfill a variety of tasks. The rabies virus phosphoprotein P (RABV P) exhibits numerous interactions with viral as well as host cell proteins and orchestrates many crucial aspects of the viral life cycle, making it a central "hub" protein for RABV.

Several serine phosphorylations are a common feature of the P proteins of NNS RNA virus, what is the reason for the designation as "phosphoprotein". RABV P is phosphorylated at the N-terminus at Ser63/Ser64 by a unknown kinase, whereas several C-terminal phosphorylations (serine residues 162/219/271) are mediated by protein kinase C (PKC) (Gupta et al., 2000). The phosphorylated moieties at the C-terminus have been reported to modulate the trafficking behavior of RABV P between nucleus and cytosol (Moseley et al., 2007). However, no clear essential function for the viral life cycle could be attributed yet to RABV P phosphorylation (Gigant et al., 2000). In contrast, phosphorylation of the P protein of vesicular stomatitis virus (VSV), another member of the *Rhabdoviridae* family, was shown to be essential for growth of this virus (Das and Pattnaik, 2004).

RABV P is a rather small protein of 297 amino acids length and a molecular mass of about 33 kDa. Due to its various phosphorylations, P has an apparent size of 37 kDa in SDS-PAGE gels. RABV P is organized in distinct structured domains that are connected by intrinsically disordered regions (Figure 4A). This organization and the ability to form homo-oligomers, as well as functions in the viral life cycle, are shared among phosphoproteins of the *Mononegavirales*, however no sequence similarities can be found in sequence alignments (Gerard et al., 2009). The intrinsically disordered regions are very susceptible to proteolysis, therefore only structural data of the proteolysis resistant central domain (CED) (Ivanov et al., 2010) and C-terminal domain (CTD) (Mavrakis et al., 2004) could be determined by x-ray crystallography.

The structured central domain of RABV P mediates dimerization (Jacob et al., 2001) and consists of two α-helices connected by a short loop (residues 92 to 131), forming a charged and a hydrophobic surface, while the latter forms the dimer interface (Gerard et al., 2009; Ivanov et al., 2010). Using this hydrophobic interface, the monomers form a face-to-face interaction and

cross with an angle of about 46° (Ivanov et al., 2010). The dimerization domain was shown to be dispensable for transcriptional activity in minigenome assays (Jacob et al., 2001).

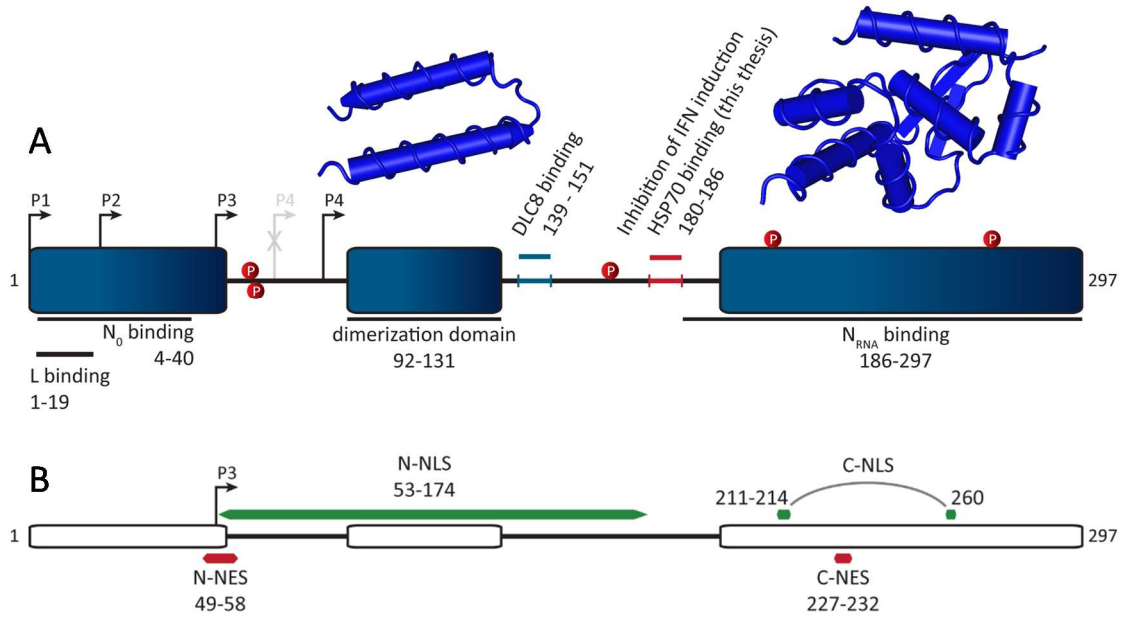

Figure 4: Domain organization and trafficking signals of the rabies virus phosphoprotein.
A) RABV P consists of structured domains which are connected by intrinsically disordered regions. It is a central "hub" protein for the virus, since it is essential in many aspects of the viral life cycle. Together with L, it forms the viral polymerase complex and links it to the RNP with its N_{RNA} binding region. RABV P keeps newly synthesized N (N_0) free from cellular RNAs, in order to ensure correct enwrapping of viral genomes and antigenomes. A self-association domain mediates dimerization of the protein. In addition, RABV P is associated with host cell factors like DLC8. In this thesis, a region previously identified as essential for inhibition of RIG-I mediated IFN induction will be characterized as binding motif for HSP70 family members. Structural data available for the dimerization domain (PDB ID 3L32) and C-terminal domain (PDB ID 3OA1) were visualized with Cn3D software by NCBI **B)** Overview over the RABV P trafficking signals. In full length P, a strong N-terminal NES dominates and causes a mainly cytoplasmic localization. In N-terminally truncated P isoforms the N-NES can be absent, leading to enhanced nuclear localization by the N-NLS (reported for CVS-strain P) and C-NLS. Additionally a C-NES, which is regulated by phosphorylation, affects the subcellular distribution.

Full length RABV P (P_1) exhibits a size of 297 amino acids, but several additional N-terminally truncated versions of the protein are expressed, due to leaky scanning of the ribosome on the P mRNA, resulting in translation start on alternative downstream in-frame start codons. This generates shorter P versions starting at amino acid positions 20 (P_2), 53 (P_3), 69 (P_4) and 83 (P_5) in the CVS strain P, which can also be found in virions (Chenik et al., 1995). Whereas P_{1-3} are conserved, the start codon at position 69 is missing in the SAD-L16 strain of rabies virus, which is mainly used in this project. Therefore, SAD-L16-P_4 is referring to P versions starting at residue 83 in this thesis. Although alternative start codons are well conserved among the *Lyssavirus* genus, successful rescue of a recombinant SAD-L16 virus containing eGFP-P (Finke et al., 2004) or P with deleted P_2/P_3/P_4 start codons (Brzózka et al., 2005), which are unable to produce shortened P isoforms, indicates that these variants are not essential for the viral life cycle.

RABV P isoforms exhibit differential subcellular localization, due to a strong CRM1-dependent N-terminal nuclear export signal (NES), which is only present in P_1 and P_2 and mediates cytoplasmic localization (Chenik et al., 1995; Pasdeloup et al., 2005) (overview over trafficking signals of RABV P in Figure 4B). Mutations which render this NES non-functional have been associated with a loss of pathogenicity and impaired inhibition of IFN-signaling in the attenuated Nishigahara-CE strain (Ito et al., 2010). In P_3, this NES is truncated and non-functional. This leads to a strong nuclear localization mediated by nuclear localization signal (NLS) within the C-terminal domain (Pasdeloup et al., 2005) and for P_3 of CVS strain by an additional N-terminal NLS, which localizes to residues 53-174 and only gets active upon truncation of the N-terminal 52 amino acids (Oksayan et al., 2012). The C-terminal NLS activity strictly requires the moieties lysine 214 and arginine 260, which are in close proximity within the tertiary structure and form a positively charged stretch, constituting a conformational NLS (Mavrakis et al., 2004; Pasdeloup et al., 2005). Additionally, the C-terminal domain was reported to contain another NES, which partly overlaps with the CT-NLS and is regulated by PKC mediated phosphorylation of an adjacent residue (Moseley et al., 2007).

The N-terminal truncation in the shorter isoforms also impairs other functions of the corresponding P products. The P proteins of the *Rhabdoviridae* are essential non-catalytic cofactors for the viral RNA-dependent RNA polymerase L (Emerson and Wagner, 1972; Emerson and Yu, 1975). In the case of RABV, the first 19 amino acids of the phosphoprotein are essential and sufficient to mediate association with the C-terminal domain of L (Chenik et al., 1998). Therefore, only the full length P_1 form is able to act as a cofactor for the viral polymerase.

RABV P also exhibits two distinct binding sites for the N protein, which are localized to the N- and C-terminus respectively (Chenik et al., 1994; Fu et al., 1994). Co-expression of both N and P protein is sufficient to induce the formation of intracellular inclusions similar to Negri-Bodies, which contain associated N and P proteins in a ratio 1:2 (Chenik et al., 1994; Mavrakis et al., 2003). In the absence of P, the RABV N protein forms stable complexes with endogenous cellular RNAs, which exhibit a morphology and N:RNA stoichiometry similar to viral nucleocapsids (Iseni et al., 1998). For *Sendai virus* and VSV, the P protein was shown to bind newly synthesized N (N_0) with its N-terminal domain, in order to prevent unspecific association of N with cellular RNAs (Curran et al., 1995; Masters and Banerjee, 1988), defining P as a molecular chaperone for N in regard to the encapsidation of viral RNAs. For rabies virus, this ability to associate with N_0 was localized to P residues 4-40, which are predicted to form a conserved negatively charged α-helix (Mavrakis et al., 2006). Mavrakis et al. (2006) speculated that this domain mimics the negative charge of the RNA backbone and thus interacts with the RNA association domain of N. Since N_0

and L binding sites partially overlap, these two functions are thought to be mutually exclusive (Mavrakis et al., 2006).

The C-terminal domain of RABV P (aa 186-297) mediates binding to N_{RNA} complexes, thereby linking the viral polymerase to its template using the N-terminal L binding site (Chenik et al., 1998; Mavrakis et al., 2004; Mellon and Emerson, 1978).

Besides self-association and interactions with other viral proteins, RABV P interacts with several host-cell factors. *Lyssavirus* P proteins exhibit a strong and conserved binding site for cytoplasmic dynein light chain LC8-type 1 (DLC8) which could be mapped to the central part of RABV P adjacent to the dimerization domain (Jacob et al., 2000; Raux et al., 2000). Further studies could localize the binding motif precisely to the RABV P region 139-151 and showed an essential contribution of the residues D143 and Q147 (Poisson et al., 2001). Although this motif was initially assumed to be involved in axonal transport of rabies virus (Rasalingam et al., 2005), another study suggested that DLC8 binding by P is rather important for efficient transcription and replication of RABV in neurons (Tan et al., 2007). Further, the C-terminal domain of RABV P has been reported to associate with the promyelocytic leukemia (PML/TRIM19) protein and sequester PML in the cytoplasm (Blondel et al., 2002), while overexpression of the PML-IV isoform was shown to suppress transcription and replication of the CVS strain of RABV (Blondel et al., 2010). Recently, the focal adhesion kinase (FAK) was reported to be involved in viral RNA replication by association with RABV P (Fouquet et al., 2015). Moreover, RABV P of the CVS strain interacts with the mitochondrial complex I, resulting in mitochondrial dysfunction and oxidative stress (Alandijany et al., 2013; Kammouni et al., 2015). These studies suggest that the generation of reactive oxygen species (ROS) and malfunction of mitochondria contribute to virus-induced neuronal pathogenesis.

In addition to the different functions in the viral life cycle, RABV P is a very potent interferon antagonist, which circumvents the cellular innate immune response and thus helps the virus to evade the host's immune system. This is important for the establishment of a viral infection, since cytosolic 5'-triphosphate RNAs of viral origin are readily recognized by RIG-I-like receptors (RLR), resulting in the induction of type I interferon genes (Yoneyama et al., 2004). *In vitro* transcribed RNA corresponding to the RABV leader sequence, RNA isolated from viral particles and synthetic 5'-ppp RNAs containing the sequence of the complementary panhandle genome ends of rabies virus have been reported as potential triggers for RIG-I (Hornung et al., 2006; Schlee et al., 2009). Intriguingly, the P protein is able to interfere with innate immune signaling on two distinct levels.

First, RABV P is able to prevent transcription of type I interferon genes by blocking phosphorylation of the crucial interferon transcription factor IRF3 by the kinases TBK1 and IKKε (Brzózka et al., 2005). This was initially demonstrated by the generation of recombinant viruses with attenuated production of P, which induced high amounts of IFN. Further, *in vitro* assays employing ectopic expression of the phosphoprotein clearly identified it as a very potent antagonist of IFN induction (Brzózka et al., 2005; Marschalek et al., 2009). The suppression of IRF3 phosphorylation and nuclear accumulation is strictly dependent on the P region 176-186, which is absent in the PΔInd1/2 mutant that was characterized by previous work in this group (Rieder et al., 2011). Mutant viruses with deletions in this region of the P protein exhibited reduced mortality when injected intracerebrally into mice, indicating an involvement of inhibition of IFN-induction in viral pathogenicity. However, the nature of the inhibitory mechanism and why this region is essential for preventing interferon induction remained enigmatic. To clarify this issue and to identify potential molecular binding partners associated with this P region is a major goal of the current thesis.

Second, in addition to interfering with induction of interferons, RABV P also blocks interferon signaling. Normally, secreted type I interferons initiate downstream signaling by an interaction with the heterodimeric IFNAR receptor (IFNAR1 and IFNAR2), in an autocrine and paracrine fashion. Activation of the IFNAR receptor leads to phosphorylation of intracellular residues by the Janus kinases (JAKs) JAK1 and TYK2, resulting in recruitment of signal transducer and activator of transcription (STAT) 1 and STAT2. Subsequently, the STATs get phosphorylated at their tyrosine residues Y701 and Y689 by the active JAKs, which are still bound to the cytosolic components of the IFNAR receptor. Phosphorylation of STATs leads to their hetero-dimerization and nuclear translocation, where they induce the transcription of interferon-stimulated genes (ISGs) by binding to interferon-stimulated response elements (ISREs) in their promoter regions (Platanias, 2005). This process is abrogated by RABV P by binding specifically to activated STATs, thereby preventing their nuclear accumulation and transcriptional activity (Brzózka et al., 2006). This effect strictly requires the CTD of RABV P and truncation of the 10 C-terminal residues abrogates the interaction with STATs (Brzózka et al., 2006; Vidy et al., 2005). In addition to the prevention of nuclear localization of STATs, the nuclear P isoform P_3 was reported to interfere with transcriptional activity by suppressing the binding of STAT1 to target DNA sequences in the nucleus (Vidy et al., 2007). This would delineate an alternative inhibitory mechanism for repression of ISG induction by RABV P. STAT-inhibition deficient RABV was shown to be highly susceptible to IFN-treatment, while displaying significantly reduced pathogenicity in mice after intracerebral inoculation (Ito et al., 2010; Wiltzer et al., 2014). Taken together, the control of an

innate immune response on the levels of interferon induction and signaling by RABV P are both important determinants for viral pathogenicity (Immune evasion by RABV P reviewed in Rieder and Conzelmann (2011)).

As shown above, RABV P is a prime example for the highly multifunctional proteins typically found in small RNA viruses. This illustrates how RNA viruses were forced by the limited coding capacity of their genomes to develop extremely efficient proteins capable of carrying out various tasks which are essential for the viral life cycle in many aspects.

2.2. Innate immunity

The cells of our body are under a permanent threat by a magnitude of different invading pathogens from bacteria, fungi, and protozoa to viruses. During the course of evolution, the development of several countermeasures to deleterious pathogens was crucial. The innate immune system is the first line of defense and is able to detect special molecular characteristics that are primarily associated with pathogens, since they are normally not present inside a healthy eukaryotic cell or in its extracellular environment. These specific molecular markers, which have been defined as pathogen-associated molecular pattern (PAMPs), are therefore used by our cells to discriminate between harmless self and potentially deleterious non-self structures (Janeway and Medzhitov, 2002). Since not only pathogens but also commensal microorganisms may display structures which are detected by our cells, the alternative term microbe-associated molecular pattern (MAMPs) has been suggested (Didierlaurent et al., 2005).

This is achieved by several pattern recognition receptors (PRRs), which specifically detect their targets and act as cellular sensors for PAMPs. Foreign nucleic acids are prominent ligands that indicate a threat to the cellular genomic integrity and can be recognized by members of the Toll-like receptor (TLR) and RIG-I-like receptor (RLR) family (Kawai and Akira, 2008). TLRs are a family of transmembrane PRRs which localize to the endolysosomal compartment and detect bacterial GpC motif containing DNA (TLR9, Krieg et al. (1995), Hemmi et al. (2000)), double strand (ds)RNA (TLR3, Alexopoulou et al. (2001)) and single strand (ss)RNA (TLR7/8, Heil et al. (2004)). Whereas the TLRs recognize their ligands mostly in endosomes, the RIG-I-like receptors retinoic acid-inducible gene I (RIG-I), melanoma-differentiation-associated factor 5 (MDA5) and laboratory of genetics and physiology 2 (LGP2) detect dsRNAs in the cytosol (Loo and Gale, 2011). The recognition of non-self virus-derived nucleic acids in the cytosol by RLRs and in endosomes by TLR3/7/8 is central in the response to infections with RNA viruses. Depending on the activated receptors, different signaling cascades are initiated. Although distinct pathways are triggered by

their respective PRRs, they merge in the production of type I interferons and inflammatory cytokines. These signaling molecules elicit a broad anti-microbial cellular immune response through the induction of a multitude of interferon-stimulated genes (ISGs), such as Mx proteins, protein kinase R (PKR), 2'-5'-oligoadenylate synthase (2'-5'-OAS) and RNaseL (Haller et al., 2007). Additionally, IFNs contribute to activation of the pathogen specific adaptive immune system, for instance by facilitating a CD8+ T-cell response (Goodbourn et al., 2000; Kolumam et al., 2005).

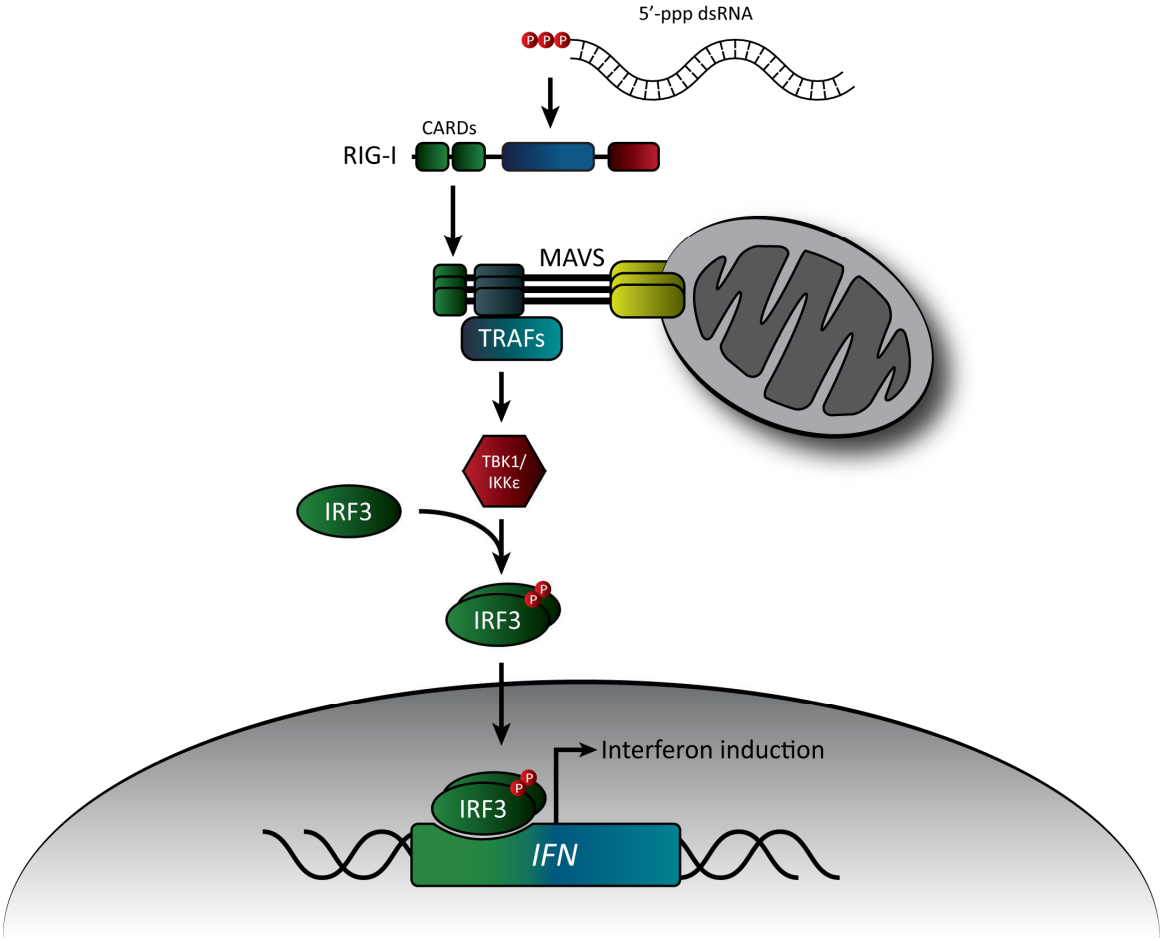

Figure 5: Interferon induction upon activation of RIG-I signaling.
Virus derived 5'-triphosphate (5'-ppp) dsRNA products are able to bind the helicase domain of RIG-I and mediate downstream signaling to MAVS in an ATP-dependent fashion (Loo and Gale, 2011). MAVS is a mitochondrial signaling platform and functions as an adaptor for numerous proteins involved in regulating IFN-induction. In concert with TRAFs and other adaptor proteins, MAVS activates TBK1/IKKε, leading to the phosphorylation of IRF3 (Belgnaoui et al., 2011). IRF3 dimerizes and translocates to the nucleus, were it activates transcription of type I interferon genes, together with NF-κB and ATF2/C-Jun (Hiscott, 2007).

RLRs recognize a present RNA virus infection and mediate downstream signaling to the mitochondrial antiviral-signaling protein (MAVS) after binding to certain virus-derived dsRNA species (Figure 5). MAVS is anchored to outer mitochondrial and to some extend peroxisomal membranes and acts as a signaling platform that accumulates further regulatory adaptor

proteins and initiates activation of TBK1 and IKKε (Dixit et al., 2010; Loo and Gale, 2011; Seth et al., 2005). These effector kinases mediate the phosphorylation and consequently nuclear translocation of interferon regulatory factor 3 (IRF3), which is the central transcription factor of type I interferon genes (Hiscott, 2007).

Upon transcription and secretion of IFN and other pro-inflammatory cytokines, the activated cell itself and other cells in proximity enter an antiviral state in an auto- and paracrine fashion, respectively, characterized by the expression of interferon-stimulated genes (ISGs) via JAK-STAT signaling (Goodbourn et al., 2000). A more precise overview about the molecular mechanisms of the signaling cascade leading to induction of interferons after RLR activation by virus derived ligands is given below, including novel insights reported in the recent years.

2.2.1. RLR recognition of viral nucleic acids

Whereas professional interferon producing cells like plasmacytoid dendritic cells (pDCs) rather use the TLR-system for viral detection, RIG-I-like receptors (RLRs) are crucial for the induction of type I interferons in conventional DCs (cDCs) and fibroblasts (Kato et al., 2005). The DExD/H box RNA helicase RIG-I is the prototypic member of the RLR family and was the first cytosolic receptor identified to trigger a dsRNA dependent antiviral response by mediating activation of NF-κB and IRF3 (Yoneyama et al., 2004). RIG-I exhibits two caspase recruitment domains (CARDs) at its N-terminus, which are essential and sufficient to mediate signaling and a central helicase domain with intact ATPase activity (Yoneyama et al., 2004). MDA5 and LGP2 are the other two RIG-I related proteins found in humans. MDA5 shares the domain organization including the tandem CARD repeat with RIG-I and is a similar positive regulator of antiviral signaling (Yoneyama et al., 2005). In contrast, LGP2 completely lacks any CARD domains and has been characterized as a negative modulator of IFN-induction after viral infection (Rothenfusser et al., 2005; Yoneyama et al., 2005) (overview RLR domain structure see Figure 6).

Both RIG-I and MDA5 respond to dsRNA depending on their ATPase activity. Whereas the tandem CARDs of both proteins are sufficient and essential for signaling, only RIG-I mutants lacking the CARD domains or ATPase activity exhibit a dominant negative inhibition of antiviral signaling (Yoneyama et al., 2005; Yoneyama et al., 2004). Both CARD domains within the tandem repeat are essential for mediating downstream signaling and binding to MAVS (mitochondrial antiviral-signaling protein), the mitochondria-associated signaling platform downstream of RLRs (Saito et al., 2007; Seth et al., 2005). RIG-I and LGP2 both contain a C-terminal repressor domain (RD) that prevents signaling of the CARDs in absence of a ligand. The RD of LGP2 is even able to

suppress RIG-I signaling when co-expressed *in trans*. Removal of this regulatory domain renders RIG-I constitutively active (Saito et al., 2007).

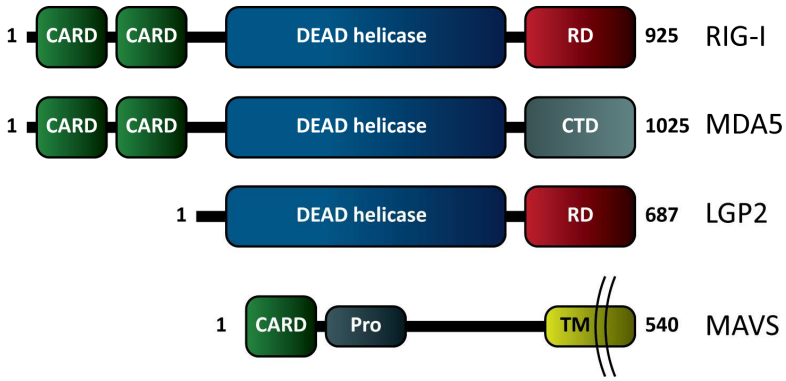

Figure 6: Schematic representation of the RLRs and their adaptor protein MAVS.
Schematic representation of RLR and MAVS structural domains involved in antiviral signaling. RIG-I and MDA5 exhibit N-terminal tandem CARD domains, which are essential and sufficient to mediate downstream signaling by interacting with the homologous CARD domain of MAVS. The helicase domains bind dsRNA and mediate signaling in an ATP dependent way. LGP2 lacks any CARD domains and is a negative modulator of RLR signaling. RIG-I and LGP2, but not MDA5, contain a repressor domain at the C-terminal region, which blocks signaling in absence of a ligand (Loo and Gale, 2011). MAVS is a mitochondria-associated protein that contains an integral membrane anchor at its C-terminus. Adjacent to the N-terminal CARD domain, a proline rich motif regulates interactions with various regulatory proteins that enhance or modulate further downstream signaling (Belgnaoui et al., 2011).

Even though RIG-I and MDA5 seem very similar in their domain organization and downstream signaling, they detect an almost non-redundant set of distinct viral pathogens. Whereas MDA5 is essential for recognizing members of the *Picornaviridae* family such as EMCV (Gitlin et al., 2006; Kato et al., 2006), RIG-I detects a broader range of RNA viruses encompassing among others the *Rhabdoviridae* VSV and rabies virus (Hornung et al., 2006; Kato et al., 2005; Yoneyama et al., 2005), as well as members of the *Orthomyxo*- (Influenza A/B) and *Paramyxoviridae* (Sendai virus, measles) families (Kato et al., 2005; Kato et al., 2006; Loo et al., 2008; Plumet et al., 2007; Yoneyama et al., 2005). A simultaneous contribution to antiviral signaling of both RIG-I and MDA5 could only be shown for infections with members of the *Flaviviridae* and *Reoviridae* (Kato et al. (2006); Kato et al. (2008); Loo et al. (2008); for review see Loo and Gale (2011)).

In the last decade, a lot of effort was put into the characterization of the RNA ligands responsible for triggering RIG-I and MDA5. Some aspects of this topic have been quite controversial, since some of the findings were contradictory to some degree. Although RIG-I was at first described as a cytosolic receptor that detects RNA viruses and is able to bind to the synthetic dsRNA analog poly I:C (Yoneyama et al., 2004), studies employing mice deficient in different RLRs could show that poly I:C is recognized by MDA5 but not RIG-I (Gitlin et al., 2006; Kato et al., 2006). Kato et al. (2008) could demonstrate later that poly I:C shortened by RNase III treatment was a ligand for

RIG-I, but no longer for MDA5. This provided some evidence that the differential dsRNA sensing of RIG-I and MDA5 might be length dependent. In other independent studies, the presence of a triphosphate group at the 5' end (5'-ppp) of different short *in vitro* transcribed RNA species was shown to be essential for detection of both ssRNA and dsRNA by RIG-I (Hornung et al., 2006; Pichlmair et al., 2006). The apparent absence of dsRNA in cells infected with influenza A virus (Weber et al., 2006), an infection that is detected by RIG-I (Kato et al., 2006), hinted at a role for 5'-ppp ssRNA as a ligand. This was strictly dependent on the 5'-ppp-structure, since phosphatase treatment abrogated the antiviral response to influenza A viral RNA (vRNA) purified from virions (Pichlmair et al., 2006). Concomitantly, Kato et al. (2008) reported that total RNA isolated from influenza A infected cells almost completely lost stimulatory capacity upon phosphatase treatment. In contrast, RNA isolates derived from VSV infected cells exhibited only a moderate reduction in their capacity to induce IFNs after phosphatase treatment, providing some evidence for the ability of certain dsRNA species to induce RLR signaling independent of a 5'-ppp structure. Concomitantly, chemically synthesized 70 bp dsRNA with a 5' hydroxyl end were shown to induce IFN-β to a comparable low, however significant level, strictly depending on RIG-I (Kato et al., 2008). Furthermore, Saito et al. (2008) reported that a 5'-ppp is an essential prerequisite but not alone sufficient for detection of *in vitro* transcribed ssRNA and that a poly-U/UC rich RNA in the 3' non-coding region of the hepatitis C virus genome is triggering RIG-I signaling upon infection with this RNA virus. Later work by Schlee et al. (2009) seriously challenged former findings that 5'-ppp-ssRNA can be considered a RIG-I ligand by introducing completely chemically synthesized and thus very precisely characterized 5'-ppp RNAs. The authors reported that synthetic 5'-ppp-ssRNAs are in contrast to the corresponding RNAs generated by *in vitro* transcription not a trigger of antiviral signaling. Addition of a fully synthetic complementary single strand fully restored the stimulatory capacity. This at first seemingly contradictory finding was explained with the inherent property of the T7 polymerase, which is frequently used for *in vitro* transcription, to readily create self-coded 3' end prolongations with complementarity to the correct transcript, thus creating in fact partly dsRNA species (Triana-Alonso et al., 1995). Using clearly defined chemically synthesized 5'-ppp-dsRNAs, it could further be shown that efficient recognition of dsRNAs by RIG-I requires blunt ends, while 3'-overlaps are tolerated to some degree, in contrast to 5'-overhangs which abrogate recognition (Schlee et al., 2009). In summary, according to the current literature, the ideal RIG-I ligand is a short, blunt end 5'-triphosphate or 5'-diphosphate dsRNA lacking 2'-O-methylation of the first nucleotide (Schuberth-Wagner et al., 2015), although it is acknowledged that longer dsRNAs without 5'-ppp might also trigger signaling, however much less efficiently (for review see Schlee and Hartmann

(2010) and Roers et al. (2016)). Apart from *in vitro* transcribed or synthetic RNAs, complete RNA virus nucleocapsids containing 5'-ppp dsRNA "panhandle" structures are able to elicit RIG-I signaling (Weber et al., 2013). Moreover, in addition to its signaling functions, RIG-I was recently shown to have certain antiviral effector functions itself, possibly by displacement of viral proteins from dsRNA (Chan and Gack, 2015; Sato et al., 2015; Yao et al., 2015).

Even when the correct ligand is bound to RIG-I and the tandem CARD (2CARD) domains are released from the auto-inhibitory repressor domain (Saito et al., 2007), further downstream signaling is tightly controlled and modulated by several proteins and post-translational modifications, in order to prevent erroneous and potential deleterious IFN-induction. RIG-I signaling is positively regulated by K63-polyubiquitination of Lys172 mediated by the RING-finger E3 ubiquitin ligase TRIM25 (Gack et al., 2007) and negatively regulated by a phosphorylation at Thr170, which antagonizes ubiquitination at Lys172 (Nistal-Villan et al., 2010). Blockage of TRIM25-mediated polyubiquitination of RIG-I is a viral immune evasion strategy employed by the influenza A virus protein NS1 (Gack et al., 2009). Moreover, also non-covalently bound K63-polyubiquitin chains were reported to facilitate RIG-I signaling by inducing the formation of tandem CARD oligomers (Jiang et al., 2012; Zeng et al., 2010). Abnormal signaling by an ATPase deficient RIG-I mutant, the cause of atypical Singleton-Merten syndrome, was recently shown to signal constitutively through endogenous RNAs, emphasizing the importance of correct discrimination between self and non-self structures (Jang et al., 2015; Lassig et al., 2015).

In addition to a further characterization of the ligands for RIG-I, also many new insights about how RIG-I mediates downstream signaling to MAVS have been reported in the recent years. *In vitro* studies could reveal that RIG-I binds to 5'-ppp dsRNA ends and subsequently forms elongated filaments as it moves along the dsRNA from the ends to the interior of the molecule in an ATP-dependent manner. Thereby, using the RNA as a scaffold, multiple RIG-I tandem CARD domains are brought in close proximity resulting in the K63-ubiquitin independent formation of CARD oligomers. Induced proximity is sufficient for the formation of 2CARD oligomers, which are able to induce unidirectional polymerization of the homologous MAVS CARDs as visualized by electron microscopy (Peisley et al., 2013).

According to this proposed model, RIG-I and MDA5 mediate downstream signaling to MAVS by inducing prion-like polymer formation of homologous MAVS CARD domains (Hou et al., 2011; Peisley et al., 2013; Wu et al., 2013), as depicted in Figure 7. In contrast, oligomerization of isolated CARDs strictly requires binding of K63-polyubiquitin chains in an *in vitro* reconstituted signaling system (Jiang et al., 2012; Zeng et al., 2010). A crystal structure of RIG-I CARD oligomers

in complex with K63-Ub_2 could recently be determined, revealing a tetrameric architecture of four 2CARDs with three bound K63-Ub_2 molecules exhibiting a helical "lock-washer" structure (Peisley et al., 2014).

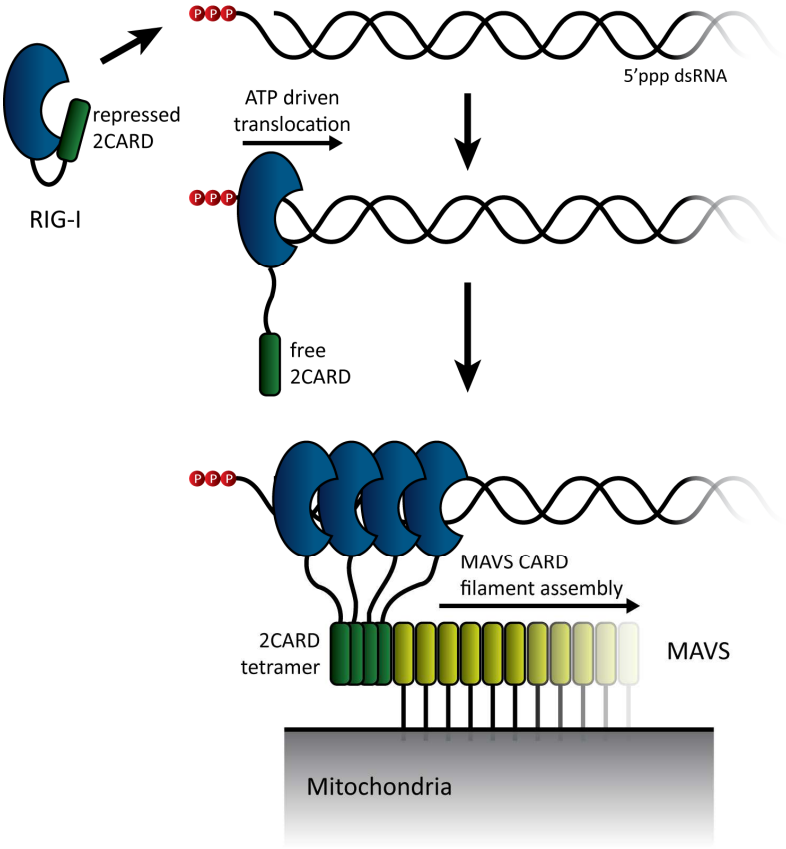

Figure 7: Model of MAVS activation by filament formation.
Schematic representation of the current model of MAVS activation after triggering of RIG-I. The 2CARD domains of RIG-I are auto-repressed in the absence of a ligand. Upon binding to the end of a 5'-ppp dsRNA molecule, the repression is released, freeing the 2CARD domain. RIG-I migrates to the dsRNA interior in an ATP dependent way, forming filaments of multiple RIG-I molecules. This process brings several 2CARD domains in close proximity, leading to the formation of 2CARD tetramers. RIG-I 2CARD tetramers are then able to imprint their structure on the similar MAVS CARD domains, resulting in the propagation of MAVS CARD filament formation. Thereby, induction of MAVS aggregation leads to downstream signal transduction and eventually to type I IFN induction (Peisley et al., 2013; Wu et al., 2014).

Further, a cryo-EM approach revealed that the MAVS-CARD oligomer displays a common single-stranded left-handed helix symmetry shared by the RIG-I 2CARD tetramer (Wu et al., 2014). Engineering of a tetrameric MAVS CARD fusion construct that is unable to oligomerize any further enabled the determination of the crystal structure of a $2CARD^{RIG\text{-}I}$:$CARD^{MAVS}$ complex. This structure strongly suggested a mechanism how RIG-I 2CARD tetramers seed the formation of MAVS oligomers by imprinting their helical architecture on MAVS CARDs, resulting in a growing filament with the same symmetry (Wu et al., 2014). This provides a precise molecular

model how RIG-I CARD oligomerization leads to the assembly of an oligomerized MAVS signaling platform on the mitochondrial membrane to initiate a cellular antiviral response.

2.2.2. MAVS as antiviral signaling adaptor

The mitochondrial antiviral-signaling (MAVS) protein is the central adapter protein for the RLR pathway and essential for mounting an antiviral response (Seth et al., 2005; Sun et al., 2006). Initially, MAVS was independently characterized by different groups and is therefore alternatively knows as IPS-1 (Kawai et al., 2005), VISA (Xu et al., 2005) or Cardif (Meylan et al., 2005). The 57 kDA protein contains an N-terminal CARD domain, homologous to the 2CARDs of RIG-I and MDA5, which is essential for signal transduction from RLR (described in the previous chapter), an adjacent proline rich region and a C-terminal transmembrane anchor localizing MAVS mainly to the mitochondria (Figure 8). Although MAVS is primarily a mitochondrial protein, it is also associated with other cellular compartments such as peroxisomes (Dixit et al., 2010) and a certain compartment of the endoplasmic reticulum (ER), the mitochondria-associated membranes (MAMs) (Horner et al., 2011). Even though the mechanism underlying the differential sorting of MAVS to the different cellular compartments is poorly characterized, its signaling activity strictly relies on membrane anchoring (Seth et al., 2005). In accordance with the requirement for membrane localization, Hepatitis C virus attacks MAVS by using its NS3-4A protease to cleave the protein adjacent to the C-terminal membrane anchor, resulting in cytosolic relocalization of MAVS and thus abrogation of antiviral signaling (Hiscott et al., 2006; Meylan et al., 2005).

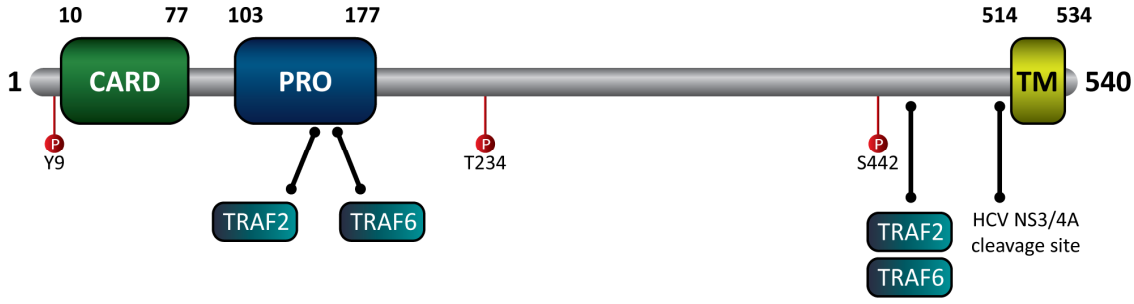

Figure 8: Domain organization of MAVS.
Schematic representation of MAVS, including selected interactors and modifications. MAVS contains an N-terminal CARD domain, which is essential for oligomerization and downstream signaling. The adjacent proline-rich region (PRO) contains two distinct TRAF interaction motifs (TIMs) for TRAF2 and TRAF6, respectively. Another TIM for TRAF2 and TRAF6 is located in proximity to the C-terminal transmembrane anchor (TM). MAVS function can be positively (Y9 and S442) and negatively (T234) regulated by posttranslational phosphorylation (Belgnaoui et al., 2011; Vazquez and Horner, 2015).

On the level of MAVS, the RLR pathway branches into antiviral IFN-signaling and inflammatory response, by activation of the corresponding transcription factors IRF3 and NF-κB (Seth et al., 2005; Sun et al., 2006). Although MAVS is associated with numerous regulating and signaling proteins, activation dependent interactions with members of the TNF receptor-associated family (TRAF) are central for different downstream signaling functions. MAVS contains two distinct TRAF-interaction motifs (TIM) in the N-terminal proline rich region and another TIM at the C-terminus adjacent to the membrane anchor (Saha et al., 2006; Xu et al., 2005). However, the precise mechanism and which TRAFs are essential for IRF3 and NF-κB activation, respectively, is highly controversial, with partly contradictory reports in the literature. TRAF3, which is also an essential factor in TLR-mediated IRF3 activation (Hacker et al., 2006), was reported to be crucially involved in the activation of IRF3 in the RLR pathway (Oganesyan et al., 2006; Saha et al., 2006). Thereby, the C-terminal TRAF3 binding site of MAVS was shown to be essential for antiviral signaling (Paz et al., 2011). In contrast, TRAF2 and TRAF6 were associated with the activation of NF-κB downstream of MAVS (Xu et al., 2005). Further studies challenged the view that TRAF3 is essential for MAVS mediated IFN-induction and suggested that rather TRAF2, TRAF5 and TRAF6, which were previously linked to NF-κB activation, mediate also activation of IRF3 in a redundant manner, depending on their E3 ligase activity (Liu et al., 2013a; Zeng et al., 2009). Recently, a study could demonstrate that the different TRAF interaction motifs in MAVS are inhibited by adjacent regions in inactive monomeric MAVS, leading to an autoinhibition of signaling activity. This inhibitory effect is thought to be released upon MAVS filament formation, proposing a model how MAVS forms an active signaling platform by oligomerization (Shi et al., 2015) (MAVS signaling reviewed in Belgnaoui et al. (2011) and Vazquez and Horner (2015)).

Although the specific contribution of the distinct TRAFs in MAVS signaling is not fully understood, the downstream adaptor protein NEMO (also known as IKKγ) is essential for both IRF3 and NF-κB activation, depending on its ability to bind K63-linked polyubiquitin chains (Yamaoka et al., 1998; Zhao et al., 2007). Further, the ability of NEMO to bind K63-linked polyubiquitinated TBK1 has been reported to be essential for activation of the kinase and subsequent IRF3 activation (Wang et al., 2012). This is consistent with the overall necessity for K63-linked polyubiquitination in IRF3 activation (Zeng et al., 2009). Originally, NEMO was characterized as regulatory subunit of the inhibitor of NF-κB (IκB) kinase (IKK) complex with its catalytic subunits IKKα and IKKβ. In the canonical variant of the pathway, the NF-κB subunits p50 and Rel A are present in an inactive form bound to IκB. IKK activation leads to phosphorylation of IκB, triggering its polyubiquitination and subsequent proteasomal degradation. This process leads to a release of NF-κB and nuclear translocation. NF-κB is activated by several cell surface

receptors such as TNF receptors, IL-1 receptors and toll-like receptors (TLRs), a process which is dependent on various adaptor proteins and TRAF family members (Chen, 2005). Additionally, NF-κB is activated following MAVS activation by RLR signaling (Kawai et al., 2005; Seth et al., 2005; Yoneyama et al., 2004). This is mediated by the adaptor proteins FADD (Fas-associated death domain) and RIP1 (receptor interacting protein 1) (Kawai et al., 2005).

On the IRF3 activating branch of the MAVS signaling cascade, the TNFR-associated death domain (TRADD) protein is involved in downstream activation of the kinases TBK1 and IKKε by interactions with TRAF3 and TRAF family member-associated NF-κB activator (TANK) (Michallet et al., 2008). Besides TANK, also NAP1 and SINTBAD have been identified as potential adaptors mediating activation of the downstream kinases TBK1 and IKKε (Guo and Cheng, 2007; Ryzhakov and Randow, 2007; Sasai et al., 2006). These three adaptor proteins exhibit mutually exclusive interactions with TBK1 and are thought to trigger trans-autophosphorylation-mediated activation of TBK1 by inducing a high subcellular local concentration of the kinase, for example at the sites of signaling MAVS aggregates (Goncalves et al., 2011; Helgason et al., 2013; Hou et al., 2011; Ma et al., 2012).

2.2.3. IRF3 activation by the effector kinases TBK1/IKKε

Initially, the two kinases TBK1 and IKKε were characterized as NF-κB activating kinases (Bonnard et al., 2000; Tojima et al., 2000). However, this theory was later discarded and the kinases were shown to be essential for the activation of interferon regulatory factor 3 (IRF3) and the subsequent induction of type I interferon genes (Fitzgerald et al., 2003; Hemmi et al., 2004; McWhirter et al., 2004; Sharma et al., 2003). Cells lacking TBK1 were shown to be defective at triggering IRF3 phosphorylation in a RIG-I dependent way (Yoneyama et al., 2004)(TBK1/IKKε regulation reviewed in Chau et al. (2008)).

The viral induction of type I interferons relies on the transcription factors IRF3 and IRF7 (Malmgaard, 2004; Sato et al., 2000). This antiviral response is triggered by activation of a transcription factor complex consisting of IRF3 and CBP/p300 (Yoneyama et al., 1998), while posttranslational activation of IRF3 depends on several serine phosphorylations (Yoneyama et al., 2002). Both IRF3 and IRF7, which are activated after RIG-I signaling (Paz et al., 2006), are targeted by the kinases TBK1 and IKKε *in vitro* (Sharma et al., 2003). A recent study could show that activation of IRF3 by TBK1 depends on interactions with one of its upstream adaptors MAVS, TRIF or STING. This association depends on phosphorylation of the adaptors at a common pLxIS motif (where p is a hydrophilic residue and x any residue) by TBK1 and IKK (Liu et al., 2015).

IRF3 is able to bind to MAVS using a pLxIS binding motif and is subsequently activated by phosphorylation on several residues in a Ser/Thr rich cluster in the C-terminal domain by TBK1/IKKε, whereby Ser386 and Ser396 have been identified as critical moieties (Mori et al., 2004; Servant et al., 2003). Phosphorylation of these residues leads to a conformational change in IRF3 that allows for dimerization and CBP/p300 association. Ser396 of IRF3 is also part of a pLxIS motif that is used by IRF3 for self-association via its pLxIS binding motif. This interaction is similar to the binding of IRF3 to its upstream adaptors during activation, as revealed by structural studies (Zhao et al., 2016). The Rotavirus NSP1 protein employs such a motif to bind IRF3, thus targeting it for degradation (Zhao et al., 2016). Dimerization of IRF3 subsequently leads to nuclear localization and association with CBP/p300. This phosphorylation dependent association with CPB/p300 leads to the transcription of IFN-β among other genes (IRF3 activation reviewed in Hiscott (2007)). Efficient induction of IFN-β relies on the cooperative activity of IRF3, NF-κB and AP-1 to form an enhanceosome that drives IFN-β transcription (Kim et al., 2000; Thanos and Maniatis, 1995). In addition to the induction of type I interferons, IRF3 is also able to directly stimulate certain interferon-stimulated genes (ISGs), such as ISG15, by interaction with an interferon-stimulated response element (ISRE) containing promoter, independently of IFN signaling (Au et al., 1995).

In summary, although many adaptor and regulatory proteins have been identified, the precise molecular mechanisms leading to IRF3 phosphorylation after MAVS activation is still not fully understood. To determine the molecular mechanism of inhibitors of this pathway, such as the rabies virus phosphoprotein (Brzózka et al., 2005), might contribute to a further characterization of this remarkably complex signaling cascade and the identification of new key players.

2.2.4. Antiviral interferon signaling

Once type I interferons have been induced and secreted, they bind a common receptor located to the cell surface, the type I IFN receptor, consisting of the two subunits IFNAR1 and IFNAR2. The intracellular part of these subunits is associated with the Janus activated kinases (JAKs) TYK2 and JAK1, respectively. Upon ligand binding, the receptor subunits dimerize, leading to activation of the JAKs by autophosphorylation. The active JAKs in turn phosphorylate the members of the signal transducer and activator of transcription (STAT) family, in the case of type I interferon signaling mainly STAT1 and STAT2, on several tyrosine residues. This leads to STAT1-STAT2 heterodimerization and association with IRF9, forming a complex known as ISG factor 3 (ISGF3). ISGF3 localizes to the nucleus and triggers transcriptional activity of numerous interferon-

stimulated genes (ISGs) by binding to interferon-stimulated response elements (ISREs) (Levy et al., 1988) present within their promotor region (interferon signaling reviewed in Platanias (2005)).

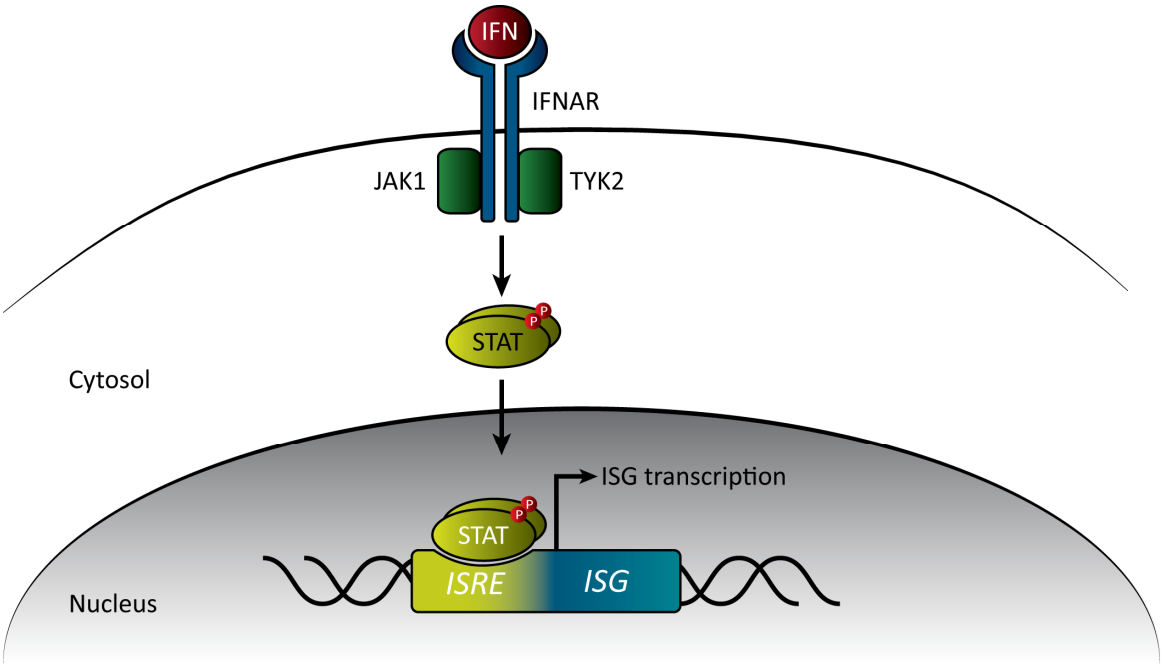

Figure 9: IFN-signaling triggers ISG induction via JAK-STAT signaling.
The antiviral function of type I interferons is based on their ability to trigger the expression of interferon-stimulated genes (ISGs), coding for a variety of effector proteins and transcription factors with broad antiviral activities. IFN binds to the extracellular domain of the heterodimeric IFNAR receptor, leading to intracellular activation of the tyrosine kinases JAK1 and TYK2. These kinases in turn activate signal transducer and activator of transcription (STAT) family members, which heterodimerize (STAT1 and STAT2 for type I IFNs), translocate to the nucleus and induce ISG expression (Platanias, 2005).

Although IRF3 can also trigger some ISGs like ISG15 and ISG56 directly in an interferon-independent manner (Au et al., 1995; Grandvaux et al., 2002), the major antiviral response is driven by interferon induced ISG expression. The phosphoproteins of rabies virus and other members of the *Lyssavirus* genus exhibit a conserved mechanism to evade the induction of antiviral ISGs by binding to activated STATs and thereby preventing their nuclear localization and transcriptional activity (Brzózka et al., 2006; Vidy et al., 2005; Wiltzer et al., 2012).

In addition to genes coding for antiviral effector proteins, also components of the antiviral signaling cascade such as RIG-I-like receptors, IRFs and STAT1 are upregulated upon interferon induced JAK-STAT signaling (Der et al., 1998). Together with the expression of transcription factors such as IRF1, which activates ISGs itself in an interferon-independent way, a powerful positive feedback loop is initiated. In total, several hundred ISGs have been identified, depending on IFN dose and cell type. Antiviral effector proteins, such as MX1, RNaseL and PKR, exhibit strong activity against a broad range of viral pathogens. However, defects in single or multiple

strong ISGs are not leading to a total loss of antiviral function, indicating that many effector proteins contribute to protection in a redundant way. Many ISGs have a rather weak activity when acting alone, but may still exhibit a significant suppression of viral replication when numerous components act in parallel in a cooperative manner (antiviral effector functions of ISGs reviewed in Schoggins and Rice (2011)).

2.3. HSP70 – a molecular chaperone

2.3.1. The heat shock response

Exposure to heat is a major stressor nearly all living organisms have to deal with. Since proteins need to exhibit a certain conformational flexibility in order to fulfill their designated tasks, they are only slightly stable at the normal growing temperature of an organism. Therefore, elevation of the optimal temperature by just a few degrees can already lead to unfolding and aggregation of proteins, rendering them non-functional. Consequently, this heat shock condition disturbs the cellular protein homeostasis, strongly impairing protein function and integrity of the cytoskeleton. Additionally, heat shock has a negative impact on membranes and several cellular compartments such as the ER and the mitochondria. To counteract this deleterious process, the heat shock response, a complex and in some parts highly conserved cellular program, is initiated, leading to the significant induction of approximately 50-200 genes (Richter et al., 2010). Initially, HSPs were identified as a group of proteins which are transcriptionally upregulated during heat stress in *Drosophila melanogaster* (Ashburner and Bonner, 1979; Tissieres et al., 1974), coining the term “heat shock proteins”. The appearance of chromosomal puffs after heat shock, indicating enhanced transcriptional activity, was used to map the genetic loci of some of the responsible genes (Peterson et al., 1979). Other studies revealed that this effect of upregulation of certain genes upon temperature increase is also occurring in other eukaryotes and prokaryotes, showing that the heat shock response is an ancient mechanism that is conserved among the domains of life (Kelley and Schlesinger, 1978; Lemaux et al., 1978). The major class of heat stress induced proteins are heat shock proteins (HSPs), nowadays defined as molecular chaperones that assist in correct (re-)folding of denatured proteins and are able to dissolve protein aggregates or even prevent their formation, thus mediating protection from this harmful condition. Generally, molecular chaperones are not imparting any structural information to their client proteins, but contribute to correct folding by preventing or dissolving aberrant intra- or

intermolecular interactions. Misfolded proteins are recognized by their increased exposure of hydrophobic amino acid residues. The molecular chaperones are comprised of the conserved protein families HSP100, HSP90, HSP70, HSP60 and small heat shock proteins (sHSPs). Besides their role in stress protection, several heat shock proteins are also constitutively expressed under normal conditions and are required for the correct folding of newly synthesized proteins and participate in the modulation of numerous cellular processes (For review on heat shock response see Richter et al. (2010)).

2.3.2. The heat shock protein 70 kDa family

The heat shock protein 70 kDa (HSP70) family is well conserved even among the domains of life. The prokaryotic homolog DnaK exhibits about 60 % sequence identity with its eukaryotic homologs (Richter et al., 2010). HSP70 consists of a nucleotide binding domain (NBD) of 45 kDa and a substrate binding domain (SBD) of about 25 kDa, connected by a short disordered linker. The NBD is formed by two subdomains and is able to bind and hydrolyze ATP. The SBD is divided into a β-sandwich subdomain of 15 kDa and an adjacent C-terminal α-helical domain referred to as “lid” (Mayer and Bukau, 2005). The crystal structure of functionally intact HSC70 of bovine origin, a constitutively expressed member of the HSP70 family, could be resolved (Figure 10, Jiang et al. (2005)).

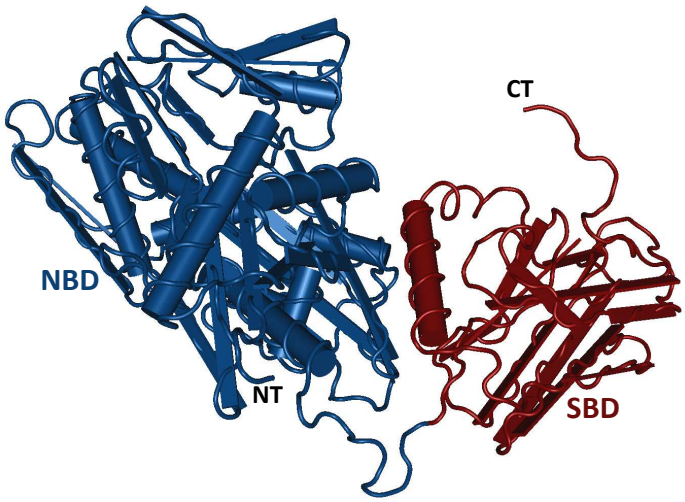

Figure 10: Structural representation of mammalian HSC70.
Structure of HSC70 of bovine origin, as resolved by x-ray crystallography (Jiang et al. (2005), PDB ID 1YUW; illustration with Cn3D by NCBI). Members of the HSP70 family are comprised of a nucleotide binding domain (depicted in blue) and a substrate binding domain (depicted in red) connected by a short disordered linker. The SBD is comprised of a β-sandwich followed by an α-helical lid. In concert with HSP40 co-chaperones, substrate binding to the SBD greatly increases the ATP hydrolysis rate of the NBD. Upon ATP hydrolysis, the C-terminal lid closes on the substrate, resulting in a high affinity interaction.

The HSP70 proteins assist in the correct folding of newly synthesized proteins, help to prevent the formation of aggregates and are even able to mediate the solubilization and refolding of denatured and already aggregated proteins. In addition, HSP70 interacts with central regulators of numerous cellular pathways and therefore is involved in the modulation of cell homeostasis, proliferation, differentiation and cell death, illustrating that its functions go well beyond mere assistance in protein folding or heat stress response. Together with HSP40 co-chaperones and cooperating HSPs of other families, mainly HSP90 and HSP100, the HSP70 proteins form a complex network that controls many aspects of the cellular life cycle (Mayer and Bukau, 2005).

HSP70 recognizes exposed hydrophobic stretches within its client proteins using the substrate binding domain. The SBD is able to interact with approximately seven, mainly hydrophobic, disordered residues (Zhu et al., 1996). In the ATP bound form, HSP70 exhibits rather weak and transient interactions with its target proteins. Therefore, the interaction of HSP70s with their substrates is modulated by ATP hydrolysis, since the binding to the target residues is significantly stronger in the ADP bound form. Although the binding of a substrate to HSP70 increases its ATP hydrolysis rate, co-chaperones of the HSP40 family, the eukaryotic homologs of the bacterial DnaJ, are required for efficient client binding. The HSP40, or J-domain co-chaperones are important modulatory cofactors for HSP70 that are able to bind client proteins and mediate their recruitment to HSP70. In concert with substrate binding, the shared J-domain of HSP40s greatly enhances the ATPase activity of the HSP70 NBD. ATP hydrolysis leads to a conformational change in the protein and the lid of the SBD closes on the substrate, resulting in a strong interaction between HSP70 and its client protein. HSP70 alone exhibits rather limited selectivity in client binding. Functional specificity is thought to be mediated by the protein family of the HSP40 co-chaperones, enabling HSP70 to fulfill its multiple tasks in cellular protein homeostasis under normal and thermal stress conditions (Kampinga and Craig, 2010). In order to release the bound substrate, ADP has to be replaced by a new ATP molecule, a step mediated by a diverse class of proteins, the so called nucleotide exchange factors (NEFs). They associate only with ADP bound HSP70, leading to the release of ADP and the substrate protein, and dissociate from the chaperone upon binding of a new ATP molecule. At this point, a new cycle of substrate binding and ATP hydrolysis can begin. HSP70 therefore always cycles between an ATP and ADP bound state. Since NEFs define the kinetics of substrate release, they regulate the chaperoning activity of HSP70 in concert with the HSP40 co-chaperones (molecular functions of HSP70 chaperones reviewed in Mayer and Bukau (2005)). This cooperative mode of function between different HSP70 family members and their even more diverse cofactors leads to an enormous number of

potential combinations, proposing a model how substrate specificity and the functional diversity of the HSP70 system is achieved.

2.3.3. HSP70 in cellular processes and disease

As mentioned above, the functions of the HSP70 chaperone machinery go beyond the correct re-folding of proteins during heat stress. While the almost identical homologs HSP70-1A/1B are the major HSP70s induced upon heat shock, heat shock cognate 71 kDa protein (HSC70, also known as HSPA8) is constitutively expressed under normal conditions and fulfills important housekeeping functions. Additional HSP70 family members exist in human cells which are localized to certain cellular compartments, such as the mitochondria-associated GRP75 (HspA9) or BiP (GRP78, HspA5), which localizes to the lumen of the endoplasmic reticulum (For a list of members of the diverse human HSP70 family see Table 1 (adapted from Radons (2016)).

Besides its role in dissolving denatured protein aggregates, HSP70 family members are also essential to disassemble a number of native protein complexes. HSC70 was identified as the central uncoating ATPase for clathrin-coated vesicles (Chappell et al., 1986). Clathrin-mediated endocytosis is an important route for the internalization of cellular receptors and extracellular ligands, as well as an essential process for neuronal cells to recycle synaptic vesicles, which would otherwise be used up rapidly by fusion events with the presynaptic membrane during signal transduction (Slepnev and De Camilli, 2000). The uncoating of these vesicles relies on the concerted action of HSC70, its J-domain containing cofactor auxilin and a number of NEFs such as HSP110 or Bag1 (Schuermann et al., 2008; Ungewickell et al., 1995). Uncoating of clathrin-coated vesicles during neuronal endocytosis was shown to be abrogated by targeting the interaction between HSP70 and its critical cofactors with specific peptides, or by introducing dominant negative HSP70 mutant proteins defective in ATPase activity or ATP binding (Morgan et al., 2013; Morgan et al., 2001; Newmyer and Schmid, 2001). Suppression of vesicle uncoating lead to impaired endocytosis and consequently a significantly enlarged presynaptic membrane, indicating a crucial function for HSC70 in maintaining membrane integrity during synaptic transmission (Morgan et al., 2013). Moreover, distinct members of the HSP70 family are involved in the transport of proteins across membranes of subcellular components. BiP (also known as GRP78/HSPA5) and mtHSP70 (also known as GRP75/HSPA9) facilitate translocation of substrates into the lumen of the ER and the mitochondrial matrix, respectively. BiP interacts with the Sec complex on the luminal side of the ER and participates in posttranslational import by binding to the substrate and thus providing unidirectional transport in an ATP-dependent

manner (Matlack et al., 1999; Matlack et al., 1997). Using a similar mechanism, mtHSP70 assists in the import of proteins across the inner mitochondrial membrane. On the side of the mitochondrial matrix mtHSP70 is associated with the Tim44 subunit at the exit of the translocase of the inner membrane (TIM) complex and binds to its target substrate, thereby acting as a molecular ratchet that prevents retrograde movement of the incoming polypeptide (Moro et al., 1999; Okamoto et al., 2002). Whether HSP70s implicated in transmembrane trafficking only work as rather passive molecular ratchets or apply power strokes to move the substrate and actively participate in its unfolding is controversial. Goloubinoff and De Los Rios (2007) suggested an "entropic pulling" model, in which the force applied by the HSP70 chaperone is of entropic origin, thus trying to unify the models of "molecular ratchet" and "power stroke".

Protein	UniProt ID	Alternative names	Cellular localization	Length (aa)
HspA1A	P0DMV8	Hsp70-1, Hsp72, HspA1, Hsp70-1A, Hsp70i	Cytosol, nucleus, cell membrane, extracellular exosomes	641
HspA1B	P0DMV9	Hsp70-2, Hsp70-1B	Cytosol, nucleus, extracellular exosomes	641
HspA1L	P34931	Hsp70-1L, Hsp70-hom, Hsp70-1t, Hum70t	Cytosol, nucleus	641
HspA2	P54652	Heat shock 70kD protein 2, Hsp70.2	Cytosol, nucleus, cell membrane, extracellular exosomes	639
HspA5	P11021	Hsp70-5, BiP, Grp78, Mif-2	ER, extracellular exosomes	654
HspA6	P17066	Hsp70-6, Hsp70B'	Cytosol, extracellular exosomes	643
HspA7	P48741	Hsp70-7, Hsp70B	Blood microparticles, extracellular exosomes	367
HspA8	P11142	Hsp70-8, Hsc70, Hsc71, Hsp71, Hsp73	Cytosol, nucleus, cell membrane, extracellular exosomes	646
HspA9	P38646	Hsp70-9, Grp75, HspA9B, MOT, MOT2, PBP74, mot-2, mtHsp70, mortalin	Mitochondria, nucleus	679
HspA12A	O43301	Hsp70-12A, FLJ13874, KIAA0417	Intracellular, extracellular exosomes	675
HspA12B	B7ZLP2	Hsp70-12B, RP23-32L15.1, 2700081N06Rik	Endothelial cells, intracellular, blood plasma	685
HspA13	P48723	Hsp70-13, Stch	ER, extracellular exosomes, microsomes	471
HspA14	Q0VDF9	Hsp70-14, Hsp70L1	Cytosol, membrane	509

Table 1: Members of the human HSP70 family. Protein names corresponding to gene names.

Although HSP70 activity is important for cellular survival in regard to its involvement in protein homeostasis, HSP70s additionally exhibit direct anti-apoptotic functions on several levels of the programmed cell-death pathway. HSP70 family members have been reported to interfere with activation of the pro-apoptotic c-jun N-terminal kinases (JNKs), mitochondrial release of cytochrome c and the oligomerization of Apaf-1 (reviewed in Beere and Green (2001)). Further, levels of the survival kinase Akt are regulated by HSP70 in an ATPase-dependent way (Koren et al., 2010).

Due to this influence on cell survival, molecular chaperones, such as members of the HSP70 family, are upregulated in the cells of many cancer types. Additionally, elevated levels of heat shock proteins help aberrant cancer cells to deal with the presence of many mutated, and thus frequently misfolded proteins. Therefore, in addition to targeting HSP90, the modulation of HSP70 function is an emerging strategy in the development of new therapeutic options for cancer treatment (Ma et al., 2014; Murphy, 2013; Powers et al., 2008). HSP70 binding aptamers and peptides were shown to sensitize tumors to cisplatin treatment in a melanoma mouse model (Rerole et al., 2011). Another study reported that depletion of HSP70 leads to massive death in a human breast cancer cell-line (Nylandsted et al., 2000). These findings emphasize that targeting of molecular chaperones might be a promising generalized strategy in the future that could be applied to tumors of diverse origins.

Protein misfolding and aggregation are not exclusively occurring during heat stress conditions. Between the unfolded and the correctly folded state, proteins can take numerous possible conformations within the energy landscape. Although the native state of a protein is supposed to be its most stable conformation, many alternative conformations exist that can form potentially deleterious aggregates and fibrillary amyloid structures, a process that is facilitated by mutations and stress conditions. The accumulation of amyloid protein aggregates is shared among many neurodegenerative diseases, such as Alzheimer's, Parkinson's, Huntington's disease, amyotrophic lateral sclerosis and prion encephalopathies, which have been therefore described as protein-misfolding diseases. The appearance of such toxic aggregates is accompanied by inflammation, oxidative stress and cell death, leading to strongly impaired neuronal function and survival. There is growing evidence that molecular chaperones such as HSP70 are part of a complex cellular network which attempts to counteract such harmful changes in protein homeostasis. Concurring, the progressive failure of multicellular organisms to induce elevated levels of heat shock proteins during aging might explain the onset of neurodegenerative diseases in the late phases of life. New experimental therapeutic approaches aim at sustaining high levels of chaperone activity, in order to reduce the toxic effect of protein

aggregates in neurodegenerative and other age-related diseases (reviewed in Hinault et al. (2006)).

2.3.4. Viruses and heat shock proteins

Some members of the different heat shock protein families belong to the most abundant and important proteins in our cells. Therefore, it is not surprising that viruses evolved means to use this complex machinery for their own purposes. It is a commonly observed phenomenon, that viruses upregulate heat shock proteins upon infection. In general, a productive viral infection is accompanied by extensive production of viral proteins that require correct de-novo folding. The newly translated viral polypeptides are thought to compete HSP70 away from Hsf1, the central eukaryotic heat shock transcription factor, freeing Hsf1, which in turn induces a heat shock response (Richter et al., 2010). In addition, expression of heat shock proteins is further induced by disease-mediated fever (Hasday and Singh, 2000). The elevated levels of molecular chaperones might contribute to the expression of viral proteins and thus viral replication. Notably, several DNA viruses such as adenovirus, herpes simplex virus (HSV) and *Simian virus 40* (SV40) directly induce expression of HSP70s on a transcriptional or posttranscriptional level (reviewed in Mayer (2005)).

Besides the upregulation of chaperones in order to favor viral protein translation, several viral proteins have been shown to directly interact with HSP70s, suggesting specific functions for heat shock proteins in the viral life cycle. Measles virus and the closely related canine distemper virus, which belong to the *Morbillivirus* family and belong together with *Lyssaviruses* to the order *Mononegavirales*, react to a cellular heat shock response and elevated HSP70 levels with a significant increase in viral transcription and replication (Oglesbee et al., 1996; Parks et al., 1999). The cytoplasmic tail of the measles virus N protein (N_{TAIL}) has been identified as molecular binding partner of HSP70 (Zhang et al., 2002). The HSP70 binding motif in N_{TAIL} partially overlaps with the phosphoprotein binding region. During transcription and replication, P links the polymerase L to the N-encapsidated genome. Measles virus containing a N protein version unable to bind HSP70 is unresponsive to heat shock induction in regard to transcription (Zhang et al., 2005). It is speculated that the N-HSP70 interaction might assist in transiently weakening the N-P interaction, in order to promote repeated N-P binding, a process that is essential for transcription and replication along the RNP (Bourhis et al., 2006).

Rabies virus was reported to be positively regulated by HSP70 in a similar way (Lahaye et al., 2012). HSP70 interacts with purified RNPs containing only the N-protein, suggesting a N-HSP70

interaction. This is supported by the presence of HSP70 in viral particles (Sagara and Kawai, 1992). Additionally, HSP70 co-localizes with Negri body-like structures, a certain type of inclusion bodies which have been identified as the sites of replication and transcription of rabies virus, illustrating the close connection between the viral life cycle and the cellular chaperone machinery (Lahaye et al., 2009).

Association with HSP70 is also a known feature for several other RNA viruses. For example, HSP70 is recruited to the viral inclusion bodies of Mumps virus (MuV) and regulates the ubiquitin-proteasome-dependent degradation of MuV-P (Katoh et al., 2015). An interaction between HSC70 and the *Orthoreovirus* nonstructural protein µNS recruit the heat shock protein to viral factories, the sites of particle assembly, independently of chaperone function (Kaufer et al., 2012). In a HRSV (*Human respiratory syncytial virus*) infection, HSP70 interacts with the viral polymerase within lipid rafts, dependent on ATPase function (Brown et al., 2005). HSP70 and several other cellular chaperones were further identified as proviral host-factors for HRSV (Munday et al., 2015). Heat shock proteins of the HSP70 and HSP90 are components of the *Dengue virus* (DENV) receptor complex (Reyes-Del Valle et al., 2005). Accordingly, depletion of HSP70 by RNA interference or abrogation of HSP70 function by small molecule inhibitors significantly reduced DENV replication (Howe et al., 2016; Padwad et al., 2010). This illustrates that HSP70 has a role as potential target in antiviral strategies.

The numerous examples given above show that an interplay between the cellular chaperone machinery and viral life cycles are rather a common phenomenon than the exception. Thereby, the functions of HSP70s seem to go well beyond their chaperoning function and support of viral protein folding. New insights about this interesting relationship might also reveal new functions of the complex and not yet fully understood HSP70 system.

2.4. Aims of the Thesis

The ability of viruses to interfere with the induction of an IFN-mediated antiviral cellular state is critically required to establish a productive infection and therefore an important prerequisite for pathogenicity. For rabies virus, the phosphoprotein (RABV P) is very efficient at antagonizing innate immune signaling on two distinct levels. RABV P suppresses RIG-I mediated IFN-induction by blocking IRF3 phosphorylation (Brzózka et al., 2005) as well as IFN-mediated STAT-signaling (Brzózka et al., 2006; Vidy et al., 2005). While the abrogation of STAT-signaling can be explained with a sequestration of activated STATs in the cytosol, the mode of inhibition in regard to IRF3 activation is enigmatic. Previous research in our group could show that RABV P internal truncation mutants lacking residues 176-186 exhibit a defect in regard to inhibition of IFN-induction (Rieder et al., 2011). However, a clear function or direct molecular binding partner could not be identified for this sequence.

A major goal of this thesis is to obtain new experimental evidence on how RABV P interferes with activation of IRF3, the central transcription factor of type I IFNs. To this end, features and domains of the P protein shall be assayed for their contribution to inhibitory function by site-directed mutagenesis, in order to identify the minimal RABV P residues which are essential for inhibition of IFN-induction. Further, RABV P mutant constructs as well as RABV P derived fusion peptides encompassing residues 176-186 are to be analyzed by co-immunoprecipitation experiments and an unbiased mass spectrometry approach. Potential hits shall be examined in terms of a potential involvement in innate immune signaling by additional interaction studies using wild type and inhibition deficient RABV P versions. Target proteins exhibiting a correlation between P binding and inhibition of IFN-induction can then be further assayed in regard to a potential general contribution to RLR-mediated IFN-induction, possibly identifying new key players in this pathway.

3. Materials & Methods

3.1. Materials

3.1.1. Chemicals

Chemical	Manufacturer
Acetic acid, 100 %	Roth
Acetone, Rotipuran 99.8 %	Roth
Acrylamide Rotiphorese® Gel 30 (37.5 : 1)	Roth
Agar	BD
Agarose, UltraPure	Invitrogen
Albumin Fraction V (BSA)	Roth
Ammonium chloride (NH4Cl)	Merck
Ammonium persulfate	Sigma-Aldrich
Ampicillin sodium salt (Amp)	Roth
Bis-Tris	Santa Cruz Biotech.
Bromophenole blue	Sigma-Aldrich
Coomassie Brilliant Blue G-250	Biorad
Deoxycholic acid (DOC)	Sigma-Aldrich
Dimethyl sulfoxide (DMSO)	Roth
Dimethylformamide	Merck
Disodium hydrogen phosphate	Merck
Ethanol	Merck
Ethidium bromide solution 1 %	Roth
Ethylenediamine tetraacetic acid (EDTA)	Sigma
G418	Roth
Glycerol , Rotipuran 99.5 %	Roth
HEPES	Roth
Hydrochloric acid, Rotipuran 37 %	Merck
Imidazole	Merck
Isopropanol	Merck
Kanamycin monofulfate	Sigma-Aldrich
Leptomycin B (LMB)	Santa Cruz Biotech.
Magnesium chloride hexahydrate ($MgCl_2 \bullet 6H_2O$)	Fluka
Magnesium sulfate heptahydrate ($MgSO_4 \bullet 7H_2O$)	Merck
Methanol	Roth
Milk powder, blotting grade	Roth

MOPS (3-(N-morpholino)propanesulfonic acid)	Roth
Nonidet™ P40 Substitute	Fluka
Orange G	Fluka
ortho-Phosphoric acid, 85 %	Merck
Paraformaldehyde (PFA)	Merck
Poly-D-lysine hydrobromide	Sigma-Aldrich
Polyethylenimine, branched	Sigma-Aldrich
Potassium acetate, extra pure (CH_3CO_2K)	Merck
Potassium chloride (KCl)	Merck
Potassium dihydrogen phosphate	Merck
Sodium bisulfite ($NaHSO_3$)	Sigma
Sodium chloride (NaCl)	Merck
Sodium dihydrogen phosphate	Merck
Sodium dodecyl sulfate (SDS)	Serva
Sodium hydroxide	VWR Chemicals
Sodium orthovanadate (Na_3VO_4)	Sigma-Aldrich
Tetramethylethylenediamine (TEMED)	Roth
Tris, Pufferan 99.9 %	Roth
Triton X-100	Merck
Tryptone	BD
Tween-20	Roth
Yeast Extract	BD
β-Mercaptoethanol	Sigma-Aldrich

Table 2: Chemicals used in this thesis.

3.1.2. Media & cell culture additives

The following cell culture media and additives have been acquired from *Gibco*:

- D-MEM (L-Glutamine, high glucose)
- G-MEM (L-Glutamine, high glucose)
- Opti-MEM® I Reduced Serum Medium
- DPBS (no calcium, no magnesium)
- L-Glutamine (200 mM)
- Penicillin-Streptomycin (Pen Strep), 10000 units/ml
- Tryptose Phosphate Broth
- MEM Amino Acids (50x)
- Trypsin-EDTA 0.25 %

The following media compositions have been used for cultivation of mammalian cell lines (for 500 ml medium):

- **D-MEM 3+**: 10 % FBS, 2.5 ml Pen Strep, 5 ml L-Glutamine.
- **G-MEM 4+**: 10 % FBS, 2.5 ml Pen Strep, 5 ml Tryptose Phosphate Broth, 10 ml MEM Amino Acids.

The following media have been used for cultivating *E. coli* bacteria:

- **LB-Medium:** 5 g NaCl, 10 g Bactotryptone, 5 g Yeast extract in 1 l with 1 mM $MgSO_4$
- **LB++ Medium:** LB medium containing additional 10 mM $MgSO_4$ and 2.5 mM KCl

3.1.3. Buffers

- **20 x MOPS buffer**: 1 M Tris, 1 M MOPS, 20 mM EDTA, 2 % SDS.
- **1 x MOPS buffer**: Diluted from 20 x MOPS buffer with addition of 2 ml of 2.5 M Sodium Bisulfite stock solution per liter (final concentration of 5 mM).
- **Extra-Dry blotting buffer**: 48 mM Tris, 20 mM Hepes, 1 mM EDTA, 1.3 mM Sodiumbisulfite, 1.3 mM Dimethylformamide (Garic et al., 2013).
- **PBS**: 137 mM NaCl, 2.7 mM KCl, 1.18 mM KH_2PO_4, 6.4 mM N_2HPO_4, pH 7.4
- **PBS-T**: PBS containing 0.05 % Tween-20.
- **TBS**: 50 mM Tris, 150 mM NaCl, pH 7.4 (adjusted with HCl).
- **TBS-T**: TBS containing 0.05 % Tween-20.
- **Co-IP buffer**: 50 mM Tris, 150 mM NaCl, 2 mM EDTA, 0.5 % Nonidet™ P40 Substitue, pH 7.4 (adjusted with HCl).
- **SDS sample buffer**: 62 mM Tris/HCl pH 6.8, 10 % SDS, 15 % β-Mercaptoethanol, 0.012 % Bromophenole blue, 30 % Glycerol.
- **3.5 x Bis-Tris**: 1.25 M Bis-Tris HCl pH 6.8.
- **Stacking gel mix (6 %)**: 1x Bis-Tris, 6 % acrylamide/bisacrylamide 37.5:1.
- **Stacking gel**: 10 ml stacking gel mix, 100 µl 10 % APS, 10 µl TEMED (for one gel).
- **Separating gel mix (10 %)**: 1x Bis-Tris, 10 % acrylamide/bisacrylamide 37.5:1.
- **Separating gel**: 25 ml stacking gel mix, 250 µl APS, 10 µl TEMED (for one gel).
- **Flexi I**: 100 mM Tris, 10 mM EDTA, 200 µg/ml RNAse, pH 7.5.
- **Flexi II**: 200 mM NaOH, 1 % SDS.

- **Flexi III**: 3 M Potassium acetate in 100 % acetic acid.
- **Colloidal Coomassie**: 0.02 % (w/v) CBB-250, 5 % (w/v) aluminium sulfate-(14-18)-hydrate, 10 % (v/v) ethanol, 2 % (v/v) orthophosphoric acid (Dyballa and Metzger, 2012).
- **Coomassie destainer**: 10 % (v/v) ethanol, 2 % (v/v) orthophosphoric acid.
- **Recombinant purification buffer**: 300 mM NaCl, 50 mM Na_2HPO_4, pH 8.0.
- **Purification buffer A**: Recombinant purification buffer containing 15 mM imidazole, 400 µl DNase/RNase stock solution each per 50 ml and a Roche Complete Protease Inhibitor EDTA-free tablet added freshly prior to use.
- **Purification Buffer B**: Recombinant purification buffer containing 15 mM imidazole.
- **Elution Buffer**: Recombinant purification buffer containing 300 mM imidazole.

3.1.4. Kits

Kit	Manufacturer
SilverQuest™ Silver Staining Kit	novex, Life Technologies
NucleoBond Xtra Midi	Macherey-Nagel
QIAquick Gel Extraction Kit	Qiagen
QIAquick PCR Purification Kit	Qiagen
Dual Luciferase® Reporter Assay System	Promega
RNeasy Mini Kit	Qiagen
Mammalian Transfection Kit	Agilent Technologies
QuantiNova SYBR Green PCR kit	Qiagen

Table 3: Kits used in this thesis.

3.1.5. Enzymes

Enzyme	Manufacturer
Restriction Enzymes	New England Biolabs
Phusion DNA Polymerase	NEB/Thermo Fisher Scientific
T4 DNA ligase	New England Biolabs
Alkaline Phosphatase, Calf Intestinal (CIAP)	New England Biolabs
Instant Sticky-End Ligase Master Mix	New England Biolabs
DNase, RNase-free	Qiagen
Transcriptor Reverse Transcriptase	Roche
RNase	Macherey-Nagel
Lysozyme	Fluka

Table 4: Enzymes used in this thesis.

3.1.6. Cell lines & Bacteria strains

HEK 293T, HeLa, HEp-2 and BSR T7 cells were used in mammalian cell culture for various experimental settings as described in the methods section of this thesis.

The *Escherichia coli* strain XL-1 blue (*Stratagene*) was used for cloning and preparation of plasmid DNA. Purification of recombinant proteins was conducted using *E. coli* strain Rosetta™ (DE3) (*Novagen*) (3.2.12).

3.1.7. Primary antibodies

The following list shows the primary antibodies used in this thesis. If not indicated otherwise, the column "Dilution" is referring to the dilution used for Western blotting. Number in brackets after epitope relates to the manufacturer's identification number for the corresponding antibody.

Epitope (#)	Host	Dilution	Manufacturer
HA-tag (Y-11)	Rabbit	1 : 1000	Santa Cruz Biotech.
HSP70 (H-300)	Rabbit	1 : 1000	Santa Cruz Biotech.
Actin (20-33)	Rabbit	1 : 1000	Sigma-Aldrich
RABV P (160-5)	Rabbit	1 : 50000	*In house*
DLC8 (FL-89)	Rabbit	1 : 1000	Santa Cruz Biotech.
Flag-tag (F7425)	Rabbit	1 : 2000	Sigma-Aldrich
IRF3-pS396 (4D4G)	Rabbit	1 : 1000	Cell Signaling Technology
IRF3 (FL-425)	Rabbit	1 : 1000	Santa Cruz Biotech.
HSC70 (B6)	Mouse	1 : 1000	Santa Cruz Biotech.
MAVS (3993)	Rabbit	1 : 1000	Cell Signaling Technology
TBK1 (D1B4)	Rabbit	1 : 1000	Cell Signaling Technology
TBK1pS172 (D52C2)	Rabbit	1 : 1000	Cell Signaling Technology
RABV P (25E6)	Mouse	1 : 500 (IF)	*Kindly provided by D. Blondel*
RABV N/P (S50)	Rabbit	1 : 20000	*Kindly provided by J. Cox*

Table 5: Primary antibodies used in this thesis.

3.1.8. Secondary antibodies

Alexa Fluor© labeled secondary antibodies were used for immunostaining in confocal microscopy, horseradish-peroxidase (HRP) coupled antibodies were used for Western blotting.

Epitope	Conjugate	Host	Dilution	Manufacturer
Rabbit IgG	Alexa-488	Goat	1 : 200	Molecular Probes (Invitrogen)
Rabbit IgG	Alexa-555	Goat	1 : 200	

Mouse IgG	Alexa-488	Goat	1 : 200	
Mouse IgG	Alexa-555	Goat	1 : 200	
Rabbit IgG	HRP	Goat	1 : 20000	Jackson ImmunoResearch Laboratories
Mouse IgG	HRP	Goat	1 : 20000	

Table 6: Secondary antibodies used in this thesis.

3.1.9. Laboratory equipment

Equipment	Manufacturer
Incubators	
Certomat BS-1	Sartorius
Cell culture incubator	Sanyo
37 °C incubator	Heraeus
Centrifuges	
Centrifuge 5417 R	Eppendorf
Centrifuge 5804 R	Eppendorf
Centrifuge 5418	Eppendorf
Varifuge 3.0R	Heraeus
Table centrifuge Z160-M	Hermle
Microscopes	
Axiovert 35	Zeiss
Light micoscrope *TMS*	Nikon
UV-Light microscope *IX71*	Olympus
Freezers	
Premium No Frost	Liebherr
-80 °C II Shin	Nunc
Forma ULT deep freezer	Thermo Scientific
Miscellaneous	
Chemiluminescence developing system (Fusion FX7)	Vilber-Lourmat
Luminometer Centro LB 960	Berthold
Magnetic stirrer/heater	VELP Scientifica
pH-meter	VWR International
PIPETBOY acu	IBS
Pipettes (2/10/200/1000 µl)	Eppendorf; Gilson
Polyacrylamid gel electrophoresis system	Peqlab
Agarose gel electrophoresis system	Peqlab
Roller mixer SRT2	Stuart
Semi-Dry blotting system	Peqlab
Spectrophotometer Nanodrop ND-1000	Peqlab
Thermocycler T3	Biometra
Thermomixer 5436	Eppendorf
Thermostated hot-block 5320	Eppendorf

Horizontal shaker Swip SM-25	Edmund Bühler GmbH
Digital Sonifier® Cell Disruptor	Branson
GJ Balance	Kern

Table 7: Laboratory equipment.

3.1.10. Laboratory consumables and miscellaneous

Consumables	Manufacturer
SUPERase•In™ RNase Inhibitor	Ambion (Life Technologies)
Pierce™ Anti-HA Magnetic Beads	Thermo Fisher Scientific
Lipofectamine® 2000	Thermo Fisher Scientific
TO-PRO®-3	Thermo Fisher Scientific
FITC Anti-Rabies Monoclonal Globulin	Fujirebio Diagnostics
WesternBright ECL Spray	Advansta
Microscope slides, frosted end	Roth
Microscope cover glasses, 12 mm Ø	Roth
Recombinant human HSP70 Protein	StressMarq
Leptomycin B	Santa Cruz Biotech.
Universal Type I Interferon	PBL Assay Science
HisPur™ Cobalt Superflow Agarose	Thermo Fisher Scientific
Cell culture plates (6-well, 24-well, 96-well)	Sarstedt
1.5/2.0 ml reaction tubes	Eppendorf
15/50 ml falcons	Sarstedt
Cell culture flasks (T25/T75)	Falcon
Pierce™ Centrifuge Columns, 10 ml	Thermo Fisher Scientific
Vectashield HardSet Antifade Mounting Medium	Vector Laboratories
Precision Plus Protein™ Standard	Biorad
1 kb DNA ladder	New England Biolabs
PCR Marker	New England Biolabs
Oligo(dT)$_{12-18}$ Primer	Thermo Fisher Scientific
SeV-DI preparations	*Kindly provided by D. Garcin*

Table 8: Consumables and miscellaneous.

3.1.11. Plasmids

The following list contains the plasmids which have been used for the experiments in this thesis. The source is indicated if the construct was not created during this thesis. If not mentioned otherwise, “P” refers to the RABV L16-strain phosphoprotein. Constructs which contain previously reported or not self-explanatory mutations are further described.

Plasmid name	Source if not this thesis	Description
RABV P expression plasmids		
pCAGGS-HA-GST-P		RABV P fused to HA-GST.
pCAGGS-HA-GST-P-130-188		RABV P truncation constructs fused to HA-GST.
pCAGGS-HA-GST-P-130-297		
pCAGGS-HA-GST-P-153-188		
pCAGGS-HA-GST-P-168-188		
pCAGGS-HA-GST-P-170-188		
pCAGGS-HA-GST-P-176-188		
pCAGGS-HA-GST-P-180-185		
pCAGGS-HA-GST-P-180-186		
pCAGGS-HA-GST-P-180-188		
pCAGGS-HA-GST-P-83-188		
pCAGGS-HA-GST-P-83-197		
pCAGGS-HA-GST-P-83-297		
pCAGGS-HA-GST-P-83-297Δdim		P truncation construct with alanine substitutions F114A, W118A and I125A, impairing dimerization (Ivanov et al., 2010).
pCAGGS-HA-GST-P-scr. Peptide		Peptide fused to HA-GST based on P residues 176-188 in randomized order.
pCR3-HA-CVS-P		N-terminally HA-tagged CVS-strain P.
pCR3-HA-CVS-P-P179S		HA-tagged CVS-strain P containing a P179S substitution.
pCR3-HA-NLS-P		RABV P N-terminally fused to HA and a SV40-TAg-NLS.
pCR3-HA-NLS-P-1-188		P truncation construct containing an N-terminal HA tag and a SV40-TAg-NLS.
pCR3-HA-NLS-P-K214A		The indicated P mutant containing an N-terminal HA tag and a SV40-TAg-NLS.
pCR3-HA-NLS-P-R260A		The indicated P mutant containing an N-terminal HA tag and a SV40-TAg-NLS.
pCR3-HA-P	Master thesis M. Wachowius	Full length RABV P, N-terminally HA-tagged. Cloned from untagged version created by K. Brzózka.
pCR3-HA-P_1	Master thesis M. Wachowius	RABV P lacking internal alternative start-codons, N-terminally HA-tagged. Cloned from untagged version created by K. Brzózka.
pCR3-HA-P-1-174		N-terminally HA-tagged C-terminal

pCR3-HA-P-1-186		RABV P truncation mutants.
pCR3-HA-P-1-186+A		
pCR3-HA-P-1-186+D		
pCR3-HA-P-1-187		
pCR3-HA-P-1-188		
pCR3-HA-P-1-197		
pCR3-HA-P-D143A-Q147A		P mutant with impaired DLC8 binding (Jacob et al., 2000).
pCR3-HA-PΔdim	Master thesis M. Wachowius	P construct with alanine substitutions F114A, W118A and I125A, impairing dimerization (Ivanov et al., 2010).
pCR3-HA-P-K214A		Alanine substitution mutant impairing the CTD conformational NLS of P. Created from a non-tagged version by K. Brzózka.
pCR3-HA-P-P181A-W186A		
pCR3-HA-P-R260A		Alanine substitution mutant impairing the CTD conformational NLS of P. Created from a non-tagged version by K. Brzózka.
pCR3-HA-P-S179P		
pCR3-HA-P-T189A		
pCR3-HA-P-T189D		
pCR3-HA-P-W186A		
pCR3-HA-P-Δ176-181		HA-tag added to original construct from K. Brzózka (P-ΔInd1).
pCR3-HA-P-Δ176-186		HA-tag added to original construct from K. Brzózka (P-ΔInd1/2).
pCR3-HA-P-Δ182-186		HA-tag added to original construct from K. Brzózka (P-ΔInd2).
pCR3-HA-THA-P		N-terminally HA-tagged THA-strain P. Cloned from full length THA-strain construct obtained from H. Bourhy.
pCR3-P-K214A	K. Brzózka	Mutant RABV P constructs containing an impaired CTD conformational NLS (Pasdeloup et al., 2005).
pCR3-P-R260A	K. Brzózka	
pCR3-P-WAMA	D. Aberle	RABV P construct containing the alanine substitutions W265A and M287A.
pCR3-tagRFP-P_4		RABV P-83-297 containing the indicated mutations and N-terminally fused to tagRFP.
pCR3-tagRFP-P_4-K214A		
pCR3-tagRFP-P_4-R260A		
pET28a-HA-$(H_6)_2$-GST-P		Constructs for bacterial expression and purification. The indicated P sequences were fused to HA-tag, two
pET28a-HA-$(H_6)_2$-GST-P-176-188		

pET28a-HA-$(H_6)_2$-GST-P-176-188-scrambled		His_6-tag repeats and a GST-tag.
Other expression plasmids		
pcDNA5/FRT/TO GFP HSPA1A	H. Kampinga (Addgene plasmid # 19483)	
pcDNA5/FRT/TO GFP HSPA1L	H. Kampinga (Addgene plasmid # 19484)	
pcDNA5/FRT/TO GFP HSPA8	H. Kampinga (Addgene plasmid # 19487)	
pCR3-Flag-HSC70		Created from GFP-tagged version obtained from addgene.
pCR3-Flag-HSC70-190-511		
pCR3-Flag-HSP70-1A		Created from GFP-tagged version obtained from addgene.
pCR3-Flag-HSP70-1A-190-511		
pCR3-Flag-HSP70-1A-362-511		
pCR3-Flag-HSP70-1A-394-511		
pCR3-Flag-HSP70-1A-K71E		HSP70-1A mutant lacking ATPase activity (Zeng et al., 2004). Cloned from GFP-tagged version obtained from addgene.
pCR3-Flag-HSP70-1A-NBD		Construct coding for the NBD (aa 1-385) of HSP70-1A.
pCR3-Flag-HSP70-1A-NBD-GG-DE		HSP70-1A-NBD with G201D and G202E substitutions, impairing ATP binding (Morgan et al., 2013).
pCR3-Flag-HSP70-1A-NBD-K71E		HSP70-1A-NBD mutant lacking ATPase activity (Zeng et al., 2004).
pCR3-Flag-HSP70-1A-SBD		Flag-tagged substrate binding domain (aa 394-641) of HSP70-1A.
pCR3-HA-HSP70-1A		
pEGFP-HSP70-1A-K71E	L. Greene (Addgene plasmid # 15216)	HSP70-1A mutant lacking ATPase activity (Zeng et al., 2004).
pCR3-Flag-TBK1	K. Schumann	
pEFBos-Flag-ΔRIG-I	A. Krug	Expression construct coding for the CARDs of RIG-I (Yoneyama et al., 2004).
pCR3-Flag-IKKε	K. Schumann	
pCR3 (empty vector)	Invitrogen	Mammalian expression plasmid.
pCAGGS (empty vector)	A. Garcia-Sastre	Mammalian expression plasmid.
pET28a	Invitrogen	Plasmid for bacterial expression.

pCAGGS-HA-GST		
pFLAG-IRF3	M. Rieder	
pTIT-N	Finke and Conzelmann (1999)	T7 polymerase and EMCV-IRES-dependent expression of the corresponding RABV proteins.
pTIT-P		
pTIT-L		
Reporter gene constructs		
p125-Firefly-Luciferase	T. Fujita	Construct coding for Firefly luciferase under control of the IFN-β promoter.
p55A2-Firefly-Luciferase	T. Fujita	Construct coding for Firefly luciferase under control of repeated IFN-β promoter PRDII elements; responsive to NF-κB.
p55C1B-Firefly-Luciferase	T. Fujita	Construct coding for Firefly luciferase under control of repeated IFN-β promoter PRDI elements; IRF3 responsive.
pCMV-Renilla-Luciferase	Promega	Construct coding for *Renilla* luciferase under control of the CMV promoter.
pISRE-Firefly-Luciferase	Clontech	Construct coding for Firefly luciferase under control of the ISRE promoter.
pTK-Renilla-Luciferase	Promega	Construct coding for *Renilla* luciferase under control of the HSV-thymidine kinase promoter.
Full length Rabies virus rescue constructs		
pSAD-T7-HH-L16-SC	Ghanem et al. (2012)	Full length L16 cDNA rescue construct.
pSAD-T7-HH-L16-P-W186A-SC		L16 full length rescue constructs containing the indicated mutations in the P gene.
pSAD-T7-HH-L16-P-K214A-SC		

Table 9: List of plasmids used in this thesis.

3.1.12. Recombinant Viruses

Recombinant rabies viruses were created from cDNA with a reverse genetics approach (Ghanem et al., 2012; Schnell et al., 1994). For rescue procedure see 3.2.13. The following recombinant viruses were used in this thesis:

- SAD-L16 (wild type vaccine strain)
- SAD-L16 P-W186A (described in this thesis)
- SAD-L16 P-K214A (described in this thesis)

3.2. Methods

3.2.1. Polymerase chain reaction (PCR)

With a polymerase chain reaction (PCR), specific DNA sequences can be amplified *in vitro* by repetitive steps of double strand melting, annealing of specific primers and elongation by a heat resistant DNA polymerase. In this thesis, a T3 Thermocycler (*Biometra*) was used for the reactions. The correct size of the generated DNA fragments was validated by agarose gel electrophoresis and a 1 kb DNA Ladder (NEB) as size standard. Reaction products were purified using the QIAquick® PCR Purification Kit. The following buffer components and reaction properties were used for the corresponding PCR reactions:

- **Standard PCR reaction**

Enzyme/buffer	Volume
Template	1 µl (1 pg – 10 ng)
Primer 1 (10 µm)	5 µl
Primer 2 (10 µm)	5 µl
5 x buffer	20 µl
dNTPs	1 µl
DMSO	3 µl
Phusion DNA Polymerase	1 µl
ddH_2O	64 µl

Reaction settings: 30 s 95 °C, 10 s 95 °C, 30 s 56 °C, 15 s/kb 72 °C (30 cycles), 10 min 72 °C.

- **Mutagenesis PCR**

Enzyme/buffer	Volume
Template	1 µl (1 pg – 10 ng)
Primer 1 (10 µm)	2.5 µl
Primer 2 (10 µm)	2.5 µl
10 x buffer	10 µl
dNTPs	1 µl
Pfu DNA Polymerase	1 µl
H_2Odd	82 µl

Reaction settings: 3 min 95 °C, 40 s 95 °C, 1 min 50 °C, 12 min 72 °C (30 cycles), 10 min 72 °C.

3.2.2. Plasmid construction

- **Digest and purification**

For the construction of expression plasmids, specific DNA restriction sites and epitope tags were attached to the desired inserts by PCR amplification and suitable primers. The purified PCR product (QIAquick PCR Purification Kit) and approximately 5 µg of the target plasmid were digested with 20 units each of the corresponding restriction enzymes (incubation at 37 °C, 2 h or over-night) according to the manufacturer's (*NEB*) instructions. To prevent re-ligation, the vector reaction mix was incubated for at least 1 h at 37 °C with 1 µl CIAP after the digestion. Insert and plasmid DNA were subsequently purified by agarose gel purification (QIAquick Gel Extraction Kit) and taken up in a volume of 30 µl ddH_2O.

- **Ligation reaction**

The ligation reaction was carried out at RT for 30 min or at 4 °C overnight using T4 DNA ligase (NEB) in a volume of 20 µl according to the manufacturer's manual. Alternatively, "Instant Sticky-End Ligase Master Mix" (NEB) was used to perform ligations according to the manufacturer's instruction. For the creation of expression constructs with specific mutations the mutagenesis PCR products were at first incubated with 1 µl DpnI at 37 °C for 3 h prior to agarose gel purification. This way, the template DNA of the PCR reaction which does not contain the desired mutation can be specifically degraded, since DpnI only cuts methylated DNA, a modification which is found in bacterial DNA, such as the PCR template.

- **Transformation**

50 µl of chemically competent *E. coli* (XL-1 blue, *Stratagene*) were mixed with either 10 µl ligation reaction or 10 µl of mutagenesis PCR product and incubated for 5 min on ice. After a 42 °C, 2 min heat shock and 2 min on ice the cells were supplemented with 250 µl LB++ medium and shaken for 30 min at 37 °C. The bacteria suspension was then transferred to selective LB plates containing 100 µg/ml ampicillin or kanamycin and incubated at 37 °C o/n.

- **Mini preparation**

Colonies grown o/n on selective LB-plates were picked and transferred to 1 ml selective LB medium and incubated on a shaker at 37 °C o/n. After harvesting by centrifugation (14 000 rpm, 1 min) the cell pellet was resuspended using 200 µl Flexi I solution. The cell suspension was then lysed by incubation with Flexi II for 5 min at RT and neutralized with 200 µl Flexi III (5 min on ice). After removal of cell debris (7 min, 14 000 rpm) the DNA was precipitated from the supernatant with 400 µl isopropanol. After another centrifugation step (7 min, 14 000 rpm) the DNA pellet

was washed with 200 µl 70 % ethanol, dried at RT and solubilized in 50 µl ddH_2O. The success of the plasmid construction was examined by test digestion and agarose gel electrophoresis, using a 1 kb marker to validate the correct insert size. Promising mini preparation samples were then send in for validation by sequencing (performed by *GATC Biotech*).

- **Midi preparation**

To obtain a midi preparation of DNA plasmids, 1 µl mini- or midi-preparation of a construct was first transformed into chemically competent XL-1 blue *E. coli* as described previously. Single colonies grown o/n were used to inoculate 50 ml selective LB-medium. The bacteria were incubated in shaking culture at 37 °C o/n and subsequently harvested by centrifugation (3500 rpm, 20 min). Plasmid DNA was then extracted from the pellets using the Nucleobond® Xtra Midi kit (*Macherey & Nagel*) according to the manufacturer's instructions.

3.2.3. Cell culture

HEK 293T, BSR T7, HeLa and HEp-2 cells were used in this thesis and stored in incubators at 37 °C with 5 % CO_2. The cells were cultured in T25 or T75 culture flasks under sterile conditions with the media described in the materials section. Cell growth was monitored and cells were passaged every 3 - 4 days and detached by removal of media and incubation in an appropriate volume of Trypsin-EDTA 0.25 % (*Gibco*), followed by 1:8 – 1:12 dilution with the corresponding media (D-MEM 3+ for HEK 293T, HeLa and HEp-2 and G-MEM 4+ for BSR T7).

3.2.4. Immunofluorescence imaging

HeLa cells grown to confluency in a T25 cell culture flask were trypsinized and resuspended with 20 ml fresh D-MEM 3+. A volume of 250 µl of this cell suspension was seeded in a total volume of 600 µl onto 12 mm Ø microscope cover glasses placed into 24-well plates. After incubation overnight the cells were transfected with expression plasmids coding for the protein of interest using Lipofectamine™ 2000 in Opti-MEM. In case fluorescent proteins were used, all following incubation steps were conducted in the dark to prevent photobleaching. 24 h p. t. the medium was removed, cells were washed once with PBS and fixed with cold 4 % PFA in PBS for 20 min at RT. Fixation and the following steps, including the staining procedure, were carried out with the cover glasses still inside 24-well plates. Cells were washed with PBS and incubated with 50 mM NH_4Cl in PBS for 10 min at RT. After another PBS washing step the cells were incubated with 0.5 % Triton X-100 in PBS for 10 min in order to permeabilize cellular membranes. Cells were

subsequently washed three times with PBS and blocked for 20 min with 2.5 % milk in PBS. Following a PBS washing step, cells were incubated with primary antibodies diluted in PBS for 1 h at 37 °C in a cell culture incubator. The wells were washed thrice with PBS and incubated with secondary antibodies coupled to a fluorescent dye and TO-PRO®-3 diluted in PBS. Finally the samples were washed again three times with PBS, once with deionized water and the cover glasses with the fixed and stained cells were mounted to microscope slides using Vectashield HardSet Antifade Mounting Medium (*Vector Laboratories*). After hardening of the mounting medium overnight the specimen were monitored using a Axiovert 35 confocal laser scanning microscope (*Zeiss*).

3.2.5. Transfection

Cells cultivated in T25 or T75 culture flasks and grown to confluence were used for seeding. The cells were trypsinized and resuspended in 10 ml (T25) or 30 ml (T75) of the appropriate medium.

The following cell amounts were seeded in the corresponding culture dishes and incubated o/n if not indicated otherwise:

Culture dish	Cell number	Total volume
100 mm dish	$1.6 * 10^6$	12 ml
60 mm dish	$6.2 * 10^5$	3.5 ml
6-well plate	$3.1 * 10^5$	2.0 ml
24-well plate	$5.2 * 10^4$	600 µl
96-well plate	$1,6 * 10^4$	100 µl

Cell growth was monitored by microscopy. Transfection of plasmids was performed using 2.5 µl Lipofectamine™ 2000 (*Invitrogen*) or (polyethyleneimine, 1 mg/ml) per µg DNA. Transfection reagent and DNA were pre-incubated separately with D-MEM w/o additives or Opti-MEM for 5 min. DNA solution and media with Lipofectamine™ 2000 or PEI were then mixed and incubated for 20 min, before the mixture was added to the cells.

3.2.6. Dual luciferase reporter gene assay

To analyze the influence of different protein constructs on innate immune signaling pathways, the Dual Luciferase® Reporter Assay System (*Promega*) was used for reporter gene assays. This reporter system employs luminescence resulting from Firefly luciferase expression under the

control of the promoter of interest. In this thesis, Luciferase expression driven by the IFN-promoter (p125-FF-Luc.), artificial IRF3-promoter (p55C1B-FF-Luc.), NFκB-promoter (p55A2-FF-Luc.) and the ISRE-promoter (pISRE-Luc.) were used as reporter plasmids. The luminescence of constitutive TK- (HSV-thymidine kinase) or CMV-(human cytomegalovirus immediate-early) promoter driven Renilla luciferase expression was used for normalization.

100 ng of the reporter plasmid and 10 ng pCMV-Renilla or pTK-Renilla were co-transfected with the plasmids of interest into HEK 293T cells in a 24-well cell culture plate. Mock transfections were carried out using empty vector plasmid DNA. Cells were lysed 24 h p. t. using 200 µl passive lysis buffer (PLB, *Promega*) and 40 µl lysate was subsequently subjected to luminescence measurement using a Centro LB 960 Luminometer (*Berthold*). The samples were each first incubated with 40 µl firefly-substrate to measure reporter activity, followed by injection of 40 µl renilla substrate to obtain luminescence values for normalization from the constitutively expressed renilla luciferase construct. Protein expression levels from the lysates were examined using SDS-PAGE and Western blotting.

3.2.7. Real-time PCR

In order to measure IFN gene transcription in response to different stimuli, IFN-β mRNA levels were examined using real-time PCR. HEK 293T cells in 24-well culture plates were transfected with the plasmids coding for the proteins of interest, infected with recombinant rabies virus or treated with SeV-DIs according to the experimental setup. Cells were harvested 48 h after infection and total RNA was extracted using the "RNeasy mini kit" from *Quiagen* following the manufacturer's protocol. RNA was transcribed into cDNA by first incubating 6.5 µl RNA with 0.5 µl oligodT primer dilution at 65 °C for 10 min. Subsequently, 5x reaction buffer (2 µl), RNAsin (0.25 µl), dNTPs (25 mM, 0.4 µl) and RT enyzme (0.25 µl) were added and the rection mix was incubated at 55 °C for 30 min, followed by a final incubation step at 85 °C for 10 min. The resulting cDNA was used as template in a real-time PCR reaction with the QuantiNova SYBR Green PCR kit (*Quiagen*) using a *Roche* LightCycler 96. The PCR data was relatively quantified to mock controls using the $2^{-\Delta\Delta C_t}$ method (Livak and Schmittgen, 2001). TATA binding protein (TBP) mRNA levels were used for normalization.

Primer	Sequence
IFN-β forward	TCC AAA TTG CTC TCC TGT TG
IFN-β reverse	GCA GTA TTC AAG CCT CCC AT
RABV P forward	ATGGTCACAGACCGTAGAAG

RABV P reverse	GATGATTGGCTTTCTCTCTG
TBP forward	TGC ACA GGA GCC AAG AGT GAA
TBP reverse	CAC ATC ACA GCT CCC CAC CA

Table 10: Primers used for real-time RT-PCR.

3.2.8. Co-Immunoprecipitation (Co-IP)

Co-immunoprecipitation was used to identify protein-protein interactions. HEK 293T cells were seeded in a 6 cm dish or in 6-well plates and transfected with plasmid constructs coding for the proteins of interest. One of the potential interaction partners was fused to a tag suitable for immunoprecipitation (HA-, or Flag-tag). 24 h p. t. the cells were detached from the dish with 1 ml PBS. After centrifugation (5 min, 4 °C, 2500 rpm), the cell pellets were lysed with 500 µl Co-IP buffer. Following 30 min – 2 h incubation, cellular debris was removed by another centrifugation step (10 min, 4 °C, 14 000 rpm) and 10% of the sample (50 µl) was taken as a control for the total amount of protein expression. The remaining supernatant was incubated with a suitable amount of anti-HA magnetic beads (*Pierce*) for 3 h or overnight.
Using this method, FLAG- or HA-tagged proteins can be specifically bound to an affinity matrix, which carries immobilized antibodies against the corresponding epitope tags. Untagged proteins that bind specifically to the target protein can thus be co-precipitated. Unspecifically bound proteins were removed by washing three times with 500 µl Co-IP buffer. After the last washing step and removal of supernatant, the samples were eluted with 75 µl SDS sample buffer and further examined by SDS-PAGE and Western blotting.

3.2.9. Denaturing polyacrylamide gel electrophoresis (SDS-PAGE)

Bis-Tris polyacrylamide gels (developed by Updyke & Engelhorn for *Invitrogen*, US patent 6162338) were used to separate proteins by their apparent molecular weight. A 6 % stacking gel was used on top of a 10 % separating gel in a *Peqlab* gel chamber (for gel composition see 3.1.3). Protein lysates were incubated with an appropriate volume of SDS sample buffer and heated to 95 °C for 10 min. Precision Plus Protein™ Standard (*Biorad*) was loaded in addition to the samples as a marker for size determination of protein bands. Using 1x MOPS as running buffer, the gels were run at 175 V for about 2.5 h under water-cooling. Subsequently, the protein bands on the gel were where either stained directly (3.2.10) or visualized by immunostaining after Western blotting (3.2.11).

3.2.10. SDS-PAGE gel staining methods

In order to directly visualize protein bands on SDS-gels, staining with colloidal coomassie was performed. The solution was prepared as previously described (Dyballa and Metzger, 2012). First, the gel was washed three times for 10 min on a horizontal shaker with deionized water. Subsequently the gel was covered in colloidal coomassie staining solution and incubated for 2 - 6 h until the desired staining intensity. After staining, the gel was rinsed twice with deionized water and incubated for 10 – 60 min with destainer. After destaining the gel was rinsed with water twice and stored in water for further analysis and imaging (Dyballa and Metzger, 2012).
For a more sensitive staining the SilverQuest™ Silver Staining Kit (*Life Technologies*) was used according to the manufacturer's instruction.

3.2.11. Western blotting

The transfer buffer used for Western blotting in this thesis (here termed "extra-dry") was previously described (Garic et al., 2013). A semi-dry blotting system (*Peqlab*) and Immobilon PVDF-membranes (*Millipore*) were used for Western blotting. PVDF Membranes were activated by soaking shortly in pure methanol. Separating gels from SDS-PAGE and activated membranes were separately equilibrated with extra-dry buffer for 10 min under constant agitation. Blotting chambers were assembled by putting the gel on top of a membrane in between extra-dry buffer soaked stacks of three blotting paper sheets. The electro-blotting was performed for 45 min with 1000 mA for 2 gels and at 650 mA for 1 gel. Using this method, proteins can be transferred from a denaturing polyacrylamide gel onto a membrane and thus be immobilized. To avoid unspecific binding of antibodies, the membrane was blocked with either 2.5 % milk powder or 2.5 % BSA in TBS-T for at least 30 min at RT. To visualize specific protein bands, primary antibodies diluted in TBS-T (dilutions as described in the materials section) were applied and incubated on the membrane overnight at 4 °C under constant agitation. After three 10 min washing steps with TBS-T, suitable secondary antibodies were applied and incubated for 2 h at RT on a horizontal shaker. All secondary antibodies used for Western blotting in this thesis were conjugated with HRP (horseradish peroxidase). After incubation the membrane was washed three times with TBS-T for 10 min. For the final detection step WesternBright ECL Spray (*Advansta*) was applied to the membrane according to the manufacturer's instructions. The chemiluminescence was directly imaged using the Fusion FX7 system (*Vilber-Lourmat*).

3.2.12. Purification of recombinantly expressed proteins

Electrocompetent Rosetta strain *E. coli* were transformed with about 500 ng pET28a expression plasmid coding for the His_6-tagged protein of interest on **day 1**, transferred to a selective LB plate containing 100 µg/ml kanamycin and incubated overnight at 37 °C. A single colony from the selective LB plate was used on **day 2** to inoculate 100 ml selective LB medium that was grown overnight in a cell culture incubator at 37 °C. 1 l selective LB medium was inoculated using 15 ml of the overnight culture on **day 3** and incubated with agitation at 37 °C. Bacteria growth was monitored by measuring OD_{600} values using a Nanodrop ND-1000 Spectrophotometer. Between an OD_{600} of 0.5 and 0.8 protein expression was induced with 0.5 mM IPTG and the culture was incubated at 20 °C overnight. On **day 4** the bacteria were harvested by centrifugation at 4000 g, 4 °C for 20 min, resuspended on ice in 30 ml cold purification buffer A and incubated with a spatula tip of lysozyme for 1 - 2 h at 4 °C in a 50 ml falcon under constant agitation. Subsequently the cells were disrupted by sonication for 3 min total pulse time with 3 s pulses interrupted by a 2 s pause in an ice cooled water bath. Cell debris and undisrupted cells were removed by centrifugation at 8000 g, 4 °C for 45 min. 1.5 ml HisPur™ Cobalt Superflow Agarose (*Thermo Fisher Scientific*) was added to a 10 ml centrifuge column and equilibrated with 2 column volumes of purification buffer B by gravity flow. Afterwards the lysates previously cleared by centrifugation were loaded onto the column and samples were collected from the flow through fraction. The column was washed 4 times with 10 ml purification buffer B and samples were taken from each of these washing fractions. Subsequently, the bound protein was eluted in three fractions with 3 ml elution buffer each. Success of the purification process was evaluated by subjecting the collected samples to SDS-PAGE (3.2.9) and colloidal coomassie staining (3.2.10).

3.2.13. Virus rescue

A rescue of replication competent rabies virus particles from cDNA requires the generation of functional viral RNA genomes in the cytoplasm of a cell as well as the production of viral structural proteins necessary for transcription and replication. This method relies on the BSR T7 cell line, which expresses T7 polymerase constitutively (Buchholz et al., 1999). Co-transfection of different T7 promoter driven expression plasmids leads to the generation of genomic RNA transcripts in the cytosol and the viral structure proteins N, P and L. With a certain chance, encapsidation of the genomic RNA with nucleoprotein N occurs, leading to the generation of a

functional genome, which can act as new template for both viral transcription and replication by the Polymerase L and its cofactor P. Such a rescue event results in the ongoing propagation of viral particles (Schnell et al., 1994). This method was further optimized in the Conzelmann group by usage of self-processing ribozymes in the full length genomic construct leading to correct processing of the ends of the genomic RNA and therefore a significant increase in successful rescue events (Ghanem et al., 2012). Since the template for the generation of viral genomic RNA is a DNA plasmid, the sequence can be determined by standard molecular biological techniques. This enables the introduction of mutations and deletions as well as the insertion of recombinant proteins in the rabies virus genome.

As a first step in the virus rescue procedure, a T25 cell culture flask of BSR T7 cells grown to confluency was split 1:20 on **day 1** and 2 ml of cell suspension (approximately $3*10^5$ cells) was seeded per 6 well. 1 h prior to transfection of rescue constructs, cells were washed once with D-MEM (no additives) and 1 ml D-MEM (no additives) was added to the cells. The following transfections were carried out using the Mammalian Transfection Kit (*Agilent Technologies*) based on the $CaPO_4$ method. 10 µg of the viral cDNA rescue construct in a volume of 40 µl was mixed with 50 µl of a mix containing 5 µg pTIT-N, 2.5 µg pTIT-P and 2.5 µg pTIT-L coding for the corresponding viral proteins (NPL-mix). In order to evaluate the transfection efficiency, 10 µg pTIT-eGFP was used as control in a separate sample. The DNA solution was mixed with 10 µl of transfection reagent #1 and put on ice for 5 min. Subsequently, 100 µl of transfection reagent #2 was added and after incubation at room temperature for 10 – 20 min the transfection mix was added to the cells dropwise (1 h after the cells have been initially washed with D-MEM). 3.5 h after transfection the medium was removed, cells were washed once with G-MEM 4+ and supplemented with 2 ml G-MEM 4+. On **day 3** success of transfection was monitored by confirming green fluorescence in cells transfected with pTIT-eGFP control plasmid using a fluorescence microscope. Fresh BSR T7 cells grown to confluency were split 1:10 on **day 5** and 1 ml cell suspension (approximately $3*10^5$ cells) was seeded per 6-well. 2 h later, the supernatant of the previously transfected rescue cells was cleared from cell debris by centrifugation and added to the newly seeded BSR T7 cells (passage 1) and replaced by fresh G-MEM 4+. On **day 8** rescue cell supernatants were passaged for a second time to newly seeded cells like on day 5. Cells previously incubated with passage 1 on day 5 were stained for viral N protein using FITC Anti-Rabies Monoclonal Globulin (for fixation and staining procedure see 3.2.14) and monitored for viral foci indicating successful rescue. In addition, the transfected rescue cells were detached using 500 µl trypsin-EDTA and taken up in 1.5 ml G-MEM 4+. 1.5 ml of this cell suspension was transferred to a T25 flask and taken up in a total volume of 8 ml GMEM-4+. 1.5 ml G-MEM 4+

were added to the remaining 500 µl cell suspension and seeded again into 6-well plates. On **day 10** the cells incubated with passage 2 supernatant as well as the rescue cells split to 6-wells on day 8 were fluorescence labeled for viral proteins and also monitored for successful rescue. In case of a positive rescue 8 ml supernatant of rescue cells previously split to a T25 cell culture flask was taken, cleared from cell debris by centrifugation at 1800 rpm, 5 min, 4 °C and stored at -80 °C in 1 ml aliquots. The cells were provided with 8 ml fresh G-MEM 4+ and supernatants were taken and stored again on **day 12**. Rescue supernatants were subsequently titrated to obtain the amount of focus forming units per volume (3.2.15) and used at a defined MOI in order to create virus stocks (3.2.16).

3.2.14. Fluorescence labeling of RABV infected cells

In order to label rabies virus infected cells for fluorescence microscopy, the supernatant was disposed and cells were washed once with PBS and once with cold 80 % acetone. Subsequently, cells were fixed by adding cold 80 % acetone and incubation for 20 min at 4 °C. Acetone was removed and the fixed cells were air dried before of a suitable amount of FITC Anti-Rabies Monoclonal Globulin (*Fujirebio Diagnostics*) was added and incubated for 2 h at 37 °C in a cell culture incubator. Afterwards, cells were washed 2 times with PBS and monitored under a fluorescence microscope.

3.2.15. Titration of virus preparations

In order to determine the amount of infectious particles per volume (focus forming units per ml, ffu/ml) in viral supernatants, BSR T7 cells were infected with serial dilutions as described below, stained for virus infected cells (3.2.14) and the number of viral foci was determined. Confluent BSR T7 cells in a T25 cell culture flask were detached with trypsin and resuspended in 20 ml G-MEM 4+. 100 µl of the cell suspension per well were seeded to 96-wells. 450 µl medium was mixed with 50 µl of the original viral supernatant or the previous dilution step. Thus 7 serial dilutions were created, ranging from 10^{-2} – 10^{-8}. BSR T7 cells were infected in duplicates with 100 µl of the original supernatant or the serial dilutions and fixed and stained 48 h p. i. (3.2.14). Wells containing a numerable amount of foci were counted and used for calculating viral titers for the corresponding supernatants.

3.2.16. Virus stock production

For the production of viral stocks BSR T7 cells grown to confluency were split 1:3 and transferred to a new T25 flask in a total volume of 8 ml G-MEM 4+ on **day 1**. 3 h later, cells were infected with a defined MOI of 0.01 of a previously titrated virus rescue supernatant. On day 3, the supernatant of the cells was transferred to a 15 ml falcon tube, cleared form cell debris by centrifugation at 1800 rpm, 5 min at 4 °C, split up in 1 ml aliquots and stored at - 80 °C. Cells were supplied again with 8 ml fresh G-MEM 4+. Supernatant was harvested again in the same way on day 5. Subsequently, titers of the viral stocks were determined (3.2.15) and used for further experiments.

3.2.17. Virus growth curves

Growth kinetics of specific viruses were examined by determination of viral titers of the supernatant at 4.5 h, 24 h, 48 h, 72 h and 96 h past infection. BSR T7 cells grown to confluency were split 1:3 to a T25 flask (approximately $1*10^6$ cells) in total volume of 8 ml G-MEM 4+ and infected 3 h later with a MOI of 0.01. 4.5 h past infection, directly before harvesting the first supernatant, cells were washed once with medium in order to remove input virus and supplied again with 8 ml G-MEM 4+. For every time point 1 ml of the supernatant was harvested and stored at -80 °C in two 500 µl aliquots, while the volume of removed supernatant was replenished with fresh medium. All supernatants were subsequently titrated (3.2.15) and the results plotted to obtain a time-dependent growth curve.

4. Results

4.1. Mapping of RABV P residues essential for inhibition of IFN-induction

The rabies virus phosphoprotein (RABV P) is one of the most potent known interferon antagonists. It exercises its dual function on two different levels of innate immune signaling, making it a very efficient inhibitor of the antiviral response. First, RABV P circumvents induction of Interferon-β (IFN-β) after RIG-I activation by blocking phosphorylation of interferon regulatory factor 3 (IRF3), which is the central IFN-β transcription factor (Brzózka et al., 2005; Hiscott, 2007). In addition, also signal transduction of type I interferons is suppressed by a specific binding of RABV P to activated STATs (Brzózka et al., 2006). This results in cytosolic retention of STAT molecules, thus preventing the induction of interferon-stimulated genes (ISGs). Due to this dual strategy, RABV P exhibits a very strong suppressive capacity in regard to cellular innate immunity. While RABV P region 176-186 could previously be identified as crucially required for inhibition of IFN-β induction and viral pathogenicity (Rieder et al., 2011), its precise function or mechanistic role in inhibition is still unknown. In order to pin down the RABV P regions critical for the inhibitory function, several truncation- as well as amino acid substitution mutants of P were created and assayed for their ability to inhibit IFN-β induction under different conditions. This is particularly interesting, since the RABV P region identified to be crucial for inhibition is located in a domain of the protein that is considered to be intrinsically disordered (Gerard et al., 2009). Narrowing down inhibitory function to a disordered region might allow for future application as a peptide that retains suppressive capacity. If not mentioned otherwise, in this thesis “P” is always referring to the SAD-L16 strain rabies virus phosphoprotein.

4.1.1. Inhibition of TBK1 mediated IFN-β promoter activity

Tank-binding kinase 1 (TBK1) and IKK-related kinase epsilon (IKKε) were identified as the kinases required for phosphorylation and thus activation of interferon regulatory factor 3 (IRF3), the major transcription factor driving induction of type I interferon genes (Fitzgerald et al., 2003; Malmgaard, 2004; Sato et al., 2000; Sharma et al., 2003). Overexpression of the kinases alone is sufficient for mediating type I IFN-induction. TBK1 could be shown to be critically involved in RLR signaling, since IRF3 activation mediated by overexpressing constitutionally active RIG-I and MDA5 mutants was significantly impaired in TBK1-deficient MEFs (Yoneyama et al., 2005).

The N-terminal region of RABV P, which is absent in the P_4 isoform, was previously shown to be non-essential for inhibition of TBK1 overexpression-mediated IFN-β induction (Master thesis M. Wachowius (2012)). To examine whether the C-terminus of P is essential for its suppressive capacities, two truncations constructs were created: HA-P-1-197, which lacks the highly conserved C-terminal structured domain, and HA-P-1-174, which is further truncated and lacks the residues 176-186 which have been previously identified to be essential for inhibition by studies characterizing the PΔInd1/2 deletion mutant (Rieder et al., 2011).

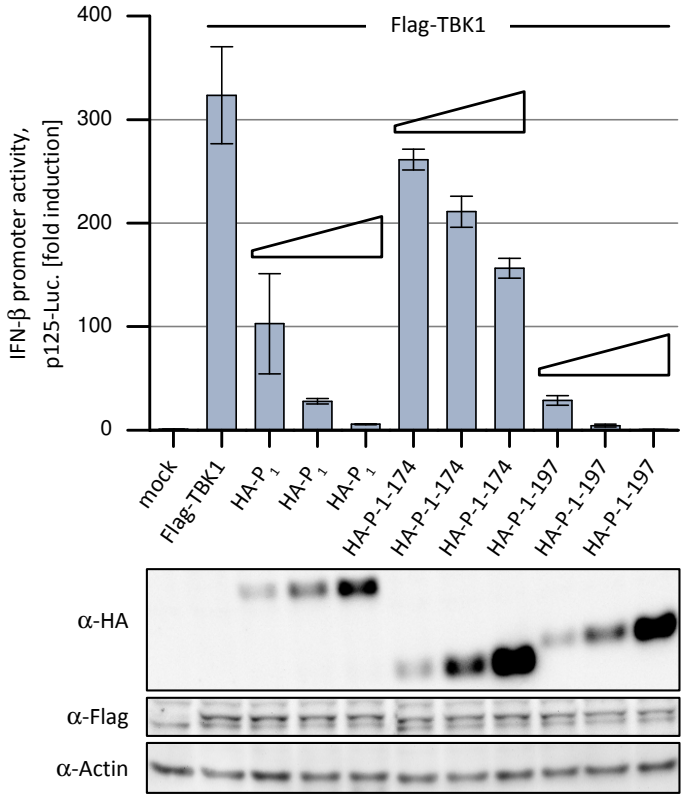

Figure 11: RABV P CTD is non-essential for inhibition of TBK1-mediated IFN-β induction.
HEK 293T cells were transfected with the reporter plasmids (100 ng p125-FF/10 ng pCMV-RL) and increasing amounts of the indicated constructs (200 ng Flag-TBK1, 25, 50 and 100 ng P constructs plasmid DNA). Cells were lysed 24 h p. t. and subjected to dual luciferase assays in order to examine the ability of different P constructs to interfere with TBK1 overexpression-mediated IFN-β promoter activity. While the presence of the ΔInd region (contained in 175-197) is required for inhibition, the entire CTD (residues 197-297) is not. The bars represent the means and the error bars the standard deviations of biological duplicates. The lysates were subjected to SDS-PAGE followed by Western blotting and immunostaining with the indicated antibodies to confirm expression of the constructs.

Together with HA-P_1, a RABV P construct which only produces the full length protein due to mutated alternative internal start codons, the new truncation constructs were assayed for their ability to interfere with TBK1 overexpression-mediated IFN-β promoter activity using dual luciferase reporter gene assays (Figure 11). Whereas HA-P-1-197 abrogated IFN-β promoter activity in a dose dependent way even more efficiently than full length HA-P_1, especially at lower

concentrations, HA-P-1-174 almost completely lost its inhibitory function. This suggests that the structured C-terminal domain of RABV is not essential for counteracting TBK1-mediated IFN-β induction and underlines the importance of the 176-186 region and potentially additional amino acids between positions 186 and 197.

A number of additional C-terminal truncations were created in order to further narrow down RABV P residues involved in inhibition and so to find the shortest C-terminal truncation still able to interfere with TBK1 overexpression-mediated IFN-β reporter activity. Therefore, the new constructs were again subjected to IFN-β promoter dependent dual luciferase assays (Figure 12A).

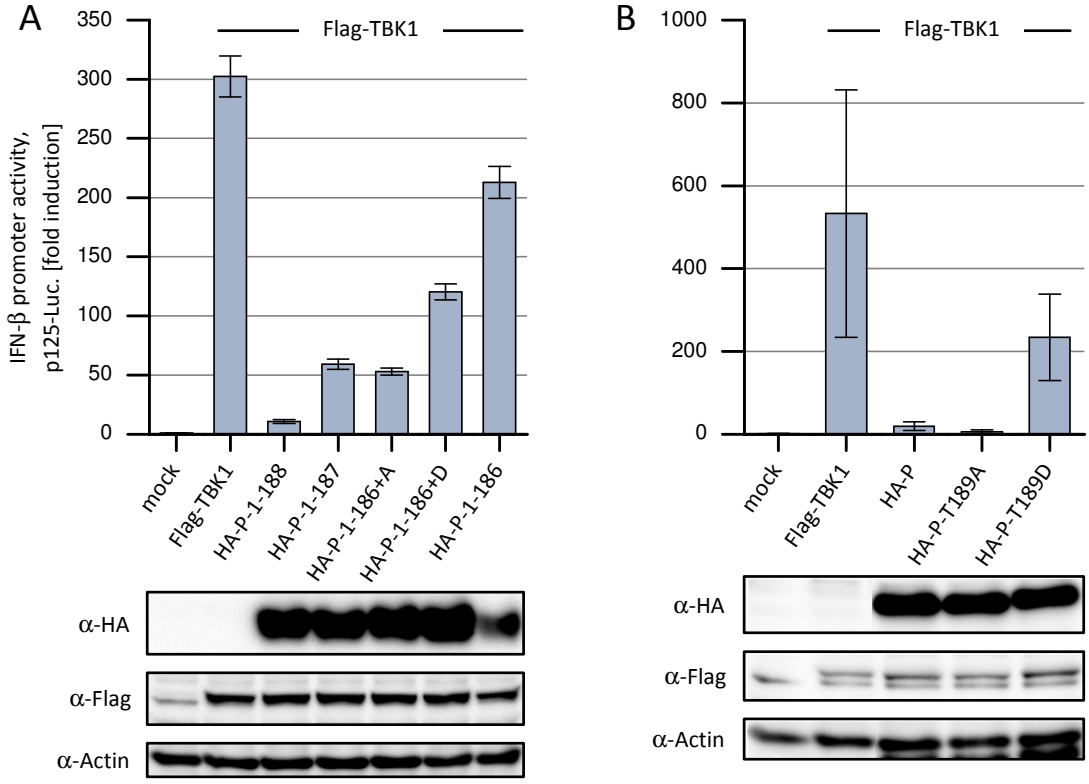

Figure 12: Importance of the RABV P residues C-terminal of the ΔInd sequence.

A) While the RABV P-1-188 truncation exhibits strong inhibitory capacities, truncation by two more residues (resulting in P-1-186) almost completely abrogates inhibition. Position shows no preference for a serine residue, since a substitution by alanine, in contrast to an aspartate substitution, has no negative impact on inhibition. **B)** The substitution of T189, which is in close proximity to the ΔInd region, by an aspartate residue impairs the inhibitory function of RABV P. Experimental conditions for both **A)** and **B)**: HEK 293T cells were transfected with the reporter plasmids (100 ng p125-FF/10 ng pCMV-RL) and the indicated constructs (200 ng Flag-TBK1, 200 ng P constructs plasmid DNA). Cells were lysed 24 h p. t. and subjected to dual luciferase assays in order to examine the ability of different P constructs to interfere with TBK1-mediated IFN-β promoter activity. The bars represent the means and the error bars the standard deviations of biological duplicates. The lysates were subjected to SDS-PAGE followed by Western blotting and immunostaining with the indicated antibodies to confirm expression of the constructs.

P-1-188 was the shortest C-terminal truncation still able to fully inhibit IFN-β promoter activity. Further truncation by two amino acids (P-1-186) lead to an almost complete loss of inhibitory

function. P-1-187 retained some inhibitory abilities but was already impaired in comparison to P-1-188. No significant difference between P-1-187 and P-1-187-S187A (P-1-186+A) could be detected, whereas the phosphomimetic mutant P-1-187-S187D (P-1-186+D) exhibited a stronger defect. This indicates that serine 187 or phosphorylation of this residue are rather not involved in inhibitory function of the RABV P truncation mutants.

In addition to C-terminal truncations, RABV P threonine 189, which is in close proximity to the ΔInd region (primary sequence, ΔInd underlined: 176-QIASGPPALEWSA**T**-189), was examined for a possible involvement in inhibition (Figure 12B). While an alanine substitution at this position showed no phenotype in regard to RABV P inhibitory function, the aspartate mutant was significantly impaired, showing that artificial introduction of charged residues close to the critical ΔInd region (P-176-186) is able to impair the suppressive capacity of P.

As aforementioned, the shortest C-terminal truncation that still allows for suppressive capacity could be identified to be RABV P-1-188. In addition, we further wanted to examine the involvement of the N-terminal domains of RABV P. N-terminal truncations of RABV P corresponding to the P_4 isoform (P-83-297) could already be shown to be not impaired in their ability to interfere with TBK1 overexpression-mediated IFN-β promoter activity (Master thesis M. Wachowius). Therefore, we wanted to examine further N-terminally truncated P proteins in order to find the shortest construct that retains inhibitory efficacy and to determine whether a P-derived peptide alone might be sufficient for the suppressive function. P_4 still contains the dimerization domain ending at amino acid 130, followed by a disordered region, which contains a DLC8 binding site that is conserved among the *Lyssavirus* genus (Jacob et al., 2000), as well as the ΔInd motif. We wanted to examine whether one of these specific features directly contributes to inhibition. However, only weak and insufficient expression levels for some N-terminally truncated RABV P constructs were observed (data not shown). To ensure good and comparable expression levels, a HA-GST construct (Figure 13B) was fused to N-terminally truncated P forms, as well as P-derived peptides. The HA-tag was introduced for detection and use in pulldown experiments, while GST (*Schistosoma japonicum* glutathione S-transferase) was included for stabilization (Smith, 2000). RABV P residue 188 was used as most C-terminal amino acid according to the results obtained before. P peptides of different length ranging from residue 130 (lacking the dimerization domain), 153 (lacking the DLC8 binding site, Jacob et al. (2000)), 168, 170, and 176 to the common C-terminal residue 188 were cloned into the HA-GST construct and assayed for their ability to interfere with Flag-TBK1 overexpression mediated IFN-β promoter activity (Figure 13A).

The HA-GST-P-176-188 construct, consisting only of the ΔInd1/2 motif and the following two amino acids (amino acid sequence: QIASGPPALEWSA) was found to be completely deficient in inhibition. All the other investigated peptides showed inhibitory abilities to some degree. Removal of the DLC8 binding site (from residue 130 to 153) showed no appreciable change in suppressive capacity. Even though full length HA-P showed a significantly stronger inhibition compared to all peptide constructs, partial inhibition of TBK1 overexpression mediated IFN-β promoter activity could be achieved with short, disordered P-derived peptides. Oddly, the degree of inhibition did not change significantly with removal of specific features, but correlated rather with overall construct length.

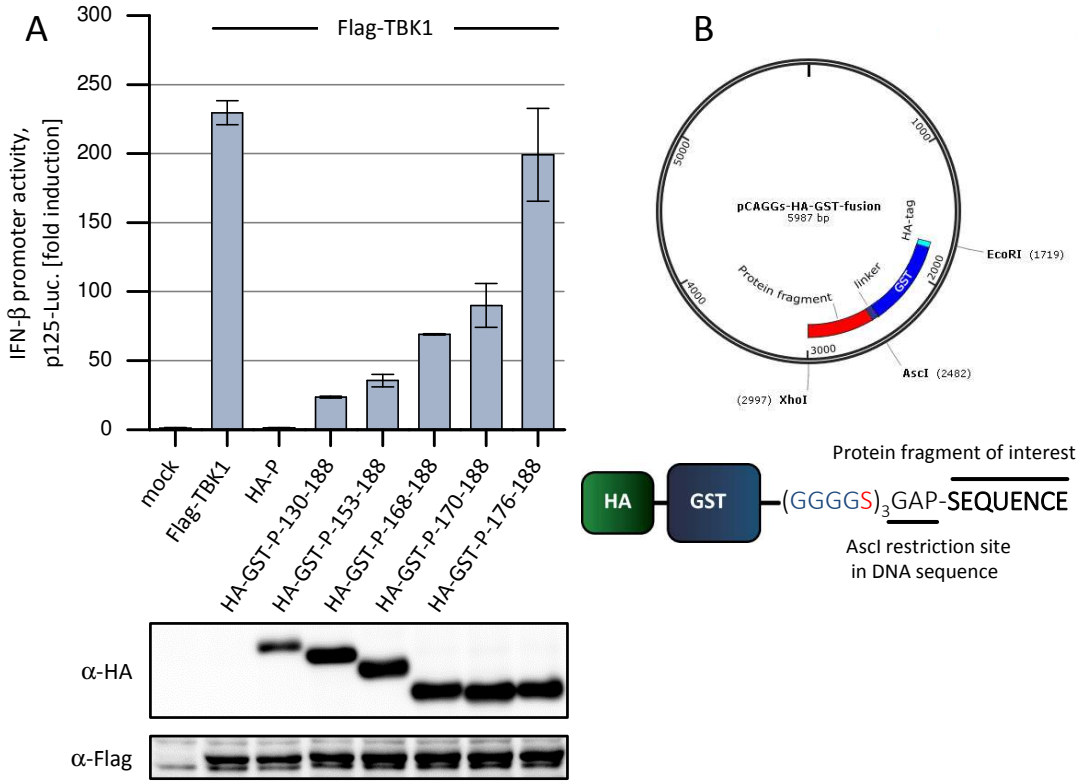

Figure 13: P fragments containing the ΔInd-region inhibit TBK1-mediated IFN-β induction with increasing N-terminal extension.

A) While only wild type HA-P suppresses reporter activity to basal levels, the HA-GST fusion peptides encompassing residues 176-186 (ΔInd region) exhibit some inhibitory function with increasing N-terminal extension. The shortest construct HA-GST-P-176-188 exhibits no suppression of IFN-β reporter activity. HEK 293T cells were transfected with reporter plasmids (100 ng p125-FF/10 ng pCMV-RL) and the indicated constructs (200 ng Flag-TBK1, 200 ng P constructs plasmid DNA). Cells were lysed 24 h p. t. and subjected to dual luciferase assays in order to examine the ability of different GST-P fusion constructs to interfere with IFN-β promoter activity mediated by Flag-TBK1 overexpression. The bars represent the means and the error bars the standard deviations of biological duplicates. The lysates were subjected to SDS-PAGE followed by Western blotting and immunostaining with the indicated antibodies to confirm expression of the constructs. **B)** Plasmid map and schematic figure of HA-GST-construct. AscI/XhoI restriction sites allow easy insertion of different P-derived sequences into the plasmid, resulting in HA-GST-tagged versions.

In the previously shown experiment, interferon promoter activity was induced by overexpression of TBK1. Together with IKKε, this kinase is responsible for activation of IRF3 (Fitzgerald et al., 2003; Sharma et al., 2003). The N-terminal tandem CARD domain of RIG-I (ΔRIG-I) was previously shown to be essential and sufficient for signal transduction and constitutively induces transcription of IFN-β (Yoneyama et al., 2004). In the absence of triggering PAMPs, the CARD domains of RIG-I are normally auto-inhibited to prevent signaling (Saito et al., 2007). Therefore, overexpression of ΔRIG-I is an effective method to mimic active RIG-I signaling. To elucidate whether truncated forms of RABV P also inhibit RLR pathway signaling when employing different stimuli than TBK1 overexpression, the following reporter gene experiment was conducted using ΔRIG-I. RABV P Inhibition of IFN-β promoter activity induced either by Flag-TBK1 or Flag-ΔRIG-I (RIG-I residues 1 to 229) overexpression was examined in reporter gene assays using HA-GST-P-83-297 (P_4 isoform) and its truncation HA-GST-P-83-197, which lacks the structured C-terminal domain (Figure 14A). HA-GST-P-83-297 and HA-GST-P-83-197 both very efficiently inhibited Flag-TBK1-mediated IFN-β promoter activity. Strikingly, HA-GST-P-83-197 completely failed to influence IFN-β promoter activity after ΔRIG-I stimulation. This unexpected result strongly indicates that C-terminally truncated P-constructs cannot be considered a direct inhibitor of TBK1, since TBK1 is supposed to be activated following RIG-I activation or overexpression of ΔRIG-I. A direct inhibitor of TBK1, comparable to a small molecule inhibiting the kinase function, would therefore be expected to inhibit IFN-β promoter activity under both conditions. In addition to TBK1 activation, RIG-I signaling could also trigger the related kinase IKKε, therefore the ability of RABV P and several C-terminal truncations to interfere with IKKε mediated IFN-β induction was examined (Figure 14B). Only HA-P-1-174, which lacks the crucial 176-186 region, failed to abrogate promoter activity. All other P constructs included in the experiment strongly suppressed promoter activation, indicating that RABV P is able to suppress both TBK1 and IKKε overexpression-mediated IFN-β promoter activity. Overexpression of the IRF3 activating kinases TBK1 and IKKε is a rather artificial system for IFN induction and P inhibition might be due to a different mode of action in this case, as compared to normal inhibition of RIG-I mediated IRF3 activation. Due to this discrepancy, RABV P inhibition was further examined in the context of ΔRIG-I stimulation, since we could no longer safely assume that P inhibits natural IFN-β induction downstream of TBK1/IKKε.

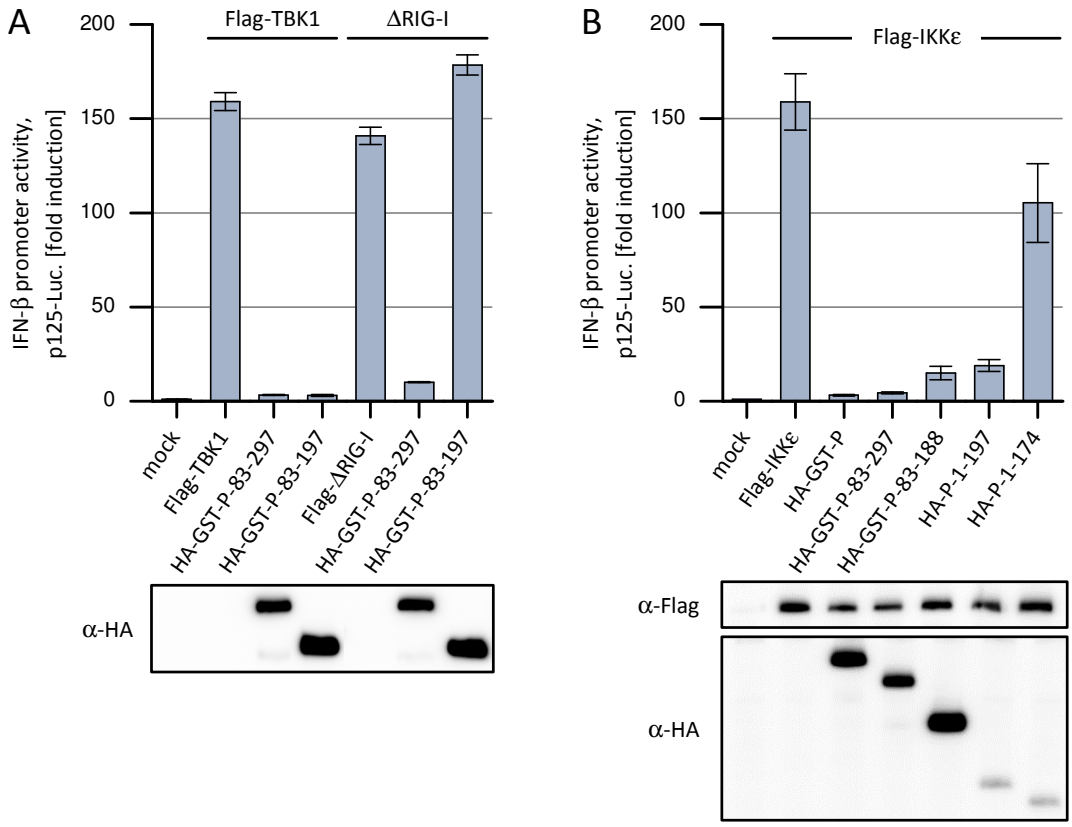

Figure 14: RABV P lacking the C-terminal domain is deficient in inhibiting ΔRIG-I, but not TBK1 or IKKε mediated IFN-β promoter activity.

A) While HA-GST-P-83-297 and HA-GST-P-83-197 interfere very efficiently with TBK1 stimulation, HA-GST-P-83-197, lacking the C-terminal domain, completely fails to prevent ΔRIG-I mediated IFN-β promoter activity. **B)** C-terminal RABV P truncation constructs are able to inhibit IKKε mediated IFN-promoter induction, similar to results obtained before with TBK1. Only HA-P-1-174, which lacks the ΔInd region, fails to interfere with IFN-reporter activity. Experimental conditions for both **A)** and **B)**: HEK 293T cells were transfected with reporter plasmids (100 ng p125-FF/10 ng pCMV-RL) and the indicated constructs (100 ng Flag-ΔRIG-I, 200 ng Flag-TBK1 or Flag-IKKε and 200 ng P constructs plasmid DNA). Cells were lysed 24 h p. t. and subjected to dual luciferase assays in order to examine the ability of different P constructs to interfere with TBK1, ΔRIG-I or IKKε mediated IFN-β promoter activity. The bars represent the means and the error bars the standard deviations of biological duplicates. The lysates were subjected to SDS-PAGE followed by Western blotting and immunostaining with the indicated antibodies to confirm expression of the constructs.

4.1.2. RABV P CTD is essential for inhibition of ΔRIG-I mediated IFN-β induction

The data shown previously provide some evidence for differential inhibitory abilities of certain RABV P truncation constructs in regard to different RLR pathway triggers. Whereas HA-GST-P-83-197 very efficiently suppressed TBK1-mediated IFN-β promoter activity, it completely lacked any inhibitory capacity when ΔRIG-I was used for pathway stimulation (Figure 14). Therefore, the ability of different RABV P constructs to suppress IFN-induction was further

examined for ΔRIG-I activation. HA-GST-tagged versions of full length P, the P_4 isoform as well as the truncations P-83-188, P-130-188 and P-168-188 were examined for their ability to interfere with ΔRIG-I mediated IFN-β promoter induction (Figure 15A).

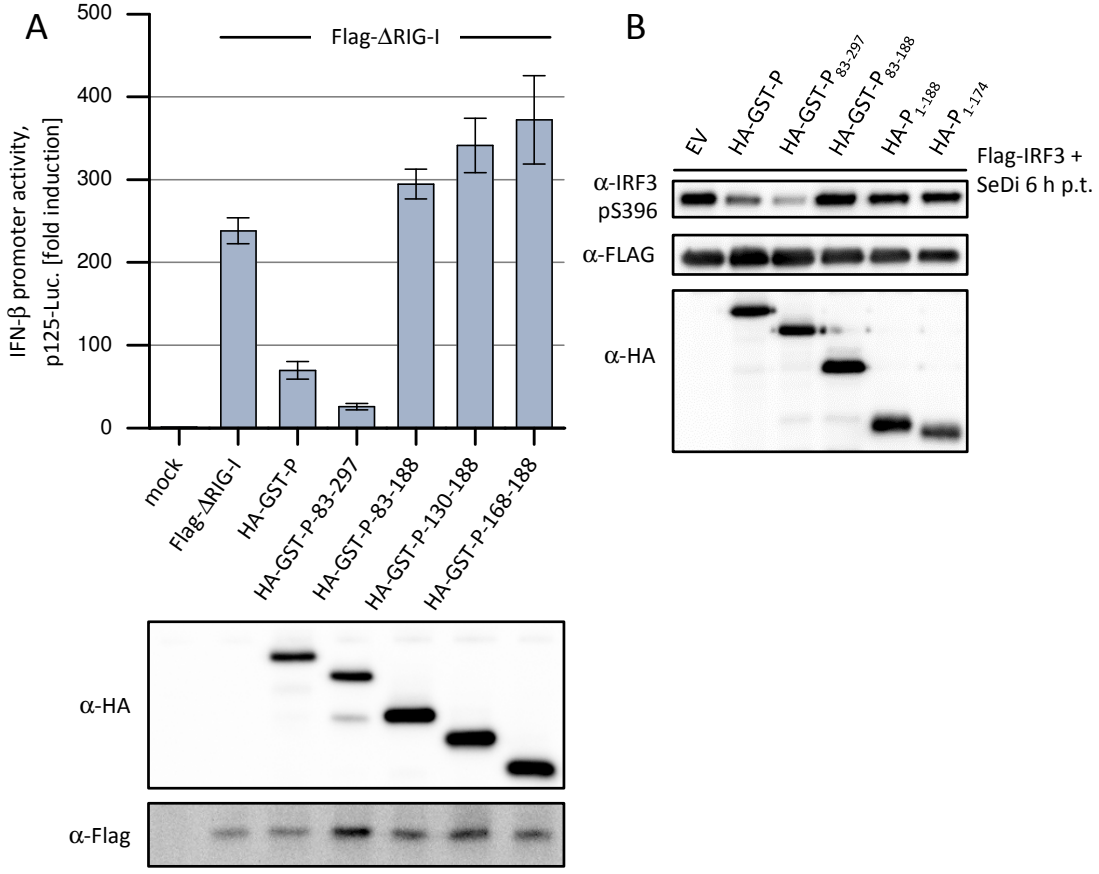

Figure 15: P constructs lacking the CTD fail to inhibit ΔRIG-I and SeDi stimulation.
A) HEK 293T cells were transfected with reporter plasmids (100 ng p125-FF/10 ng pCMV-RL) and the indicated constructs (100 ng Flag-ΔRIG-I, 200 ng P constructs plasmid DNA). Cells were lysed 24 h p. t. and subjected to dual luciferase assays in order to examine the ability of different P constructs to interfere with ΔRIG-I-mediated IFN-β promoter activity. The bars represent the means and the error bars the standard deviations of biological duplicates. Samples were subjected to SDS-PAGE followed by Western blotting and immunostaining with the indicated antibodies to confirm expression of the constructs. **B)** HEK 293T cells were transfected with 1 µg plasmid DNA coding for Flag-IRF3, 2 µg of the indicated P constructs and treated with SeDI 6 h post-transfection. Cells were lysed 24 h p. t. and samples were subjected to SDS-PAGE followed by Western blotting and immunodetection using the indicated antibodies.

HA-GST-P and HA-GST-P-83-297 significantly inhibited IFN-β promoter activity. All further truncation constructs lacking the C-terminus, HA-GST-P-83-188, HA-GST-P-130-188 and HA-GST-P-168-188, were clearly deficient in inhibitory function. This is again in contrast to previous experiments employing IFN-β promoter stimulation by TBK1 overexpression, where at least partial inhibition by P-130-188 and P-168-188 constructs could be observed (Figure 13A).

Interferon regulatory factor 3 (IRF3) is the crucial transcription factor responsible for activation of the interferon promoter after phosphorylation by TBK1/IKKε upon triggering of the RLR

signaling cascade (Fitzgerald et al., 2003; Sato et al., 2000; Sharma et al., 2003; Yoneyama et al., 2005). It exercises its function in concert with NF-κB and AP-1, forming an enhanceosome that triggers IFN transcription (Kim et al., 2000; Thanos and Maniatis, 1995). In addition to measuring IFN-promoter activity in reporter gene assays, the influence of different RABV P constructs on IRF3 serine 396 phosphorylation, an important marker of activation (Servant et al., 2003), was examined by Western blotting using a phospho-specific antibody. In order to activate the RLR signaling in a way that rather resembles a viral infection, *Sendai Virus* defective interfering particles (SeDI) were used (SeDI preparations were kindly provided by D. Garcin, Université de Genève). SeDIs were previously reported to strongly stimulate IFN-induction (Johnston, 1981; Strahle et al., 2006). Using this approach, we wanted to elucidate whether RABV P C-terminal truncation constructs also fail to inhibit SeDI mediated IFN-promoter induction. Flag-IRF3 was co-expressed with different P constructs and IRF3 phosphorylation after SeDI treatment was subsequently examined by Western blotting (Figure 15B).

HA-GST-P and HA-GST-P-83-297 were both able to significantly inhibit IRF3 serine 396 phosphorylation. HA-GST-P-83-188, as well as the C-terminal P truncations HA-P-1-188 and HA-P-1-174, however, showed no reduction in IRF3 phosphorylation compared to the EV control. IRF3 phosphorylation levels in the samples with HA-GST-P, HA-GST-P-83-297 and HA-GST-P-83-188 exhibited a good correlation with the results of the reporter gene assays conducted previously (Figure 15A). This indicates that IRF3 phosphorylation state is indeed correlating with the IFN-β promoter activity observed in reporter gene assays under the given experimental settings. Furthermore, SeDI treatment leads to a stimulation comparable to ΔRIG-I overexpression in regard to the ability of RABV P to suppress IFN-promoter induction. Therefore, it can be assumed that ΔRIG-I pathway stimulation is preferable to TBK1 overexpression in order to investigate P inhibition, because it leads to results comparable to SeDI treatment, which is closer to the setting of a natural viral infection. In summary, these findings provide some evidence that the C-terminal domain of RABV P is in fact essential for inhibition of IFN-induction, what contrasts the data obtained previously from reporter gene assays utilizing Flag-TBK1 overexpression.

4.1.3. RABV P dimerization domain and DLC8 binding in inhibition

HA-GST-P-83-297 (P_4) could previously be shown to be able to fully inhibit ΔRIG-I and SeDI treatment mediated IFN-β induction, while RABV P C-terminal domain could be identified as essential for inhibition. The P_4 isoform of the phosphoprotein still contains, among other

features, the dimerization domain and a well conserved DLC8 binding motif, which has been implicated in viral transcription and replication in neurons (Tan et al., 2007). Therefore, RABV P mutants deficient in DLC8 binding, P-D143A-Q147A (ΔDLC8, Jacob et al. (2000)), and dimerization, P-F114A-W118A-I125A, were used to examine whether these features might be implicated in the inhibitory abilities of RABV P. The critical contribution to dimerization of the P residues F114, W118 and I125, which are substituted with alanine in the monomeric P mutant (PΔDim), could be shown previously in a yeast two-hybrid system (Ivanov et al., 2010) and was confirmed by native-PAGE assays in the master thesis of M. Wachowius (2012). Co-IP experiments followed by SDS-PAGE and Western blotting were conducted to confirm that HA-PΔDLC8 is indeed DLC8 binding deficient (Figure 16C). Reporter gene assays were performed with HA-PΔDLC8 and HA-GST-P-83-297-ΔDim to examine the constructs for their ability to interfere with IFN-β induction (Figure 16A). DLC8 binding deficient P was hardly impaired in regard to inhibitory function, whereas HA-GST-P-83-297-ΔDim clearly exhibited reduced suppression in comparison to HA-GST-P-83-297 (P_4). However, dimerization deficient P was impaired to a lesser degree than HA-PΔ176-186 (PΔInd1/2) which has been shown to be defective in inhibition of IFN-β induction previously (Rieder et al., 2011). To further investigate a possible involvement of the RABV P dimerization domain, a construct lacking the dimerization domain and N-terminus completely, HA-GST-P-130-297, was created und subjected to reporter gene assays (Figure 16B). In comparison to HA-GST-P-83-297 (P_4), HA-GST-P-130-297 almost completely lost its inhibitory function, hinting at a critical involvement of the dimerization domain in inhibition. This is in agreement with the results obtained using the dimerization deficient P-mutant.

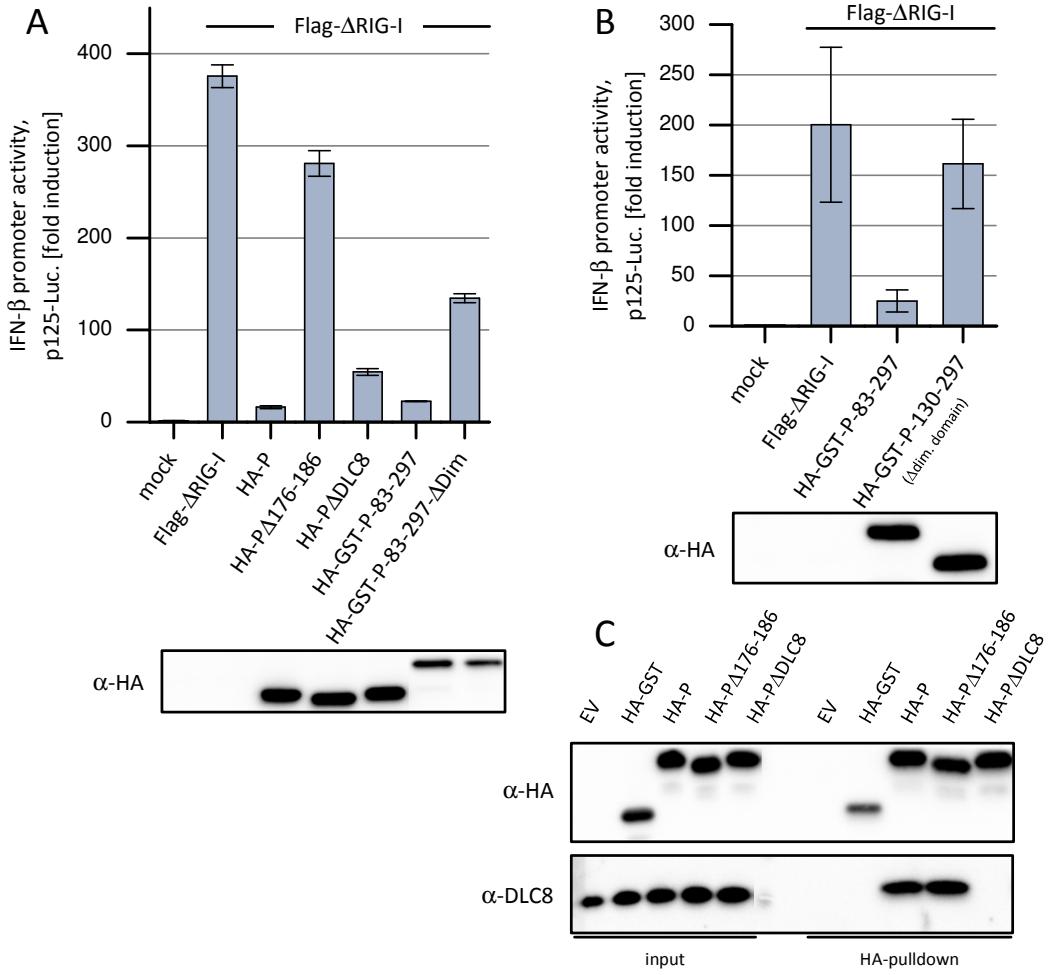

Figure 16: Role of DLC8 binding and dimerization of RABV P in ΔRIG-I inhibition.
A) The DLC8 binding deficient RABV P construct HA-PΔDLC8 exhibits no substantial loss of inhibitory function. HA-GST-P-83-297-ΔDim, a construct containing three alanine substitutions leading to impaired dimerization, shows reduced suppressive function. **B)** HA-GST-P-130-297, a RABV P construct lacking both N-terminus and dimerization domain, is unable to interfere with ΔRIG-I mediated IFN-reporter activity. Experimental conditions for both **A)** and **B)**: HEK 293T cells were transfected with reporter plasmids (100 ng p125-FF/10 ng pCMV-RL) and the indicated constructs (100 ng Flag-ΔRIG-I, 200 ng P constructs plasmid DNA). Cells were lysed 24 h p. t. and subjected to dual luciferase assays in order to examine the ability of different P constructs to interfere with ΔRIG-I-mediated IFN-β promoter activity. The bars represent the means and the error bars the standard deviations of biological duplicates. Samples from cell lysates were taken and subjected to SDS-PAGE followed by Western blotting and immunostaining with the indicated antibodies to examine expression levels of the constructs. **C)** The HA-PΔDLC8 mutant fails to interact with DLC8, as previously reported. 293T cells were transfected with 3 µg plasmid DNA coding for the indicated constructs, lysed 24 h p. t. and subjected to Co-IP experiments. Samples from input and pulldown fractions were examined by SDS-PAGE followed by Western blotting and immunostaining with the indicated antibodies.

4.1.4. RABV P CTD-NLS mutants exhibit inhibitory deficiency

The distribution of RABV P and its different isoforms within the cell is determined by several trafficking signals. P contains an N-terminal nuclear export signal (NES, residues 49-58) and a

conformational nuclear localization signal (NLS) in its C-terminal domain (CT-NLS), with lysine 214 and arginine 260 both playing a crucial role (Pasdeloup et al., 2005). However, no critical function in the viral life cycle could yet be attributed to the RABV P CTD-NLS. Since removal of the C-terminal domain of RABV P, which contains the conformational CTD-NLS, lead to a loss of suppressive capacity, we wanted to investigate whether P trafficking might be associated with inhibition of IFN-β induction. The RABV P amino acid substitutions K214A and R260A have been reported previously to impair NLS activity of the CVS-strain P protein (Pasdeloup et al., 2005).

Therefore, the SAD-L16 strain RABV P CTD-NLS defective mutants K214A and R260A were co-expressed with Flag-ΔRIG-I and assayed for their ability to interfere with interferon induction in dual luciferase assays using IFN-β promoter driven luciferase expression (Figure 17A). HA-tagged wild type P and inhibition deficient PΔ176-186 (ΔInd1/2) (Rieder et al., 2011) were used as positive and negative controls, respectively. While HA-P strongly repressed IFN-β promoter activity, P-K214A and P-R260A mutants were impaired in their inhibitory function equally to HA-PΔ176-186. Since expression levels of the mutants were not impaired, these results hint at an involvement of the C-terminal conformational NLS of RABV P in inhibition of IFN-induction.

To investigate whether the observed defect is really due to impaired nuclear localization, RABV P wild type and the K214A and R260A mutant versions were N-terminally fused to a recombinant SV40-NLS. It has been shown that this amino acid sequence mediates nuclear import of the Simian virus 40 (SV40) large T antigen and is able to restore nuclear localization of NLS defective mutant versions of this protein when fused additionally to the N-terminus (Kalderon et al., 1984a; Kalderon et al., 1984b). HA-P, HA-P-K214A and HA-P-R260A as well as their SV40-NLS containing versions were co-transfected with Flag-ΔRIG-I and assayed for their ability to suppress IFN-β promoter activity in reporter gene assays (Figure 17B). Both HA-tagged mutants P-K214A and P-R260A were strongly impaired in their inhibitory abilities, with P-K214A being slightly less affected. HA-NLS-P, containing a recombinant SV40-NLS, abrogated IFN-β promoter activity even more efficiently than wild type HA-P. Strikingly, HA-NLS-P-K214A and HA-NLS-P-K260A showed an inhibitory effect comparable to wild type P. This demonstrates that the suppressive defect in the P mutants containing a K214A or R260A substitution is indeed associated with impaired nuclear trafficking since inhibition can be rescued by complementing this function with an ectopic recombinant SV40 nuclear localization signal. Furthermore, the finding that even wild type P suppression profits slightly from an additional NLS suggests that nuclear localization plays a role in the inhibitory mode of action.

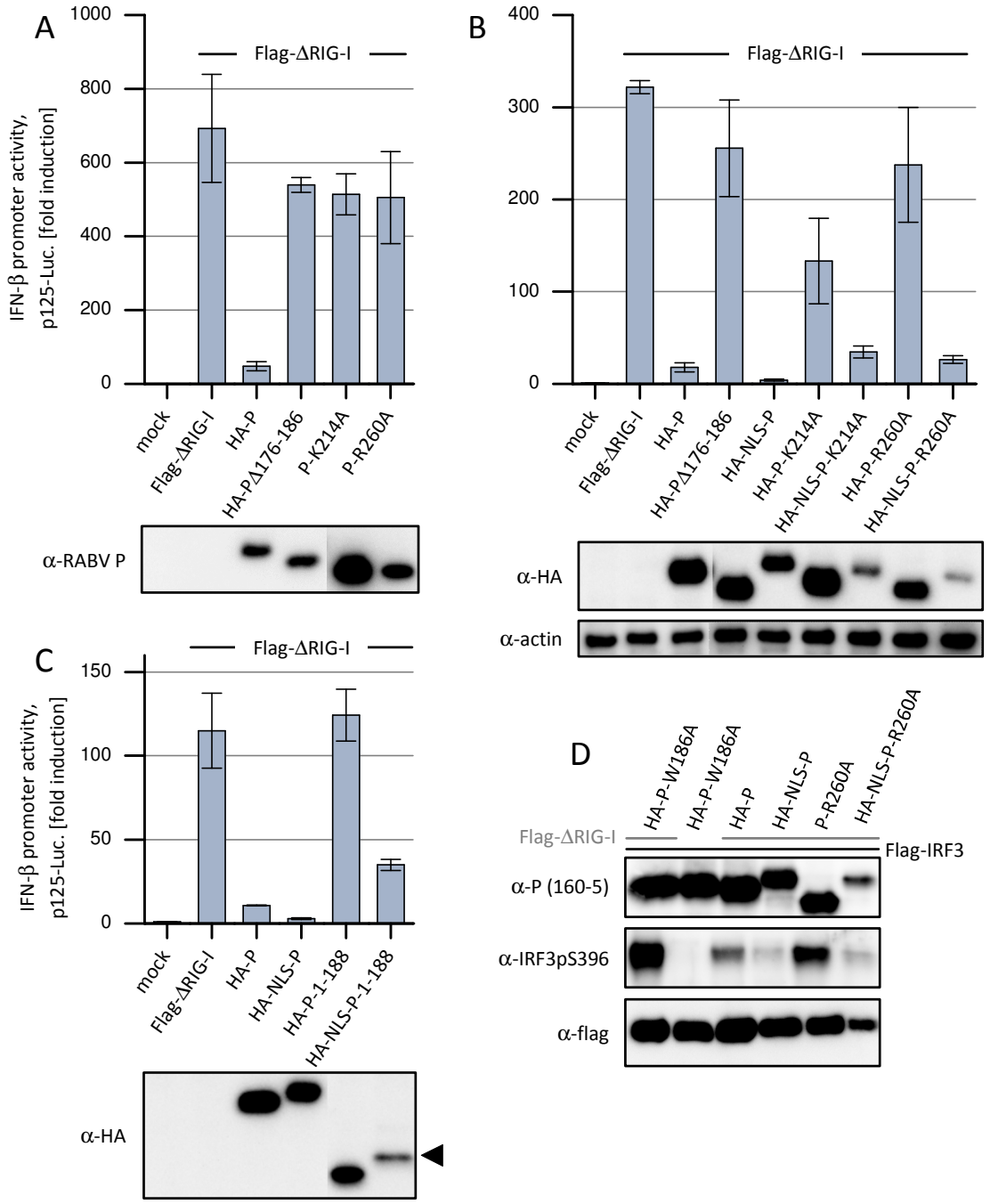

Figure 17: Inhibitory deficiency of RABV P CTD-NLS mutants can be rescued by fusion to a SV40-NLS.
A) RABV P mutants containing single alanine substitutions in the C-terminal conformational NLS exhibit an inhibitory defect similar to HA-PΔ176-186. **B)** Fusion of the defective RABV P mutants P-K214A and P-R260A to a recombinant SV40-NLS rescues the inhibitory defect. **C)** In regard to inhibition, the RABV P CTD can be partially substituted by a recombinant SV40-NLS. Experimental conditions for **A)**, **B)** and **C)**: HEK 293T cells were transfected with reporter plasmids (100 ng p125-FF/10 ng pTK-RL) and the indicated constructs (100 ng Flag-ΔRIG-I, 200 ng P constructs plasmid DNA). Cells were lysed 24 h p. t. and subjected to dual luciferase assays in order to examine the ability of different P constructs to interfere with ΔRIG-I-mediated IFN-β promoter activity. The bars represent the means and the error bars the standard deviations of biological duplicates. Cell lysates were examined by Western blotting in order to determine expression levels of the constructs used. **D)** While P-R260A is unable to suppress ΔRIG-I mediated IRF3 Ser396 phosphorylation, HA-NLS-P-R260A impairs IRF3 phosphorylation comparable to wild type RABV P. 293T cells were transfected with 1 µg Flag-IRF3, 2 µg of different P-constructs and 500 ng Flag-ΔRIG-I. 24 h p. t. cells were lysed,

subjected to SDS-PAGE and Western blotting and immunostained with the indicated antibodies in order to examine the influence of different P-constructs on IRF3 phosphorylation.

In previous experiments it has already been shown that the C-terminal domain of RABV P is essential for inhibition of IFN induction under experimental settings using either Flag-ΔRIG-I or SeDI stimulation of RLR signaling. Given that the nuclear localization signal investigated before is also located in the C-terminal domain of P, this raised the question whether the inhibitory defect in C-terminal truncations is just due to absence of the CTD-NLS. In order to examine whether, in regard to inhibitory function, the C-terminal domain of RABV P can be substituted using a recombinant NLS, a HA-NLS-P-1-188 construct was created. HA-P, the C-terminal truncation HA-P-1-188 and their respective HA-NLS-versions were co-transfected with Flag-ΔRIG-I and examined for their inhibitory abilities in IFN-promoter dependent reporter gene assays (Figure 17C). HA-P-1-188 had no influence on IFN-β promoter induction, concurrent with previous observations. Conversely, HA-NLS-P-1-188 was able to interfere with ΔRIG-I mediated IFN-reporter activity in a solid way, especially considering the relatively low expression level observed for this construct (see arrowhead in Figure 17C). This indicates that the P-CTD is mainly essential for the inhibitory function of RABV P because it contains a nuclear localization signal.

In addition to reporter gene assays, HA-P, the NLS defect mutant P-R260A and HA-NLS-P-R260A, containing the recombinant SV40-NLS, were co-expressed with Flag-ΔRIG-I and Flag-IRF3 in order to examine IRF3 serine 396 phosphorylation as a marker of IRF3 activation (Figure 17D). The non-inhibitory P mutant HA-P-W186A (this RABV P mutant will be characterized in 4.2) was used as a negative control in this assay and displayed no inhibition of IRF3 phosphorylation. P-R260A was clearly significantly impaired in its ability to interfere with IRF3 S396 phosphorylation, whereas wild type HA-P, as well as both SV40-NLS fused constructs HA-NLS-P and HA-NLS-P-R260, exhibited a strong inhibitory effect. Thus, the results obtained from the IRF3 phosphorylation assays were in agreement with the data previously observed in reporter gene experiments.

In addition to circumventing IFN-induction, RABV P is also able to suppress the expression of interferon-stimulated genes (ISGs). RABV P blocks IFN-signal transduction by binding and thereby preventing nuclear translocation of phosphorylated STATs (Brzózka et al., 2006; Vidy et al., 2005). Since P mutants defective in NLS activity could be shown to have impaired inhibitory abilities in regard to IFN induction, also a possible involvement of P nuclear trafficking in inhibition of IFN-signaling was examined. To this end, the NLS defective P mutants P-K214A and P-R260A as well as the SV40-NLS fused construct HA-NLS-P-R260A were examined for their ability to block IFN signal transduction after treatment with type I interferon using ISRE-

promoter dependent dual luciferase assays (Figure 18). P-WAMA (P-W265A-M287A, created and characterized by Dr. D. Aberle), a mutant deficient in inhibiting IFN-signaling (unpublished data), was used as a negative control. P-K214A suppressed ISRE-promoter activity after interferon treatment equally to wild type P, while addition of an SV40-NLS to wild type P did not result in enhanced inhibition. P-R260A could be observed to be impacted by the mutation to some degree. However, in contrast to the deficiency observed in regard to IFN-induction, the defect could not be reversed by addition of a SV40-NLS. The RABV P mutant HA-P-W186A, which is deficient in inhibition of IFN-induction (characterized in 4.2), was not impaired in its ability to inhibit IFN-signaling. P-R260A might be impaired due to proximity of arginine 260 to tryptophan 265 which is critical for STAT-binding and changed to alanine in the defective P-WAMA mutant. Taken together, these results suggest that nuclear localization of P is important for suppression of IRF3 activation, but rather not involved in inhibition of IFN-signaling.

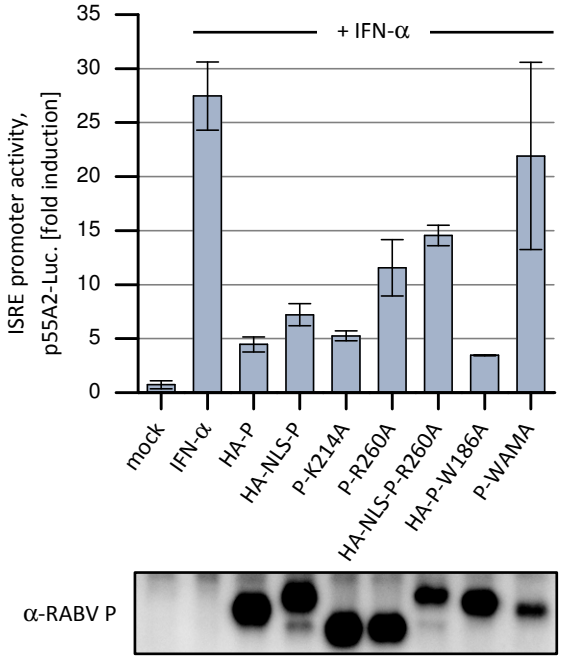

Figure 18: RABV P nuclear trafficking is not involved in the inhibition of JAK/STAT signaling.
The RABV P-K214A mutant was not affected in the ability to suppress IFN-mediated ISRE-promoter activity, indicating that the RABV P CTD-NLS plays no role in inhibition of JAK/STAT signaling. HA-P-W186A was used as a control mutant that is only impaired in the inhibition of IFN-induction but not JAK/STAT signaling (this mutation will be characterized later in this thesis), while P-WAMA was used as a deficient negative control. Fusion of P constructs to a recombinant SV40-NLS rather had a negative on suppression. The phenotype of the P-R260A mutant might be readily explained with the proximity of R260 to residues which contribute to STAT-binding. HEK 293T cells were transfected with reporter plasmids (100 ng pISRE-FF/10 ng pTK-RL) and 200 ng plasmid DNA coding for the indicated RABV P constructs. Cells were treated with 100 units universal type I interferon (human recombinant IFN-α) per 24-well 6 h post-transfection. Cells were lysed 24 h p. t. and subjected to dual luciferase assays in order to examine the ability of different P constructs to interfere with ISRE promoter activity. The bars represent the means and the error bars the standard deviations of biological duplicates. Cell lysates were examined by Western blotting in order to determine expression levels of the transfected constructs.

4.1.5. RABV P requires a functional NLS for inhibition of IFN-β induction

Functional reporter gene and IRF3 phosphorylation assays indicated a crucial role of nuclear trafficking of RABV P in its ability to interfere with IFN induction. To support this, we examined the intracellular localization of P constructs with mutations in the C-terminal NLS (P-K214A, P-R260A), as well as the corresponding RABV P constructs fused to the recombinant SV40-NLS. Full length RABV P is normally enriched in the cytoplasm due to a strong N-terminal nuclear export signal (NES) (Pasdeloup et al., 2005). Therefore, leptomycin B (LMB) treatment was employed which was previously shown to inhibit CRM-1 dependent nuclear export of RABV P, revealing impaired nuclear localization in mutant P_3 isoforms (Fornerod et al., 1997; Oksayan et al., 2012; Pasdeloup et al., 2005). Recently, it could be shown that the RABV P C-terminal NLS is also involved in nuclear trafficking of full length P_1 and mediates IMPα2/IMPβ1-dependent nuclear import (Rowe et al., 2016). Subcellular localization of wild type RABV P, the NLS defective mutants P-K214A and P-R260A and their corresponding versions fused to SV40-NLS was examined with and without LMB treatment 3 h prior to fixation using confocal immunofluorescence imaging (Figure 19). Differential subcellular localization could be observed between non-treated cells and cells treated with LMB as well as between constructs with and without recombinant SV40-NLS. LMB treatment lead to a significant increase in nuclear localization in every case. The same is true for the P constructs fused to SV40-NLS. However, all SV40-NLS containing constructs showed a significantly stronger nuclear localization, demonstrating the effectivity of this sequence in combination with different P proteins. Unfortunately, no significant differences between wild type P and the K214A and R260A alanine substitution mutants could be observed under these experimental conditions. In order to quantify this impression, the ratio between nuclear fluorescence and cytosolic fluorescence (F_n/F_c) of the different P constructs was determined using the ImageJ software with the plugin "Intensity Ratio Nuclei Cytoplasm Tool" (Schneider et al., 2012). Five representative images were taken for every condition and subjected to F_n/F_c calculation. Higher values represent a stronger nuclear enrichment. The average results for every condition were plotted as bars with the standard deviation shown as error bars (Figure 20). Between HA-P, HA-P-K214A and HA-P-R260A (green bars) no significant difference was observed with or without LMB treatment, confirming the preceding observation. Differential localization was observed only between LMB treated/non-treated samples and constructs with (red bars) or without (green bars) SV40-NLS. This might be due to fact that RABV P is a relatively small protein with a molecular mass of 34 kDa and therefore probably able to diffuse passively through the nuclear pores relatively fast

(Gorlich and Kutay, 1999). Consequently, it might be possible that the defect in nuclear localization of the P NLS-mutants is not visible because active nuclear import is overlaid by passive diffusion upon shutdown of nuclear export by LMB treatment. Since all SV40-NLS constructs almost completely localize to the nucleus upon LMB treatment, it can be assumed that the P C-terminal NLS is weaker in comparison to the SV40-NLS.

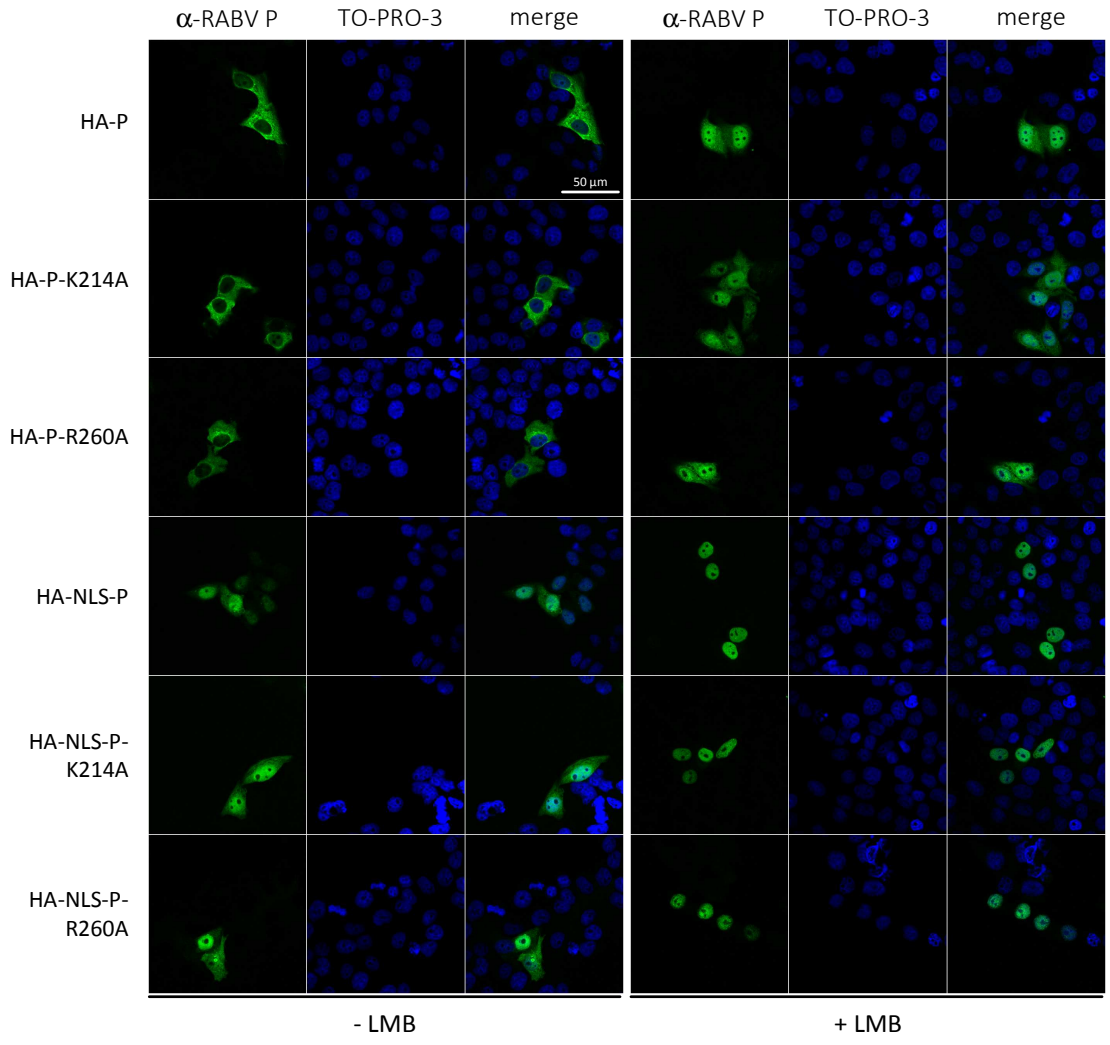

Figure 19: A recombinant SV40-NLS strongly confers nuclear localization to RABV P fusion constructs.
While the effect of the recombinant SV40-NLS on localization is clearly visible, RABV P mutants P-K214A and P-R260A show no differential subcellular localization upon LMB treatment. HeLa cells previously seeded on microscope slides in 24-wells were transfected with 400 ng plasmid DNA coding for the indicated P constructs. Cells were treated with 50 nM leptomycin B (LMB) for 3 h before fixation 24 h post-transfection. Cells were stained with the indicated antibodies and TO-PRO-3 and monitored by confocal laser scanning microscopy.

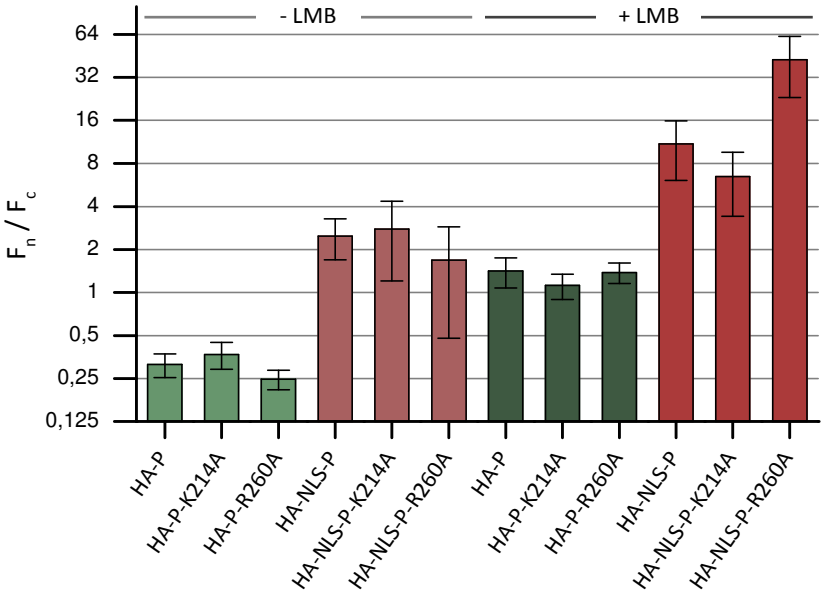

Figure 20: RABV P mutations K214A and R260A cause no apparent difference in localization.
Of the experiment depicted in Figure 19 for every condition the ratio between nuclear fluorescence and cytosolic fluorescence F_n/F_c of the different P constructs was calculated using ImageJ with the "Intensity Ratio Nuclei Cytoplasm Tool". The bars show the means and the errors the standard deviations of F_n/F_c ratios of five representative pictures. A $\log_2$ scale was employed in this figure for a better simultaneous illustration of very low and very high values.

In order to examine whether a difference in localization between NLS mutants and wild type RABV P can be detected in constructs which are big enough to prevent significant passive diffusion through the nuclear pores, tagRFP-tagged P-83-297 (P_4) was used. Constructs comprising RABV P residues 83-297 have been shown to be able to inhibit IFN-induction before (4.1.2). In contrast to tagRFP-P_4, the mutant proteins tagRFP-P_4-K214A and tagRFP-P_4-R260A were confirmed to be significantly impaired in inhibition of IFN-promoter activity in luciferase assays (Figure 21B, experiment conducted by H.-S. Luu during his research internship under supervision of the author of this thesis), comparable to the previously examined HA-tagged full length P constructs. Exhibiting a molecular mass of about 51 kDa, tagRFP-P_4 is assumedly too big for efficient passive diffusion, since even ovalbumin, which has a molecular mass of 44 kDa, could be shown previously to diffuse to the nucleus only at a very slow negligible rate (Bonner, 1975; Gorlich and Kutay, 1999). Therefore, subcellular localization experiments were repeated with the RABV P constructs tagRFP-P_4 (wild type) and the CTD-NLS mutants tagRFP-P_4-K214A and tagRFP-P_4-R260A with and without LMB treatment. Again, at least five pictures were taken from each condition with typical representatives depicted in Figure 21A. While a nuclear enrichment upon LMB treatment is visible for tagRFP-P4, both mutants are significantly impaired in nuclear localization. This observation was confirmed by calculating F_n/F_c values for all conditions (Figure 21C).

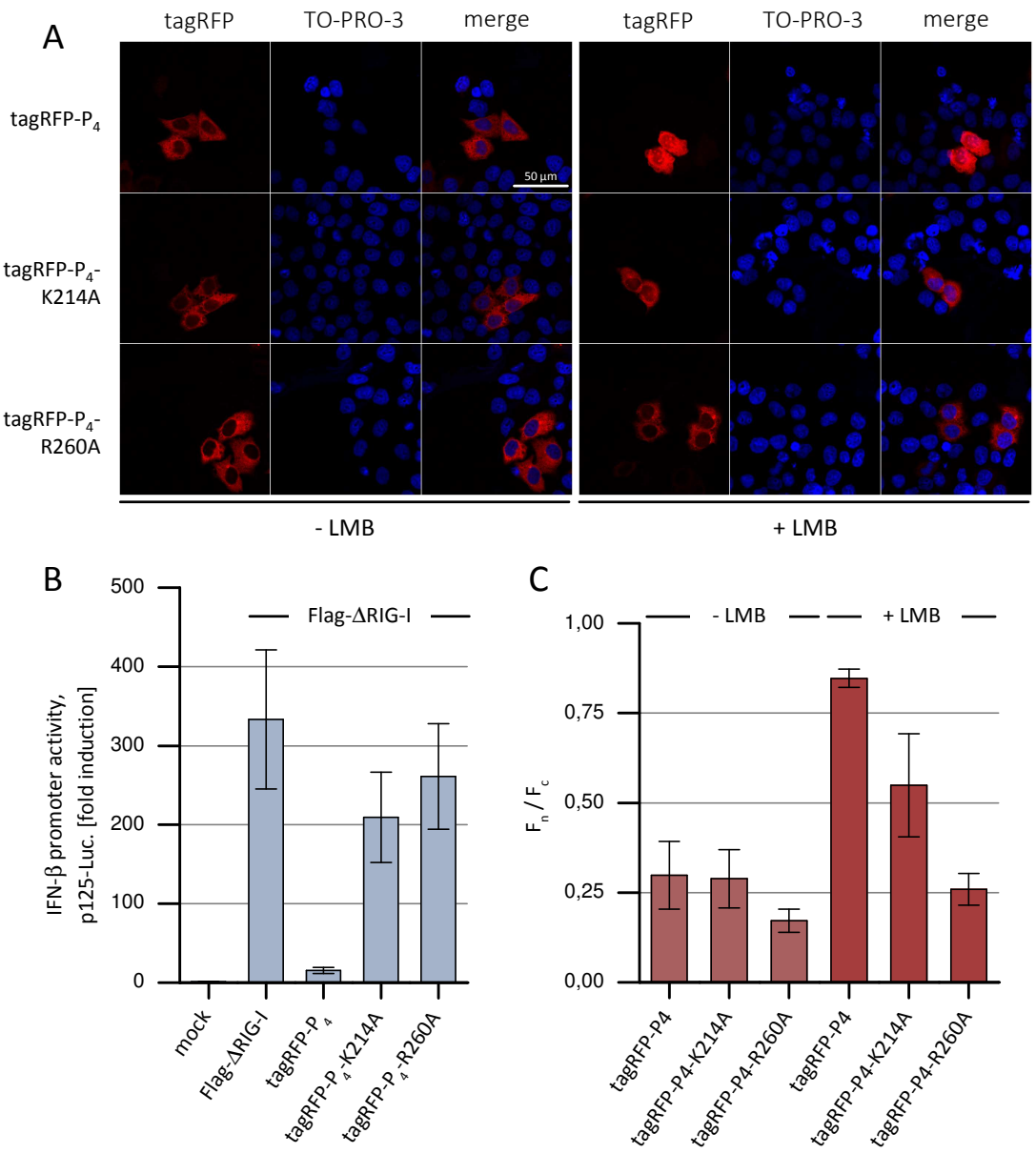

Figure 21: tagRFP-P$_4$ NLS mutants are substantially impaired in regard to nuclear accumulation.
A) LMB treatment reveals the impaired ability of tagRFP-P$_4$-K214A and tagRFP-P$_4$-R260A to be actively transported to the nucleus. HeLa cells previously seeded on microscope slides in 24-wells were transfected with 400 ng plasmid DNA coding for the indicated P constructs. Cells were treated with 50 nM leptomycin B (LMB) for 3 h before fixation 24 h post-transfection. Cells were stained with TO-PRO-3 and monitored by confocal laser scanning microscopy. **B)** Dual luciferase assays show that the RABV P mutants tagRFP-P$_4$-K214A and tagRFP-P$_4$-R260A are strongly impaired in regard to inhibition of ΔRIG-I mediated IFN-β reporter activity, as compared to tagRFP-P$_4$. HEK 293T cells were transfected with reporter plasmids (100 ng p125-FF/10 ng pTK-RL) and the indicated constructs (100 ng Flag-ΔRIG-I, 50 ng tagRFP-P$_4$ constructs plasmid DNA). Cells were lysed 24 h p. t. and subjected to dual luciferase assays in order to examine the ability of different P constructs to interfere with ΔRIG-I-mediated IFN-β promoter activity. The bars represent the means and the error bars the standard deviations of biological duplicates. **C)** The ratio between nuclear fluorescence and cytosolic fluorescence F_n/F_c of the different P constructs was calculated using ImageJ with the "Intensity Ratio Nuclei Cytoplasm Tool" for every condition. The bars show the means and the errors the standard deviations of F_n/F_c ratios of five representative pictures.

tagRFP-P_4-R260A is more significantly excluded from the nucleus than wild type tagRFP-P4, even without addition of LMB, and hardly responds to LMB treatment. tagRFP-P_4-K214A is less impaired in regard to nuclear accumulation compared to tagRFP-P_4-R260A upon LMB treatment, but still exhibits a significant difference to wild type tagRFP-P_4. In general, nuclear enrichment upon LMB treatment is much less prominent for tagRFP-P_4 than for wild type HA-P examined previously. This discrepancy might be attributed to the different sizes of the protein constructs and their ability to passively diffuse to the nucleus in addition to active transport. Thus, using the tagRFP-P_4 constructs, the difference in active nuclear transport between wild type P and K214A and R260A mutants could be confirmed. Previous studies in the literature characterizing these mutations also employed RABV P versions tagged with fluorescent proteins like eGFP, thus also made use of constructs which are in size above the threshold for passive diffusion (Oksayan et al., 2012; Pasdeloup et al., 2005; Rowe et al., 2016).

Taken together, the results described in 4.1.4 and 4.1.5 provide some evidence that active nuclear translocation by a functional NLS is an essential requirement for inhibition of RIG-I mediated IFN induction by RABV P.

4.2. A novel HSP70 binding motif in RABV P is essential for inhibition of IFN-induction

RABV P residues 176-186 (absent in the PΔInd1/2 deletion mutant) could be identified previously as crucial for inhibition of IFN-induction after RLR activation and TBK1 overexpression. In the viral context, these residues were found to be involved in viral pathogenicity (Rieder et al., 2011). However, no mechanistic role or potential interaction partner for this sequence could be identified so far. In order to obtain new insights about this RABV P region and to elucidate whether the inhibitory deficiency in PΔ176-186 can be attributed to loss of a specific binding partner, several pulldown studies were conducted by co-immunoprecipitation (Co-IP) using full length RABV P constructs as well as peptide constructs of different length encompassing residues 176-186.

4.2.1. RABV P co-precipitates HSP70 family members

HA-GST-tagged RABV P peptides of different length were used in an attempt to identify a possible molecular binding partner associated with the residues 176-186 lacking in PΔInd1/2. Therefore, the constructs HA-GST-P-130-188, HA-GST-P-168-188 and HA-GST-P-176-188, previously examined in regard of their ability to interfere with TBK1 and ΔRIG-I overexpression mediated IFN-β induction, were used in Co-IP experiments employing anti-HA affinity matrix. We could not exclude that P interacts with a host cell protein in an activation dependent manner, like the binding to activated STATs after IFN-signaling (Brzózka et al., 2006). Therefore, we optionally stimulated cells with SeDI treatment, to induce RLR-mediated innate immune signaling in the pulldown assays (Johnston, 1981; Strahle et al., 2006). Empty vector transfection and expression of HA-GST were used as controls for specificity. Pulldown fractions of the experiment were visualized by silver staining on a SDS-PAGE gel (Figure 22A).

A prominent band with the size of approximately 70 kDa (white arrowhead) could be detected with and without SeDI treatment in all GST-P fusion peptide pulldowns but not in the control fractions. The 70 kDa gel bands were excised and examined by mass spectrometry (analysis conducted by Dr. T. Fröhlich, Arnold Lab, Gene Center, LMU). The peptides detected in the band could be assigned to HSP70 family members. To confirm the data obtained from mass spectrometry, full length HA-P was used together with HA-GST and EV transfection as controls in Co-IP experiments. Using an antibody with specific reactivity towards inducible HSP70 family members (tested previously, data not shown), input and pulldown fractions were examined for

co-immunoprecipitation of endogenous HSP70 (Figure 22B). Association of RABV P with dynein light chain LC8-type 1 (DLC8) (Jacob et al., 2000) confirmed success of the pulldown experiment. HSP70 co-precipitated with RABV P but not the controls, confirming the association detected in MS analysis.

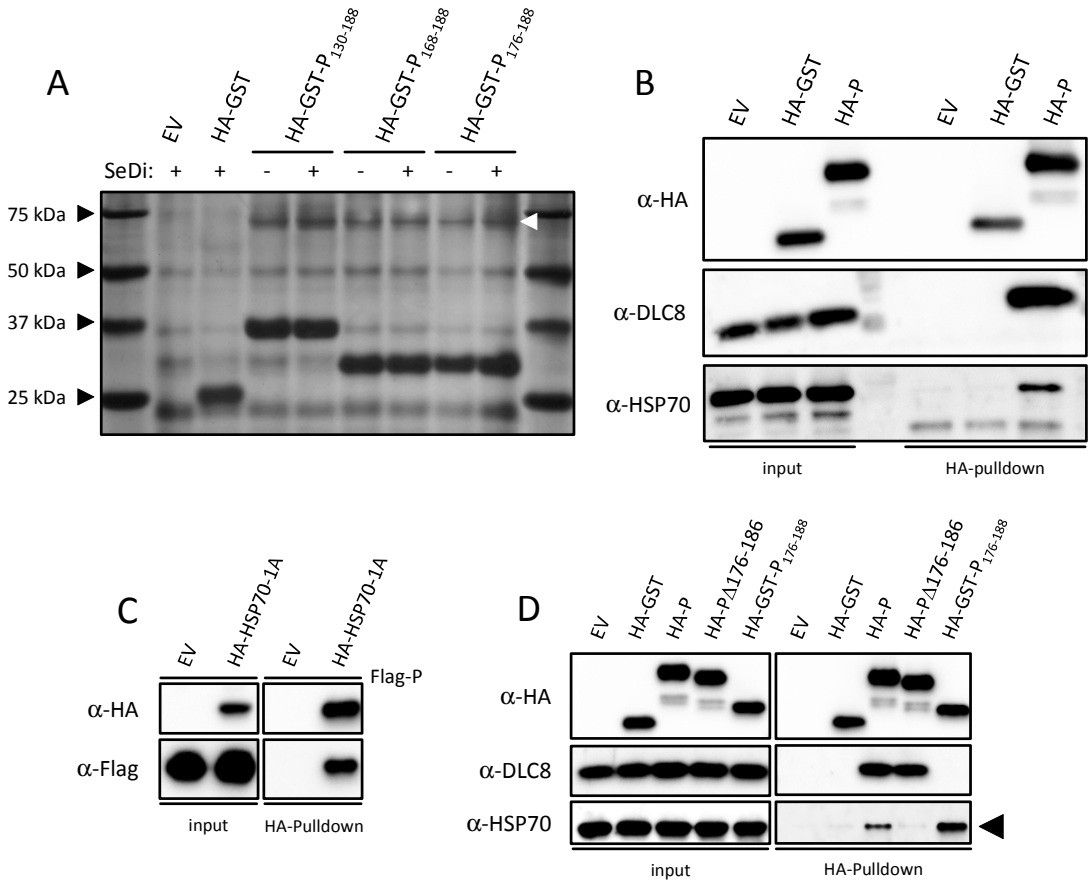

Figure 22: RABV P interacts specifically with HSP70 depending on P residues 176-186.
A) Silver staining of protein fractions separated by SDS-PAGE reveals that a protein of a size of approximately 70 kDa (white arrowhead) is specifically co-precipitated by different P-derived fusion peptides. HEK 293T cells in 10 cm dishes were transfected with 20 µg plasmid DNA coding for the indicated constructs, lysed 24 h p. t. and subjected to Co-IP experiments. The pulldown fractions were examined by silver staining of SDS-PAGE gels. **B)** Co-IP and Western blotting show that endogenous HSP70 co-precipitates with full length HA-P. 293T cells were transfected with 3 µg plasmid DNA coding for the indicated constructs, lysed 24 h p. t. and subjected to Co-IP experiments. Samples from input and pulldown fractions were examined by SDS-PAGE followed by Western blotting and immunostaining with the indicated antibodies. **C)** Flag-P co-precipitates with HA-HSP70-1A. 293T cells were transfected with 2 µg plasmid DNA coding for HA-HSP70-1A and 2 µg Flag-P constructs. Cells were lysed 24 h p. t. and subjected to Co-IP experiments. Pulldown samples were examined by SDS-PAGE followed by Western blotting and immunostaining with the indicated antibodies. **D)** In contrast to HA-P and a HA-GST-P-176-188 fusion construct, HA-PΔ176-186 fails to co-precipitate HSP70. 293T cells were transfected with 2 µg plasmid DNA coding for Flag-HSP70-1A and 2 µg of the indicated P constructs. Cells were lysed 24 h p. t. and subjected to Co-IP experiments. Pulldown samples were examined by SDS-PAGE followed by Western blotting and immunostaining with the indicated antibodies.

To examine whether the P–HSP70 interaction can also be shown in a reciprocal way, HA-affinity matrix pulldowns using HA-HSP70-1A (HSPA1A) and Flag-P were conducted (Figure 22C). HA-

HSP70-1A was able to co-precipitate Flag-P very efficiently, showing that the association can be observed in Co-IP experiments regardless of which protein is immobilized on the matrix during the procedure.

In the pulldown experiment shown in Figure 22A all fractions with P-derived HA-GST-fusion peptides contain a similar 70 kDa band identified as HSP70. This is also true for the 13 amino acids long fusion construct HA-GST-P-176-188, what raised the questions whether this short sequence might alone be responsible for mediating association with HSP70. Consequently, the fusion peptide HA-GST-P-176-188 and the inhibition defective HA-PΔ176-186 construct, which has a deletion nearly identical to the peptide, and wild type HA-P were compared in regard to their ability to co-precipitate endogenous HSP70 using again HA-GST and EV transfection as controls. In fact, HA-GST-P-176-188 exhibited an even stronger association with HSP70 than wild type HA-P (Figure 22D, black arrowhead). In contrast, HA-PΔ176-186 did not show any detectable association with HSP70, while pulldown efficiency was again confirmed by the co-precipitation of DLC8. Taken together, these results provide evidence that residues 176-188 are alone sufficient and essential to mediate association of RABV P with HSP70. This is of some significance, since HA-PΔ176-186 has also been shown to be deficient in regard to inhibition of IFN-induction, revealing a correlation between the inhibitory capacity of RABV P and HSP70 association.

The heat shock 70 kDa protein family consists of heat shock inducible members that have a crucial cytoprotective function under cellular stress conditions. Also under normal conditions these molecular chaperones contribute to correct folding of de-novo synthesized proteins (Mayer and Bukau, 2005). In addition, HSP70s have a role in assembly and disassembly of native protein complexes as well as in protein trafficking across certain cellular membranes (Chappell et al., 1986; Matlack et al., 1999; Okamoto et al., 2002). HSP70 binds to short stretches of approximately seven amino acids with a preference for hydrophobic and basic residues (Flynn et al., 1991; Gragerov et al., 1994; Zhu et al., 1996). In order to exclude that HA-GST-P-176-188 is only being bound by HSP70 due to the chemical properties of its amino acid residues, a HA-GST-peptide containing the residues of P-176-188 in a random order was created (176-QIASGPPALEWSA-188 to APIAAQLWSEPGS). This was achieved by cloning artificially synthesized DNA oligo nucleotides coding for the intended amino acid sequence into the HA-GST expression vector. To obtain new information regarding the minimal HSP70 binding motif, another P-derived peptide further N-terminally shortened by four amino acids was created (HA-GST-P-180-188). The scrambled construct (“HA-GST-scr. peptide” in the figure) and HA-GST-P-180-188

were compared to the other P constructs previously examined (Figure 22D) in regard to their ability to associate with Flag-tagged HSP70 in Co-IP experiments (Figure 23).

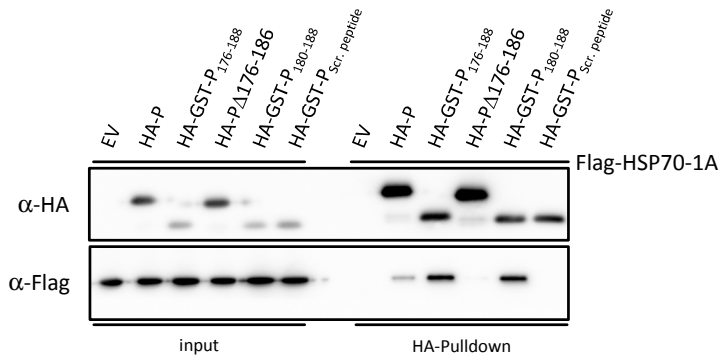

Figure 23: Binding of RABV P-derived peptides to HSP70-1A is sequence specific.
While HA-P and the P-derived fusion constructs HA-GST-P-176-188 and HA-GST-P-180-188 co-precipitate HSP70-1A, no interaction can be detected for a HA-GST-peptide containing the RABV P residues 176-188 in a randomized order. HEK 293T cells were transfected with 2 µg plasmid DNA coding for HA-HSP70-1A and 2 µg of different P constructs. Cells were lysed 24 h p. t. and subjected to Co-IP experiments. Pulldown samples were examined by SDS-PAGE followed by Western blotting and immunostaining with the indicated antibodies.

Notably, the HA-GST-P-180-188 fusion peptide was still able to co-precipitate HSP70. Conversely, the scrambled version of HA-GST-P-176-188 failed completely to associate with HSP70, comparable to HA-PΔ176-186. This demonstrates that RABV P amino acids 180-188 are sufficient to mediate interaction with HSP70. Moreover, the interaction is sequence specific, since a scrambled version of HA-GST-176-188 which contains the same amino acids in a different order, shows no association to HSP70. This underlines the importance of RABV P region 176-186 and identifies HSP70 as molecular binding partner of this motif.

Many different strains of rabies virus are available and are currently being used in research. Since viral assays in the Conzelmann group are usually conducted using the attenuated, vaccine-strain derived SAD-L16 clone (Schnell et al., 1994), also experiments studying single viral proteins were mainly carried out using the L16 variant. In the experiments shown above, it was indicated that L16-P is associated with HSP70 family members in Co-IP experiments. In order to put these results in a wider context, the ability of RABV P to associate with HSP70 was also examined for other rabies virus strains. The phosphoproteins of Thailand-(THA) and CVS-strain were chosen for these assays. THA-strain is a wild type virus isolated from a human case that occurred after a dog bite in Thailand. A full length rescue construct for THA-strain rabies virus was kindly provided by the lab of Hervé Bourhy (Institut Pasteur, France). CVS-strain (challenge virus standard) is a fixed laboratory strain with lethal pathogenicity frequently used for studying viral infection employing *in vivo* models (Park et al., 2006). Together with SAD-L16, which is a cell culture attenuated vaccine strain, three very different types of rabies viruses were covered. HA-

tagged versions of the Thailand-strain phosphoprotein (HA-THA-P) and of CVS-strain P (HA-CVS-P) were created in order to examine whether they are also capable of associating with HSP70. The constructs were co-transfected with HA-L16-P as positive control and the binding deficient HA-L16-PΔ176-186 deletion mutant as negative control (Figure 24). Furthermore, the RABV P mutant HA-P-W186A was created and included in this assay, to examine whether the exchange of a single amino acid within the essential P region 176-186 is also able to impair binding comparable to a complete deletion. Tryptophan 186 was chosen due to its high conservation among different *Lyssavirus* species phosphoproteins and its outstanding chemical properties within the ΔInd motif.

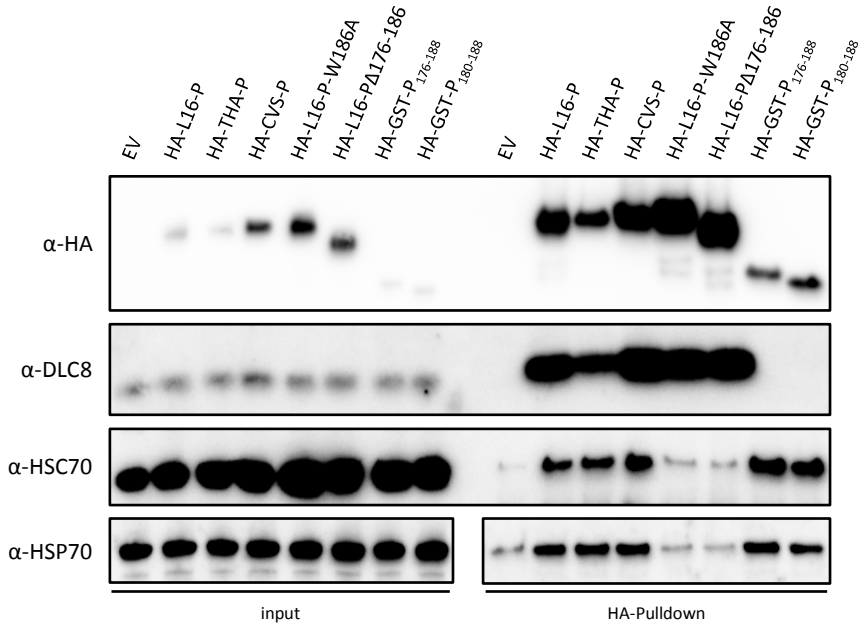

Figure 24: RABV P proteins of different strains interact with HSP70 and HSC70.
The rabies virus phosphoproteins of the L16, THA and CVS-strain equally co-precipitate HSP70 and HSC70. In contrast, no binding can be detected for HA-L16-PΔ176-186 and the single alanine substitution mutant HA-L16-P-W186A, identifying W186 as a critical residue for the observed interaction. HEK 293T cells were transfected with 3 µg plasmid DNA coding for the indicated constructs, lysed 24 h p. t. and subjected to Co-IP experiments. Samples from input and pulldown fractions were examined by SDS-PAGE followed by Western blotting and immunostaining with the indicated antibodies.

The HA-tagged rabies virus proteins of L16, THA and CVS strain were equally able to associate with endogenous HSP70 (HSPA1A/1B), whereas L16-PΔ176-186 failed to do so as observed before. In addition to HSP70, Western blots were also stained for HSC70 (HSPA8) using a specific antibody. Cross-reactivity between epitopes for the employed HSP70 and HSC70 antibodies was excluded by separate experiments (data not shown). In comparison to HSP70, HSC70 associated equally well with the phosphoproteins of different rabies virus strains. Also the HA-GST fusion peptides HA-GST-P-176-188 and HA-GST-180-188 interacted equally well with both HSP70 family

members. Strikingly, HA-L16-W186A showed the same deficiency in regard to association with HSP70 as the deletion mutant HA-L16-PΔ176-186. This strongly indicates that RABV P tryptophan 186 is an essential amino acid for the observed interaction.

4.2.2. P–HSP70 association correlates with inhibitory function

RABV P could be shown above to co-precipitate HSP70, while both mutants PΔ176-186 and P-W186A failed to do so. Since PΔ176-186 is deficient as well in inhibition of IFN-induction, a correlation between binding of HSP70 and suppressive capacity was suggested. Therefore, also HA-P-W186A was assayed in regard to inhibitory function in IFN-β promoter dependent reporter gene assays and compared to HA-P and HA-PΔ176-186 (Figure 25A). HA-P-W186A was found to be impaired in its suppressive capacity equally to the HA-PΔ176-186 deletion mutant. The observed defect of both mutant proteins was not due to impaired expression levels, since all P constructs including wild type HA-P were equally well expressed. This confirms that RABV P residue W186 is crucially involved in HSP70 association and inhibitory function alike.

Furthermore, different RABV P deletion mutants HA-PΔ176-181 (ΔInd1), HA-PΔ182-186 (ΔInd2) and HA-PΔ176-186 (ΔInd1/2) (previously described by Rieder et al. (2011)) were compared to HA-P-PA-WA (P181A-W186A), which contains an amino acid substitution in the ΔInd1 region (P181A) and another in the ΔInd2 region (W186A). In IFN-β dependent reporter gene assays (Figure 25B), all mutant constructs were equally impaired in their inhibitory abilities, underlining the reported importance of the ΔInd region (Rieder et al., 2011). The same P constructs were assayed in addition for their ability to co-precipitate HSP70 in Co-IP experiments (Figure 25C). All RABV P mutants examined in this assay displayed a significant deficiency to co-precipitate HSP70. Only HA-PΔ176-181 displayed residual binding to HSP70, indicating that the ΔInd2 (182-186) region is more important for the observed interaction. This is concurring with the previous finding that HA-GST-P-180-188 is sufficient for co-precipitation of HSP70 (Figure 22D) and the fact that the essential residue W186 is also located in the ΔInd2 stretch. Moreover, the correlation of HSP70 binding and RABV P inhibition is further supported by these findings.

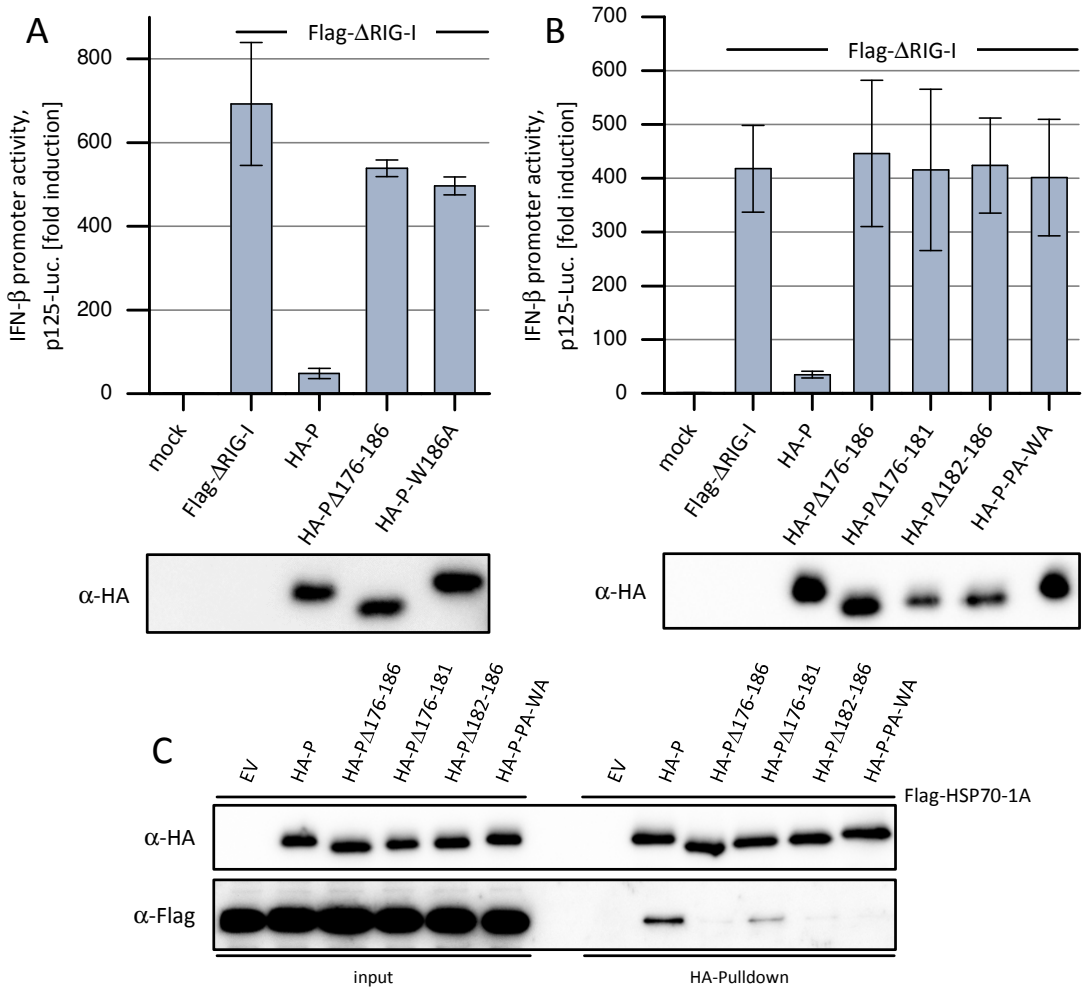

Figure 25: A HSP70 binding motif is essential for the suppressive function of RABV P.
Different RABV P mutants with deletions or alanine substitutions (P-W186A, P-P181A-W186A) in the region 176-186 exhibit a deficiency in regard to the inhibition of ΔRIG-I mediated IFN-reporter activity. Experimental conditions for both **A)** and **B)**: HEK 293T cells were transfected with reporter plasmids (100 ng p125-FF/10 ng pTK-RL) and the indicated constructs (100 ng Flag-ΔRIG-I, 200 ng P constructs plasmid DNA). Cells were lysed 24 h p. t. and subjected to dual luciferase assays in order to examine the ability of different P constructs to interfere with ΔRIG-I-mediated IFN-β promoter activity. The bars represent the means and the error bars the standard deviations of biological duplicates. Cell lysates were examined by Western blotting in order to determine expression levels of the constructs used. **C)** The binding of RABV P to HSP70 critically depends on residues in the region 176-186. HEK 293T cells were transfected with 3 µg plasmid DNA coding for the indicated constructs, lysed 24 h p. t. under native conditions and subjected to Co-IP experiments. Samples from input and pulldown fractions were examined by SDS-PAGE and Western blotting and subsequently immunostained with the indicated antibodies.

4.2.3. Mapping of the RABV P–HSP70 interaction

In order to further map the HSP70 association motif of RABV P on the C-terminal side with single amino acid precision, three different C-terminal RABV P truncation constructs differing in length only by one amino acid were examined. We hypothesized that binding to HSP70 might correlate

with inhibition of TBK1 overexpression by RABV P C-terminal truncations previously observed (Figure 12A). To validate this hypothesis, HA-P-1-188, HA-P-1-187 and HA-P-1-186 were examined for their ability to co-precipitate HSP70 in Co-IP assays (Figure 26A). Although expression of C-terminal deletion constructs was in general very low compared to full length P controls, even the shortest P-1-186 was functional in co-precipitating HSP70. This indicates that the crucial residues within the HSP70 binding motif in RABV P range up to W186, which has been identified to be essential for inhibition of IFN-induction before (Figure 25A).

A RABV P peptide starting with amino acid 180 has been shown to interact with HSP70 before (Figure 24). Taking into account the results observed for the C-terminal truncations in regard to HSP70 association, the new HA-GST fusion constructs HA-GST-P-180-186 and HA-GST-P-180-185 were created, in order to obtain the shortest RABV P derived peptide able to associate with HSP70. HA-GST-P-180-185 was presumed to be binding deficient due to absence of the central residue W186.

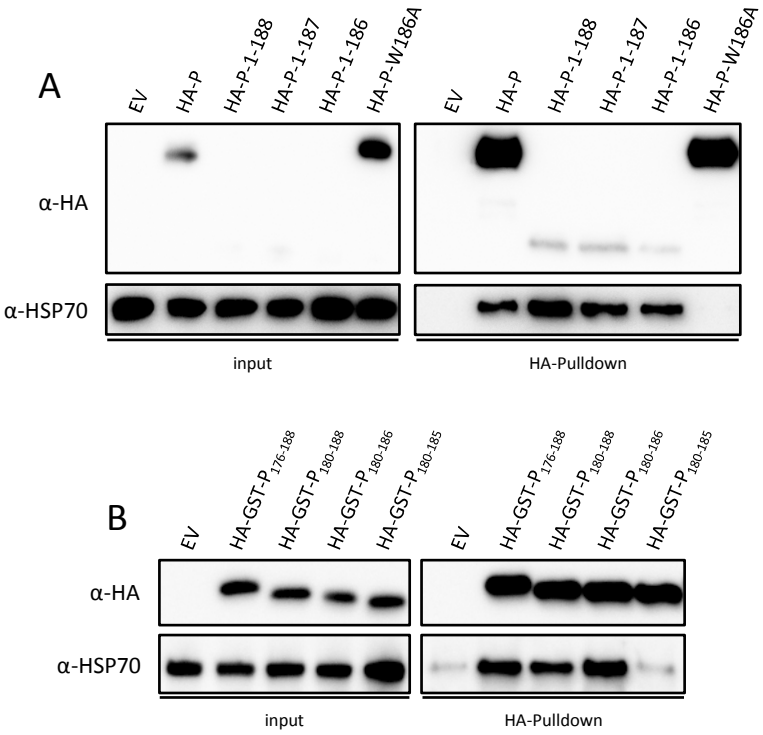

Figure 26: RABV P region 180-186 is sufficient to mediate an interaction with HSP70.
A) and **B)** 293T cells were transfected with 3 µg plasmid DNA coding for the indicated P constructs and lysed 24 h p. t. under native conditions. Subsequently, the lysates were subjected to Co-IP experiments and samples from input and pulldown fractions were subjected to by SDS-PAGE. After Western blotting, specific protein bands were visualized using the indicated antibodies.

The HA-GST fusion constructs P-176-188, P-180-188, P-180-186 and P-180-185 were therefore subjected to Co-IP analysis and examined for their ability to co-precipitate HSP70 (Figure 26B).

HA-GST-P-176-188, HA-GST-P-180-188 and HA-GST-P-180-186 associated strongly with HSP70, whereas HA-GST-P-180-185, being only truncated by one more residue (W186), failed completely to bind HSP70. This provides good evidence that the seven amino acids long RABV P-derived peptide with the sequence "GPPALEW" (HA-GST-P-180-186) is the minimal binding motif in the phosphoprotein that is alone sufficient for mediating the interaction.

With the binding motif for HSP70 in the rabies virus phosphoprotein identified, we wanted to determine which region or domain of HSP70 mediates the observed interaction. Therefore, different Flag-tagged HSP70-1A and HSC70 truncation mutants were investigated (full length HSC70 structure is depicted in Figure 27A). HSP70 is the major inducible heat shock protein in mammalian cells and is encoded by the nearly identical paralogs HSP70-1A and HSP70-1B. In contrast, HSC70 (heat shock cognate 71 kDa protein, HSPA8) is constitutively expressed and is an essential housekeeping factor involved in many different cellular functions under normal conditions. HSP70 family members are characteristically comprised of a nucleotide binding domain (NBD), containing the ATPase function of the protein, and a substrate binding domain with an adjacent "lid" region.

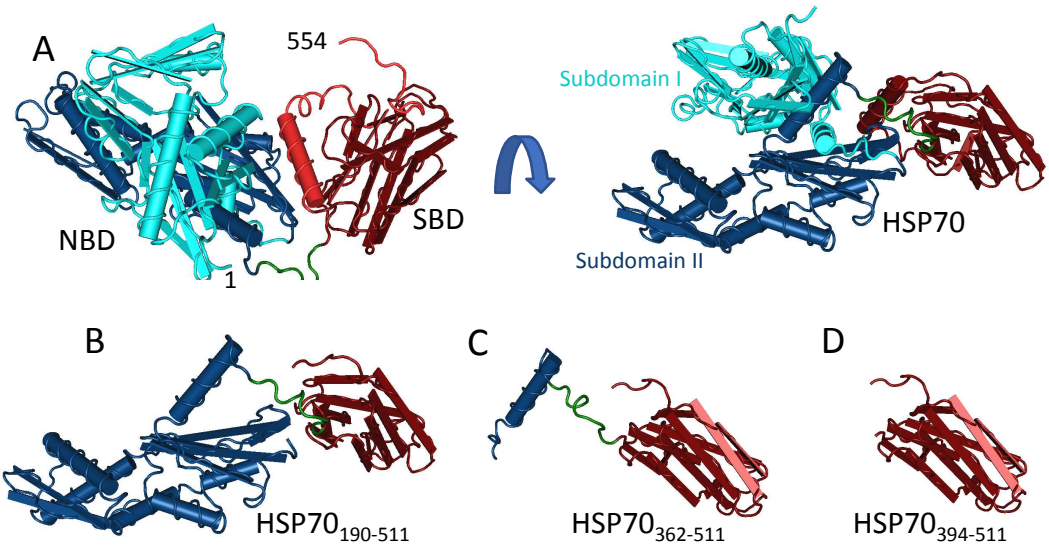

Figure 27: Different HSP70 truncation mutants used in pulldown studies.
Schematic representations of the structure of HSP70 and different HSP70 truncation mutants based on the structure of bovine HSC70, for which a crystal structure comprising both domains is available (Jiang et al. (2005), PDB ID 1YUW; illustration with Cn3D by NCBI). Members of the HSP70 family consist of two separate domains, the nucleotide binding domain (NBD) and substrate binding domain (SBD) which are connected by a short linker (green). The NBD can be further divided into subdomain I and II (depicted in blue and turquoise). The SBD is comprised of a core of β-sheets with an adjacent α-helical region, referred to as "lid" (depicted in light red). The absent residues in the truncation mutants were just hidden, therefore these representations are based on the full length protein and do not represent authentic structural data.

Upon substrate binding, the ATPase function of HSP70 is triggered and enhanced by HSP40 co-chaperones. Hydrolysis of ATP to ADP leads to a conformational switch that closes the lid on the

substrate, resulting in a stronger binding of the client. Bound substrates can be released by replacement of ADP with a new ATP molecule, a process that is modulated by nucleotide exchange factors (NEFs), another class of important HSP70 cofactors. In order to identify the HSP70 domain which is responsible for the interaction with RABV P, separate constructs coding for the Flag-tagged NBD (residues 1-385) and SBD (residues 394-641) of HSP70 were created and assayed for their ability to interact with RABV P in Co-IP experiments (Figure 28). Flag-tagged versions of the NBD and SBD of HSP70 could successfully be expressed individually. Whereas the NBD shows no binding (black arrowhead), the SBD co-precipitates with HA-P (gray arrowhead), however to a lesser degree than full length HSP70-1A. This indicates that the SBD is essential and sufficient for binding, but that other parts of the protein might contribute to a considerably stronger interaction as observed for full length HSP70.

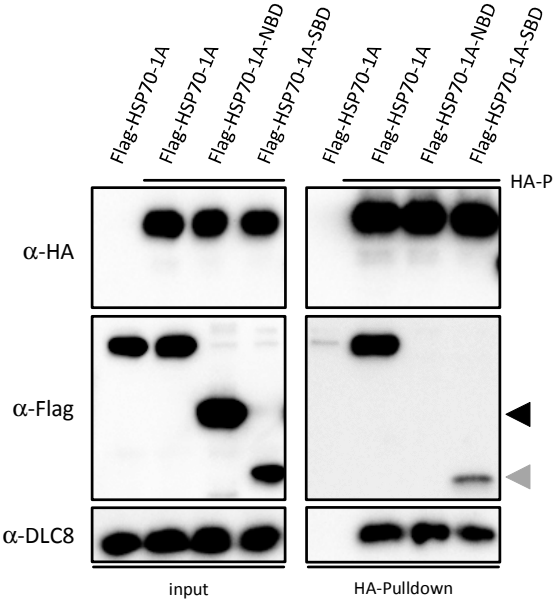

Figure 28: RABV P interacts with the SBD but not the NBD of HSP70-1A.
While HA-P co-precipitates full length HSP70-1A very efficiently, the SBD alone is only bound to a lower extent (gray arrowhead), whereas no interaction is apparent for the NBD (black arrowhead). HEK 293T cells were transfected with the indicated expression plasmids (2 µg HSP70 constructs, 2 µg HA-P) and lysed 24 h p. t. under native conditions. The lysates were subsequently subjected to Co-IP experiments and samples from input and pulldown fractions were subjected to by SDS-PAGE. After Western blotting specific protein bands were visualized using the indicated antibodies.

To identify which residues of HSP70 are essential to confer the strong interaction detected for full length HSP70, further truncation mutants were created. For both HSP70 and HSC70 constructs containing residues 190-511 were created, lacking subdomain I (aa 1-189) of the nucleotide binding domain (NBD) and the C-terminal lid, which is a part of the substrate binding domain (SBD) (Figure 27B). Truncation constructs and full length versions of both heat shock

proteins were assayed for their ability to associate with HA-GST-P-176-188 in Co-IP experiments using anti-HA affinity matrix (Figure 29A).

Both truncation versions of HSP70 and HSC70 retained their ability to co-precipitate with the RABV P derived peptide. Oddly, the Flag-tagged full length HSC70 construct displayed only residual interaction, whereas endogenous untagged HSC70 has been shown before to interact with RABV P equally well compared to HSP70. This was also indicated by mass spectrometry analysis of whole pulldown fractions (data not shown). The differential binding observed might be due to the N-terminal tag. HSP70 and HSC70 are in general well conserved (86 % sequence identity), but a number of amino acids at the N-terminus differ significantly and might account for the differential binding of N-terminal tagged constructs (MAKAAAI.. for HSP70 and MSKGPAV.. for HSC70). This is supported by the fact that the further N-terminally truncated HSC70 construct Flag-HSC70-190-511 is again able to interact with the P-peptide. In summary, these findings indicate that subdomain I of the NBD as well as the lid region of HSP70 proteins are not involved in interaction with RABV P. Since HSP70-190-511 comprises a truncated NBD, lacking the central catalytically important lysine 73, it is non-functional in regard to ATP hydrolysis (O'Brien et al., 1996). For this reason, ATPase function of HSP70 supposedly plays no role in the mode of interaction.

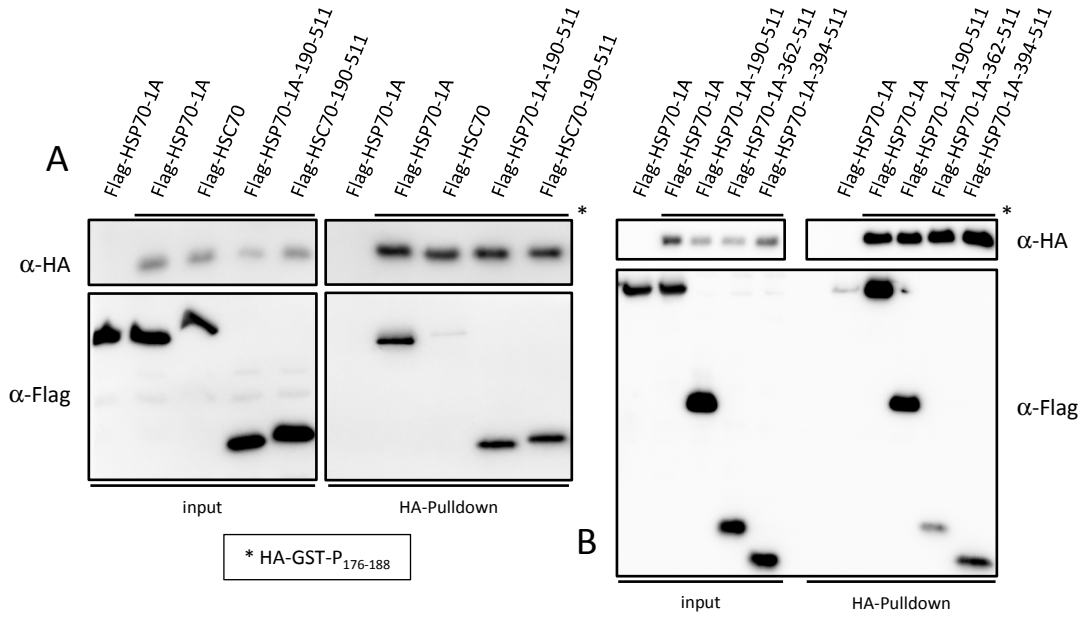

Figure 29: RABV P-176-188 co-precipitates the SBD (residues 394-511) of HSP70.

While HA-GST-P-176-188 co-precipitates full length HSP70 and an HSP70-1A-190-511 truncation construct very efficiently, the SBD (394-511, the core region lacking the lid) is co-precipitated to a lesser extent. For an overview over the constructs used see Figure 27. Experimental conditions for both **A)** and **B)**: 293T cells were transfected with the indicated expression plasmids (2 µg HSP70 constructs, 2 µg HA-GST-P-176-188) and lysed 24 h p. t. under native conditions. The lysates were subsequently subjected to Co-IP experiments and samples from input and pulldown

fractions were subjected to SDS-PAGE. After Western blotting specific protein bands were visualized using the indicated antibodies.

Since HSP70-1A-190-511 was still fully able to interact with HA-GST-P-176-188, additional truncations were created to elucidate the minimal binding site. In Flag-HSP70-1A-362-511 the N-terminal NBD is further truncated, with only the last helix before the linker to the SBD remaining (Figure 27C). Flag-HSP70-1A-394-511 only contains the SBD of HSP70-1A beginning in the linker region (Figure 27D). Both constructs were created lacking the lid region, because these residues have been shown before to be nonessential for the interaction. Full length Flag-HSP70-1A, as well as the truncations Flag-HSP70-190-511, Flag-HSP70-362-511 and Flag-HSP70-394-511 were assayed for their ability to co-precipitate with HA-GST-P-176-188 (Figure 29B). Even the smallest construct Flag-HSP70-394-511, consisting only of the core SBD without the lid region, was able to associate with the P-derived peptide. However, Flag-HSP70-190-511 exhibited a stronger interaction. This provides some evidence that RABV P interacts with the substrate binding domain of HSP70 family members, independently of the lid. Additionally, these observations suggest that HSP70 NBD subdomain II might stabilize the interaction, since interaction of HA-P-GST-176-188 is significantly stronger with HSP70-190-511 compared to Flag-HSP70-362-511 and Flag-HSP70-394-511.

4.2.4. Recombinantly purified P-constructs co-precipitate HSP70

Previously in this thesis, an interaction between HSP70 and RABV P residues 180-186 was described. This association was, however, observed in Co-IP experiments with overexpressed proteins in a human cell line. Therefore, an indirect interaction or mode of association requiring additional cofactors could not be excluded. We wanted to elucidate whether recombinantly expressed P derived peptides are able to co-precipitate HSP70 from cell lysate or *in vitro*, to provide some evidence for a direct interaction between the proteins.

For recombinant expression and purification from *E. coli*, HA-$(H_6)_2$-GST-fusion constructs were cloned into the bacterial expression vector pET28a. This construct was created to comprise an HA-tag for detection and purification using anti-HA affinity matrix, two His_6-tags for purification from bacteria and a GST tag for stabilization (schematic representation in Figure 31A). Full length P, P-176-188 and the scrambled version of the P-176-188 peptide, which has been shown to be unable to associate with HSP70 (Figure 23), were fused to this construct. The proteins were expressed and purified from *E. coli* as described in the Methods section of this thesis (3.2.12) and success of purification was validated by SDS-PAGE. Samples of elution fractions E1 - E3 of

the purifications were separated on a gel and stained with colloidal coomassie as shown in Figure 30. The fusion peptides HA-$(H_6)_2$-GST-P-176-186 as well as its scrambled version with a size of 32 kDa could be stably expressed and purified with a good yield. The full length RABV P fusion construct HA-$(H_6)_2$-GST-P (64 kDa) could also be expressed and purified, however to a lower concentration compared to the fusion peptides and containing more by-products. The smaller fragments in the full length P elution fractions might be bacterial contaminations binding to P, or C-terminal P degradation products still containing the N-terminal affinity tag, since they also strictly co-purify with the main product. The latter seems more likely, since RABV P has been reported previously to be prone to proteolysis due to the presence of intrinsically disordered regions (Mavrakis et al., 2004).

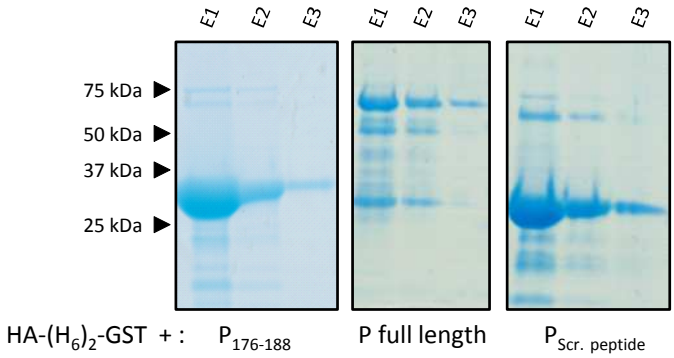

Figure 30: Elution fractions of different P constructs purified from *E. coli*.
The indicated proteins were expressed in *E. coli* and purified as described in 3.2.12. Samples of the elution fractions E1 – E3 for each protein were analyzed by SDS-PAGE and colloidal coomassie staining.

HA-$(H_6)_2$-GST-P-176-186 as well as the scrambled version were first used in order to elucidate whether a recombinantly expressed, short RABV P derived peptide is able to co-precipitate HSP70 from 293T cell lysate. Therefore, anti-HA affinity matrix was incubated in Co-IP buffer with an excess of the corresponding elution fractions of the bacterial purification. After removal of unbound proteins by several washing steps, 293T cell lysate was added and the normal Co-IP protocol was conducted (Figure 31B). Cellular HSP70 co-precipitated well with the recombinantly expressed HA-$(H_6)_2$-GST-P-176-186, whereas only background level association could be observed for the HA-$(H_6)_2$-GST-Scr.-peptide. This shows that a recombinant RABV P derived peptide is able to co-precipitate HSP70 from cell lysates.

In order to obtain evidence on the mode of interaction between HSP70 and RABV P, *in vitro* pulldowns were conducted using the RABV P proteins and peptides previously purified and recombinant human HSP70 purchased from *StressMarq*. Again, the different RABV P

HA-$(H_6)_2$-GST fusion proteins P-176-188, P-Scr.-peptide and full length P were incubated with HA-affinity matrix. After removal of unbound proteins by three washing steps, 4 µg of recombinant HSP70 per sample were taken up in Co-IP buffer and incubated with the protein loaded matrix (Figure 31C, input).

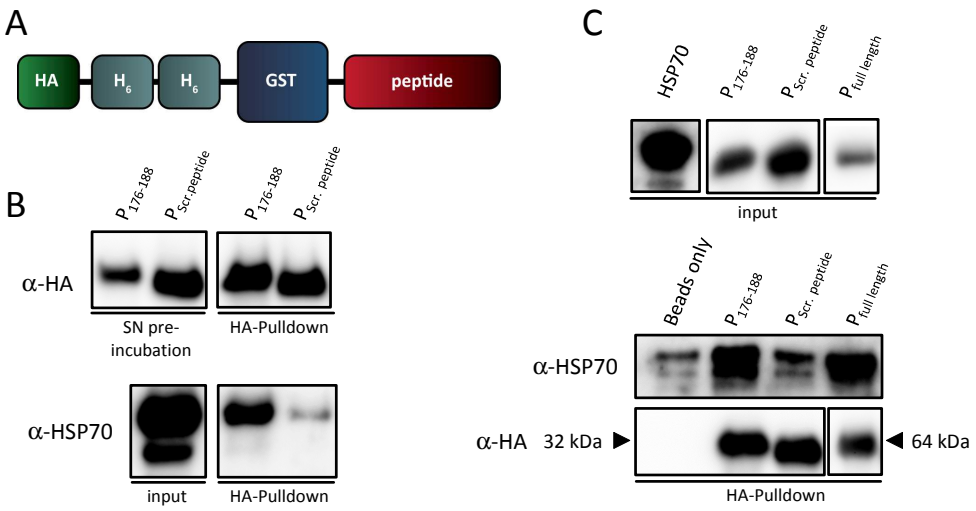

Figure 31: RABV P peptides purified from *E. coli* interact with HSP70.
A) Schematic representation of the HA-$(H_6)_2$-GST-fusion constructs used for bacterial expression. **B)** A RABV P-derived fusion peptide containing residues 176-188 co-precipitates HSP70 from HEK 293T cell lysate, in contrast to the scrambled negative control construct. Samples from the corresponding elution fractions of the bacterial purifications were incubated with HA-affinity matrix. As shown in the "SN pre-incubation" panel the recombinant proteins were used in excess. After washing, 293T cell lysate was added, followed by conduction of the standard Co-IP protocol. **C)** Purified full length RABV P and a P-176-186 fusion protein are able to co-purify recombinant human HSP70. A purified fusion peptide containing RABV P residues 176-188 in a randomized order was used as negative control. Samples from the corresponding elution fractions of the bacterial purifications were incubated with HA-affinity matrix. After removal of unbound proteins by three washing steps, the matrix was incubated with 4 µg of recombinant human HSP70. Subsequently, the standard Co-IP protocol was conducted.

While only minor background binding could be detected for empty matrix control (no pre-incubation with HA-tagged protein) and the scrambled P-peptide, P-176-186 and full length P were both able to interact with HSP70 (Figure 31C, HA-Pulldown). This provides some evidence for a direct interaction between RABV P region 176-188 and HSP70, because no other eukaryotic proteins that might mediate association are present in this *in vitro* setting. The observed interaction could be shown to be sequence specific for the identified residues, since the scrambled version of the P-derived peptide failed to associate with HSP70, equally to Co-IP experiments conducted previously employing co-expression of constructs in HEK 293T cells.

4.2.5. The mutant viruses SAD-L16-P-W186A and P-K214A induce IFN

The rabies virus phosphoprotein mutants P-W186A and P-K214A have been shown before in this thesis to be deficient in inhibiting interferon induction. We wanted to further elucidate whether this effect can also be observed in the viral context. Therefore, the corresponding mutations were inserted into the P gene of the full length virus rescue construct pSAD-HH-L16-SC (Ghanem et al., 2012). Using these constructs, recombinant rabies virus could be successfully rescued as described in the methods section of this thesis (3.2.13). Cloning of the viral full length rescue constructs and rescue of SAD-L16-P-K214A were conducted in cooperation with Dr. D. Aberle. Supernatants from rescue experiments were titrated and used to infect BSR-T7 cells with a defined MOI of 0.01 in order to grow stocks of the corresponding recombinant viruses. For L16-P-W186A, viral titers equal to the parental wild type L16 strain in the range of 10^8 ffu/ml could be obtained. L16-P-K214A only reached titers of 10^5 ffu/ml, exhibiting a significant growth defect.

In order to evaluate the growth kinetics of both L16 mutants on different cell lines, BSR-T7, HEp-2 and HEK 293T cells were infected with an MOI of 0.01, including SAD-L16 wild type virus as a control. HEp-2 and HEK 293T are human cell lines with an intact interferon system. Consequentially, virus mutants which fail to interfere with interferon induction might display impaired growth, although P still suppresses IFN signaling. Supernatants were taken 4.5, 24, 48, 72 and 96 h after infection and the viral titers were determined for each time point (Figure 32). SAD-L16-P-W186A exhibited growth kinetics comparable to wild type SAD-L16 on all different cell lines used, indicating that defective inhibition of IFN-induction is not crucial for viral growth even on IFN-competent cell lines. A possible explanation is that the RABV P mutant P-W186A is deficient in inhibition of IFN-induction, but still capable to block JAK-STAT signaling, thereby preventing the induction of antiviral ISGs. SAD-L16-P-K214A was significantly impaired in growth on all cell lines examined. This suggests that the defect is probably not mainly due to the inhibitory deficiency of the mutant P in regard to IFN-induction. RABV P binding to N_{RNA} involves the C-terminal domain (Chenik et al., 1994; Fu et al., 1994), consequently this function might be impaired in the P-K214A mutant leading to the observed severe attenuation in growth.

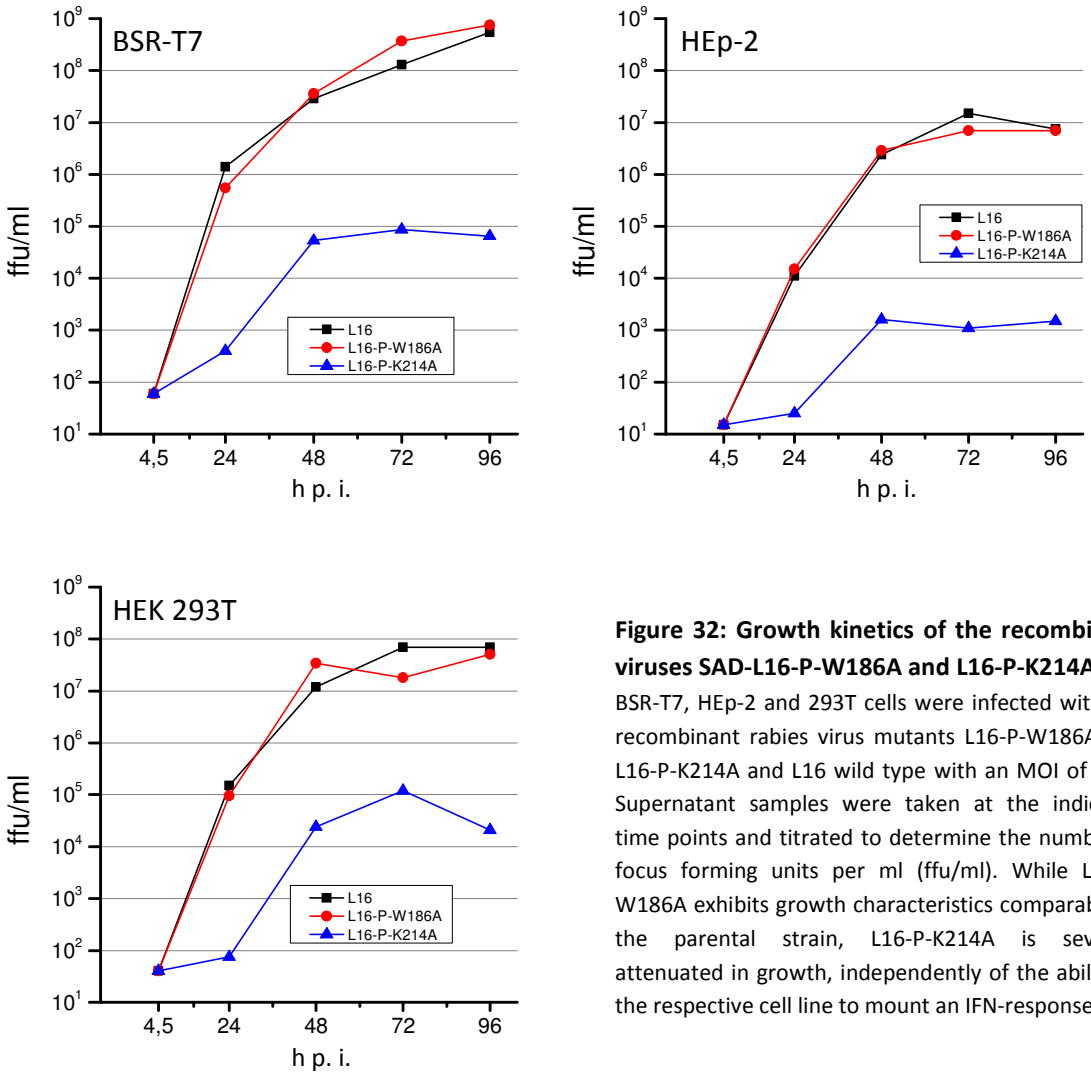

Figure 32: Growth kinetics of the recombinant viruses SAD-L16-P-W186A and L16-P-K214A.
BSR-T7, HEp-2 and 293T cells were infected with the recombinant rabies virus mutants L16-P-W186A and L16-P-K214A and L16 wild type with an MOI of 0.01. Supernatant samples were taken at the indicated time points and titrated to determine the number of focus forming units per ml (ffu/ml). While L16-P-W186A exhibits growth characteristics comparable to the parental strain, L16-P-K214A is severely attenuated in growth, independently of the ability of the respective cell line to mount an IFN-response.

In order to monitor IRF3 phosphorylation and induction of IFN-β mRNA upon infection with the different recombinant RABV mutants, HEK 293T cells were infected in triplicates with a MOI of 0.01 and harvested 48 h post-infection. SeDI treatment was used as a positive control for IFN-induction. From the triplicates, two samples each were subjected to RNA extraction and one sample was used for Western blotting analysis. Total RNA isolates were transcribed to cDNA and used in real-time RT-PCR assays to determine the levels of IFN-β and RABV P mRNA relative to mock infection (Figure 33A).

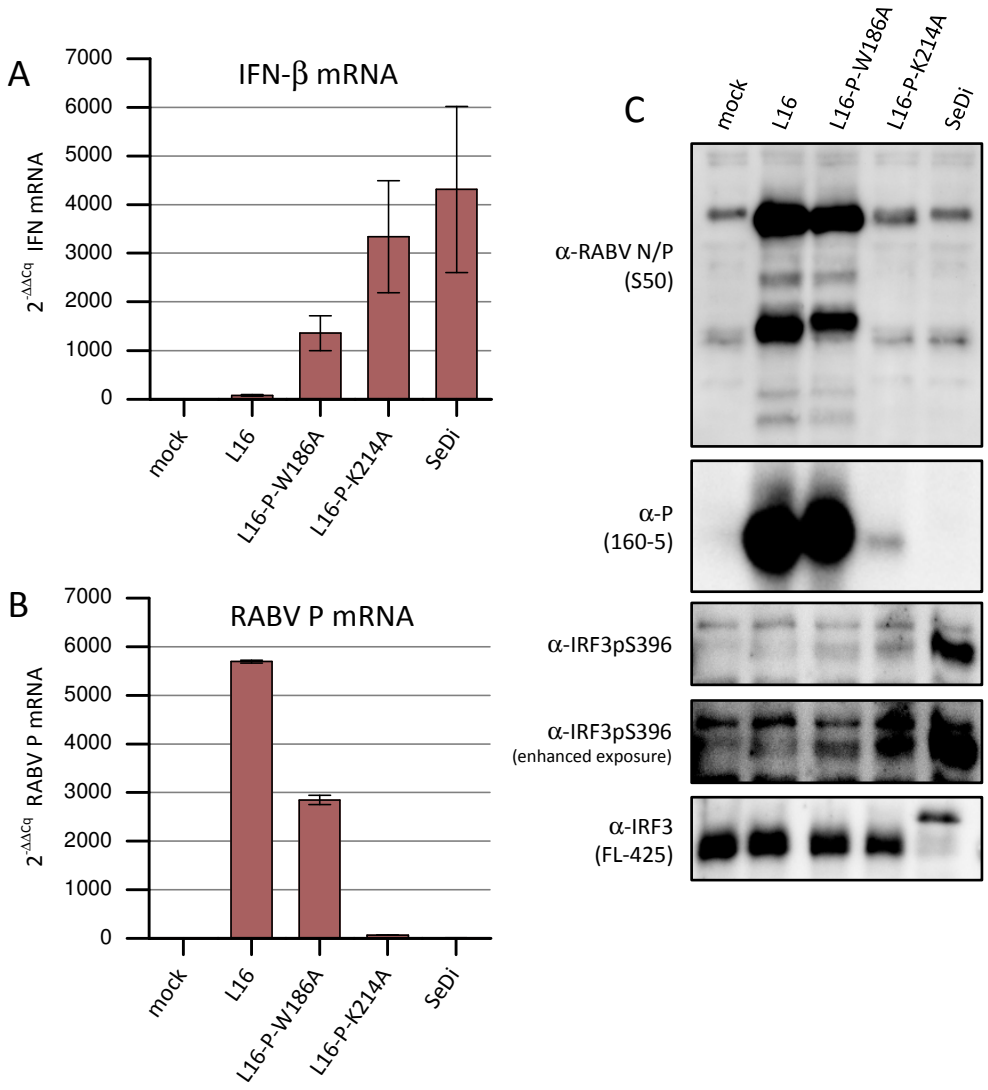

Figure 33: SAD-L16-P-W186A and L16-P-K214A induce transcription of IFN-β mRNA.
293T cells were infected with an MOI of 0.01 of the indicated recombinant viruses or treated with SeDIs in triplicates and harvested 48 h post-infection. **A)** and **B)** Two samples for each condition were used as duplicates in total RNA extraction and reverse transcription into cDNA. Real-time PCR was conducted using IFN-β (A) and RABV P (B) specific primers to determine the corresponding transcription levels. **C)** The remaining samples were subjected to SDS-PAGE and Western blotting. Specific protein bands were visualized using the indicated antibodies. While the levels of viral proteins for L16-P-W186A and the parental strain are comparable, the severe growth defect of L16-P-K214A is reflected in the hardly detectable signals for N and P in the corresponding lysates.

Whereas infection with the wild type L16 virus only lead to minor induction, L16-P-W186A infected cells exhibited a solid upregulation of IFN-β mRNA transcription. Normalized to L16 wild type, the induction by L16-P-W186A is about 16-fold higher, what is in the range that has been reported previously for the L16-PΔInd viruses, which likewise exhibit a defect in controlling IFN-induction (Rieder et al., 2011). Additionally, a low but detectable endogenous level of IRF3 S396 phosphorylation could be observed by Western blotting (Figure 33B, panel with enhanced exposure). Expression levels of the viral proteins N and P were similar for L16 and L16-P-W186A,

however P mRNA levels were reduced twofold in the mutant virus. This provides good evidence that RABV phosphoprotein tryptophan 186 is indeed crucial for a functional inhibition of IRF3 phosphorylation and circumvention of IFN-β mRNA induction in the viral context.
Surprisingly, infection with L16-P-K214A lead to a very strong IFN-β mRNA induction comparable to SeDI treatment. This is contrasted by the strongly impaired growth which is also reflected by very low P mRNA levels and N and P protein levels. These findings hint at an increase in PAMP generation in L16-P-K214A, since induction is even much higher than in cells infected with L16-P-W186A, despite significantly reduced growth.

4.2.6. CVS-strain P is deficient in inhibition of IFN-induction

As described before, we could show that the rabies virus phosphoproteins of the different strains L16, THA and CVS interacted with HSP70 and HSC70 equally well (Figure 24). In addition, the abilities of the different RABV P proteins to interfere with IRF3 activation was assayed in IFN-β promoter dependent reporter gene assays. Pathway stimulation was carried out with ΔRIG-I or TBK1 overexpression (Figure 34). Like L16-P, THA-P abrogated the reporter activity to almost basal levels. Remarkably, HA-CVS-P was found to be deficient in interfering with IFN-β promoter activity equally to HA-L16-P-W186A. This defect was observed for pathway stimulation with either ΔRIG-I and TBK1 and could not be attributed to impaired expression, since Western blotting did not reveal a correlation between protein levels and inhibition. This finding is surprising, since CVS strain is a lethal virus frequently used for studying rabies virus infection in animal models (Park et al., 2006) and the ability to suppress IFN induction was assumed to be important for viral pathogenicity of the SAD-L16 strain (Rieder et al., 2011).
In order to find an explanation for the differential inhibitory capacities, we wanted to elucidate which sequence differences between the well conserved phosphoproteins are responsible for the defect observed in CVS-P. Therefore a number of rabies and other *Lyssavirus* P sequences were aligned and monitored for notable variations, especially in proximity of the HSP70 binding motif (Figure 35). The selection of rabies virus P sequences (highlighted with red overlay) contains vaccine strains, other fixed laboratory strains as well as wild type isolates. In general, the rabies virus P sequences included are quite highly conserved in the observed region. However, the inhibition deficient CVS-strain P protein shows an outstanding proline residue at position 179, where all other RABV P sequences exhibit a serine residue (highlighted as red dot).

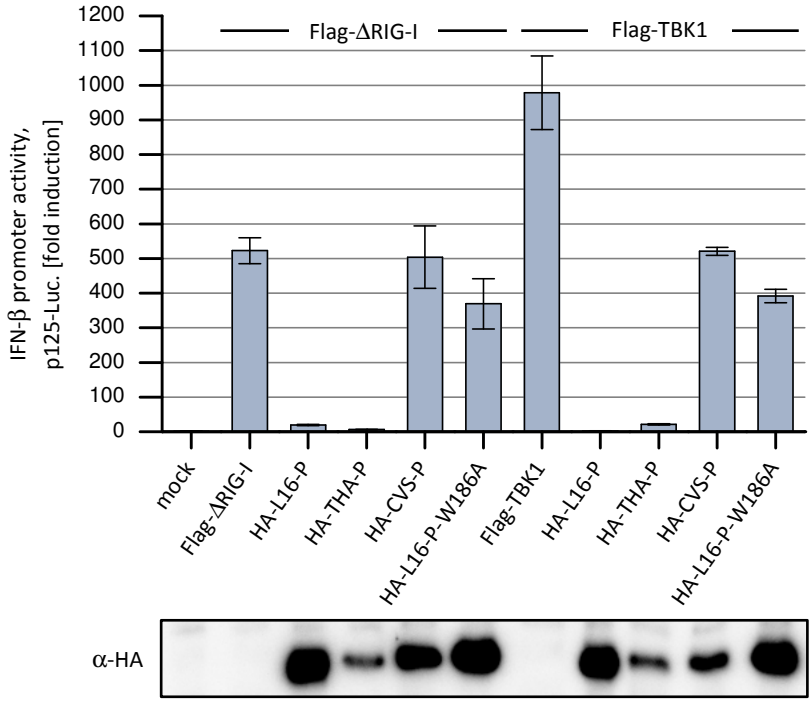

Figure 34: CVS strain RABV P is deficient in inhibiting IFN-β promoter activity.
While THA-strain RABV P interferes with IFN-promoter activity like L16-P, CVS-P exhibits an inhibitory defect comparable to the mutant L16-P-W186A. HEK 293T cells were transfected with reporter plasmids (100 ng p125-FF/10 ng pTK-RL) and the indicated constructs (100 ng Flag-ΔRIG-I, 200 ng Flag-TBK1, 200 ng P constructs plasmid DNA). Cells were lysed 24 h p. t. and subjected to dual luciferase assays in order to examine the ability of different P constructs to interfere with ΔRIG-I and TBK1 overexpression mediated IFN-β promoter activity. The bars represent the means and the error bars the standard deviations of biological duplicates. Cell lysates were examined by Western blotting in order to determine expression levels of the constructs used.

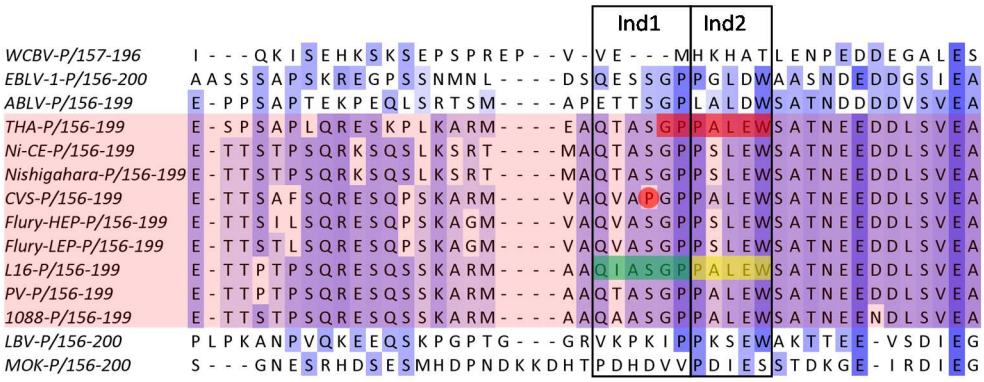

Figure 35: Alignment of different rabies and *Lyssavirus* phosphoprotein sequences.
Phosphoprotein sequences of different rabies virus strains (red overlay) and other *Lyssaviruses* were aligned using the "Clustal Omega" online tool of EMBL-EBI (European Bioinformatics Institute) and visualized with Jalview (Waterhouse et al., 2009). Ind1 (green) and Ind2 (yellow), the sequences missing in the respective deletion mutants, and the minimal HSP70 binding (red) region are annotated.

This residue came especially in the focus of interest, because P181 is located in the Ind1 region and ΔInd1 deletions have been shown to be deficient in inhibition before (Figure 25; Rieder et al. (2011)). EBLV-1-P, a *Lyssavirus* proteins that has been previously shown to be able to inhibit

IFN-β induction (unpublished observation, Conzelmann group), also exhibits a serine residue at this position. Consequently, we hypothesized that CVS-P residue 179 might be responsible for the inhibitory defect.

To further examine this, the mutant proteins HA-L16-P-S179P and HA-CVS-P-P179S were created. In these constructs, proline 179 in CVS-P has been replaced by a serine residue normally found in L16-P, and the other way round. Together with HA-L16-P, HA-CVS-P and HA-L16-P-W186A as controls, the new mutants were examined for their ability to interfere with ΔRIG-I mediated IFN-β promoter activity in reporter gene assays (Figure 36).

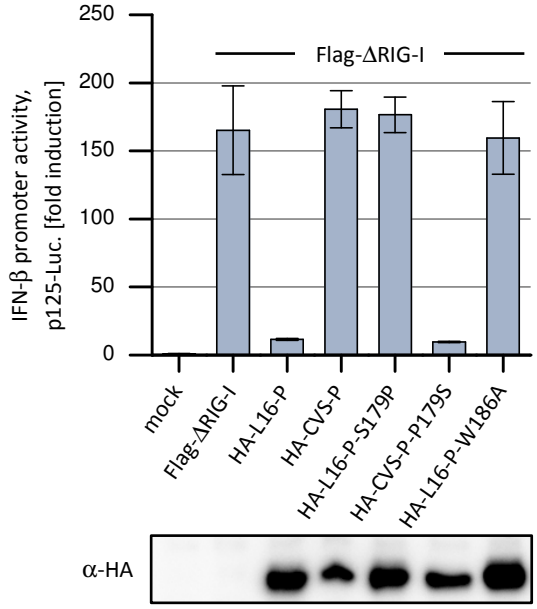

Figure 36: CVS-P inhibitory deficiency can be restored by a P179S substitution.
HEK 293T cells were transfected with reporter plasmids (100 ng p125-FF/10 ng pTK-RL) and the indicated constructs (100 ng Flag-ΔRIG-I, 200 ng P constructs plasmid DNA). Cells were lysed 24 h p. t. and subjected to dual luciferase assays in order to examine the ability of different P constructs to interfere with ΔRIG-I-mediated IFN-β promoter activity. The bars represent the means and the error bars the standard deviations of biological duplicates. Cell lysates were examined by Western blotting in order to determine expression levels of the constructs used.

HA-L16-P inhibited induction very strongly, whereas for HA-CVS-P again no significant influence on promoter activity could be observed. HA-L16-P-S179P exhibited the same deficiency as CVS-P in regard to suppressive capacity. In contrast, HA-CVS-P-P179S impaired IFN-β promoter induction equally well as HA-L16-P, while the observed expression levels for the different proteins were comparable. Thus, the P179S substitution was able to rescue the defect in CVS-P, whereas L16-P was impaired by a S179P mutation. Taken together, this provides strong evidence that indeed P179 in the CVS strain phosphoprotein sequence is alone responsible for the inhibitory deficiency. Since CVS-P also binds HSP70, it can be concluded that this interaction alone is not sufficient, however essential for the suppressive capacities of RABV P. This has also

been the case for RABV P mutants deficient in nuclear trafficking previously examined, which contain the intact HSP70 binding motif but fail to interfere with IFN-β induction.

4.3. Impact of HSP70 and heat shock on RLR signaling

Previously in this thesis, an intact to HSP70 binding motif could be identified as a crucial feature in inhibition of IFN-β induction by RABV P. This raised the question whether HSP70 family members might be in general involved in the regulation of IFN induction via the RLR pathway and how P could utilize heat shock proteins to exert its suppressive functions. To further investigate this issue, several experiments with overexpression of different heat shock protein constructs were conducted, in order to monitor a possible impact on innate immune signaling.

4.3.1. P inhibition is not impaired by HSP70 overexpression

Since RABV P targets HSP70, we wanted to elucidate whether further hints can be obtained that this interaction is indeed responsible for the inhibitory abilities of RABV P. HSP70 is a ubiquitously expressed protein family and involved in a magnitude of cellular processes not limited to protein folding and stress response (Beere and Green, 2001; Chappell et al., 1986; Matlack et al., 1999). Therefore, we wanted to obtain a general overview by examining whether overexpression of HSP70 might interfere with IFN-β promoter activity or either impair or support the inhibitory function of P. Therefore, Flag-HSP70 (HSPA1A) and Flag-HSC70 were co-expressed with ΔRIG-I or TBK1 in the absence or presence of RABV P and IFN-β promoter activity was measures in luciferase reporter gene experiments (Figure 37). Sole expression of Flag-HSP70 or HSC70 did not lead to any promoter activation. Whereas Flag-HSC70 expression left induction by ΔRIG-I unaffected, Flag-HSP70 impaired IFN-β promoter activity to some degree. Co-expression of either heat shock protein with P displayed no significant change in the inhibitory abilities of RABV P. The same pattern could be observed for promoter induction with Flag-TBK1 overexpression.

Consequently, RABV P inhibition of IFN-β promoter induction could not be compensated or stimulated by overexpression of additional heat shock proteins. However, Flag-HSP70 overexpression lead to some reduction of promoter activity, providing a first hint that heat shock proteins might be involved in the modulation of RLR signaling.

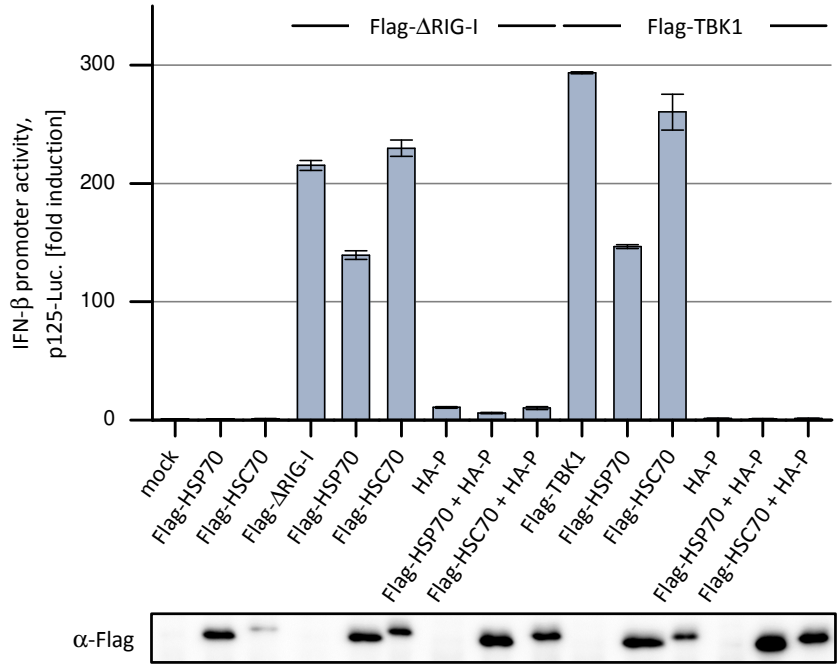

Figure 37: Overexpression of HSP70s has no impact on the inhibitory function of RABV P.
HEK 293T cells were transfected with reporter plasmids (100 ng p125-FF/10 ng pTK-RL) and the indicated constructs (100 ng Flag-ΔRIG-I, 200 ng Flag-TBK1, 200 ng HSP70/P construct plasmid DNA). Cells were lysed 24 h p. t. and subjected to dual luciferase assays in order to examine the ability of different P and HSP70 constructs to interfere with ΔRIG-I-mediated IFN-β promoter activity and whether HSP70 co-expression is able to interfere with the suppressive capacity of RABV P. The bars represent the means and the error bars the standard deviations of biological duplicates. Cell lysates were examined by Western blotting in order to determine expression levels of the HSP70 constructs used.

4.3.2. Dominant negative HSP70 constructs inhibit IFN induction

To get a further insight into how members of the HSP70 family might interfere with innate immune signaling pathways, we examined wild type heat shock proteins and mutants deficient in chaperoning activity and their effect on different parts of the IFN-promoter. Therefore, an ATPase deficient Flag-HSP70-K71E mutant (based on HSPA1) was created (Zeng et al., 2004). The ability of Flag-P, Flag-HSP70 (HSPA1), Flag-HSP70-K71E and Flag-HSC70 to interfere with ΔRIG-I mediated induction of several promoters was examined. In addition to the natural IFN-β promoter (p125), the impact on the artificial reporter constructs p55C1B (multiple IRF3 binding sites) and p55A2 (multiple NF-κB binding sites) was examined (Yoneyama et al., 1996). IRF3 and NF-κB normally activate transcription in a cooperative way on the native IFN-β promoter (Kim et al., 2000). Using this reporter system, it is possible to distinguish the activation states of the two transcription factors that separately drive expression from the corresponding reporters (Figure 38).

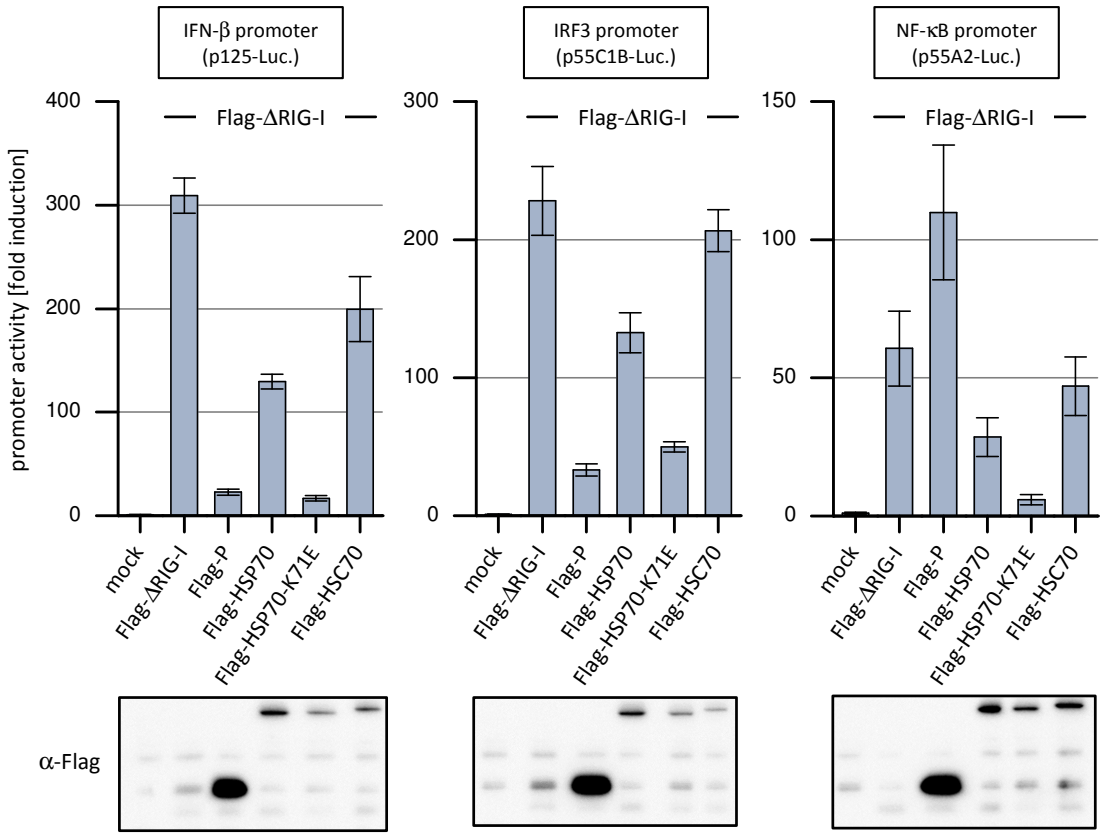

Figure 38: Expression of ATPase deficient HSP70-K71E significantly impairs ΔRIG-I mediated signaling.
200 ng plasmid DNA coding for the indicated RABV P or HSP70 constructs was co-transfected into HEK 293T cells together with 100 ng Flag-ΔRIG-I and the indicated reporter constructs (100 ng reporter plasmid/ 10 ng pTK-RL for normalization). 24 h. p. t. cells were harvested and subjected to dual luciferase assays in order to examine the capacity of the indicated constructs to interfere with the induction of IFN-β, IRF3 or NF-κB promoter by ΔRIG-I overexpression. The bars represent the means and the error bars the standard deviations of biological duplicates. Results for the different reporters are shown in separate plots. Cell lysates were examined by Western blotting in order to determine expression levels of the constructs used.

RABV P inhibited IFN-β and IRF3 promoter activity efficiently, reflecting its ability to block activation of IRF3. In contrast, NF-κB promoter activity was significantly enhanced by RABV P, indicating that inhibition of the IFN-promoter is exclusively due to impaired IRF3 phosphorylation. Flag-HSP70 overexpression lead to a reduction in activity for all promoters investigated. Flag-HSC70 only impaired IFN-promoter activity, however to a lesser degree than HSP70. The ATPase deficient mutant Flag-HSP70-K71E repressed activity of all examined reporters very efficiently. In contrast to RABV P, this was also true for NF-κB promoter induction. This shows that overexpression of wild type or dominant negative ATPase defective HSP70 family members can significantly impair RLR signaling, however, not with precisely the same mechanism as RABV P, since NF-κB promoter activity is suppressed as well.

In addition to K71E, also other mutations in HSP70 lead to dysfunctional and potentially dominant negative heat shock proteins. A construct based on the nucleotide binding domain of

HSC70 with glycine 201 and 202 substituted by aspartate and glutamate, respectively (GG-DE mutation), was previously shown to inhibit synaptic vesicle endocytosis (Morgan et al., 2013). Heat shock proteins with this mutations are unable to bind ATP, because the charge of the aspartate and glutamate residues block positioning of the gamma-phosphate of ATP. Normally, nucleotide exchange factors (NEFs), a family of HSP70 cofactors, bind to the chaperone after hydrolysis of ATP in order to replace ADP by a new molecule of ATP, so that the substrate can be released and a new hydrolytic cycle can start. The NEF–HSP70 binding dissolves upon ATP binding. Since this binding is blocked in case of the GG-DE mutant, NEFs are stuck on the protein and are no longer available in the cellular pool, leading to impaired nucleotide exchange function. This results in decreased chaperone activity and consequently a blockage in HSC70 dependent uncoating of clathrin-coated endocytosed synaptic vesicles (Morgan et al., 2013).

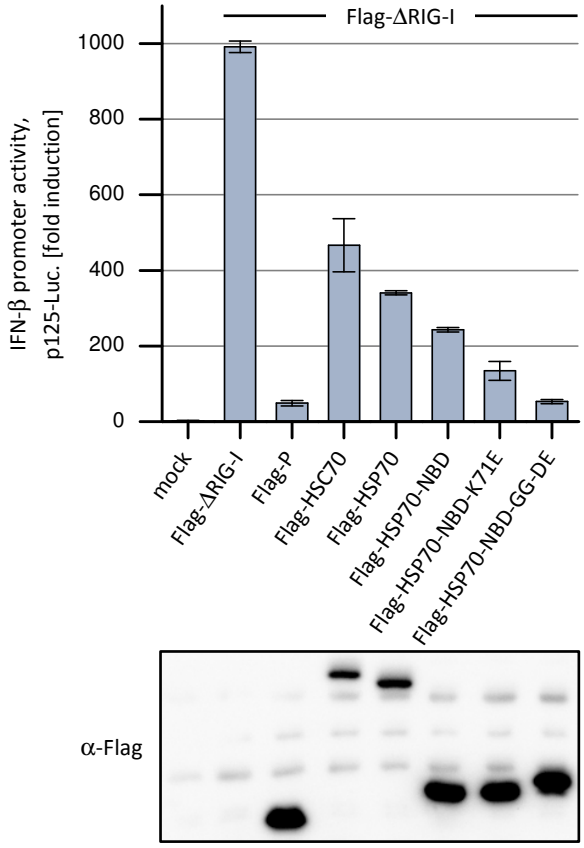

Figure 39: Different HSP70 mutants interfere efficiently with IFN-β promoter activity.
The HSP70 NBD mutants K71E (ATPase deficient) and GG-DE (ATP binding deficient) interfere substantially with ΔRIG-I mediated IFN-reporter activity. HEK 293T cells were transfected with reporter plasmids (100 ng p125-FF/10 ng pTK-RL) and the indicated constructs (100 ng Flag-ΔRIG-I, 200 ng P/HSP70 construct plasmid DNA). Cells were lysed 24 h p. t. and subjected to dual luciferase assays in order to examine the ability of the indicated constructs to interfere with ΔRIG-I-mediated IFN-β promoter activity. The bars represent the means and the error bars the standard deviations of biological duplicates. Cell lysates were examined by Western blotting in order to determine expression levels of the constructs used.

We wanted to elucidate whether HSP70 constructs other than full length K71E mutants might be able to interfere with the induction of IFN-β as well. Therefore HSP70-1A-NBD versions of the K71E and the G201D-G202E mutant were created and assayed for their ability to suppress ΔRIG-I induced IFN-β reporter activity (Figure 39). Wild type HSP70-NBD alone suppressed the activity slightly better than the full length heat shock proteins investigated in this experiments. The mutant NBD constructs both inhibited IFN-β promoter activity very efficiently, while Flag-HSP70-NBD-GG-DE exhibited the strongest inhibitory effect.

Taken together, the results obtained from studying ATPase or ATP-binding deficient HSP70 provide a hint that these constructs exhibit a dominant negative effect that not only impairs the cellular heat shock machinery, but also induction of IFN following RLR activation.

4.3.3. Heat-shock treatment impairs RLR signaling but not IFN signaling

In the current thesis it could be shown that overexpression of wild type and, to a much greater extent, deficient heat shock proteins can significantly impair IFN-β promoter activity upon ΔRIG-I stimulation in dual luciferase reporter gene assays. As the name suggests, heat shock proteins are normally upregulated in conditions of cellular stress resulting from elevated temperatures, leading to denaturation of proteins (Richter et al., 2010). Therefore, we wanted to examine whether direct heat shock (HS) treatment of HEK 293T cells might also influence interferon induction via RLR signaling, or impair the suppressive capacity of RABV P.

It can be difficult to determine whether an observed effect associated with heat shock proteins is in fact specific, since HSP70 is involved in a plethora of different cellular functions, especially in regard to protein homeostasis (Balchin et al., 2016). This has to be handled with particular care when reporter gene experiments are employed, since the observed readout is also partly depending on correct folding and stability of the luminescent reporter protein. To circumvent this and to support a specific activity on RLR signaling, we also investigated the impact of heat shock on JAK-STAT signaling by using ISRE-promoter driven luciferase expression and type I IFN treatment. This pathway is also a part of the cellular innate immune response, but mechanistically unrelated to the RIG-I pathway. Stimulation by ΔRIG-I and TBK1 overexpression and inhibition by RABV P with and without heat shock treatment were investigated in the IFN-β promoter dependent reporter system. The same was simultaneously conducted for stimulation with type I interferon treatment using an ISRE-reporter (Figure 40A, different reporters plotted separately).

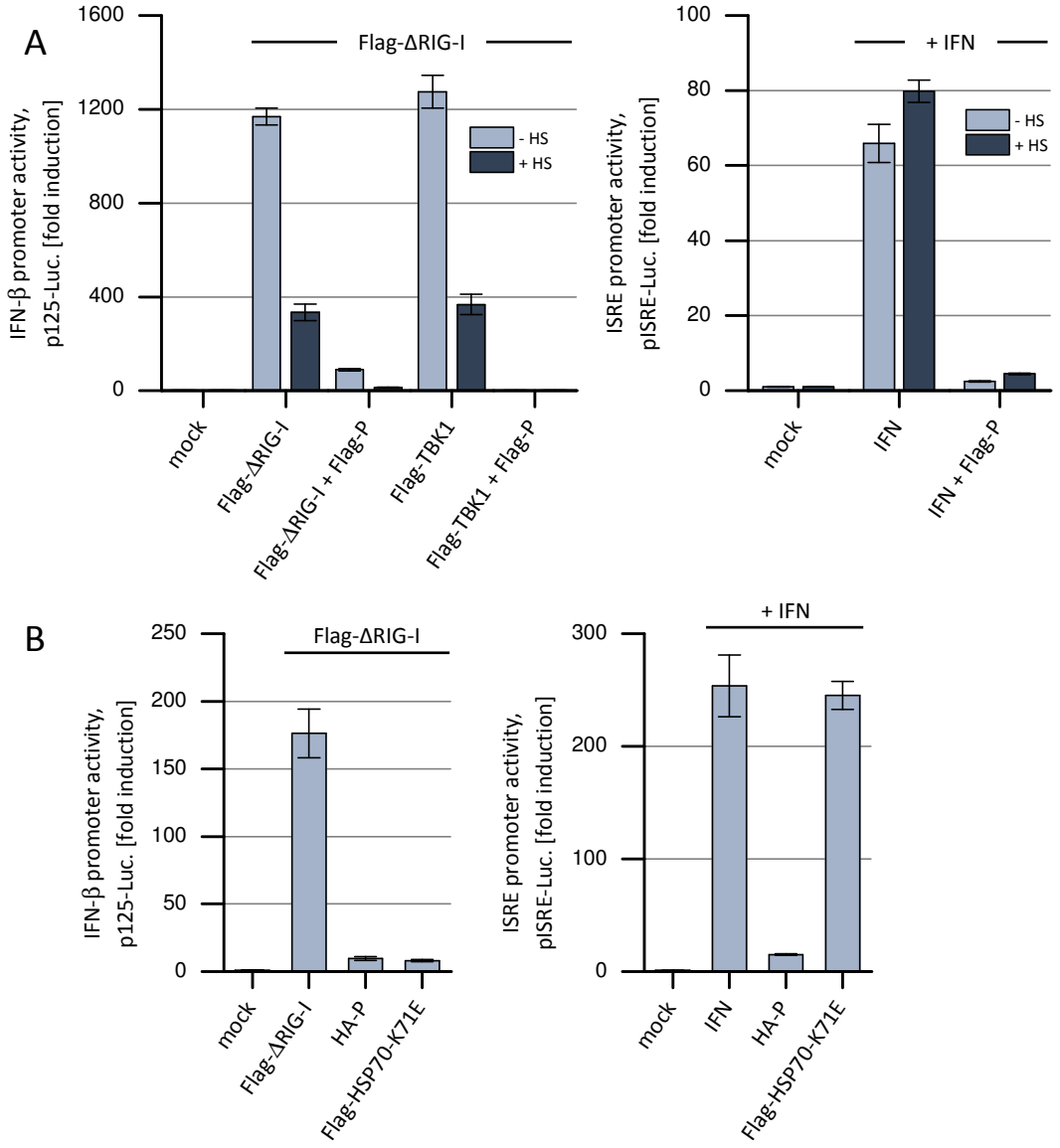

Figure 40: HS and HSP70-K71E impair IFN-β promoter induction but not IFN signaling.

A) Heat shock treatment of cells strongly interferes with ΔRIG-I and TBK1 mediated IFN-β reporter activity, while IFN-mediated ISRE-reporter activity is slightly increased. The inhibitory abilities of RABV are not affected in both cases. HEK 293T cells were transfected with reporter plasmids (100 ng p125-FF or pISRE-FF, 10 ng pTK-RL) and the indicated constructs (100 ng Flag-ΔRIG-I, 200 ng Flag-TBK1 and 200 ng P construct plasmid DNA). Heat shock treatment was conducted 3 h p. t. at 45 °C for 30 min and 100 units type I interferon were added to the cells per 24-well 6 h p. t. as indicated. Cells were lysed 24 h p. t. and subjected to dual luciferase assays in order to examine the ability of heat shock treatment to interfere with IFN-β or ISRE promoter activity or the suppressive capacity of RABV P. The bars represent the means and the error bars the standard deviations of biological duplicates. Results for the different reporters are shown in separate plots. **B)** While Flag-HSP70-K71E expression strongly impairs ΔRIG-I mediated IFN-induction, IFN-mediated ISRE-reporter activity is not affected. HEK 293T cells were transfected with reporter plasmids (100 ng p125-FF or pISRE-FF, 10 ng pTK-RL) and the indicated constructs (100 ng Flag-ΔRIG-I and 200 ng P/HSP construct plasmid DNA). 100 units type I interferon were added to the cells per 24-well 6 h p. t. as indicated. Cells were lysed 24 h p. t. and subjected to dual luciferase assays in order to examine the ability of ATPase deficient HSP70 to interfere with IFN-β or ISRE promoter activity. The bars represent the means and the error bars the standard deviations of biological duplicates. Results for the different reporters are shown in separate plots.

Interestingly, IFN-β reporter activity mediated by ΔRIG-I as well as TBK1 overexpression was significantly reduced upon HS. This is concurrent with the suppression previously observed with heat shock protein overexpression. Notably, the inability of HS treatment to impair ISRE-reporter activity after IFN-treatment demonstrates that the suppression observed with the IFN-β promoter dependent system is not only due to impaired stability or expression of firefly luciferase after heat shock. Consequently, it can be assumed that the luciferase reporter system yields specific results, also when investigating heat shock proteins by overexpression or heat shock treatment. Regardless of heat shock treatment, RABV P was able to very efficiently suppress ΔRIG-I and TBK1 overexpression mediated IFN-β promoter induction, as well as ISRE-reporter activity after addition of type I IFN. Heat shock treatment thus could not impair the inhibitory capacities of RABV P, rather a slightly supportive activity on IFN-signaling was suggested by the data.

To further ensure the reliability of the reporter assay, we wanted to compare the suppressive capacities of the HSP70-1A-K71E mutant on ΔRIG-I induced IFN-β promoter activity with a potential impact on ISRE-reporter activity after IFN treatment, similar to the previous experiment (Figure 40B, different reporters plotted separately). In accordance with previous results, HA-P and Flag-HSP70-K71E suppressed IFN-β promoter activity very efficiently. In contrast, whereas HA-P also impaired ISRE-promoter induction after type I IFN treatment, Flag-HSP70-K71E exhibited no significant influence on reporter activity. This provides again strong evidence that suppression of promoter induction with the HSP70-K71E mutant observed in the IFN-β dependent system is not due to impaired stability of the firefly luciferase reporter. Consequently, this indicates that expression of dominant negative ATPase deficient heat shock proteins indeed specifically impairs the mechanisms responsible for IFN-β induction after RIG-I activation.

Since an involvement of HSP70 family members in induction of IFN-β was suggested by previous results, we wanted to examine whether the inducible heat shock protein HSP70-1A is essential for induction or inhibition by RABV P. To examine this, a HEK 293T HSP70-1A/1B knockout cell line was used in IFN-β promoter dependent reporter gene assays. This cell line was previously generated in our laboratory by Dr. K. Sparrer and W. Greulich using the CRISPR-Cas9 system (Mali et al., 2013). Both genes, HSP70-1A and HSP70-1B, were targeted simultaneously by the same gRNA, since they exhibit an identical sequence in the corresponding target region. Overall, HSP70-1A and HSP70-1B differ only in two amino acids on the protein level and can therefore be considered functionally identical. HA-P was co-expressed with ΔRIG-I or TBK1 in HSP70-1A/1B-KO or wild type cells and optionally subjected to heat shock treatment (HS) (Figure 41).

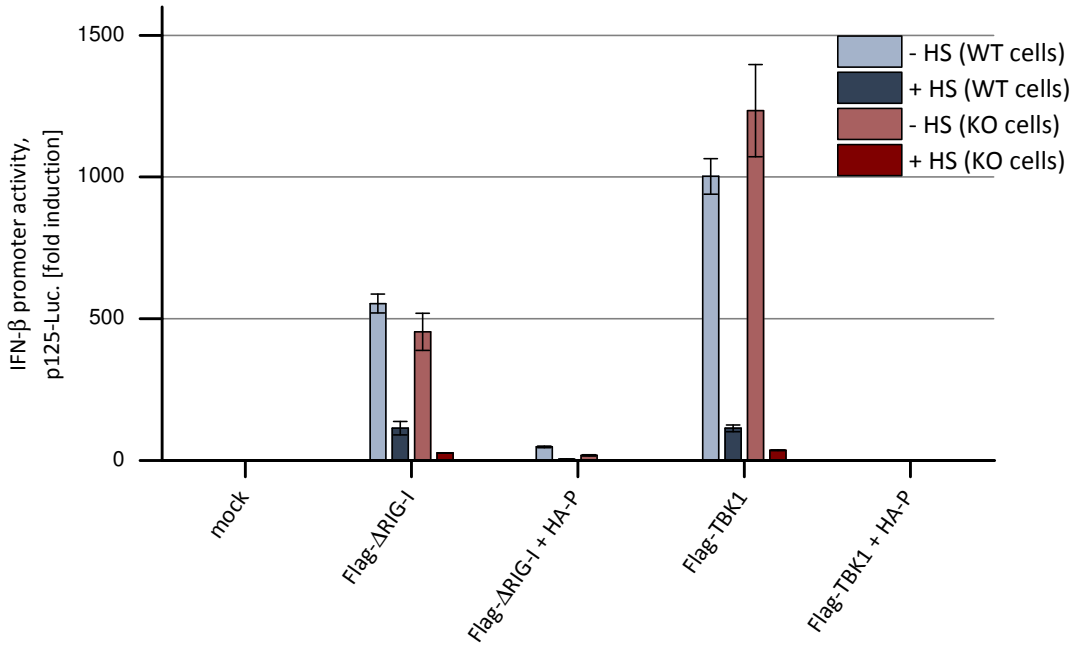

Figure 41: IFN induction and inhibition by P is not affected in 293T HSP70-1A/1B KO cells.
Induction of IFN-promoter activity by ΔRIG-I or TBK1 and inhibition by RABV P or heat shock treatment are not differing substantially between HEK 293T wild type and HSP70-1A/1B KO cells. HEK 293T wild type or HSP70-1A/1B KO cells were transfected with reporter plasmids (100 ng p125-FF/10 ng pTK-RL) and the indicated constructs (100 ng Flag-ΔRIG-I, 200 ng Flag-TBK1 and 200 ng P construct plasmid DNA). Heat shock treatment was conducted 3 h p. t. at 45 °C for 30 min. Cells were lysed 24 h p. t. and subjected to dual luciferase assays in order to examine the ability of the indicated constructs to interfere with ΔRIG-I-mediated IFN-β promoter activity with or without heat shock treatment in wild type and HSP70-1A/1B KO cells. The bars represent the means and the error bars the standard deviations of biological duplicates.

IFN-β promoter activity was not impaired in HSP70-1A/1B KO cells compared to wild type HEK 293T cells. Likewise, the suppressive capacities of RABV P remained unaffected in the knockout cells. Heat shock treatment impaired reporter activity equally in wild type and KO cells, similar to previously observed results (Figure 40A). In summary, no significant difference could be observed between wild type and HSP70-1A/1B KO cells in this experimental setting. Although HS seemed to have an even greater inhibitory effect in the KO cells, this indicates that HSP70-1A/1B is either not significantly involved in RLR signaling or RABV P inhibition, or the functional contribution of heat shock proteins to this pathway exhibits a high degree of redundancy. The latter possibility should especially be considered, since there are many conserved members of the HSP70 family that also might be involved in multiple cellular functions, such as the constitutively expressed HSC70 and several other HSP70-like proteins.

5. Discussion

All forms of life are constantly threatened by numerous invading microbial pathogens. The main goal of viruses, obligate intracellular parasites, is to introduce their genetic information into their host cells, an essential prerequisite for replication and viral propagation. This poses a significant danger to the genomic integrity of the target cell. In order to counteract this pathogenic threat and to protect the whole organism, a sophisticated immune system developed in the course of human evolution. The adaptive immune system, comprising diverse specialized immune cells and antibodies, is highly efficient and very specifically directed against a certain pathogen but reacts rather slowly. In contrast, the innate immune system is able to mediate protection against a wide range of pathogens on a cellular level without a substantial delay. It is a first line of defense that contributes to the initiation of an adaptive immune response but also confers anti-microbial activity directly via the interferon system. The innate immune system utilizes germ-line encoded receptors in order to detect pathogen-associated molecular pattern (PAMPs), which are chemically or in regard to their subcellular localization distinct from self-structures, such as viral RNAs (Roers et al., 2016). Triggering of these receptors by their ligands, such as viral RNA for RIG-I, results in the activation of a complex signaling cascade leading to the production of type I interferons and inflammatory cytokines. These signaling molecules elucidate a potent antiviral state that can potentially suppress the replication of many pathogens on different levels. However, most viruses successfully adapted and evolved means to circumvent the innate immune reaction, in order to establish an infection (Randall and Goodbourn, 2008).

The Rabies virus phosphoprotein P is able to interfere with innate immune signaling on two distinct levels. P suppresses IRF3 activation and consequently IFN induction (Brzózka et al., 2005) and further abrogates IFN-signaling on the level of STAT signal transduction (Brzózka et al., 2006; Vidy et al., 2005). This dual function makes P one of the most potent known viral IFN-antagonists. Whereas it is well establishes that the inhibition of IFN-signaling is based on a blockage of nuclear accumulation of STATs by RABV P, the mode of inhibition of IRF3 activation remains opaque. P residues 176-186, part of an intrinsically disordered region connecting dimerization domain and C-terminal domain, were shown to be critically involved in inhibition of IRF3 phosphorylation, however no clear function or binding partner could be identified (Rieder et al., 2011).

In this thesis, some light could be shed on the domains and functions of RABV P that are essential for suppression of IFN induction. Whereas the N-terminal domain of RABV was not involved in inhibition, the C-terminus and a conformational NLS located in this domain could be

shown to be required for inhibition of IRF3 activation. Further, an interaction of the previously identified RABV P stretch 176-186 with members of the HSP70 family could be characterized. P residues 180-186 were identified as minimal interaction motif. *In vitro* pulldowns employing recombinantly purified proteins suggested a direct mode of interaction. Tryptophan 186 was identified as essential residue for this interaction and, most importantly, also for the ability of RABV P to interfere with IFN induction, suggesting a correlation between HSP70 binding and inhibitory capacities. When investigating the phosphoproteins of different RABV strains, the CVS-strain P was found to be deficient in inhibition of IFN induction, due to an outstanding serine to proline mutation at position 179. Further, recombinant rabies viruses containing mutant phosphoproteins with a W186A or a CTD-NLS associated K214A substitution could be successfully rescued. L16-P-W186A showed growth kinetics similar to the parental strain, whereas L16-P-K214A exhibited severely attenuated growth. Real-time PCR experiments revealed that L16-P-W186A induces significant amounts of IFN, comparable to the phenotype of the previously reported L16-PΔ176-186 mutant (Rieder et al., 2011). L16-P-K214A induced high amounts of IFN despite its poor growth, indicating defects that go beyond the loss of inhibition of IFN induction. Since phosphoproteins defective in association with HSP70 were also shown to be defective in inhibition of IRF3 activation, a possible involvement of HSP70 family members on innate immune signaling and P inhibition was investigated. Overexpression of HSP70 family members, as well as heat shock treatment of the cells significantly impaired IFN-β promoter activity using ΔRIG-I or TBK1 overexpression as stimuli. Different dominant negative HSP70 constructs significantly impaired IFN-β promoter activity. In contrast to IFN induction, ISRE-reporter activity after IFN treatment was not altered by heat shock treatment or transfection of dominant negative HSP70 versions, suggesting that this observed effect is rather specific for IFN induction.

5.1. RABV P domains and functions involved in inhibition

At the beginning of this project, the RABV P residues 176-186 were already identified as a region critically involved in the inhibition of IFN induction (Rieder et al., 2011). However, there was no clear indication for the function of this motif leading to suppression of IRF3 activation. Therefore, a major goal of this thesis was the identification of further regions and functions of RABV P that might contribute to inhibition and possibly to assign a role or molecular target to the P region 176-186. Initial experiments employed RABV P truncation mutants that were assayed with IFN-promoter dependent dual luciferase assays for their ability to suppress

reporter activity in order to identify RABV P domains which are crucial for inhibitory function. Previously, TBK1 and IKKε were characterized as the central kinases responsible for the activation of IRF3, and overexpression of these proteins is alone sufficient to induce IFN-β transcription (Fitzgerald et al., 2003; Sharma et al., 2003). Since RABV P was reported to inhibit TBK1-overexpression mediated IRF3 activation (Brzózka et al., 2005), this stimulus was also used for initial experiments in this thesis.

5.1.1. RABV P derived peptides inhibit TBK1-overexpression mediated IFN induction

Reporter gene assays utilizing different RABV P truncation constructs could demonstrate that the C-terminal domain of RABV P is not essential for suppression of TBK1-mediated IFN-promoter activity (Figure 11). In contrast, RABV P region 176-186 was confirmed to be essential, since HA-P-1-174 left IFN-promoter activity unchanged. In further experiments RABV P-1-188 could be identified as the shortest C-terminal truncation still fully able to inhibit TBK1-mediated IFN-β induction (Figure 12). Since the RABV P region 176-186 is located to a disordered region of the protein, we wanted to elucidate whether a P derived peptide alone might be applicable as inhibitor for TBK1-mediated IFN induction. Therefore, N-terminal truncation constructs were introduced to identify the minimal RABV P region necessary for inhibition. Since N-terminally truncated P constructs and isoforms could not be expressed to a satisfactory level (data not shown), they were fused N-terminally to a HA-GST dual-tag connected by three G_4S linker repeats. The RABV P isoform P_4 (residues 83-297) was shown to be capable of inhibition of IFN induction previously (Master thesis M. Wachowius (2012)), suggesting that the N-terminal amino acids 1-82 are not involved in inhibition. In order to find the smallest functional P variant, N-terminal truncation mutants starting with different RABV P residues and ending at the previously identified amino acid 188 were created and assayed for their ability to interfere with TBK1-mediated IFN-β induction in reporter gene assays (Figure 13A, schematic representation of constructs used in Figure 42). Oddly, although P-derived HA-GST-fusion peptides of different length were partly able to interfere with IFN-promoter activity, the grade of inhibition correlated directly with the length of the constructs, however not significantly with distinct functions like dimerization (absent in HA-GST-P-130-188) or DLC8 binding (absent in HA-GST-P-153-188, Jacob et al. (2000)). Inhibition decreased with further N-terminal shortening, with HA-GST-P-170-188 being the shortest construct that still exhibited some degree of suppressive capacity. HA-GST-P-176-188 had no influence on promoter activity. This gradual loss of inhibitory function with

decrease in length of the P-derived peptide made it difficult to draw any conclusions in regard to clear functions of the phosphoprotein that are required for inhibition. Nevertheless, it could be shown that inhibition of TBK1 overexpression-mediated IFN induction is possible using P-derived peptides.

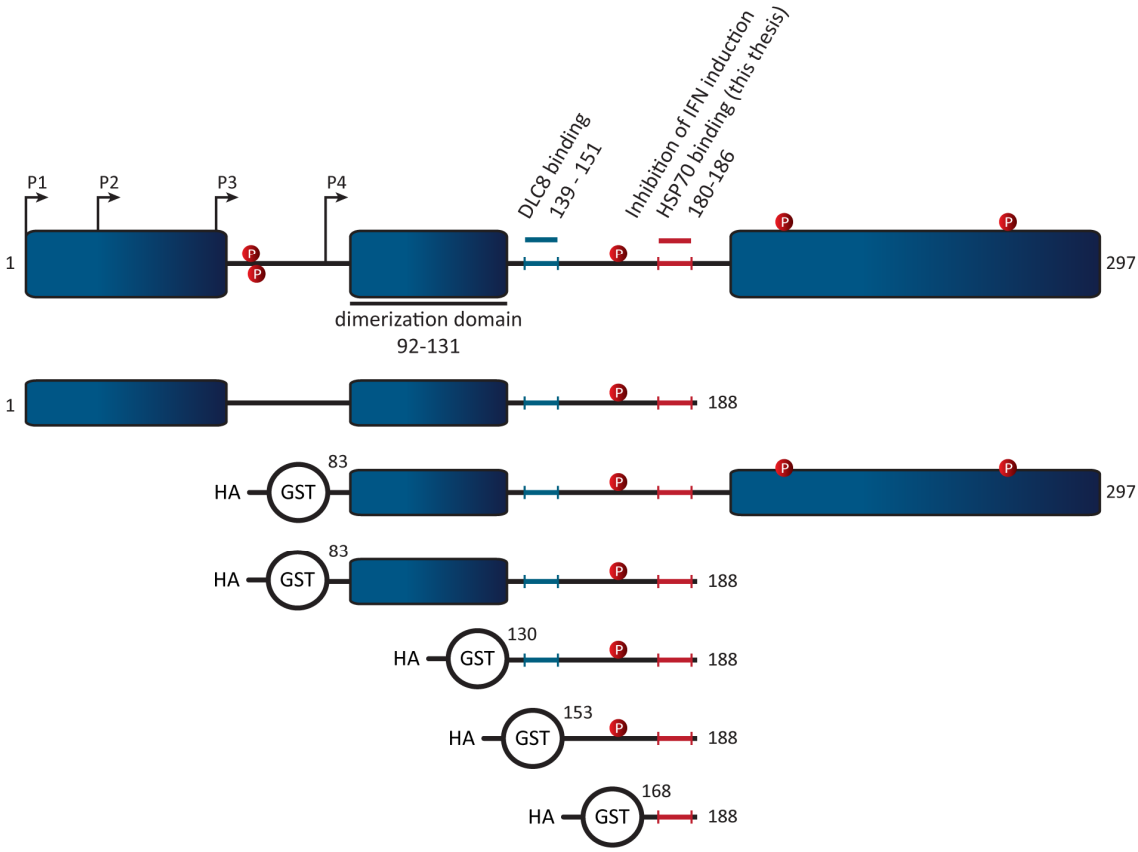

Figure 42: RABV P truncation constructs inhibiting TBK1-mediated IFN induction.
Schematic representation of select HA-GST-P fusion constructs used in this thesis. Since N-terminal truncation construct could only be expressed insufficiently (data not shown), these constructs were N-terminally fused to HA-GST. The RABV P derived fusion peptides lack distinct P features with further shortening, such as the dimerization domain, DLC8-binding site (shown in blue), or the phosphoacceptor site Ser162. The C-terminus of the constructs encompasses RABV P amino acids 176-186, which have been previously shown to be essential for inhibition of IFN induction (Rieder et al., 2011).

5.1.2. Differential inhibition of TBK1 and ΔRIG-I mediated IFN induction by P truncations

In order to obtain new insights about the mode of inhibition observed for RABV P C-terminal truncations and P-derived fusion peptides, we additionally assayed the inhibitory function of these constructs for stimuli other than TBK1-overexpression. Since TBK1 is the kinase directly engaged in IRF3 phosphorylation (Fitzgerald et al., 2003; Sharma et al., 2003), it should be

assumed that an inhibitor which directly blocks TBK1-mediated IRF3 phosphorylation should also be effective when RLR signaling is triggered further upstream. To verify this hypothesis, we assayed C-terminal RABV P truncation mutants for their ability to interfere with IFN-promoter activity mediated by ΔRIG-I expression, a constitutively active RIG-I mutant comprising only the N-terminal CARD domains (Yoneyama et al., 2004).

Strikingly, while HA-GST-P-83-197 abrogated TBK1-mediated IFN-β promoter activity almost to the basal level, the same construct failed completely to interfere with ΔRIG-I mediated IFN induction, albeit the levels of reporter induction by the respective stimuli were nearly identical (Figure 14A). This provides strong evidence, that the C-terminal RABV P truncation mutants are not targeting the kinase activity of TBK1 directly, otherwise the mode of activation should not have an impact. Potentially RIG-I signaling also activates additional factors different from TBK1, such as IKKε. Notably, a recent study indicates that the phosphoproteins of select rabies virus strains contribute to IFN antagonism by binding and blocking IKKε (Masatani et al., 2016). In order to rule out that the C-terminal truncation constructs fail to inhibit due to a defect in suppression of IKKε mediated IFN-promoter activity, we conducted further reporter gene assays to clarify this. Several C-terminal RABV P truncation mutants were found to efficiently interfere with IKKε mediated IFN-promoter activity, similar to experiments with TBK1-overexpression (Figure 14B). Only the HA-P-1-174 construct, lacking the Ind1/2 region (Rieder et al., 2011), failed to inhibit, as already observed for TBK1 (Figure 11). Although this indicates that TBK1 and IKKε are inhibited almost equally by the RABV P truncation mutants, it remains enigmatic why promoter activity is not influenced after ΔRIG-I stimulation. Reporter gene assays including the RABV P derived peptide fusion constructs HA-GST-P-130-188 and HA-GST-P-168-188 showed similar results (Figure 15A), indicating a loss of inhibitory function for constructs lacking the C-terminal domain, including peptide constructs which previously exhibited a significant degree of inhibition in assays using TBK1-overexpression (Figure 13). The ability of different RABV P truncation constructs and peptides to interfere with TBK1 and ΔRIG-I mediated IFN-β promoter activation is summarized in Table 11.

To verify these surprising results, several RABV P constructs were assayed for their ability to interfere with IRF3 Ser396 phosphorylation after treatment with *Sendai virus* defective interfering particles (SeDI), which have been shown to induce IFN induction through RIG-I signaling (Johnston, 1981; Strahle et al., 2006) (Figure 15B). These experiments confirmed the results previously obtained with reporter gene assays using ΔRIG-I stimulation and indicated that C-terminal truncation mutants are unable to interfere with ΔRIG-I or SeDI mediated IRF3 activation. Since infection with SeDIs, potently triggering RIG-I activation (Kato et al., 2005;

Yoneyama et al., 2005), and transfection with ΔRIG-I lead to the identical outcome in regard to P inhibition, it could be concluded that ΔRIG-I stimulation is in this case a preferential model which, in comparison to TBK1 overexpression, more closely resembles the setting of a viral infection triggering RIG-I. This suggests that RABV P C-terminal truncation mutants only inhibit IFN-β promoter activity induced by the overexpression of TBK1 but are unable to interfere with TBK1 function in the normally activated RIG-I/MAVS/IRF3 signaling cascade.

RABV P construct	TBK1 inhibition	ΔRIG-I inhibition
HA-P (1-297)	+++	+++
HA-P-1-197	+++	-
HA-P-1-188	+++	-
HA-P-1-174	-	-
HA-GST-P-83-297 (P_4)	+++	+++
HA-GST-P-83-197	+++	-
HA-GST-P-83-188	+++	-
HA-GST-P-130-188	++	-
HA-GST-P-168-188	+	-

Legend

+++ strong inhibition

++ robust inhibition

+ weak inhibition

- no inhibition

Table 11: Inhibition of TBK1/ΔRIG-I mediated IFN induction by different RABV P constructs.

Although inhibition of both ΔRIG-I and TBK1 overexpression-mediated IFN induction relies on RABV P residues 176-186, as demonstrated by the deficiency of full length PΔ176-186 and the P-1-174 truncation construct, the reason for this discrepancy remains elusive. Possibly an explanation lies in the mode of activation of TBK1. Normally activation of TBK1 downstream of MAVS requires its upstream adaptor proteins TANK, NAP1 or SINTBAD (Guo and Cheng, 2007; Ryzhakov and Randow, 2007; Sasai et al., 2006). These proteins interact mutually exclusive with the coiled-coil 2 motif (also referred to as adaptor binding (AB) motif) at the C-terminus of TBK1 (Goncalves et al., 2011). Using this motif, TBK1 is thought to be recruited to active signaling complexes by its adapters, resulting in a high subcellular local concentration of the kinase. Close proximity of multiple TBK1 homodimers then leads to interdimer interactions and trans-autophosphorylation of TBK1 Ser172 by activation loop-swapping, activating the kinase (Ma et al., 2012). Once active, TBK1 readily phosphorylates the activation loops of further TBK1 molecules as a substrate, resulting in the rapid activation of the unphosphorylated TBK1 pool (Helgason et al., 2013; Ma et al., 2012). Moreover, also substrate specificity is thought to be mediated by TBK1 subcellular localization, since TBK1 activation leads only to phosphorylation of a subset of potential targets, depending on the upstream stimulus (Helgason et al., 2013). Due to this mode of tightly regulated activation, TBK1 strictly requires the AB motif when expressed at endogenous levels. However, under overexpression conditions TBK1 is able to stimulate IFN-β

promoter activity without activation of upstream signaling components and even independent of the AB motif, as shown by truncation mutants (Goncalves et al., 2011). This indicates an artificial mode of auto-activation that is significantly different from the natural induction of TBK1 activity. While RABV P constructs lacking the C-terminus are able to counteract IRF3 phosphorylation under TBK1 overexpression conditions, they completely fail to do so when an upstream signal is present. In the case of physiological TBK1 signaling, the kinase and its potential substrates are thought to be recruited to their upstream signaling complexes, providing ideal conditions for the phosphorylation of TBK1 targets. To counteract this complex process, RABV P seems to need additional residues and functions located to the C-terminal domain, while constructs lacking the CTD are sufficient to abrogate rather unspecific TBK1 overexpression mediated signaling. Since the mode of auto-activation for overexpressed TBK1 is highly artificial and poorly characterized, other stimuli such as ΔRIG-I or SeDI treatment were used for further experiments in this thesis. Moreover, RABV triggers IFN induction via RIG-I activation (Hornung et al., 2006; Schlee et al., 2009), therefore upstream stimulation of the RLR pathway rather resembles the signaling events during viral infection. Although no clear explanation for the differential inhibition of C-terminal RABV P truncation mutants could be provided, this finding underlines that TBK1 activation might be fundamentally different depending on the mode of pathway activation. Therefore, the use of TBK1 overexpression as a model for IFN induction should be handled with increased caution in further studies.

5.1.3. RABV P nuclear shuttling is essential for inhibition of RIG-I mediated IFN induction

As discussed above, in order to inhibit phosphorylation of IRF3 and subsequent induction of type I interferons after upstream activation of RIG-I signaling, RABV P depends on its structured C-terminal domain (structural representation in Figure 43). This raised the question which functions or residues of the CTD are involved in inhibition of IFN induction.

RABV P is predominantly a cytosolic protein, due to a strong N-terminal nuclear export signal (NES) (Pasdeloup et al., 2005). Additionally, the C-terminal domain of P contains a conformational NLS, as revealed by inhibition of nuclear export by the CRM1 inhibitor leptomycin B (Fornerod et al., 1997; Pasdeloup et al., 2005; Rowe et al., 2016). The CTD-NLS requires the P residues Lys214 and Arg260, which are in close proximity in the protein structure and form a positively charged patch at the surface (Mavrakis et al. (2004), Figure 43B). Although RABV P is mainly cytosolic, it shuttles between the nucleus and the cytoplasm due to the

presence of both NES and NLS sequences. The C-terminal NES of P was previously reported to be involved in efficient cytosolic retention and thus suppression of STAT signaling, showing that trafficking signals of RABV P might be involved in controlling innate immune signaling (Ito et al., 2010).

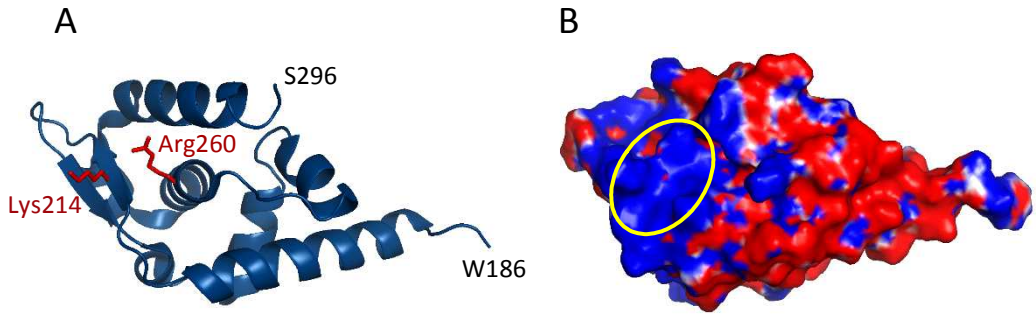

Figure 43: Structure of the C-terminal domain of RABV P.
Structural representation of the C-terminal domain of RABV P (Mavrakis et al. (2004), PDB ID 1VYI), created with PyMol (Schrodinger, 2015). **A)** Only backbone and helix objects of the RABV P-CTD are shown. Sidechains of lysine 214 and arginine 260 shown in red **B)** Surface rendering of the P-CTD, colorization based on surface potential (positive charge in blue, negative charge in red, surface map created with PyMol APBS plugin (Baker et al., 2001)). Lys214 and Arg260 strongly contribute to a positively charged patch on the protein surface (highlighted with yellow circle).

In order to examine whether the CTD-NLS might be involved in the inhibition of IRF3 activation by RABV P, the mutants P-K214A and P-R260A, which exhibit alanine substitutions that impair NLS function (Pasdeloup et al., 2005), were assayed for their capacity to suppress IFN-promoter activity in reporter gene assays. Remarkably, the constructs impaired in NLS activity exhibited a complete failure in inhibition of IFN induction comparable to PΔ176-186, a deletion mutant that was previously shown to be unable to prevent IRF3 phosphorylation (Rieder et al., 2011) (Figure 17A). This observation provided a good hint that nuclear trafficking might be indeed critically involved in the inhibition of IFN induction.

Since substitutions of polar amino acids such as lysine and arginine with hydrophobic alanine might impair the overall tertiary structure of the C-terminal domain and thus proper protein function, we wanted to validate that indeed the presence of a functional NLS was necessary for inhibition. Therefore RABV P constructs with mutated NLS (K214A and R260A) and C-terminal truncation constructs lacking the CTD completely were N-terminally fused to a SV40 large T antigen NLS, which has been previously shown to impart nuclear localization (Kalderon et al., 1984b)(schematic representation of constructs in Figure 44). IFN-promoter dependent dual luciferase assays could reveal that N-terminal addition of a recombinant NLS to the RABV P-K214A and P-R260A constructs restored inhibitory function almost to wild type levels, in spite of comparable low expression levels of the fusion constructs (Figure 17B). Notably, even wild type RABV P fused with an N-terminal SV40-NLS exhibited slightly enhanced inhibitory

capacities. Assays using IRF3 Ser396 phosphorylation as an activation marker after SeDI treatment confirmed that the SV40-NLS-P-R260A fusion construct regained inhibitory function (Figure 17D).

These findings provide strong evidence that a functional NLS signal indeed contributes to suppression of IFN induction by RABV P. Moreover, the C-terminal truncation construct P-1-188, completely lacking the CTD-NLS, exhibited a solid degree of inhibition when N-terminally fused to the SV40-NLS, suggesting that in regard to inhibition of IFN induction the CTD is mainly required due to its nuclear localization signal (Figure 17C).

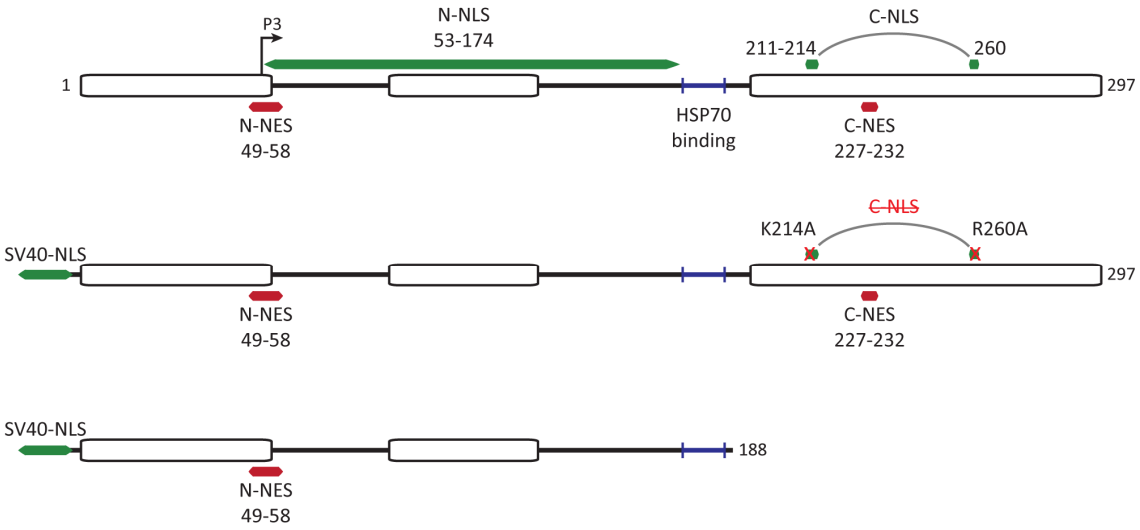

Figure 44: RABV P trafficking signals and SV40-TAg-NLS fusion constructs.
Schematic representation of RABV P domain organization including trafficking signals. The C-terminal nuclear localization signal depends on residues K214 and R260, which are in close proximity in the tertiary structure, forming a conformational NLS. In order to investigate the functional relevance of nuclear trafficking signals, different RABV P constructs with mutated (K214A, R260A) or absent CTD were N-terminally fused to the NLS of the SV40 large T antigen (Kalderon et al., 1984b).

Nuclear trafficking of RABV P seems to be exclusively required for the inhibition of IFN induction but not for suppression of STAT-signaling, since HA-P-K214A inhibited ISRE promoter activity after type I IFN treatment similar to the wild type protein (Figure 18). HA-P-R260A was impaired in regard to inhibition of JAK-STAT signaling to some degree, however this might be explained with the proximity of R260 to W265, which has been shown previously to be involved in this inhibitory function (Wiltzer et al., 2014). In addition, in this case the defect could not be rescued by fusion with a SV40-NLS, indicating that the inhibition of IFN-signaling is not connected to the NLS activity of RABV P.

In order to validate the effectivity of the SV40-NLS and to further examine the correlation of nuclear trafficking and inhibition of IFN induction, we employed immunofluorescence confocal microscopy using the RABV P constructs previously examined in reporter gene assays (Figure 19).

The N-terminal SV40-NLS fusion constructs exhibited a significantly stronger nuclear localization. Whereas the normal P versions mainly localize to the cytosol, mediated by the N-terminal nuclear export signal (Pasdeloup et al., 2005), the SV40-NLS fusions are strongly enriched in the nucleus or completely localized to the nucleus upon LMB treatment, confirming the effectivity of the SV40-NLS in the context of the P-fusion constructs. Unfortunately, RABV P wild type and the mutant versions P-K214A and P-R260A showed no differential trafficking behavior in our experiments with or without LMB treatment. Since we used only single amino acid substitutions, it cannot be excluded that the P-K214A and P-R260A mutants retained some residual NLS activity. In addition, RABV P exhibits a relatively small size of about 34 kDa which enables fast passive diffusion through the nuclear pores (Gorlich and Kutay, 1999). In combination with residual NLS activity this might blur the difference in localization upon LMB treatment. The existing studies on RABV P nuclear trafficking employed eGFP-P fusion proteins exhibiting a molecular mass of about 60 kDA (Pasdeloup et al., 2005; Rowe et al., 2016). Consequently, these constructs are most probably too big for fast passive diffusion (Bonner, 1975; Gorlich and Kutay, 1999). Since the N-terminal domain of RABV P was shown before to be not involved in suppression of IFN induction, we employed tagRFP-P4 fusion proteins with a molecular mass of about 51 kDa for further experiments. Using tagRFP-P_4 based wild type, K214A and R260A constructs, reduced nuclear import was successfully revealed by LMB treatment (Figure 21).

Taken together, these results indicate that enhanced active nuclear trafficking, mediated by a functional NLS, is important for RABV P inhibition of IRF3 activation. Especially the possibility to rescue the defect of the CTD-NLS mutants with a recombinant SV40-NLS provides strong evidence for this hypothesis. Notably, this result is rather unexpected, since recognition of nucleic acids by RLRs and activation of IRF3 are thought to be cytosolic processes and thus a connection between RABV P inhibition and nuclear trafficking cannot be drawn easily. It is further unclear, whether nuclear trafficking itself or the ability to bind importins, which mediate nuclear import (Gorlich and Kutay, 1999), is the crucial feature. For instance, a peptide derived from the NLS sequence of the NF-κB p50 subunit has been reported to impair nuclear import and thus transcriptional activity of the proinflammatory transcription factors NF-κB, AP-1 and NFAT and the interferon responsive factor STAT1, by binding to specific importin heterodimers and thereby blocking importin-transcription factor association (Torgerson et al., 1998). Possibly, a similar mechanism might contribute to the inhibition of IFN induction by RABV P to some degree, since import of both P and IRF3 is thought to depend on importin-α (Rowe et al., 2016; Zhu et al., 2015). Moreover, it could be speculated that RABV P mediates a subcellular mislocalization of specific host cell factors depending on its trafficking signals. Since RABV P could be shown in

this thesis to interact with HSP70 family members (discussed below), it is tempting to speculate that P might confer a subcellular redistribution of HSP70, however no experimental evidence could be obtained hitherto. Consequently further experiments will be necessary in the future to determine the molecular mechanism underlying the involvement of RABV P nuclear trafficking in inhibition of IFN induction.

5.2. RABV P interacts with HSP70

5.2.1. RABV P contains a novel HSP70 binding motif

The RABV P residues 176-186, located to an intrinsically disordered region of RABV P (Gerard et al., 2009), were previously reported to be involved in the blockage of IRF3 activation (Rieder et al., 2011). However, despite the identification of these critical amino acids, no clear function could be assigned to this region. It was speculated that this region might be important for the correct folding of parts of the protein or that it acts as a linker that guarantees the correct spacing of the structured domains of RABV P, enabling inhibition of IFN induction.

In order to gain new insights and possibly identify molecular interaction partners associated with this RABV P region, we assayed several RABV P derived HA-GST-fused peptides encompassing the previously identified critical residues 176-186 for potential interaction partners from HEK 293T whole cell lysates using an unbiased mass spectrometry approach. The HA-tag was introduced for detection and pulldown experiments, whereas the GST-tag was used to ensure proper expression and solubility. Initially, an interaction of all examined RABV P peptides with HSP70 family members was identified by Co-IP experiments coupled to MS analysis (Figure 22A). The observed association was subsequently verified by additional Co-IP experiments employing the full length P protein as well as the P-176-188 fusion peptide already used in the initial MS experiment (Figure 22B-D). Notably, the HSP70 interaction was absent in the HA-PΔ176-186 mutant, providing strong evidence that this motif is sufficient and essential for this association. Since the binding to disordered, partly hydrophobic peptides is among the normal functions of heat shock proteins, we were concerned about the specificity of this finding. Therefore, a plasmid coding for a fusion peptide containing RABV P residues 176-188, however in a randomized order, was created by using synthetic DNA oligos. This construct exhibited no interaction with HSP70 in Co-IP experiments, indicating that the observed binding is indeed sequence specific (Figure 23).

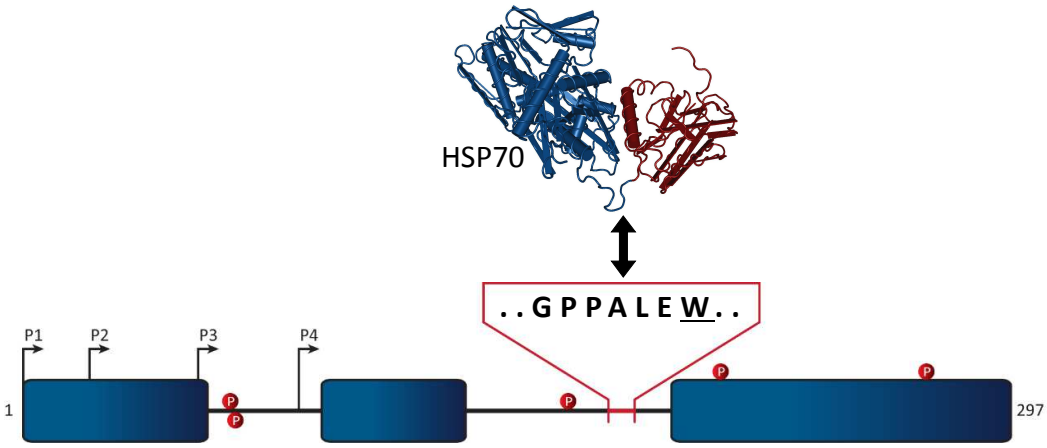

Figure 45: RABV P contains a novel binding motif for HSP70.
The RABV P residues 180-186 could be identified as a novel motif that mediates an interaction with HSP70 family members. This region is located to an intrinsically disordered stretch of the phosphoprotein connecting CTD and dimerization domain. The identified motif is alone sufficient and essential for binding of RABV P to HSP70.

Further investigations could show that RABV P region 180-186 (amino acid sequence **GPPALEW,** Figure 45) fused to HA-GST is the shortest sequence still able to mediate binding, while removal of the C-terminal tryptophan (W186 in the full length protein) completely abrogated the interaction (Figure 26). Full length RABV P proteins of L16, THA and CVS-strain as well as L16-P-derived peptides co-purified endogenous HSP70-1A/1B and HSC70 equally well from HEK 293T whole cell lysates in Co-IP experiments (Figure 24). This was expected, since the identified HSP70 binding motif GPPALEW is conserved in these phosphoproteins. Accordingly, removal of residues 176-186 from RABV P resulted in a loss of association with both HSP70s. The same is true for a L16-P construct containing a single W186A substitution, highlighting the importance of this conserved residue already described above by truncations of the binding peptide. These findings provide good evidence, that the RABV P region 180-186 is an HSP70 binding peptide that is alone sufficient and essential to mediate this interaction, with a critical contribution of W186.

The interaction of RABV P with endogenous HSP70-1A/1B and HSC70 has been validated in Co-IP experiments. Further, the heat shock protein HSPA1L, which is normally of low abundance in HEK 293T cells, also interacts with RABV P in Co-IP assays when co-expressed (data not shown). In addition, further pulldown assays coupled to MS analysis indicated an interaction in 293T cell lysates with other HSPA family members, including mitochondrial HSP70 (mtHSP70, GRP75) and the ER-associated heat shock protein BiP (GRP78) (data not shown). An association of GRP75 and GRP78 was already observed previously by Co-IP assays and Western blotting by K. Brzózka, a former member of our group (unpublished data). However, it is questionable that these interactions with organelle-associated HSP70s are in fact present in the living cell or are a results of the disruption of cellular membranes during the Co-IP procedure. Nevertheless, this indicates

that the binding motif identified in this thesis rather indiscriminately mediates interactions with many different members of the HSP70 family.

5.2.2. Nature of the HSP70 – RABV P interaction

The RABV P binding motif for HSP70 has been narrowed down to the seven residues 180-186, whereby the most C-terminal amino acid tryptophan 186 is essential. With these findings, we further wanted to elucidate the mode of interaction between the identified peptide and HSP70 family members.

It is important to mention that the assays shown in this thesis were not conducted with isolated, synthesized peptides, but rather with HA-GST-peptide fusion constructs, containing three repeats of a G_4S linker in between GST and peptide. Therefore, theoretically it is possible that additional amino acids from the fusion construct contribute to a stable interaction. However, since the association with HSP70 is completely abrogated when the most C-terminal amino acid (W186) of the binding motif GPPALEW is removed, it is fair to assume that this P-derived binding peptide indeed mediates the interaction independently of its context. This might be verified in the future by analyzing the affinity between HSP70 and synthetic RABV P derived peptides using further *in vitro* assays.

Co-IP assays of RABV P or P-derived peptide fusion constructs provide no evidence whether the observed interaction is direct or might be indirectly mediated by additional proteins present in the cell. Although the stoichiometry observed in the silver stain gels of pulldown assays suggested a direct interaction (Figure 22A), since the protein bands on the height of HSP70s were the only significant bands that appeared specifically for the peptides tested, we wanted to evaluate this issue further by interaction studies using recombinantly purified proteins. Therefore, HA-$(His_6)_2$-GST-fusion constructs with full length P, P-176-188 and the scrambled version of the peptide were created. The corresponding fusion proteins were expressed in *E. coli* and purified using a cobalt affinity matrix (Figure 30). Eluates of these purifications were used in excess in order to saturate a specific amount of HA-affinity matrix. The pre-incubated matrix was washed and subsequently incubated with purified human HSP70-1A, purchased from *Stressgen*. These experiments revealed that full length RABV P and the fusion peptide were equally able to co-precipitate recombinant HSP70 in this *in vitro* setting, whereas the scrambled peptide version failed to do so (Figure 31). Since other eukaryotic proteins are absent under these conditions, this provides strong evidence that the interaction between RABV P and HSP70 is direct.

In order to further characterize P/HSP70 association, we wanted to elucidate which target domains and residues of HSP70 are bound by the identified RABV P motif. Since HSP70 exhibits a huge interactome encompassing not only the bound client peptides but also numerous co-modulating proteins like J-domain proteins and NEFs (Mayer, 2013), various modes of interaction are conceivable. Therefore, with the aim of narrowing down the domains and moieties involved in binding, several HSP70 truncation mutants, based on HSP70-1A, were created and assayed for their ability to interact with RABV P or P-derived peptides in Co-IP assays (HSP70 truncation constructs depicted in Figure 46).

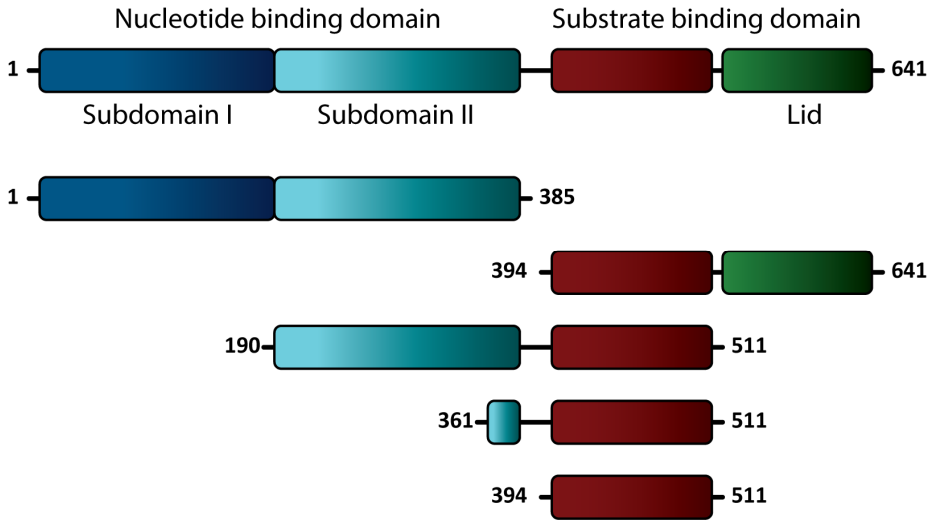

Figure 46: HSP70 truncation constructs used in this thesis.
Schematic representation of the domain organization of different HSP70 truncation constructs that were used for mapping the interaction with RABV P.

The HSP70-NBD alone completely failed to associate with RABV P. In contrast, an interaction between RABV P and the SBD was clearly detectable, however significantly weaker in comparison to full length HSP70 (Figure 28). Truncation constructs of both HSP70-1A and HSC70 lacking the C-terminal lid region, as well as subdomain I of the NBD, were shown to interact with a RABV P-176-188 fusion peptide equally well as full length HSP70 (Figure 29A). Notably, although the truncation constructs of HSP70 and HSC70 were co-precipitated to a similar extend, the Flag-tagged version of full length HSC70 hardly exhibited any association with P or RABV P derived peptides. This is strictly in contrast to the data previously obtained by pulldowns of endogenous untagged HSP70s, which clearly indicated an equal binding of HSP70-1A/1B and HSC70. Therefore, we concluded that the recombinant N-terminal Flag-tag might impair the interaction only in the case of HSC70, what might be explained by the differences in amino acid composition at the N-terminus between the two otherwise well conserved proteins (MAKAAAI.. for HSP70 and MSKGPAV.. for HSC70). Equal binding of the truncation mutants suggests an

identical mode of interaction. Furthermore, this finding provides good evidence that the lid region of HSP70, as well as subdomain I of the NBD are dispensable for binding. Subdomain I, encompassing residues 1-188 (Flaherty et al., 1990), forms one half of the ATP-binding hydrophilic pocket and contains lysine 71, a moiety which is essential for ATP hydrolysis (O'Brien et al., 1996). Insofar, it can be concluded that ATPase activity of HSP70 plays no role in binding to the identified P motif. This is further supported by the observation that Flag-HSP70-1A-K71 and wild type HSP70-1A were equally associated with HA-GST-P-176-188 in Co-IP assays (data not shown). Furthermore, a SBD construct lacking the lid region interacted with RABV P-176-188, however to a lesser extend compared to HSP70-190-511 (Figure 29B). This indicates that the SBD of HSP70 is alone sufficient and essential to mediate the interaction but that subdomain II of the NBD might have a stabilizing function, thus contributing to the interaction.

At the present time, the open question which residues of HSP70 are in contact with the RABV P motif and which conformation of HSP70 is being bound remains. Since no structural data is available of HSP70 in complex with the identified binding motif, this can only be discussed on a speculative basis by falling back on the identified involved domains as well as on the amino acid composition of the P motif.

For the bacterial HSP70 homolog DnaK structural data is available for the open ATP-bound (Figure 47A, Kityk et al. (2012)) and closed ADP-bound conformation (Figure 47B, Bertelsen et al. (2009)). In the closed conformation, the lid is closed over the substrate binding groove and the whole SBD is positioned in a certain distance from the NBD, only connected by a short linker without any visible surface interactions. In contrast, in the open conformation NBD and SBD are in direct contact stabilized by several hydrogen bonds (Kityk et al., 2015). The substrate binding cavity of the SBD is open with the lid subdomain docking to a distal site of the NBD. Our data indicated, that subdomain II might be involved in the interaction between RABV P and HSP70, since Flag-HSP70-1A-190-511 (lacking NBD-subdomain I and the lid) was co-precipitated more efficiently by P-176-188 than Flag-HSP70-1A-394-511 (only SBD lacking the lid). This implies that HSP70 is rather being bound in the open ATP-bound conformation, since NBD and SBD are at some distance in the closed conformation, making a cooperative binding of NBD subdomain II and the SBD with the P motif unlikely. This is supported by the finding that neither the lid subdomain, nor the ATPase activity of HSP70-1A are critically involved in binding to RABV P-176-188 (Figure 29B). If the P motif was bound by the closed high affinity conformation of HSP70, it could be assumed that ATP-hydrolysis and subsequent closing of the lid would be of importance.

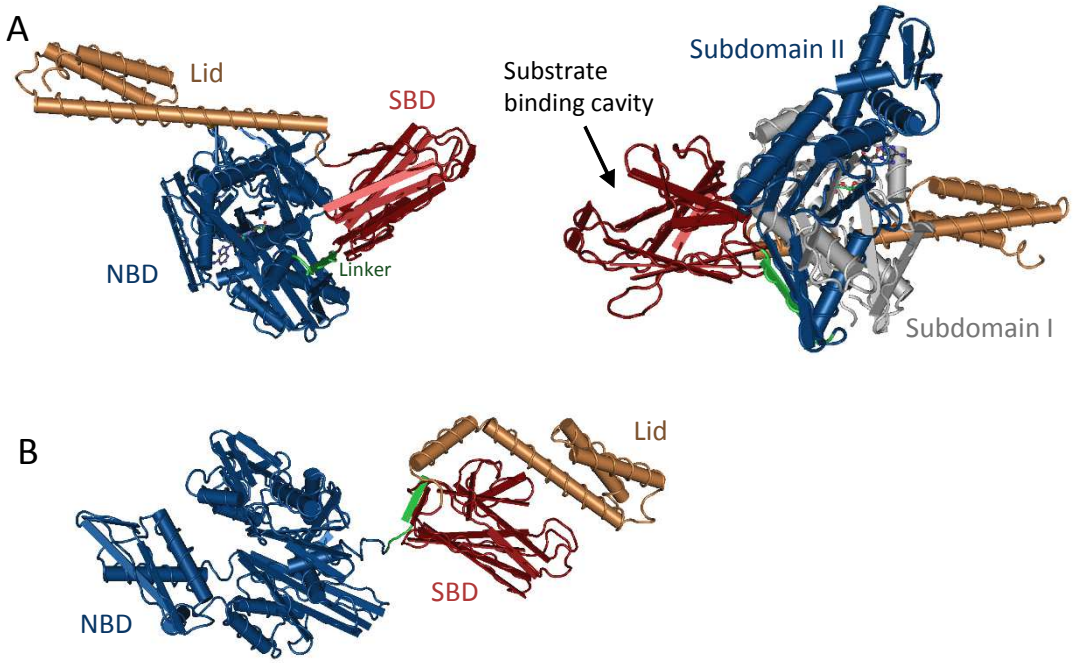

Figure 47: Structure of the bacterial HSP70 homolog DnaK in open and closed conformation.
A) Representation of bacterial HSP70 homolog DnaK in the ATP-bound open conformation depicted in two different orientations. NBD and SBD make direct contact, while the lid region is positioned at a distal site of the NBD, leaving the substrate binding groove of the SBD accessible (PDB ID 4B9Q, Kityk et al. (2012)). **B)** Bacterial HSP70 in the ADP-bound closed conformation. The lid is closed over the substrate binding groove of the SBD, while no direct contact between NBD and SBD is visible (PDB ID 2KHO, Bertelsen et al. (2009)). Illustrations were created using the Cn3D tool by NCBI.

In regard to the HSP70 residues that are contacted by the P motif, there are two options to consider: either the peptide is bound by the hydrophobic pocket of the SBD, similar to HSP70 client peptides, or the interaction occurs at a different site of the molecule in an atypical way. Crystal structures have been solved for HSP70 substrate binding domains of bacterial (Zhu et al., 1996) and human (Zhang et al., 2014) origin bound to the model substrate peptide NRLLLTG (Figure 48).

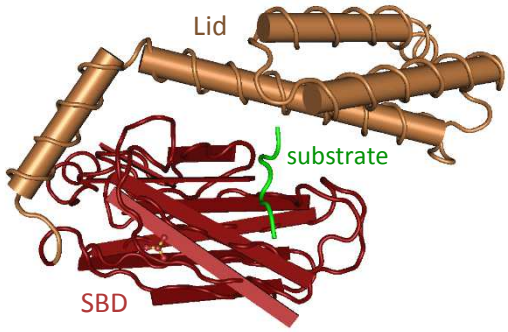

Figure 48: SBD of human inducible HSP70 in complex with peptide substrate.
Representation of human inducible HSP70 (HSP70-1A) SBD in complex with a peptide substrate (green) bound to the hydrophobic binding groove. In this closed conformation the lid is covering the substrate binding groove, resulting in high affinity binding (PDB ID 4PO2, Zhang et al. (2014)). The Illustration was created with the Cn3D tool by NCBI.

These structures reveal a binding of hydrophobic peptides to the conserved peptide binding groove of the HSP70 substrate binding domain. The length of the identified minimal RABV P binding motif for HSP70 of seven residues (GPPALEW, Figure 26) fits to the identified heptameric HSP70 binding peptides. However, the substrate binding groove within the SBD is located at some distance to the NBD, even in the open conformation of HSP70 (Figure 47A). Considering that subdomain II of the nucleotide binding domain of HSP70 might contribute to the interaction with the P-motif (Figure 29B), this gives a weak hint that the interaction might be located to a different site of the SBD.

Several studies tried to identify common peptide motifs that are bound by HSP70 by screening of libraries containing numerous potential clients with different techniques such as phage display or cellulose-bound peptide scans (Blond-Elguindi et al., 1993; Gragerov et al., 1994; Rüdiger et al., 1997a; Rüdiger et al., 1997b). Although no clear binding motif could be identified, these studies suggested the common principle that the SBD of HSP70 binds preferentially to heptameric peptides consisting of a core of five amino acids enriched in hydrophobic residues flanked by positively charged moieties. Although some hydrophobic residues are present in the GPPALEW motif, a clearly defined hydrophobic core as well as flanking basic residues are absent. In contrast, the most C-terminal tryptophan residue, which has been identified as a crucial amino acid for binding, is nonpolar and aromatic. In addition, the negatively charged and thus hydrophilic glutamate residue at position 6 of the peptide might speak against an interaction with the hydrophobic substrate binding groove. Prediction algorithms that integrate sequence information from peptide binding experiments and structural data had partial success in determining potential binding partners for specific HSP70s (Schneider et al., 2016; Van Durme et al., 2009). The resulting model proposed by Van Durme et al. (2009) for bacterial DnaK assigns a score to every amino acid of a given heptamer depending on the position. Following this model, the GPPALEW peptide obtains a negative score of approximately -28, clearly defining it as a non-binder with a disfavorable amino acid at nearly every position. Accordingly, the algorithm that has been made available by the group as a web-based tool (http://limbo.switchlab.org/) is not even detecting the experimentally identified HSP70 binding peptide in RABV P when using the “highest sensitivity” setting. Although this provides a weak hint that the RABV P might not interact with the substrate binding groove, one has to consider that the prediction is based on data obtained for bacterial HSP70. A recently published workflow for the computational prediction of binding peptides for the human HSP70 variant BiP (GRP78) is not yet available as a public tool and could therefore not be applied to predict the identified RABV P motif (Schneider et al., 2016). Anyway, these models are not completely accurate, making it essential to validate

every potential binding peptide experimentally. Moreover, still little is known about potential differences in substrate specificity of the different HSP70 family members present in mammalian cells. There is some evidence that the substrate specificity of human HSP70 isoforms may differ significantly under certain conditions (Hageman et al., 2011).

Although the RABV P derived HSP70 binding peptide identified in this thesis exhibits rather unusual properties for a HSP70 client peptide according to the available models, it cannot be excluded that it is bound by the substrate binding groove of the SBD. Further experiments are necessary in the future to clarify this issue. The most precise information about the mode of interaction could be obtained by solving of a crystal structure of HSP70 bound to the P-derived peptide or the full RABV P protein, although this might rather be a technically challenging approach. The easiest way to confirm or rule out a binding of RABV P to the substrate binding groove of HSP70 would be to employ binding assays utilizing a SBD with a V436F substitution. This mutation blocks the substrate binding cavity by the introduction of a much larger phenylalanine residue, leading to significantly impaired client binding (Mayer et al., 2000). This way, a potential involvement of the substrate binding groove could be clarified. If the HSP70 residues involved in binding could be determined, this might imply a hypothesis how RABV P manipulates HSP70 function.

5.2.3. Correlation between P-HSP70 association and inhibition

The results described in this thesis indicate a direct correlation between the ability of RABV P to bind HSP70 and its ability to interfere with IFN induction. Several experiments provided good evidence that the inhibitory defect of RABV P mutants lacking HSP70 association is not due to defective P protein folding. Protein expression was not significantly impaired in these mutants, as determined by Western blotting (Figure 24). Further, other functions of the P protein, such as inhibition of IFN-signaling, were left unchanged by mutations impairing HSP70 association (Figure 18). Most importantly, replication competent viruses containing the P-W186A mutation could be rescued and exhibited growth characteristics comparable to the parental strain (Figure 32, discussed below). This emphasizes that the P protein is intact in every regard that is important for the viral life cycle. It can be expected that aberrant folding of P would significantly impair viral growth, since the phosphoprotein is central to transcription and replication as a polymerase cofactor and N-binding protein (Chenik et al., 1994; Chenik et al., 1998; Emerson and Yu, 1975; Fu et al., 1994). Therefore, these findings strongly indicate that the observed interaction is exclusively important for inhibition of IRF3 activation. Moreover, there is some

recent evidence suggesting that rather HSP90 and its co-chaperone Cdc37 assist in correct folding of RABV P (Xu et al., 2016).

Although a clear correlation between HSP70 binding and the ability of RABV P to interfere with IFN induction could be shown, this is, strictly speaking, no definite proof that RABV P relies on members of this protein family for inhibition. An impact of different wild type and mutant HSP70 proteins and heat shock treatment on IFN induction was demonstrated in this thesis, suggesting an involvement in the regulation of RIG-I-MAVS signaling and P inhibition. However, theoretically RABV P might also bind other proteins or molecules, possibly using the same binding motif, which could not be identified yet. Due to the abundance and pleiotropic functions of HSP70s, this possibility is hard to eliminate, especially considering the binding of RABV P to various members of the HSP70 family. In addition, if heat shock protein function is manipulated experimentally, many effects could arise and a possible specific impact on innate immune signaling or P inhibition is hard to distinguish. Therefore additional research is necessary, in order to obtain further evidence and to clarify the role of HSP70 for the inhibition of IFN induction by RABV P and which specific HSP70 family members are involved.

Potentially, RABV P could influence many steps of the HSP70 chaperone cycle. Various small molecules have been shown to modulate HSP70 function either by impairing ATPase activity, targeting the substrate binding domain, or by abrogating interactions of HSP70 with distinct cofactors (Patury et al., 2009). Future research could employ the different classes of HSP70 inhibitors and screen these compounds for their potential ability to interfere with IFN induction, thus hinting at an inhibitory mechanism for RABV P. Conversely, it could be promising to determine whether RABV P or P-derived peptides could be used as modulators or inhibitors for HSP70 function, providing a new tool to investigate this interesting class of chaperones. This might be achieved in future research by examining the folding or ATPase activity of HSP70 *in vitro*, in the presence or absence of RABV P or P-derived peptides.

In addition to modulating HSP70 function, RABV P might also lead to subcellular mislocalization of possibly select heat shock proteins involved in innate immune signaling. This option seems promising for further investigation, since nuclear trafficking signals of RABV P have been identified as essential for inhibition of IFN induction. However, no impact on heat shock protein localization could be experimentally identified so far. This attempt was complicated by the need for sensitive and specific antibodies suitable for immunofluorescence imaging which are able to clearly distinguish between the different HSP70 family members. Future research with optimized detection strategies and fluorescent fusion proteins might reveal new insights into a possible connection between HSP70 binding and RABV P trafficking, two features which likewise were

identified as critical prerequisites for inhibition of IFN-induction by P. Emerging evidence suggests that subcellular localization of signaling components is a crucial determinant of innate immune pathway activation and TBK1 substrate specificity (Helgason et al., 2013), making the link between RABV P inhibition and trafficking an interesting subject of investigation.

In general, two mechanistic possibilities might be distinguished in regard to inhibition of IFN induction by RABV P and the described interaction with HSP70: First, RABV P might utilize specific or multiple HSP70 chaperones in order to interfere with innate immune signaling, whereby HSP70 is normally not critically involved in IFN induction. Second, HSP70 family members might be critical regulatory components of the RLR-MAVS signaling cascade. In this scenario RABV P would need to target this essential function in order to abrogate the induction of type I IFNs. Further research is necessary to determine which of the two possibilities is more likely. Since overexpression of heat shock proteins, heat shock treatment of cells and overexpression of HSP70 mutants defective in specific functions were shown to interfere with innate immune signaling in this project, we favor the second working hypothesis.

5.3. L16-P-W186A and L16-P-K214A induce IFN

The RABV P mutants P-W186A, P-K214A and P-R260A were identified in this thesis as deficient in inhibition of IFN induction (Figure 17, Figure 25). In order to validate these mutations in the viral context, we attempted to rescue recombinant viruses from cDNA harboring the corresponding amino acid substitutions. While the W186A substitution, similar to PΔ176-186 (Rieder et al., 2011), was shown in this thesis to be deficient in binding to HSP70 family members, the P-K214A and P-R260A mutants exhibit a deficiency in the C-terminal conformational NLS of RABV P (Pasdeloup et al., 2005; Rowe et al., 2016).

Whereas the rescue procedure resulted in the successful generation of replication competent viruses for L16-P-W186A and L16-P-K214A, the same approach failed for the L16-P-R260A mutant. Furthermore, cells transiently expressing RABV P-R260A did not support growth of a recombinant L16-ΔP-eGFP virus (data not shown), indicating an essential defect in the viral life cycle for the L16-P-R260A mutant virus. A positively charged patch on the surface of the CTD of RABV P encompassing K214A and R260A is critically involved in P–N_{RNA} binding, an interaction which is essential for viral replication (Jacob et al., 2001; Mavrakis et al., 2004; Ribeiro et al., 2009). This feature of the positively charged patch is likely the reason for the defect of L16-P-R260A, thereby emphasizing that the positively charged region of the CTD has a dual function, mediating both importin binding for nuclear trafficking and N_{RNA} binding (Rowe et al., 2016).

The L16-P-W186A mutant could be grown to titers and exhibited growth kinetics indistinguishable from those of the L16 parental strain in BSR T7, HEp-2 and HEK 293T cells. Notably, growth of the mutant virus L16-PΔ176-186, which is defective in preventing IFN induction, was previously reported to be about 10-fold reduced in comparison the L16 wild type strain (Rieder et al., 2011). In contrast to L16-P-W186A, the mutant virus L16-P-K214A was significantly attenuated in growth (Figure 32). This underlines the importance of the positively charged patch in the RABV P CTD for efficient viral replication. The RABV P residue R260 seems to be more critical for this function than K214, because a recombinant virus containing the R260A substitution could not be rescued. Since the defect in growth is also observed in BSR cells, which cannot mount an antiviral IFN-response, the observed defect in inhibition of IFN induction by RABV P-K214A is not the reason for the strongly attenuated replication. Although HEK 293T and HEp-2 cells have an intact innate immune system that might potentially impair viral replication, L16-P-W186A exhibited growth kinetics equal to the wild type strain in these cell lines. The reason for this might be the ability of RABV P to interfere not only with IFN induction, but also with IFN-mediated STAT signaling (Brzózka et al., 2006; Vidy et al., 2005), a function that is fully retained in P-W186A (Figure 18). This way, the mutant virus L16-P-W186A might induce IFN but could still block its antiviral effects by abrogating STAT signaling.

In order to examine to which extent the described mutant viruses induce an IFN-response, HEK 293T cells were infected with the parental L16 strain and the recombinant viruses L16-P-W186A and L16-P-K214A, followed by extraction of cellular RNAs 48 h post-infection. Reverse transcription of mRNAs and real-time PCR with IFN-β mRNA specific primers were used to evaluate the level of IFN induction (Figure 33A). Compared to the parental isogenic strain, L16-P-W186A infection lead to a 16-fold increase in IFN-β mRNA transcription. This ratio is in agreement with the data obtained from reporter gene assays with overexpression of wild type and mutant P proteins (Figure 25A) and with the IFN induction by L16-PΔ176-186 reported previously (Rieder et al., 2011). Thereby, the inhibitory defect of P-W186A could be confirmed in the viral context, providing good evidence that W186 is indeed crucial for both HSP70 binding and suppression of IFN induction. Further, it should be noted that the P mRNA levels were 2-fold reduced in L16-P-W186A in comparison to the wild type. However, since the P levels were comparable on the protein level as shown by Western blotting, it is unlikely that reduced transcription or mRNA stability had an impact on inhibition. This finding might provide a slight hint at a potential additional role of the characterized P-HSP70 interaction in transcription, similar to the role for N-HSP70 interaction in facilitating measles virus transcription (Bourhis et al., 2006; Zhang et al., 2005; Zhang et al., 2002).

Strikingly, in spite of the strongly attenuated growth, L16-P-K214A induced even higher amounts of interferon mRNA. This is surprising, considering the very limited viral replication as shown by Western blotting (Figure 33C). Accordingly, RABV P mRNA levels were very low for L16-P-K214A. This somewhat resembles the previously reported phenotype of the L16-ΔPLP virus, which contains a P gene shifted to a genomic position 5' of the L gene, resulting in strongly reduced P expression in relation to other viral proteins (Rieder et al., 2011).

Since RABV P is not only involved in inhibition of IFN-signaling, but also in viral replication, transcription, proper N encapsidation of viral RNAs and RNP binding (Chenik et al., 1994; Chenik et al., 1998; Curran et al., 1995; Jacob et al., 2001), the mutant virus containing the P-K214A protein might be severely impaired in one or multiple of these functions, as discussed above. It could be speculated that defects in viral transcription and replication due to defective P function might lead to aberrant generation of PAMPs, potentially specific viral nucleic acid species that strongly trigger RLRs. In this hypothesis, the P-W186A mutation unmasks the level of IFN-inducing PAMPs which is present in an otherwise natural infection, whereas additional defects in the viral life cycle, like in the L16-P-K214A mutant virus, lead to an increase in PAMP generation or reduced shielding of PAMPs due to aberrant RNA encapsidation, and thereby IFN induction.

Since L16-P-W186A exhibits wild type-like growth kinetics while inducing IFN, this newly characterized mutant is an ideal tool for investigating the mechanism and importance of IFN induction in rabies virus infection in the future. Moreover, these traits might designate this mutant virus as an interesting candidate for a rabies vaccine. Previous studies reported that the recombinant virus L16-PΔ176-181 (PΔInd1) failed in inducing higher titers of virus neutralizing antibodies in foxes after oral vaccination in comparison to the parental strain (Vos et al., 2011). L16-P-W186A might be more promising, because, in contrast to L16-PΔ176-181, its growth kinetics are comparable to the wild type virus while the inhibitory abilities of RABV P in regard to IFN induction are absent, potentially leading to an augmented immune response.

5.4. CVS-strain P is deficient in inhibition of IFN induction

The rabies virus strain CVS (challenge virus standard) is a typical fixed, laboratory adapted strain that retained pathogenicity and leads to fatal infections in laboratory animals (Park et al., 2006). Due to this properties, CVS-strain is frequently used for rabies *in vivo* studies. However, the findings reported in this thesis raised the questions whether CVS is actually a typical street virus-like rabies virus that should be considered and used as a "standard". When comparing the phosphoproteins of SAD-L16, THA and CVS strain in reporter gene assays for their ability to

interfere with ΔRIG-I and TBK1 overexpression mediated IFN-β promoter activation, we found the CVS variant to exhibit a defect similar to the inhibition deficient L16-P mutants, such as P-W186A, which were characterized in this thesis (Figure 34) and previous research (Rieder et al., 2011). By analyzing alignments of various RABV phosphoproteins, we found an outstanding variation in the primary sequence of CVS-P at position 179 (Figure 35, section below in Figure 49).

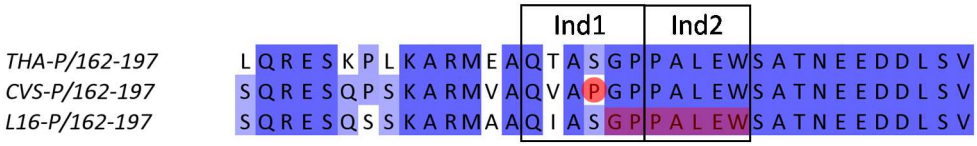

Figure 49: Sequence alignment of residues 162-197 of THA, CVS and L16-strain RABV P.
Rabies virus phosphoprotein sequence alignment for THA, CVS and L16-strain encompassing residues 162-197. Sequences were aligned using the "Clustal Omega" online tool of EMBL-EBI (European Bioinformatics Institute) and visualized with Jalview (Waterhouse et al., 2009). The minimal HSP70 binding region (GPPALEW) is annotated and CVS-P-P179 is highlighted with a red dot.

Whereas all other RABV phosphoproteins exhibit a serine residue at this position, in the case of CVS-P a proline residue is present. This position was identified as potentially important due to the otherwise strong conservation at this position and because it is located within the amino acid region which is associated with the inhibitory abilities of RABV P and is absent in the RABV PΔInd1 and PΔInd1/2 mutants described previously (Rieder et al., 2011). The exchange of a serine for a proline residue at position 179 in CVS-P restored the inhibitory function completely (Figure 36). The other way round, L16-P-S179P mutants displayed the same inhibitory defect as CVS-P or L16-P-W186A. This clearly shows that the P179 residue in CVS-P is responsible for the defect in the inhibition of IFN induction. Since all other RABV P sequences examined contain a serine residue at this position, it is well possible that the P179 in CVS-strain P is a mutation the strain acquired during passaging. Since the STAT-inhibition is still intact in this protein, the selective pressure for maintaining inhibition of IFN induction could be rather weak, especially in the artificial setting of a cell culture adapted fixed virus strain.

Rabies virus immune evasion is thought to be an important determinant of viral pathogenesis (Ito et al., 2016). The observed defect of CVS strain P raises the question whether the inhibition of IRF3 activation is strictly required for viral pathogenicity under the condition that inhibition of IFN signaling by RABV P is still intact. Although antiviral function is mostly mediated by IFN signaling, certain ISGs can also be directly induced by IRF3 independently of IFN signaling (Au et al., 1995). Expression of these gene would consequently not be suppressed by P proteins which are exclusively able to abrogate STAT signaling. The situation is severely complicated by the fact that pathogenicity of rabies virus and possibly the potential to stimulate IFN induction could be

multigenic traits that differ significantly among different rabies virus strains (Ito et al., 2010; Pulmanausahakul et al., 2008; Rieder et al., 2011; Wiltzer et al., 2014). CVS strain RABV might compensate its lack in inhibitory function in regard to IFN induction for instance with reduced PAMP generation, or a more efficient control of JAK-STAT signaling by its phosphoprotein in comparison to SAD-L16. Alternatively, RABV proteins other than P might compensate for the lack of inhibitory function, such as the matrix protein, which has been reported to target RelAp43, a class I member of the NF-κB family, leading to inhibition of the NF-κB pathway and a significant reduction of IFN-β transcription (Luco et al., 2012). A comparison of the L16 and CVS strain of rabies virus in regard to PAMP generation and analysis of corresponding chimeric recombinant viruses might reveal new interesting insights about which viral proteins and features are crucial prerequisites for immune evasion.

For the L16 strain, the ability to interfere with IFN induction was shown to be an important determinant of viral pathogenicity in a mouse model employing intracranial injection (Rieder et al., 2011). Furthermore, for Nishigahara (Ni) strain a critical connection between suppression of IFN induction and stable replication in muscle cells, enabling infection of peripheral nerves, was reported (Yamaoka et al., 2013). This underlines the importance of inhibition of IFN induction for the course of rabies virus infection. The necessity for RABV P to interfere with IRF3 activation might vary, depending on cell or tissue type and depending on the potential of the respective virus strain to induce IFN-signaling. Further research, preferably including *in vivo* studies, is necessary to clarify which viral characteristics contribute to pathogenesis.

5.5. Heat shock proteins and innate immune signaling

In this thesis a RABV P binding motif for HSP70 was identified and localized to P residues 180-186, with a critical contribution of the C-terminal residue W186. This HSP70 binding motif is contained in a RABV P region previously shown to be essential for inhibition of IFN induction (Rieder et al., 2011). All RABV P proteins deficient in HSP70 interaction also fail in inhibition of IFN induction (Figure 25). This provides strong evidence that the identified HSP70 binding motif in RABV P is essential for suppression of IRF3 activation, suggesting a connection between HSP70 chaperones and innate immune signaling.

To further evaluate this possible connection, we employed overexpression of wild type and mutant HSP70 family members as well as thermal stress (heat shock), in order to verify whether heat shock proteins might have an impact on IFN induction by RLR signaling.

Initial reporter gene experiments demonstrated that overexpression of inducible HSP70 interferes moderately with ΔRIG-I and TBK1 overexpression-mediated IFN-promoter activity (Figure 37). The ability of RABV P to interfere with IFN induction was not significantly altered by HSP70 co-expression. Further experiments revealed that HSP70-K71E, an ATPase deficient mutant (Zeng et al., 2004), significantly impaired ΔRIG-I mediation IFN-promoter induction, comparable to RABV P (Figure 38). However, in contrast to RABV P, also NF-κB activation by ΔRIG-I co-expression was significantly abrogated by HSP70-K71E. Although the observed inhibition by RABV P and HSP70-K71E was similar for IFN induction, the differential suppression in regard to NF-κB activation indicates that the modes of action are not identical. RABV P seems to interfere with IFN induction in a more specific way. Anyway, the significant impact of an ATPase deficient HSP70 mutant on IFN induction provides a further hint at a connection between the function of molecular chaperones and innate immune signaling.

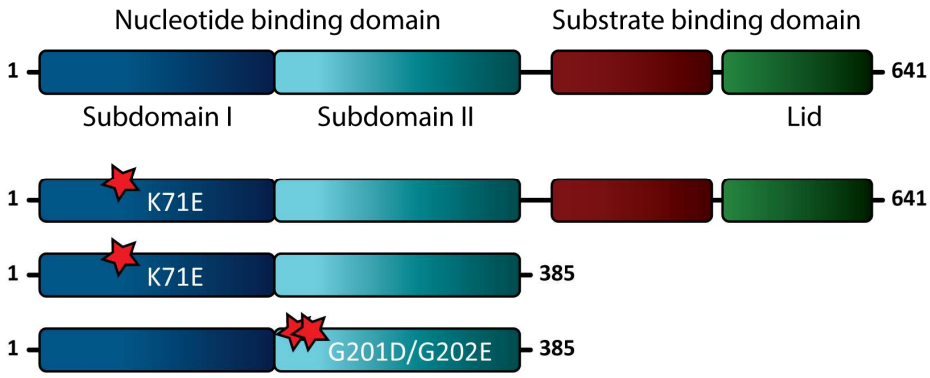

Figure 50: HSP70 mutant constructs used in this thesis.
Schematic representation of different dominant negative HSP70 constructs used in this thesis. K71 is centrally involved in ATPase activity, whereas the GG-DE mutation abrogates ATP binding.

In addition to the ATPase deficient mutant, another HSP70 mutation (G201D/G202E, termed GG-DE below) has been reported previously to interfere with HSP70 function by its inability to bind ATP, thus binding and blocking nucleotide exchange factors such as auxilin (Morgan et al., 2013). The K71E and the GG-DE mutation were separately introduced into nucleotide binding domain constructs of HSP70-1A and assayed for inhibition of IFN induction in comparison to RABV P and different HSP70 constructs (Figure 39). Both mutants, K71E and GG-DE, in the context of the HSP70-1A NBD interfered very efficiently with IFN-promoter activity. Inhibition was comparable with RABV P for the GG-DE construct, and slightly less efficient for the K71E version. Interestingly, expression of the wild type NBD alone also interfered with IFN induction significantly and moderately better than wild type full length HSP70-1A. Taken together, these experiments provide evidence that interfering with proper chaperone function in a dominant negative way may impair innate immune signaling considerably.

In further experiments we obtained some evidence that similar to heat shock protein overexpression, heat shock treatment of cells impaired ΔRIG-I and TBK1-overexpression mediated IFN-promoter activity, while the inhibitory function of RABV P remained intact (Figure 40A). In parallel, the reliability of the reporter gene assay was verified by assaying heat shock treatment for an influence on IFN-mediated ISRE promoter activity. While RABV P, which is a known inhibitor for STAT signaling (Brzózka et al., 2006; Vidy et al., 2005), abrogated reporter activity under normal and after thermal stress conditions, heat shock treatment alone had rather a slightly positive effect on ISRE-promoter activity. In a similar setting, the dominant negative mutant HSP70-K71E abrogated ΔRIG-I mediated IFN-promoter activity, but not induction of IFN-induced ISRE-reporter activation (Figure 40B). This indicates that the utilized dual luciferase assay is suitable for the employed experimental conditions and is not in general indicating reduced reporter activity after heat shock treatment or expression of dominant negative HSP70 mutants, for example due to impaired folding of the luciferase reporter. Therefore, it can be concluded that changes in cellular heat shock protein function might specifically impair IFN induction while leaving other cellular pathways unaffected.

In order to evaluate a possible involvement of inducible HSP70 family members, which exhibited a higher impact on IFN induction before, we created HSP70-1A/1B HEK 293T knock-out cells using the CRIPR/Cas9 technology (Mali et al., 2013). However, experiments conducted with this knock-out cell line did not reveal any significant differences in regard to induction of IFN-β promoter activity by TBK1 or ΔRIG-I (Figure 41). Also inhibition of IFN induction by RABV P or the reaction to heat shock treatment were not notably altered in comparison to the parental cell line. This indicates that the inducible form of HSP70 (HSP70-1A/1B) is not involved in the induction of type I interferons, or that the corresponding function might be redundant and shared with other heat shock proteins. The constitutively expressed variant HSC70 might be an interesting candidate for future research, since it is expressed in all cell types also under non-stress conditions. It might be challenging to obtain further evidence for a potential role for HSC70 in innate immune signaling, since this chaperone was shown to be essential for cell viability. This was indicated previously by the non-viability of knockout cells (Florin et al., 2004) and massive cell death upon knockdown (Rohde et al., 2005). Therefore it might be preferential in future experiments to employ small molecule inhibitors targeting the function of HSC70 or other chaperones. The compounds of the diverse pool of available HSP70 inhibitors (Patury et al., 2009) could be screened for their ability to modulate IFN induction, possibly providing further evidence for a general involvement of HSP70 chaperones in innate immune signaling. An interesting, however technically more challenging approach would be the generation of cell lines

with inducible degradation of HSC70, based on the auxin-inducible degron system (Nishimura et al., 2009) or small molecule-assisted shutoff (SMASh) technology (Chung et al., 2015).

In addition to the findings presented in this thesis, there is emerging evidence in the literature that heat shock proteins have many different roles in cellular processes besides maintaining protein homeostasis under stress and normal conditions. The drug deoxyspergualin (DSG) is a potent immunosuppressant with clinical applications (Ito et al., 1990). Although the exact mechanism of action is still unknown, it could be demonstrated that the compound binds to members of the HSP70 family (Nadler et al., 1992). Studies using different DSG analogs and inactive metabolites revealed a correlation between the ability of these molecules to interact with HSP70 and their efficacy as immunosuppressants (Nadeau et al., 1994).

In the last decade, different heat shock proteins have been further shown to be involved in different aspects of innate immune signaling. HSPD1, a mitochondria-associated member of the HSP60 chaperonin family, was shown to be involved in the positive regulation of IRF3 phosphorylation in the RLR pathway (Lin et al., 2014). HSC70, a constitutively expressed HSP70 member was reported to negatively regulate MAVS filament formation, thus impairing IFN induction (Liu et al., 2013b). However, this report could not be supported in this thesis, since HSC70 overexpression only lead to minor changes of RLR-dependent IFN induction (Figure 38). Another HSP70 family member, the ER-resident chaperone GRP78 (BiP) modulates the TLR3-dependent innate immune response in HCV infection (Wei et al., 2016). Another heat shock protein family, HSP90, was reported to regulate IRF3 activation by stabilization of TBK1 (Yang et al., 2006).

These examples and the results presented in this thesis illustrate that heat shock proteins might rather play a common and possibly underestimated role in innate immune signaling. The involvement of HSP70 chaperones in IFN induction could be further elucidated in further research using RABV P as a promising tool. It should be clarified whether RABV P exhibits selectivity towards defined HSP70 family members or targets the whole protein group, possibly by interacting with a conserved motif. This approach and further methods discussed above might lead to promising novel insights into the involvement of possibly select HSP70 chaperones in innate immune signaling.

5.6. Conclusion and outlook

In the present thesis, several novel insights about the potent IFN-antagonist RABV P could be reported. Inhibition of RIG-I signaling could be shown to depend on the C-terminal domain of the protein, while in contrast the N-terminal domain was found to be non-essential. Some evidence could be gathered that this requirement for the CTD is based on the presence of a conformational nuclear localization signal in this domain. RABV P mutants exhibiting CTD-NLS mutations lost their ability to interfere with IFN induction, similar to C-terminal truncation mutants. Notably, this defect could be rescued in both cases by N-terminal fusion with a recombinant SV40-NLS sequence, strongly suggesting that indeed active nuclear trafficking is a prerequisite for inhibition of IRF3 activation.

Further, a novel HSP70 binding peptide in RABV P was identified and characterized. It could be mapped to a seven amino acid stretch (residues 180-186) located to a part of the disordered region of the protein previously implicated in the inhibition of IFN induction (Rieder, 2012). In addition to internal deletion of this interaction motif, the binding to HSP70 could also be abrogated by a single amino acid substitution (W186A). Strikingly, all RABV constructs which exhibited defective HSP70 binding also failed in interfering with IFN induction, revealing an interesting correlation. To follow up on these results, overexpression of heat shock proteins, dominant negative HSP70 mutants and direct heat shock treatment were employed to investigate a potential connection between the molecular chaperone machinery and innate immune signaling. The obtained data indicates that interference with proper HSP70 function is impairing IFN induction, while other pathways such as STAT signaling remain unaffected. These findings provide good hints that HSP70 family members might have an important and so far not appreciated role in the regulation of innate immune signaling.

In order to shed more light on the detected RABV P-HSP70 interaction and potential functional implications a closer understanding on the binding interface between the two proteins is of great interest and could potentially provide a hint at how P modulates HSP70 function. Further mutational analysis of select HSP70s and structural studies might provide new insights about this issue. The function of HSP70s in regard to innate immune signaling could be further investigated by selectively modulating the function of one or multiple chaperones by small molecule inhibitors or genetic engineering techniques. This way, the potential involvement of this class of proteins in IFN induction could be further clarified. Since HSP70s were identified as a target of RABV P in the present thesis, this viral protein might be a valuable tool in the future to further examine the contribution of HSP70 chaperones to cellular signaling pathways. Further, it might

be interesting to evaluate, whether already available HSP70 inhibitors might be suitable for modulation of IFN induction, or conversely whether RABV P derived constructs might be able to modulate HSP70 function. This could lead to the development of novel compounds targeting HSP70, what might be promising considering that HSP70 is an emerging target for chemosensitization of cancer cells (Powers et al., 2008; Rerole et al., 2011). Moreover, molecules targeting HSP70 function might be assayed for potential interference with IFN induction. A potential modulation of IFN induction by small molecules targeting chaperone function might in this case be used as new therapeutic option in the treatment of auto-immune disorders in the future.

6. Appendix

6.1. List of Figures

6.2. List of Tables

6.3. Abbreviations

Abbreviation	Description
5’-ppp	5’-triphosphate
aa	amino acids
APS	ammonium persulfate
bp	base pair
CARD	caspase activation and recruitment domain
cDNA	copy DNA
CIAP	calf intestinal alkaline phosphatase
Co-IP	co-immunoprecipitation
CTD	C-terminal domain
Da	dalton
ddH_2O	bidestilled water
DLC8	dynein light chain LC-type 1
dsRNA	double stranded RNA
EM	electron microscopy
EV	empty vector
FCS	fetal calf serum
FF	firefly luciferase
ffu	focus forming unit
GFP	green fluorescent protein
HA	hemagglutinin tag
HRP	horseradish peroxidase
HS	heat shock
HSP	heat shock protein
IF	immunofluorescence

IFN	interferon
IFNAR	interferon-α/β receptor
IKK	IκB kinase
IRF	interferon regulatory factor
ISG	interferon-stimulated gene
ISRE	interferon-stimulated response element
IκB	inhibitor of κB
JAK	Janus kinase
KO	knock out
LGP2	laboratory of genetics and physiology 2
LMB	leptomycin B
MAMP	microbe-associated molecular pattern
MAVS	mitochondrial antiviral-signaling protein
MDA5	melanoma differentiation-associated gene 5
MOI	multiplicity of infection
MS	mass spectrometry
NBD	nucleotide binding domain
NEF	nucleotide exchange factor
NES	nuclear export signal
NF-κB	nuclear factor κB
NLS	nuclear localization signal
o/n	overnight
OD	optical density
OE	overlap extension (PCR)
p. i.	post-infection
p. t.	post-transfection
PAGE	polyacrylamide gel electrophoresis
PAMP	pathogen associated molecular pattern
PBS	phosphate buffered saline
PCR	polymerase chain reaction
PEI	polyethyleneimine
PKC	protein kinase C
PO	peroxidase
PRR	pattern recognition receptor
PVDF	polyvinylidene fluoride
RABV P	Rabies virus phosphoprotein
RD	regulatory domain
RIG-I	retinoic acid inducible I
RL	renilla luciferase
RLR	RIG-I like receptor
RNP	ribonucleoprotein
RT	room temperature
SBD	substrate binding domain
SeDI	*Sendai virus* defective interfering particles
ssRNA	single stranded RNA
STAT	signal transducer and activator of transcription

TBK1	tank-binding kinase 1
TIM	TRAF interaction motif
TLR	toll-like receptor
TRAF	TNF-receptor-associated factor
VSV	Vesicular stomatitis virus
WB	Western blotting
wt	wild type

7. References

Alandijany, T., Kammouni, W., Roy Chowdhury, S.K., Fernyhough, P., and Jackson, A.C. (2013). Mitochondrial dysfunction in rabies virus infection of neurons. J Neurovirol *19*, 537-549.

Albertini, A.A., Ruigrok, R.W., and Blondel, D. (2011). Rabies virus transcription and replication. Adv Virus Res *79*, 1-22.

Albertini, A.A., Wernimont, A.K., Muziol, T., Ravelli, R.B., Clapier, C.R., Schoehn, G., Weissenhorn, W., and Ruigrok, R.W. (2006). Crystal structure of the rabies virus nucleoprotein-RNA complex. Science *313*, 360-363.

Alexopoulou, L., Holt, A.C., Medzhitov, R., and Flavell, R.A. (2001). Recognition of double-stranded RNA and activation of NF-kappaB by Toll-like receptor 3. Nature *413*, 732-738.

Ashburner, M., and Bonner, J.J. (1979). The induction of gene activity in drosophilia by heat shock. Cell *17*, 241-254.

Au, W.C., Moore, P.A., Lowther, W., Juang, Y.T., and Pitha, P.M. (1995). Identification of a member of the interferon regulatory factor family that binds to the interferon-stimulated response element and activates expression of interferon-induced genes. Proc Natl Acad Sci U S A *92*, 11657-11661.

Baker, N.A., Sept, D., Joseph, S., Holst, M.J., and McCammon, J.A. (2001). Electrostatics of nanosystems: application to microtubules and the ribosome. Proc Natl Acad Sci U S A *98*, 10037-10041.

Balchin, D., Hayer-Hartl, M., and Hartl, F.U. (2016). In vivo aspects of protein folding and quality control. Science *353*, aac4354.

Beere, H.M., and Green, D.R. (2001). Stress management - heat shock protein-70 and the regulation of apoptosis. Trends in cell biology *11*, 6-10.

Belgnaoui, S.M., Paz, S., and Hiscott, J. (2011). Orchestrating the interferon antiviral response through the mitochondrial antiviral signaling (MAVS) adapter. Curr Opin Immunol *23*, 564-572.

Berche, P. (2012). Louis Pasteur, from crystals of life to vaccination. Clinical microbiology and infection : the official publication of the European Society of Clinical Microbiology and Infectious Diseases *18 Suppl 5*, 1-6.

Bertelsen, E.B., Chang, L., Gestwicki, J.E., and Zuiderweg, E.R. (2009). Solution conformation of wild-type E. coli Hsp70 (DnaK) chaperone complexed with ADP and substrate. Proc Natl Acad Sci U S A *106*, 8471-8476.

Blond-Elguindi, S., Cwirla, S.E., Dower, W.J., Lipshutz, R.J., Sprang, S.R., Sambrook, J.F., and Gething, M.J. (1993). Affinity panning of a library of peptides displayed on bacteriophages reveals the binding specificity of BiP. Cell *75*, 717-728.

Blondel, D., Kheddache, S., Lahaye, X., Dianoux, L., and Chelbi-Alix, M.K. (2010). Resistance to rabies virus infection conferred by the PMLIV isoform. J Virol *84*, 10719-10726.

Blondel, D., Regad, T., Poisson, N., Pavie, B., Harper, F., Pandolfi, P.P., De The, H., and Chelbi-Alix, M.K. (2002). Rabies virus P and small P products interact directly with PML and reorganize PML nuclear bodies. Oncogene *21*, 7957-7970.

Blumberg, B.M., and Kolakofsky, D. (1981). Intracellular vesicular stomatitis virus leader RNAs are found in nucleocapsid structures. J Virol *40*, 568-576.

Bonnard, M., Mirtsos, C., Suzuki, S., Graham, K., Huang, J., Ng, M., Itie, A., Wakeham, A., Shahinian, A., Henzel, W.J*., et al.* (2000). Deficiency of T2K leads to apoptotic liver degeneration and impaired NF-kappaB-dependent gene transcription. Embo j *19*, 4976-4985.

Bonner, W.M. (1975). Protein migration into nuclei. I. Frog oocyte nuclei in vivo accumulate microinjected histones, allow entry to small proteins, and exclude large proteins. The Journal of cell biology *64*, 421-430.

Bourhis, J.M., Canard, B., and Longhi, S. (2006). Structural disorder within the replicative complex of measles virus: functional implications. Virology *344*, 94-110.

Brown, G., Rixon, H.W., Steel, J., McDonald, T.P., Pitt, A.R., Graham, S., and Sugrue, R.J. (2005). Evidence for an association between heat shock protein 70 and the respiratory syncytial virus polymerase complex within lipid-raft membranes during virus infection. Virology *338*, 69-80.

Brzózka, K., Finke, S., and Conzelmann, K.K. (2005). Identification of the rabies virus alpha/beta interferon antagonist: phosphoprotein P interferes with phosphorylation of interferon regulatory factor 3. J Virol *79*, 7673-7681.

Brzózka, K., Finke, S., and Conzelmann, K.K. (2006). Inhibition of interferon signaling by rabies virus phosphoprotein P: activation-dependent binding of STAT1 and STAT2. J Virol *80*, 2675-2683.

Buchholz, U.J., Finke, S., and Conzelmann, K.K. (1999). Generation of bovine respiratory syncytial virus (BRSV) from cDNA: BRSV NS2 is not essential for virus replication in tissue culture, and the human RSV leader region acts as a functional BRSV genome promoter. J Virol *73*, 251-259.

Chan, Y.K., and Gack, M.U. (2015). RIG-I works double duty. Cell host & microbe *17*, 285-287.

Chappell, T.G., Welch, W.J., Schlossman, D.M., Palter, K.B., Schlesinger, M.J., and Rothman, J.E. (1986). Uncoating ATPase is a member of the 70 kilodalton family of stress proteins. Cell *45*, 3-13.

Chau, T.L., Gioia, R., Gatot, J.S., Patrascu, F., Carpentier, I., Chapelle, J.P., O'Neill, L., Beyaert, R., Piette, J., and Chariot, A. (2008). Are the IKKs and IKK-related kinases TBK1 and IKK-epsilon similarly activated? Trends in biochemical sciences *33*, 171-180.

Chen, Z.J. (2005). Ubiquitin signalling in the NF-kappaB pathway. Nature cell biology *7*, 758-765.

Chenik, M., Chebli, K., and Blondel, D. (1995). Translation initiation at alternate in-frame AUG codons in the rabies virus phosphoprotein mRNA is mediated by a ribosomal leaky scanning mechanism. J Virol *69*, 707-712.

Chenik, M., Chebli, K., Gaudin, Y., and Blondel, D. (1994). In vivo interaction of rabies virus phosphoprotein (P) and nucleoprotein (N): existence of two N-binding sites on P protein. J Gen Virol *75 (Pt 11)*, 2889-2896.

Chenik, M., Schnell, M., Conzelmann, K.K., and Blondel, D. (1998). Mapping the interacting domains between the rabies virus polymerase and phosphoprotein. J Virol *72*, 1925-1930.

Chung, H.K., Jacobs, C.L., Huo, Y., Yang, J., Krumm, S.A., Plemper, R.K., Tsien, R.Y., and Lin, M.Z. (2015). Tunable and reversible drug control of protein production via a self-excising degron. Nature chemical biology *11*, 713-720.

Curran, J., Marq, J.B., and Kolakofsky, D. (1995). An N-terminal domain of the Sendai paramyxovirus P protein acts as a chaperone for the NP protein during the nascent chain assembly step of genome replication. J Virol *69*, 849-855.

Das, S.C., and Pattnaik, A.K. (2004). Phosphorylation of vesicular stomatitis virus phosphoprotein P is indispensable for virus growth. J Virol *78*, 6420-6430.

Davis, B.M., Rall, G.F., and Schnell, M.J. (2015). Everything You Always Wanted to Know About Rabies Virus (But Were Afraid to Ask). Annu Rev Virol *2*, 451-471.

Der, S.D., Zhou, A., Williams, B.R., and Silverman, R.H. (1998). Identification of genes differentially regulated by interferon alpha, beta, or gamma using oligonucleotide arrays. Proc Natl Acad Sci U S A *95*, 15623-15628.

Didierlaurent, A., Simonet, M., and Sirard, J.C. (2005). Innate and acquired plasticity of the intestinal immune system. Cellular and molecular life sciences : CMLS *62*, 1285-1287.

Dixit, E., Boulant, S., Zhang, Y., Lee, A.S., Odendall, C., Shum, B., Hacohen, N., Chen, Z.J., Whelan, S.P., Fransen, M.*, et al.* (2010). Peroxisomes are signaling platforms for antiviral innate immunity. Cell *141*, 668-681.

Dyballa, N., and Metzger, S. (2012). Fast and sensitive coomassie staining in quantitative proteomics. Methods Mol Biol *893*, 47-59.

Emerson, S.U., and Wagner, R.R. (1972). Dissociation and reconstitution of the transcriptase and template activities of vesicular stomatitis B and T virions. J Virol *10*, 297-309.

Emerson, S.U., and Yu, Y. (1975). Both NS and L proteins are required for in vitro RNA synthesis by vesicular stomatitis virus. J Virol *15*, 1348-1356.

Finke, S., Brzozka, K., and Conzelmann, K.K. (2004). Tracking fluorescence-labeled rabies virus: enhanced green fluorescent protein-tagged phosphoprotein P supports virus gene expression and formation of infectious particles. J Virol *78*, 12333-12343.

Finke, S., and Conzelmann, K.K. (1997). Ambisense gene expression from recombinant rabies virus: random packaging of positive- and negative-strand ribonucleoprotein complexes into rabies virions. J Virol *71*, 7281-7288.

Finke, S., and Conzelmann, K.K. (1999). Virus promoters determine interference by defective RNAs: selective amplification of mini-RNA vectors and rescue from cDNA by a 3' copy-back ambisense rabies virus. J Virol *73*, 3818-3825.

Finke, S., and Conzelmann, K.K. (2003). Dissociation of rabies virus matrix protein functions in regulation of viral RNA synthesis and virus assembly. J Virol *77*, 12074-12082.

Finke, S., Cox, J.H., and Conzelmann, K.K. (2000). Differential transcription attenuation of rabies virus genes by intergenic regions: generation of recombinant viruses overexpressing the polymerase gene. J Virol *74*, 7261-7269.

Finke, S., Mueller-Waldeck, R., and Conzelmann, K.K. (2003). Rabies virus matrix protein regulates the balance of virus transcription and replication. J Gen Virol *84*, 1613-1621.

Fitzgerald, K.A., McWhirter, S.M., Faia, K.L., Rowe, D.C., Latz, E., Golenbock, D.T., Coyle, A.J., Liao, S.M., and Maniatis, T. (2003). IKKepsilon and TBK1 are essential components of the IRF3 signaling pathway. Nat Immunol *4*, 491-496.

Flaherty, K.M., DeLuca-Flaherty, C., and McKay, D.B. (1990). Three-dimensional structure of the ATPase fragment of a 70K heat-shock cognate protein. Nature *346*, 623-628.

Florin, L., Becker, K.A., Sapp, C., Lambert, C., Sirma, H., Muller, M., Streeck, R.E., and Sapp, M. (2004). Nuclear translocation of papillomavirus minor capsid protein L2 requires Hsc70. J Virol *78*, 5546-5553.

Flynn, G.C., Pohl, J., Flocco, M.T., and Rothman, J.E. (1991). Peptide-binding specificity of the molecular chaperone BiP. Nature *353*, 726-730.

Fornerod, M., Ohno, M., Yoshida, M., and Mattaj, I.W. (1997). CRM1 is an export receptor for leucine-rich nuclear export signals. Cell *90*, 1051-1060.

Fouquet, B., Nikolic, J., Larrous, F., Bourhy, H., Wirblich, C., Lagaudriere-Gesbert, C., and Blondel, D. (2015). Focal adhesion kinase is involved in rabies virus infection through its interaction with viral phosphoprotein P. J Virol *89*, 1640-1651.

Fu, Z.F., Zheng, Y., Wunner, W.H., Koprowski, H., and Dietzschold, B. (1994). Both the N- and the C-terminal domains of the nominal phosphoprotein of rabies virus are involved in binding to the nucleoprotein. Virology *200*, 590-597.

Gack, M.U., Albrecht, R.A., Urano, T., Inn, K.S., Huang, I.C., Carnero, E., Farzan, M., Inoue, S., Jung, J.U., and Garcia-Sastre, A. (2009). Influenza A virus NS1 targets the ubiquitin ligase TRIM25 to evade recognition by the host viral RNA sensor RIG-I. Cell host & microbe *5*, 439-449.

Gack, M.U., Shin, Y.C., Joo, C.H., Urano, T., Liang, C., Sun, L., Takeuchi, O., Akira, S., Chen, Z., Inoue, S*., et al.* (2007). TRIM25 RING-finger E3 ubiquitin ligase is essential for RIG-I-mediated antiviral activity. Nature *446*, 916-920.

Garic, D., Humbert, L., Fils-Aime, N., Korah, J., Zarfabian, Y., Lebrun, J.J., and Ali, S. (2013). Development of buffers for fast semidry transfer of proteins. Analytical biochemistry *441*, 182-184.

Gaudin, Y. (2000). Rabies virus-induced membrane fusion pathway. The Journal of cell biology *150*, 601-612.

Gerard, F.C., Ribeiro Ede, A., Jr., Leyrat, C., Ivanov, I., Blondel, D., Longhi, S., Ruigrok, R.W., and Jamin, M. (2009). Modular organization of rabies virus phosphoprotein. J Mol Biol *388*, 978-996.

Ghanem, A., Kern, A., and Conzelmann, K.K. (2012). Significantly improved rescue of rabies virus from cDNA plasmids. Eur J Cell Biol *91*, 10-16.

Gigant, B., Iseni, F., Gaudin, Y., Knossow, M., and Blondel, D. (2000). Neither phosphorylation nor the amino-terminal part of rabies virus phosphoprotein is required for its oligomerization. J Gen Virol *81*, 1757-1761.

Gitlin, L., Barchet, W., Gilfillan, S., Cella, M., Beutler, B., Flavell, R.A., Diamond, M.S., and Colonna, M. (2006). Essential role of mda-5 in type I IFN responses to polyriboinosinic:polyribocytidylic acid and encephalomyocarditis picornavirus. Proc Natl Acad Sci U S A *103*, 8459-8464.

Goloubinoff, P., and De Los Rios, P. (2007). The mechanism of Hsp70 chaperones: (entropic) pulling the models together. Trends in biochemical sciences *32*, 372-380.

Gomez-Alonso, J. (1998). Rabies: a possible explanation for the vampire legend. Neurology *51*, 856-859.

Goncalves, A., Burckstummer, T., Dixit, E., Scheicher, R., Gorna, M.W., Karayel, E., Sugar, C., Stukalov, A., Berg, T., Kralovics, R*., et al.* (2011). Functional dissection of the TBK1 molecular network. PLoS One *6*, e23971.

Goodbourn, S., Didcock, L., and Randall, R.E. (2000). Interferons: cell signalling, immune modulation, antiviral response and virus countermeasures. J Gen Virol *81*, 2341-2364.

Gorlich, D., and Kutay, U. (1999). Transport between the cell nucleus and the cytoplasm. Annual review of cell and developmental biology *15*, 607-660.

Gragerov, A., Zeng, L., Zhao, X., Burkholder, W., and Gottesman, M.E. (1994). Specificity of DnaK-peptide binding. J Mol Biol *235*, 848-854.

Grandvaux, N., Servant, M.J., tenOever, B., Sen, G.C., Balachandran, S., Barber, G.N., Lin, R., and Hiscott, J. (2002). Transcriptional profiling of interferon regulatory factor 3 target genes: direct involvement in the regulation of interferon-stimulated genes. J Virol *76*, 5532-5539.

Guichard, P., Krell, T., Chevalier, M., Vaysse, C., Adam, O., Ronzon, F., and Marco, S. (2011). Three dimensional morphology of rabies virus studied by cryo-electron tomography. J Struct Biol *176*, 32-40.

Guo, B., and Cheng, G. (2007). Modulation of the interferon antiviral response by the TBK1/IKKi adaptor protein TANK. J Biol Chem *282*, 11817-11826.

Gupta, A.K., Blondel, D., Choudhary, S., and Banerjee, A.K. (2000). The phosphoprotein of rabies virus is phosphorylated by a unique cellular protein kinase and specific isomers of protein kinase C. J Virol *74*, 91-98.

Hacker, H., Redecke, V., Blagoev, B., Kratchmarova, I., Hsu, L.C., Wang, G.G., Kamps, M.P., Raz, E., Wagner, H., Hacker, G.*, et al.* (2006). Specificity in Toll-like receptor signalling through distinct effector functions of TRAF3 and TRAF6. Nature *439*, 204-207.

Hageman, J., van Waarde, M.A., Zylicz, A., Walerych, D., and Kampinga, H.H. (2011). The diverse members of the mammalian HSP70 machine show distinct chaperone-like activities. The Biochemical journal *435*, 127-142.

Haller, O., Kochs, G., and Weber, F. (2007). Interferon, Mx, and viral countermeasures. Cytokine & growth factor reviews *18*, 425-433.

Harrist, A., Styczynski, A., Wynn, D., Ansari, S., Hopkin, J., Rosado-Santos, H., Baker, J., Nakashima, A., Atkinson, A., Spencer, M.*, et al.* (2016). Human Rabies - Wyoming and Utah, 2015. MMWR Morbidity and mortality weekly report *65*, 529-533.

Hasday, J.D., and Singh, I.S. (2000). Fever and the heat shock response: distinct, partially overlapping processes. Cell stress & chaperones *5*, 471-480.

Heil, F., Hemmi, H., Hochrein, H., Ampenberger, F., Kirschning, C., Akira, S., Lipford, G., Wagner, H., and Bauer, S. (2004). Species-specific recognition of single-stranded RNA via toll-like receptor 7 and 8. Science *303*, 1526-1529.

Helgason, E., Phung, Q.T., and Dueber, E.C. (2013). Recent insights into the complexity of Tank-binding kinase 1 signaling networks: the emerging role of cellular localization in the activation and substrate specificity of TBK1. FEBS letters *587*, 1230-1237.

Hemmi, H., Takeuchi, O., Kawai, T., Kaisho, T., Sato, S., Sanjo, H., Matsumoto, M., Hoshino, K., Wagner, H., Takeda, K.*, et al.* (2000). A Toll-like receptor recognizes bacterial DNA. Nature *408*, 740-745.

Hemmi, H., Takeuchi, O., Sato, S., Yamamoto, M., Kaisho, T., Sanjo, H., Kawai, T., Hoshino, K., Takeda, K., and Akira, S. (2004). The roles of two IkappaB kinase-related kinases in lipopolysaccharide and double stranded RNA signaling and viral infection. J Exp Med *199*, 1641-1650.

Hinault, M.P., Ben-Zvi, A., and Goloubinoff, P. (2006). Chaperones and proteases: cellular fold-controlling factors of proteins in neurodegenerative diseases and aging. Journal of molecular neuroscience : MN *30*, 249-265.

Hiscott, J. (2007). Triggering the innate antiviral response through IRF-3 activation. J Biol Chem *282*, 15325-15329.

Hiscott, J., Lacoste, J., and Lin, R. (2006). Recruitment of an interferon molecular signaling complex to the mitochondrial membrane: disruption by hepatitis C virus NS3-4A protease. Biochemical pharmacology *72*, 1477-1484.

Horner, S.M., Liu, H.M., Park, H.S., Briley, J., and Gale, M., Jr. (2011). Mitochondrial-associated endoplasmic reticulum membranes (MAM) form innate immune synapses and are targeted by hepatitis C virus. Proc Natl Acad Sci U S A *108*, 14590-14595.

Hornung, V., Ellegast, J., Kim, S., Brzozka, K., Jung, A., Kato, H., Poeck, H., Akira, S., Conzelmann, K.K., Schlee, M*., et al.* (2006). 5'-Triphosphate RNA is the ligand for RIG-I. Science *314*, 994-997.

Hou, F., Sun, L., Zheng, H., Skaug, B., Jiang, Q.X., and Chen, Z.J. (2011). MAVS forms functional prion-like aggregates to activate and propagate antiviral innate immune response. Cell *146*, 448-461.

Howe, M.K., Speer, B.L., Hughes, P.F., Loiselle, D.R., Vasudevan, S., and Haystead, T.A. (2016). An inducible heat shock protein 70 small molecule inhibitor demonstrates anti-dengue virus activity, validating Hsp70 as a host antiviral target. Antiviral research *130*, 81-92.

Iseni, F., Barge, A., Baudin, F., Blondel, D., and Ruigrok, R.W. (1998). Characterization of rabies virus nucleocapsids and recombinant nucleocapsid-like structures. J Gen Virol *79 (Pt 12)*, 2909-2919.

Ito, N., Moseley, G.W., Blondel, D., Shimizu, K., Rowe, C.L., Ito, Y., Masatani, T., Nakagawa, K., Jans, D.A., and Sugiyama, M. (2010). Role of interferon antagonist activity of rabies virus phosphoprotein in viral pathogenicity. J Virol *84*, 6699-6710.

Ito, N., Moseley, G.W., and Sugiyama, M. (2016). The importance of immune evasion in the pathogenesis of rabies virus: Veterinary Science Award Winner's (No.116) Commemorative Review. The Journal of Veterinary Medical Science *78*, 1089-1098.

Ito, S., Ueno, M., Arakawa, M., Saito, T., Aoyagi, T., and Fujiwara, M. (1990). Therapeutic effect of 15-deoxyspergualin on the progression of lupus nephritis in MRL mice. I. Immunopathological analyses. Clinical and Experimental Immunology *81*, 446-453.

Ivanov, I., Crepin, T., Jamin, M., and Ruigrok, R.W. (2010). Structure of the dimerization domain of the rabies virus phosphoprotein. J Virol *84*, 3707-3710.

Jackson, A.C. (2013). Human Disease. In: Jackson AC (ed) Rabies: scientific basis of the disease and its management.

Jacob, Y., Badrane, H., Ceccaldi, P.E., and Tordo, N. (2000). Cytoplasmic dynein LC8 interacts with lyssavirus phosphoprotein. J Virol *74*, 10217-10222.

Jacob, Y., Real, E., and Tordo, N. (2001). Functional interaction map of lyssavirus phosphoprotein: identification of the minimal transcription domains. J Virol *75*, 9613-9622.

Janeway, C.A., Jr., and Medzhitov, R. (2002). Innate immune recognition. Annu Rev Immunol *20*, 197-216.

Jang, M.A., Kim, E.K., Now, H., Nguyen, N.T., Kim, W.J., Yoo, J.Y., Lee, J., Jeong, Y.M., Kim, C.H., Kim, O.H*., et al.* (2015). Mutations in DDX58, which encodes RIG-I, cause atypical Singleton-Merten syndrome. American journal of human genetics *96*, 266-274.

Jiang, J., Prasad, K., Lafer, E.M., and Sousa, R. (2005). Structural basis of interdomain communication in the Hsc70 chaperone. Mol Cell *20*, 513-524.

Jiang, X., Kinch, L.N., Brautigam, C.A., Chen, X., Du, F., Grishin, N.V., and Chen, Z.J. (2012). Ubiquitin-induced oligomerization of the RNA sensors RIG-I and MDA5 activates antiviral innate immune response. Immunity *36*, 959-973.

Johnson, N., Arechiga-Ceballos, N., and Aguilar-Setien, A. (2014). Vampire bat rabies: ecology, epidemiology and control. Viruses *6*, 1911-1928.

Johnston, M.D. (1981). The characteristics required for a Sendai virus preparation to induce high levels of interferon in human lymphoblastoid cells. J Gen Virol *56*, 175-184.

Kalderon, D., Richardson, W.D., Markham, A.F., and Smith, A.E. (1984a). Sequence requirements for nuclear location of simian virus 40 large-T antigen. Nature *311*, 33-38.

Kalderon, D., Roberts, B.L., Richardson, W.D., and Smith, A.E. (1984b). A short amino acid sequence able to specify nuclear location. Cell *39*, 499-509.

Kammouni, W., Wood, H., Saleh, A., Appolinario, C.M., Fernyhough, P., and Jackson, A.C. (2015). Rabies virus phosphoprotein interacts with mitochondrial Complex I and induces mitochondrial dysfunction and oxidative stress. J Neurovirol *21*, 370-382.

Kampinga, H.H., and Craig, E.A. (2010). The HSP70 chaperone machinery: J proteins as drivers of functional specificity. Nature reviews Molecular cell biology *11*, 579-592.

Kato, H., Sato, S., Yoneyama, M., Yamamoto, M., Uematsu, S., Matsui, K., Tsujimura, T., Takeda, K., Fujita, T., Takeuchi, O*., et al.* (2005). Cell type-specific involvement of RIG-I in antiviral response. Immunity *23*, 19-28.

Kato, H., Takeuchi, O., Mikamo-Satoh, E., Hirai, R., Kawai, T., Matsushita, K., Hiiragi, A., Dermody, T.S., Fujita, T., and Akira, S. (2008). Length-dependent recognition of double-stranded ribonucleic acids by retinoic acid-inducible gene-I and melanoma differentiation-associated gene 5. J Exp Med *205*, 1601-1610.

Kato, H., Takeuchi, O., Sato, S., Yoneyama, M., Yamamoto, M., Matsui, K., Uematsu, S., Jung, A., Kawai, T., Ishii, K.J*., et al.* (2006). Differential roles of MDA5 and RIG-I helicases in the recognition of RNA viruses. Nature *441*, 101-105.

Katoh, H., Kubota, T., Kita, S., Nakatsu, Y., Aoki, N., Mori, Y., Maenaka, K., Takeda, M., and Kidokoro, M. (2015). Heat shock protein 70 regulates degradation of the mumps virus phosphoprotein via the ubiquitin-proteasome pathway. J Virol *89*, 3188-3199.

Kaufer, S., Coffey, C.M., and Parker, J.S. (2012). The cellular chaperone hsc70 is specifically recruited to reovirus viral factories independently of its chaperone function. J Virol *86*, 1079-1089.

Kawai, T., and Akira, S. (2008). Toll-like receptor and RIG-I-like receptor signaling. Ann N Y Acad Sci *1143*, 1-20.

Kawai, T., Takahashi, K., Sato, S., Coban, C., Kumar, H., Kato, H., Ishii, K.J., Takeuchi, O., and Akira, S. (2005). IPS-1, an adaptor triggering RIG-I- and Mda5-mediated type I interferon induction. Nat Immunol *6*, 981-988.

Kelley, P.M., and Schlesinger, M.J. (1978). The effect of amino acid analogues and heat shock on gene expression in chicken embryo fibroblasts. Cell *15*, 1277-1286.

Kim, T., Kim, T.Y., Lee, W.G., Yim, J., and Kim, T.K. (2000). Signaling pathways to the assembly of an interferon-beta enhanceosome. Chemical genetic studies with a small molecule. J Biol Chem *275*, 16910-16917.

Kityk, R., Kopp, J., Sinning, I., and Mayer, M.P. (2012). Structure and dynamics of the ATP-bound open conformation of Hsp70 chaperones. Mol Cell *48*, 863-874.

Kityk, R., Vogel, M., Schlecht, R., Bukau, B., and Mayer, M.P. (2015). Pathways of allosteric regulation in Hsp70 chaperones. Nature communications *6*, 8308.

Knobel, D.L., Cleaveland, S., Coleman, P.G., Fevre, E.M., Meltzer, M.I., Miranda, M.E., Shaw, A., Zinsstag, J., and Meslin, F.X. (2005). Re-evaluating the burden of rabies in Africa and Asia. Bull World Health Organ *83*, 360-368.

Kolumam, G.A., Thomas, S., Thompson, L.J., Sprent, J., and Murali-Krishna, K. (2005). Type I interferons act directly on CD8 T cells to allow clonal expansion and memory formation in response to viral infection. J Exp Med *202*, 637-650.

Koren, J., 3rd, Jinwal, U.K., Jin, Y., O'Leary, J., Jones, J.R., Johnson, A.G., Blair, L.J., Abisambra, J.F., Chang, L., Miyata, Y.*, et al.* (2010). Facilitating Akt clearance via manipulation of Hsp70 activity and levels. J Biol Chem *285*, 2498-2505.

Krieg, A.M., Yi, A.K., Matson, S., Waldschmidt, T.J., Bishop, G.A., Teasdale, R., Koretzky, G.A., and Klinman, D.M. (1995). CpG motifs in bacterial DNA trigger direct B-cell activation. Nature *374*, 546-549.

Lafon, M. (2005). Rabies virus receptors. J Neurovirol *11*, 82-87.

Lahaye, X., Vidy, A., Fouquet, B., and Blondel, D. (2012). Hsp70 protein positively regulates rabies virus infection. J Virol *86*, 4743-4751.

Lahaye, X., Vidy, A., Pomier, C., Obiang, L., Harper, F., Gaudin, Y., and Blondel, D. (2009). Functional characterization of Negri bodies (NBs) in rabies virus-infected cells: Evidence that NBs are sites of viral transcription and replication. J Virol *83*, 7948-7958.

Lassig, C., Matheisl, S., Sparrer, K.M., de Oliveira Mann, C.C., Moldt, M., Patel, J.R., Goldeck, M., Hartmann, G., Garcia-Sastre, A., Hornung, V.*, et al.* (2015). ATP hydrolysis by the viral RNA sensor RIG-I prevents unintentional recognition of self-RNA. eLife *4*.

Lemaux, P.G., Herendeen, S.L., Bloch, P.L., and Neidhardt, F.C. (1978). Transient rates of synthesis of individual polypeptides in E. coli following temperature shifts. Cell *13*, 427-434.

Levy, D.E., Kessler, D.S., Pine, R., Reich, N., and Darnell, J.E., Jr. (1988). Interferon-induced nuclear factors that bind a shared promoter element correlate with positive and negative transcriptional control. Genes & development *2*, 383-393.

Lin, L., Pan, S., Zhao, J., Liu, C., Wang, P., Fu, L., Xu, X., Jin, M., and Zhang, A. (2014). HSPD1 interacts with IRF3 to facilitate interferon-beta induction. PLoS One *9*, e114874.

Liu, S., Cai, X., Wu, J., Cong, Q., Chen, X., Li, T., Du, F., Ren, J., Wu, Y.T., Grishin, N.V.*, et al.* (2015). Phosphorylation of innate immune adaptor proteins MAVS, STING, and TRIF induces IRF3 activation. Science *347*, aaa2630.

Liu, S., Chen, J., Cai, X., Wu, J., Chen, X., Wu, Y.T., Sun, L., and Chen, Z.J. (2013a). MAVS recruits multiple ubiquitin E3 ligases to activate antiviral signaling cascades. eLife *2*, e00785.

Liu, Z., Wu, S.W., Lei, C.Q., Zhou, Q., Li, S., Shu, H.B., and Wang, Y.Y. (2013b). Heat shock cognate 71 (HSC71) regulates cellular antiviral response by impairing formation of VISA aggregates. Protein & cell *4*, 373-382.

Livak, K.J., and Schmittgen, T.D. (2001). Analysis of relative gene expression data using real-time quantitative PCR and the 2(-Delta Delta C(T)) Method. Methods (San Diego, Calif) *25*, 402-408.

Loo, Y.M., Fornek, J., Crochet, N., Bajwa, G., Perwitasari, O., Martinez-Sobrido, L., Akira, S., Gill, M.A., Garcia-Sastre, A., Katze, M.G.*, et al.* (2008). Distinct RIG-I and MDA5 signaling by RNA viruses in innate immunity. J Virol *82*, 335-345.

Loo, Y.M., and Gale, M., Jr. (2011). Immune signaling by RIG-I-like receptors. Immunity *34*, 680-692.

Luco, S., Delmas, O., Vidalain, P.O., Tangy, F., Weil, R., and Bourhy, H. (2012). RelAp43, a member of the NF-kappaB family involved in innate immune response against Lyssavirus infection. PLoS Pathog *8*, e1003060.

Ma, L., Sato, F., Sato, R., Matsubara, T., Hirai, K., Yamasaki, M., Shin, T., Shimada, T., Nomura, T., Mori, K.*, et al.* (2014). Dual targeting of heat shock proteins 90 and 70 promotes cell death and enhances the anticancer effect of chemotherapeutic agents in bladder cancer. Oncology reports *31*, 2482-2492.

Ma, X., Helgason, E., Phung, Q.T., Quan, C.L., Iyer, R.S., Lee, M.W., Bowman, K.K., Starovasnik, M.A., and Dueber, E.C. (2012). Molecular basis of Tank-binding kinase 1 activation by transautophosphorylation. Proceedings of the National Academy of Sciences of the United States of America *109*, 9378-9383.

Mali, P., Yang, L., Esvelt, K.M., Aach, J., Guell, M., DiCarlo, J.E., Norville, J.E., and Church, G.M. (2013). RNA-guided human genome engineering via Cas9. Science *339*, 823-826.

Malmgaard, L. (2004). Induction and regulation of IFNs during viral infections. J Interferon Cytokine Res *24*, 439-454.

Manning, S.E., Rupprecht, C.E., Fishbein, D., Hanlon, C.A., Lumlertdacha, B., Guerra, M., Meltzer, M.I., Dhankhar, P., Vaidya, S.A., Jenkins, S.R.*, et al.* (2008). Human rabies prevention--United States, 2008: recommendations of the Advisory Committee on Immunization Practices. MMWR Recomm Rep *57*, 1-28.

Marschalek, A., Finke, S., Schwemmle, M., Mayer, D., Heimrich, B., Stitz, L., and Conzelmann, K.K. (2009). Attenuation of rabies virus replication and virulence by picornavirus internal ribosome entry site elements. J Virol *83*, 1911-1919.

Masatani, T., Ozawa, M., Yamada, K., Ito, N., Horie, M., Matsuu, A., Okuya, K., Tsukiyama-Kohara, K., Sugiyama, M., and Nishizono, A. (2016). Contribution of the interaction between the rabies virus P protein and I-kappa B kinase to the inhibition of type I IFN induction signalling. J Gen Virol *97*, 316-326.

Masters, P.S., and Banerjee, A.K. (1988). Complex formation with vesicular stomatitis virus phosphoprotein NS prevents binding of nucleocapsid protein N to nonspecific RNA. J Virol *62*, 2658-2664.

Matlack, K.E., Misselwitz, B., Plath, K., and Rapoport, T.A. (1999). BiP acts as a molecular ratchet during posttranslational transport of prepro-alpha factor across the ER membrane. Cell *97*, 553-564.

Matlack, K.E., Plath, K., Misselwitz, B., and Rapoport, T.A. (1997). Protein transport by purified yeast Sec complex and Kar2p without membranes. Science *277*, 938-941.

Mavrakis, M., Iseni, F., Mazza, C., Schoehn, G., Ebel, C., Gentzel, M., Franz, T., and Ruigrok, R.W. (2003). Isolation and characterisation of the rabies virus N degrees-P complex produced in insect cells. Virology *305*, 406-414.

Mavrakis, M., McCarthy, A.A., Roche, S., Blondel, D., and Ruigrok, R.W. (2004). Structure and function of the C-terminal domain of the polymerase cofactor of rabies virus. J Mol Biol *343*, 819-831.

Mavrakis, M., Mehouas, S., Real, E., Iseni, F., Blondel, D., Tordo, N., and Ruigrok, R.W. (2006). Rabies virus chaperone: identification of the phosphoprotein peptide that keeps nucleoprotein soluble and free from non-specific RNA. Virology *349*, 422-429.

Mayer, M.P. (2005). Recruitment of Hsp70 chaperones: a crucial part of viral survival strategies. Reviews of physiology, biochemistry and pharmacology *153*, 1-46.

Mayer, M.P. (2013). Hsp70 chaperone dynamics and molecular mechanism. Trends in biochemical sciences *38*, 507-514.

Mayer, M.P., and Bukau, B. (2005). Hsp70 chaperones: cellular functions and molecular mechanism. Cellular and molecular life sciences : CMLS *62*, 670-684.

Mayer, M.P., Schroder, H., Rudiger, S., Paal, K., Laufen, T., and Bukau, B. (2000). Multistep mechanism of substrate binding determines chaperone activity of Hsp70. Nat Struct Biol *7*, 586-593.

McWhirter, S.M., Fitzgerald, K.A., Rosains, J., Rowe, D.C., Golenbock, D.T., and Maniatis, T. (2004). IFN-regulatory factor 3-dependent gene expression is defective in Tbk1-deficient mouse embryonic fibroblasts. Proc Natl Acad Sci U S A *101*, 233-238.

Mebatsion, T., Konig, M., and Conzelmann, K.K. (1996). Budding of rabies virus particles in the absence of the spike glycoprotein. Cell *84*, 941-951.

Mebatsion, T., Weiland, F., and Conzelmann, K.K. (1999). Matrix protein of rabies virus is responsible for the assembly and budding of bullet-shaped particles and interacts with the transmembrane spike glycoprotein G. J Virol *73*, 242-250.

Mellon, M.G., and Emerson, S.U. (1978). Rebinding of transcriptase components (L and NS proteins) to the nucleocapsid template of vesicular stomatitis virus. J Virol *27*, 560-567.

Menager, P., Roux, P., Megret, F., Bourgeois, J.P., Le Sourd, A.M., Danckaert, A., Lafage, M., Prehaud, C., and Lafon, M. (2009). Toll-like receptor 3 (TLR3) plays a major role in the formation of rabies virus Negri Bodies. PLoS Pathog *5*, e1000315.

Metzger, N. (2013). Battling demons with medical authority: werewolves, physicians and rationalization. Hist Psychiatry *24*, 341-355.

Meylan, E., Curran, J., Hofmann, K., Moradpour, D., Binder, M., Bartenschlager, R., and Tschopp, J. (2005). Cardif is an adaptor protein in the RIG-I antiviral pathway and is targeted by hepatitis C virus. Nature *437*, 1167-1172.

Michallet, M.C., Meylan, E., Ermolaeva, M.A., Vazquez, J., Rebsamen, M., Curran, J., Poeck, H., Bscheider, M., Hartmann, G., Konig, M.*, et al.* (2008). TRADD protein is an essential component of the RIG-like helicase antiviral pathway. Immunity *28*, 651-661.

Morgan, J.R., Jiang, J., Oliphint, P.A., Jin, S., Gimenez, L.E., Busch, D.J., Foldes, A.E., Zhuo, Y., Sousa, R., and Lafer, E.M. (2013). A role for an Hsp70 nucleotide exchange factor in the regulation of synaptic vesicle endocytosis. J Neurosci *33*, 8009-8021.

Morgan, J.R., Prasad, K., Jin, S., Augustine, G.J., and Lafer, E.M. (2001). Uncoating of clathrin-coated vesicles in presynaptic terminals: roles for Hsc70 and auxilin. Neuron *32*, 289-300.

Mori, M., Yoneyama, M., Ito, T., Takahashi, K., Inagaki, F., and Fujita, T. (2004). Identification of Ser-386 of interferon regulatory factor 3 as critical target for inducible phosphorylation that determines activation. J Biol Chem *279*, 9698-9702.

Moro, F., Sirrenberg, C., Schneider, H.C., Neupert, W., and Brunner, M. (1999). The TIM17.23 preprotein translocase of mitochondria: composition and function in protein transport into the matrix. Embo j *18*, 3667-3675.

Moseley, G.W., Filmer, R.P., DeJesus, M.A., and Jans, D.A. (2007). Nucleocytoplasmic distribution of rabies virus P-protein is regulated by phosphorylation adjacent to C-terminal nuclear import and export signals. Biochemistry *46*, 12053-12061.

Munday, D.C., Wu, W., Smith, N., Fix, J., Noton, S.L., Galloux, M., Touzelet, O., Armstrong, S.D., Dawson, J.M., Aljabr, W*., et al.* (2015). Interactome analysis of the human respiratory syncytial virus RNA polymerase complex identifies protein chaperones as important cofactors that promote L-protein stability and RNA synthesis. J Virol *89*, 917-930.

Murphy, M.E. (2013). The HSP70 family and cancer. Carcinogenesis *34*, 1181-1188.

Nadeau, K., Nadler, S.G., Saulnier, M., Tepper, M.A., and Walsh, C.T. (1994). Quantitation of the interaction of the immunosuppressant deoxyspergualin and analogs with Hsc70 and Hsp90. Biochemistry *33*, 2561-2567.

Nadler, S.G., Tepper, M.A., Schacter, B., and Mazzucco, C.E. (1992). Interaction of the immunosuppressant deoxyspergualin with a member of the Hsp70 family of heat shock proteins. Science *258*, 484-486.

Newmyer, S.L., and Schmid, S.L. (2001). Dominant-interfering Hsc70 mutants disrupt multiple stages of the clathrin-coated vesicle cycle in vivo. The Journal of cell biology *152*, 607-620.

Nishimura, K., Fukagawa, T., Takisawa, H., Kakimoto, T., and Kanemaki, M. (2009). An auxin-based degron system for the rapid depletion of proteins in nonplant cells. Nat Methods *6*, 917-922.

Nistal-Villan, E., Gack, M.U., Martinez-Delgado, G., Maharaj, N.P., Inn, K.S., Yang, H., Wang, R., Aggarwal, A.K., Jung, J.U., and Garcia-Sastre, A. (2010). Negative role of RIG-I serine 8 phosphorylation in the regulation of interferon-beta production. J Biol Chem *285*, 20252-20261.

Nylandsted, J., Rohde, M., Brand, K., Bastholm, L., Elling, F., and Jäättelä, M. (2000). Selective depletion of heat shock protein 70 (Hsp70) activates a tumor-specific death program that is independent of caspases and bypasses Bcl-2. Proceedings of the National Academy of Sciences of the United States of America *97*, 7871-7876.

O'Brien, M.C., Flaherty, K.M., and McKay, D.B. (1996). Lysine 71 of the chaperone protein Hsc70 Is essential for ATP hydrolysis. J Biol Chem *271*, 15874-15878.

Oganesyan, G., Saha, S.K., Guo, B., He, J.Q., Shahangian, A., Zarnegar, B., Perry, A., and Cheng, G. (2006). Critical role of TRAF3 in the Toll-like receptor-dependent and -independent antiviral response. Nature *439*, 208-211.

Oglesbee, M.J., Liu, Z., Kenney, H., and Brooks, C.L. (1996). The highly inducible member of the 70 kDa family of heat shock proteins increases canine distemper virus polymerase activity. J Gen Virol *77 (Pt 9)*, 2125-2135.

Okamoto, K., Brinker, A., Paschen, S.A., Moarefi, I., Hayer-Hartl, M., Neupert, W., and Brunner, M. (2002). The protein import motor of mitochondria: a targeted molecular ratchet driving unfolding and translocation. Embo j *21*, 3659-3671.

Oksayan, S., Wiltzer, L., Rowe, C.L., Blondel, D., Jans, D.A., and Moseley, G.W. (2012). A novel nuclear trafficking module regulates the nucleocytoplasmic localization of the rabies virus interferon antagonist, P protein. J Biol Chem *287*, 28112-28121.

Okumura, A., and Harty, R.N. (2011). Rabies virus assembly and budding. Adv Virus Res *79*, 23-32.

Padwad, Y.S., Mishra, K.P., Jain, M., Chanda, S., and Ganju, L. (2010). Dengue virus infection activates cellular chaperone Hsp70 in THP-1 cells: downregulation of Hsp70 by siRNA revealed decreased viral replication. Viral immunology *23*, 557-565.

Park, C.H., Kondo, M., Inoue, S., Noguchi, A., Oyamada, T., Yoshikawa, H., and Yamada, A. (2006). The histopathogenesis of paralytic rabies in six-week-old C57BL/6J mice following inoculation of the CVS-11 strain into the right triceps surae muscle. The Journal of veterinary medical science / the Japanese Society of Veterinary Science *68*, 589-595.

Parks, C.L., Lerch, R.A., Walpita, P., Sidhu, M.S., and Udem, S.A. (1999). Enhanced measles virus cDNA rescue and gene expression after heat shock. J Virol *73*, 3560-3566.

Pasdeloup, D., Poisson, N., Raux, H., Gaudin, Y., Ruigrok, R.W., and Blondel, D. (2005). Nucleocytoplasmic shuttling of the rabies virus P protein requires a nuclear localization signal and a CRM1-dependent nuclear export signal. Virology *334*, 284-293.

Patury, S., Miyata, Y., and Gestwicki, J.E. (2009). Pharmacological Targeting of the Hsp70 Chaperone. Current topics in medicinal chemistry *9*, 1337-1351.

Paz, S., Sun, Q., Nakhaei, P., Romieu-Mourez, R., Goubau, D., Julkunen, I., Lin, R., and Hiscott, J. (2006). Induction of IRF-3 and IRF-7 phosphorylation following activation of the RIG-I pathway. Cellular and molecular biology (Noisy-le-Grand, France) *52*, 17-28.

Paz, S., Vilasco, M., Werden, S.J., Arguello, M., Joseph-Pillai, D., Zhao, T., Nguyen, T.L., Sun, Q., Meurs, E.F., Lin, R*., et al.* (2011). A functional C-terminal TRAF3-binding site in MAVS participates in positive and negative regulation of the IFN antiviral response. Cell research *21*, 895-910.

Peisley, A., Wu, B., Xu, H., Chen, Z.J., and Hur, S. (2014). Structural basis for ubiquitin-mediated antiviral signal activation by RIG-I. Nature *509*, 110-114.

Peisley, A., Wu, B., Yao, H., Walz, T., and Hur, S. (2013). RIG-I Forms Signaling-Competent Filaments in an ATP-Dependent, Ubiquitin-Independent Manner. Mol Cell.

Peterson, N.S., Moller, G., and Mitchell, H.K. (1979). Genetic mapping of the coding regions for three heat-shock proteins in Drosophila melanogaster. Genetics *92*, 891-902.

Pichlmair, A., Schulz, O., Tan, C.P., Naslund, T.I., Liljestrom, P., Weber, F., and Reis e Sousa, C. (2006). RIG-I-mediated antiviral responses to single-stranded RNA bearing 5'-phosphates. Science *314*, 997-1001.

Platanias, L.C. (2005). Mechanisms of type-I- and type-II-interferon-mediated signalling. Nature reviews Immunology *5*, 375-386.

Plumet, S., Herschke, F., Bourhis, J.M., Valentin, H., Longhi, S., and Gerlier, D. (2007). Cytosolic 5'-triphosphate ended viral leader transcript of measles virus as activator of the RIG I-mediated interferon response. PLoS One *2*, e279.

Poisson, N., Real, E., Gaudin, Y., Vaney, M.C., King, S., Jacob, Y., Tordo, N., and Blondel, D. (2001). Molecular basis for the interaction between rabies virus phosphoprotein P and the dynein light chain LC8: dissociation of dynein-binding properties and transcriptional functionality of P. J Gen Virol *82*, 2691-2696.

Powers, M.V., Clarke, P.A., and Workman, P. (2008). Dual targeting of HSC70 and HSP72 inhibits HSP90 function and induces tumor-specific apoptosis. Cancer cell *14*, 250-262.

Pulmanausahakul, R., Li, J., Schnell, M.J., and Dietzschold, B. (2008). The glycoprotein and the matrix protein of rabies virus affect pathogenicity by regulating viral replication and facilitating cell-to-cell spread. J Virol *82*, 2330-2338.

Radons, J. (2016). The human HSP70 family of chaperones: where do we stand? Cell stress & chaperones *21*, 379-404.

Randall, R.E., and Goodbourn, S. (2008). Interferons and viruses: an interplay between induction, signalling, antiviral responses and virus countermeasures. J Gen Virol *89*, 1-47.

Rasalingam, P., Rossiter, J.P., Mebatsion, T., and Jackson, A.C. (2005). Comparative pathogenesis of the SAD-L16 strain of rabies virus and a mutant modifying the dynein light chain binding site of the rabies virus phosphoprotein in young mice. Virus research *111*, 55-60.

Raux, H., Flamand, A., and Blondel, D. (2000). Interaction of the rabies virus P protein with the LC8 dynein light chain. J Virol *74*, 10212-10216.

Rerole, A.L., Gobbo, J., De Thonel, A., Schmitt, E., Pais de Barros, J.P., Hammann, A., Lanneau, D., Fourmaux, E., Demidov, O.N., Micheau, O.*, et al.* (2011). Peptides and aptamers targeting HSP70: a novel approach for anticancer chemotherapy. Cancer research *71*, 484-495.

Reyes-Del Valle, J., Chavez-Salinas, S., Medina, F., and Del Angel, R.M. (2005). Heat shock protein 90 and heat shock protein 70 are components of dengue virus receptor complex in human cells. J Virol *79*, 4557-4567.

Ribeiro, A., Jr., Leyrat, C., Gerard, F.C., Albertini, A.A., Falk, C., Ruigrok, R.W., and Jamin, M. (2009). Binding of rabies virus polymerase cofactor to recombinant circular nucleoprotein-RNA complexes. J Mol Biol *394*, 558-575.

Richter, K., Haslbeck, M., and Buchner, J. (2010). The heat shock response: life on the verge of death. Mol Cell *40*, 253-266.

Rieder, M. (2012). Mechanisms of rabies virus to escape the IFN system - main actor: the phosphoprotein P. Doctoral thesis.

Rieder, M., Brzozka, K., Pfaller, C.K., Cox, J.H., Stitz, L., and Conzelmann, K.K. (2011). Genetic dissection of interferon-antagonistic functions of rabies virus phosphoprotein: inhibition of interferon regulatory factor 3 activation is important for pathogenicity. J Virol *85*, 842-852.

Rieder, M., and Conzelmann, K.K. (2009). Rhabdovirus evasion of the interferon system. J Interferon Cytokine Res *29*, 499-509.

Rieder, M., and Conzelmann, K.K. (2011). Interferon in rabies virus infection. Adv Virus Res *79*, 91-114.

Roche, S., and Gaudin, Y. (2004). Evidence that rabies virus forms different kinds of fusion machines with different pH thresholds for fusion. J Virol *78*, 8746-8752.

Roers, A., Hiller, B., and Hornung, V. (2016). Recognition of Endogenous Nucleic Acids by the Innate Immune System. Immunity *44*, 739-754.

Rohde, M., Daugaard, M., Jensen, M.H., Helin, K., Nylandsted, J., and Jaattela, M. (2005). Members of the heat-shock protein 70 family promote cancer cell growth by distinct mechanisms. Genes & development *19*, 570-582.

Rosatte, R.C. (2013). Rabies Control in Wild Carnivores. 617-670.

Rose, J.K. (1980). Complete intergenic and flanking gene sequences from the genome of vesicular stomatitis virus. Cell *19*, 415-421.

Rosner, F. (1974). Rabies in the Talmud. Med Hist *18*, 198-200.

Rothenfusser, S., Goutagny, N., DiPerna, G., Gong, M., Monks, B.G., Schoenemeyer, A., Yamamoto, M., Akira, S., and Fitzgerald, K.A. (2005). The RNA helicase Lgp2 inhibits TLR-independent sensing of viral replication by retinoic acid-inducible gene-I. Journal of immunology (Baltimore, Md : 1950) *175*, 5260-5268.

Rowe, C.L., Wagstaff, K.M., Oksayan, S., Glover, D.J., Jans, D.A., and Moseley, G.W. (2016). Nuclear Trafficking of the Rabies Virus Interferon Antagonist P-Protein Is Regulated by an Importin-Binding Nuclear Localization Sequence in the C-Terminal Domain. PLoS One *11*, e0150477.

Rüdiger, S., Buchberger, A., and Bukau, B. (1997a). Interaction of Hsp70 chaperones with substrates. Nat Struct Biol *4*, 342-349.

Rüdiger, S., Germeroth, L., Schneider-Mergener, J., and Bukau, B. (1997b). Substrate specificity of the DnaK chaperone determined by screening cellulose-bound peptide libraries. The EMBO Journal *16*, 1501-1507.

Rupprecht, C.E., Hanlon, C.A., and Hemachudha, T. (2002). Rabies re-examined. Lancet Infect Dis *2*, 327-343.

Ryzhakov, G., and Randow, F. (2007). SINTBAD, a novel component of innate antiviral immunity, shares a TBK1-binding domain with NAP1 and TANK. EMBO J *26*, 3180-3190.

Sagara, J., and Kawai, A. (1992). Identification of heat shock protein 70 in the rabies virion. Virology *190*, 845-848.

Saha, S.K., Pietras, E.M., He, J.Q., Kang, J.R., Liu, S.Y., Oganesyan, G., Shahangian, A., Zarnegar, B., Shiba, T.L., Wang, Y.*, et al.* (2006). Regulation of antiviral responses by a direct and specific interaction between TRAF3 and Cardif. Embo j *25*, 3257-3263.

Saito, T., Hirai, R., Loo, Y.-M., Owen, D., Johnson, C.L., Sinha, S.C., Akira, S., Fujita, T., and Gale, M. (2007). Regulation of innate antiviral defenses through a shared repressor domain in RIG-I and LGP2. Proceedings of the National Academy of Sciences of the United States of America *104*, 582-587.

Saito, T., Owen, D.M., Jiang, F., Marcotrigiano, J., and Gale, M. (2008). Innate immunity induced by composition-dependent RIG-I recognition of Hepatitis C virus RNA. Nature *454*, 523-527.

Sasai, M., Shingai, M., Funami, K., Yoneyama, M., Fujita, T., Matsumoto, M., and Seya, T. (2006). NAK-associated protein 1 participates in both the TLR3 and the cytoplasmic pathways in type I IFN induction. Journal of immunology (Baltimore, Md : 1950) *177*, 8676-8683.

Sato, M., Suemori, H., Hata, N., Asagiri, M., Ogasawara, K., Nakao, K., Nakaya, T., Katsuki, M., Noguchi, S., Tanaka, N.*, et al.* (2000). Distinct and essential roles of transcription factors IRF-3 and IRF-7 in response to viruses for IFN-alpha/beta gene induction. Immunity *13*, 539-548.

Sato, S., Li, K., Kameyama, T., Hayashi, T., Ishida, Y., Murakami, S., Watanabe, T., Iijima, S., Sakurai, Y., Watashi, K.*, et al.* (2015). The RNA sensor RIG-I dually functions as an innate sensor and direct antiviral factor for hepatitis B virus. Immunity *42*, 123-132.

Schlee, M., and Hartmann, G. (2010). The chase for the RIG-I ligand--recent advances. Mol Ther *18*, 1254-1262.

Schlee, M., Roth, A., Hornung, V., Hagmann, C.A., Wimmenauer, V., Barchet, W., Coch, C., Janke, M., Mihailovic, A., Wardle, G.*, et al.* (2009). Recognition of 5' triphosphate by RIG-I

helicase requires short blunt double-stranded RNA as contained in panhandle of negative-strand virus. Immunity *31*, 25-34.

Schneider, C.A., Rasband, W.S., and Eliceiri, K.W. (2012). NIH Image to ImageJ: 25 years of image analysis. Nat Methods *9*, 671-675.

Schneider, M., Rosam, M., Glaser, M., Patronov, A., Shah, H., Back, K.C., Daake, M.A., Buchner, J., and Antes, I. (2016). BiPPred: Combined sequence- and structure-based prediction of peptide binding to the Hsp70 chaperone BiP. Proteins.

Schnell, M.J., Mebatsion, T., and Conzelmann, K.K. (1994). Infectious rabies viruses from cloned cDNA. EMBO J *13*, 4195-4203.

Schoggins, J.W., and Rice, C.M. (2011). Interferon-stimulated genes and their antiviral effector functions. Current opinion in virology *1*, 519-525.

Schrodinger, LLC (2015). The PyMOL Molecular Graphics System, Version 1.8.

Schuberth-Wagner, C., Ludwig, J., Bruder, A.K., Herzner, A.M., Zillinger, T., Goldeck, M., Schmidt, T., Schmid-Burgk, J.L., Kerber, R., Wolter, S*., et al.* (2015). A Conserved Histidine in the RNA Sensor RIG-I Controls Immune Tolerance to N1-2'O-Methylated Self RNA. Immunity *43*, 41-51.

Schuermann, J.P., Jiang, J., Cuellar, J., Llorca, O., Wang, L., Gimenez, L.E., Jin, S., Taylor, A.B., Demeler, B., Morano, K.A*., et al.* (2008). Structure of the Hsp110:Hsc70 nucleotide exchange machine. Mol Cell *31*, 232-243.

Servant, M.J., Grandvaux, N., tenOever, B.R., Duguay, D., Lin, R., and Hiscott, J. (2003). Identification of the minimal phosphoacceptor site required for in vivo activation of interferon regulatory factor 3 in response to virus and double-stranded RNA. J Biol Chem *278*, 9441-9447.

Seth, R.B., Sun, L., Ea, C.K., and Chen, Z.J. (2005). Identification and characterization of MAVS, a mitochondrial antiviral signaling protein that activates NF-kappaB and IRF 3. Cell *122*, 669-682.

Sharma, S., tenOever, B.R., Grandvaux, N., Zhou, G.P., Lin, R., and Hiscott, J. (2003). Triggering the interferon antiviral response through an IKK-related pathway. Science *300*, 1148-1151.

Shi, Y., Yuan, B., Qi, N., Zhu, W., Su, J., Li, X., Qi, P., Zhang, D., and Hou, F. (2015). An autoinhibitory mechanism modulates MAVS activity in antiviral innate immune response. Nature communications *6*, 7811.

Slepnev, V.I., and De Camilli, P. (2000). Accessory factors in clathrin-dependent synaptic vesicle endocytosis. Nature reviews Neuroscience *1*, 161-172.

Smith, D.B. (2000). Generating fusions to glutathione S-transferase for protein studies. Methods in enzymology *326*, 254-270.

Smith, K.A. (2012). Louis Pasteur, the Father of Immunology? Frontiers in Immunology *3*, 68.

Smith, T.G., Wu, X., Franka, R., and Rupprecht, C.E. (2011). Design of future rabies biologics and antiviral drugs. Adv Virus Res *79*, 345-363.

Strahle, L., Garcin, D., and Kolakofsky, D. (2006). Sendai virus defective-interfering genomes and the activation of interferon-beta. Virology *351*, 101-111.

Sun, Q., Sun, L., Liu, H.H., Chen, X., Seth, R.B., Forman, J., and Chen, Z.J. (2006). The specific and essential role of MAVS in antiviral innate immune responses. Immunity *24*, 633-642.

Tan, G.S., Preuss, M.A., Williams, J.C., and Schnell, M.J. (2007). The dynein light chain 8 binding motif of rabies virus phosphoprotein promotes efficient viral transcription. Proc Natl Acad Sci U S A *104*, 7229-7234.

Thanos, D., and Maniatis, T. (1995). Virus induction of human IFN beta gene expression requires the assembly of an enhanceosome. Cell *83*, 1091-1100.

Tissieres, A., Mitchell, H.K., and Tracy, U.M. (1974). Protein synthesis in salivary glands of Drosophila melanogaster: relation to chromosome puffs. J Mol Biol *84*, 389-398.

Tojima, Y., Fujimoto, A., Delhase, M., Chen, Y., Hatakeyama, S., Nakayama, K., Kaneko, Y., Nimura, Y., Motoyama, N., Ikeda, K.*, et al.* (2000). NAK is an IkappaB kinase-activating kinase. Nature *404*, 778-782.

Torgerson, T.R., Colosia, A.D., Donahue, J.P., Lin, Y.Z., and Hawiger, J. (1998). Regulation of NF-kappa B, AP-1, NFAT, and STAT1 nuclear import in T lymphocytes by noninvasive delivery of peptide carrying the nuclear localization sequence of NF-kappa B p50. Journal of immunology (Baltimore, Md : 1950) *161*, 6084-6092.

Triana-Alonso, F.J., Dabrowski, M., Wadzack, J., and Nierhaus, K.H. (1995). Self-coded 3'-extension of run-off transcripts produces aberrant products during in vitro transcription with T7 RNA polymerase. J Biol Chem *270*, 6298-6307.

Ungewickell, E., Ungewickell, H., Holstein, S.E., Lindner, R., Prasad, K., Barouch, W., Martin, B., Greene, L.E., and Eisenberg, E. (1995). Role of auxilin in uncoating clathrin-coated vesicles. Nature *378*, 632-635.

Van Durme, J., Maurer-Stroh, S., Gallardo, R., Wilkinson, H., Rousseau, F., and Schymkowitz, J. (2009). Accurate Prediction of DnaK-Peptide Binding via Homology Modelling and Experimental Data. PLoS Computational Biology *5*, e1000475.

Vazquez, C., and Horner, S.M. (2015). MAVS Coordination of Antiviral Innate Immunity. Journal of Virology *89*, 6974-6977.

Vidy, A., Chelbi-Alix, M., and Blondel, D. (2005). Rabies virus P protein interacts with STAT1 and inhibits interferon signal transduction pathways. J Virol *79*, 14411-14420.

Vidy, A., El Bougrini, J., Chelbi-Alix, M.K., and Blondel, D. (2007). The Nucleocytoplasmic Rabies Virus P Protein Counteracts Interferon Signaling by Inhibiting both Nuclear Accumulation and DNA Binding of STAT1. Journal of Virology *81*, 4255-4263.

Vora, N.M., Basavaraju, S.V., Feldman, K.A., Paddock, C.D., Orciari, L., Gitterman, S., Griese, S., Wallace, R.M., Said, M., Blau, D.M.*, et al.* (2013). Raccoon rabies virus variant transmission through solid organ transplantation. JAMA *310*, 398-407.

Vos, A., Conzelmann, K.K., Finke, S., Muller, T., Teifke, J., Fooks, A.R., and Neubert, A. (2011). Immunogenicity studies in carnivores using a rabies virus construct with a site-directed deletion in the phosphoprotein. Advances in preventive medicine *2011*, 898171.

Wachowius, M. (2012). The rabies virus phosphoprotein P as antagonist of IRF3-mediated IFN-β induction. Master thesis.

Wang, L., Li, S., and Dorf, M.E. (2012). NEMO binds ubiquitinated TANK-binding kinase 1 (TBK1) to regulate innate immune responses to RNA viruses. PLoS One *7*, e43756.

Waterhouse, A.M., Procter, J.B., Martin, D.M., Clamp, M., and Barton, G.J. (2009). Jalview Version 2--a multiple sequence alignment editor and analysis workbench. Bioinformatics *25*, 1189-1191.

Weber, F., Wagner, V., Rasmussen, S.B., Hartmann, R., and Paludan, S.R. (2006). Double-stranded RNA is produced by positive-strand RNA viruses and DNA viruses but not in detectable amounts by negative-strand RNA viruses. J Virol *80*, 5059-5064.

Weber, M., Gawanbacht, A., Habjan, M., Rang, A., Borner, C., Schmidt, A.M., Veitinger, S., Jacob, R., Devignot, S., Kochs, G.*, et al.* (2013). Incoming RNA virus nucleocapsids containing a 5'-triphosphorylated genome activate RIG-I and antiviral signaling. Cell host & microbe *13*, 336-346.

Wei, D., Li, N.L., Zeng, Y., Liu, B., Kumthip, K., Wang, T.T., Huo, D., Ingels, J.F., Lu, L., Shang, J.*, et al.* (2016). The Molecular Chaperone GRP78 Contributes to Toll-like Receptor 3-mediated Innate Immune Response to Hepatitis C Virus in Hepatocytes. J Biol Chem *291*, 12294-12309.

Whelan, S.P., Barr, J.N., and Wertz, G.W. (2004). Transcription and replication of nonsegmented negative-strand RNA viruses. Current topics in microbiology and immunology *283*, 61-119.

Whelan, S.P., and Wertz, G.W. (2002). Transcription and replication initiate at separate sites on the vesicular stomatitis virus genome. Proc Natl Acad Sci U S A *99*, 9178-9183.

Whitt, M.A., Buonocor, L., Prehaud, C., and Rose, J.K. (1991). Membrane fusion activity, oligomerization, and assembly of the rabies virus glycoprotein. Virology *185*, 681-688.

Willoughby, R.E., Jr., Tieves, K.S., Hoffman, G.M., Ghanayem, N.S., Amlie-Lefond, C.M., Schwabe, M.J., Chusid, M.J., and Rupprecht, C.E. (2005). Survival after treatment of rabies with induction of coma. N Engl J Med *352*, 2508-2514.

Wiltzer, L., Larrous, F., Oksayan, S., Ito, N., Marsh, G.A., Wang, L.F., Blondel, D., Bourhy, H., Jans, D.A., and Moseley, G.W. (2012). Conservation of a unique mechanism of immune evasion across the Lyssavirus genus. J Virol *86*, 10194-10199.

Wiltzer, L., Okada, K., Yamaoka, S., Larrous, F., Kuusisto, H.V., Sugiyama, M., Blondel, D., Bourhy, H., Jans, D.A., Ito, N.*, et al.* (2014). Interaction of rabies virus P-protein with STAT proteins is critical to lethal rabies disease. J Infect Dis *209*, 1744-1753.

Wu, B., Peisley, A., Richards, C., Yao, H., Zeng, X., Lin, C., Chu, F., Walz, T., and Hur, S. (2013). Structural basis for dsRNA recognition, filament formation, and antiviral signal activation by MDA5. Cell *152*, 276-289.

Wu, B., Peisley, A., Tetrault, D., Li, Z., Egelman, E.H., Magor, K.E., Walz, T., Penczek, P.A., and Hur, S. (2014). Molecular imprinting as a signal-activation mechanism of the viral RNA sensor RIG-I. Mol Cell *55*, 511-523.

Xu, L.G., Wang, Y.Y., Han, K.J., Li, L.Y., Zhai, Z., and Shu, H.B. (2005). VISA is an adapter protein required for virus-triggered IFN-beta signaling. Mol Cell *19*, 727-740.

Xu, Y., Liu, F., Liu, J., Wang, D., Yan, Y., Ji, S., Zan, J., and Zhou, J. (2016). The co-chaperone Cdc37 regulates the rabies virus phosphoprotein stability by targeting to Hsp90AA1 machinery. Scientific reports *6*, 27123.

Yamaoka, S., Courtois, G., Bessia, C., Whiteside, S.T., Weil, R., Agou, F., Kirk, H.E., Kay, R.J., and Israel, A. (1998). Complementation cloning of NEMO, a component of the IkappaB kinase complex essential for NF-kappaB activation. Cell *93*, 1231-1240.

Yamaoka, S., Ito, N., Ohka, S., Kaneda, S., Nakamura, H., Agari, T., Masatani, T., Nakagawa, K., Okada, K., Okadera, K.*, et al.* (2013). Involvement of the rabies virus phosphoprotein gene in neuroinvasiveness. J Virol *87*, 12327-12338.

Yang, K., Shi, H., Qi, R., Sun, S., Tang, Y., Zhang, B., and Wang, C. (2006). Hsp90 regulates activation of interferon regulatory factor 3 and TBK-1 stabilization in Sendai virus-infected cells. Molecular biology of the cell *17*, 1461-1471.

Yao, H., Dittmann, M., Peisley, A., Hoffmann, H.H., Gilmore, R.H., Schmidt, T., Schmid-Burgk, J.L., Hornung, V., Rice, C.M., and Hur, S. (2015). ATP-dependent effector-like functions of RIG-I-like receptors. Mol Cell *58*, 541-548.

Yoneyama, M., Kikuchi, M., Matsumoto, K., Imaizumi, T., Miyagishi, M., Taira, K., Foy, E., Loo, Y.M., Gale, M., Akira, S*., et al.* (2005). Shared and Unique Functions of the DExD/H-Box Helicases RIG-I, MDA5, and LGP2 in Antiviral Innate Immunity. The Journal of Immunology *175*, 2851-2858.

Yoneyama, M., Kikuchi, M., Natsukawa, T., Shinobu, N., Imaizumi, T., Miyagishi, M., Taira, K., Akira, S., and Fujita, T. (2004). The RNA helicase RIG-I has an essential function in double-stranded RNA-induced innate antiviral responses. Nat Immunol *5*, 730-737.

Yoneyama, M., Suhara, W., and Fujita, T. (2002). Control of IRF-3 activation by phosphorylation. J Interferon Cytokine Res *22*, 73-76.

Yoneyama, M., Suhara, W., Fukuhara, Y., Fukuda, M., Nishida, E., and Fujita, T. (1998). Direct triggering of the type I interferon system by virus infection: activation of a transcription factor complex containing IRF-3 and CBP/p300. Embo j *17*, 1087-1095.

Yoneyama, M., Suhara, W., Fukuhara, Y., Sato, M., Ozato, K., and Fujita, T. (1996). Autocrine amplification of type I interferon gene expression mediated by interferon stimulated gene factor 3 (ISGF3). Journal of biochemistry *120*, 160-169.

Zeng, W., Sun, L., Jiang, X., Chen, X., Hou, F., Adhikari, A., Xu, M., and Chen, Z.J. (2010). Reconstitution of the RIG-I pathway reveals a signaling role of unanchored polyubiquitin chains in innate immunity. Cell *141*, 315-330.

Zeng, W., Xu, M., Liu, S., Sun, L., and Chen, Z.J. (2009). Key role of Ubc5 and lysine-63 polyubiquitination in viral activation of IRF3. Mol Cell *36*, 315-325.

Zeng, X.C., Bhasin, S., Wu, X., Lee, J.G., Maffi, S., Nichols, C.J., Lee, K.J., Taylor, J.P., Greene, L.E., and Eisenberg, E. (2004). Hsp70 dynamics in vivo: effect of heat shock and protein aggregation. J Cell Sci *117*, 4991-5000.

Zhang, P., Leu, J.I., Murphy, M.E., George, D.L., and Marmorstein, R. (2014). Crystal structure of the stress-inducible human heat shock protein 70 substrate-binding domain in complex with peptide substrate. PLoS One *9*, e103518.

Zhang, X., Bourhis, J.M., Longhi, S., Carsillo, T., Buccellato, M., Morin, B., Canard, B., and Oglesbee, M. (2005). Hsp72 recognizes a P binding motif in the measles virus N protein C-terminus. Virology *337*, 162-174.

Zhang, X., Glendening, C., Linke, H., Parks, C.L., Brooks, C., Udem, S.A., and Oglesbee, M. (2002). Identification and Characterization of a Regulatory Domain on the Carboxyl Terminus of the Measles Virus Nucleocapsid Protein. Journal of Virology *76*, 8737-8746.

Zhao, B., Shu, C., Gao, X., Sankaran, B., Du, F., Shelton, C.L., Herr, A.B., Ji, J.Y., and Li, P. (2016). Structural basis for concerted recruitment and activation of IRF-3 by innate immune adaptor proteins. Proc Natl Acad Sci U S A *113*, E3403-3412.

Zhao, T., Yang, L., Sun, Q., Arguello, M., Ballard, D.W., Hiscott, J., and Lin, R. (2007). The NEMO adaptor bridges the nuclear factor-kappaB and interferon regulatory factor signaling pathways. Nat Immunol *8*, 592-600.

Zhu, M., Fang, T., Li, S., Meng, K., and Guo, D. (2015). Bipartite Nuclear Localization Signal Controls Nuclear Import and DNA-Binding Activity of IFN Regulatory Factor 3. Journal of immunology (Baltimore, Md : 1950) *195*, 289-297.

Zhu, X., Zhao, X., Burkholder, W.F., Gragerov, A., Ogata, C.M., Gottesman, M.E., and Hendrickson, W.A. (1996). Structural analysis of substrate binding by the molecular chaperone DnaK. Science *272*, 1606-1614.